UNIVERSIDADE FEDERAL DE SÃO CARLOS
DEPARTAMENTO DE ENGENHARIA QUÍMICA
PROGRAMA DE PÓS-GRADUAÇÃO EM ENGENHARIA QUÍMICA

Ana Bárbara Moulin Cansian

Soybean Oil Deodorizer Distillate (SODD) as feedstock for esters production: Techno-economic-environmental analysis of enzymatic routes

Destilado da Desodorização do Óleo de Soja (DDOS) como matéria-prima na produção de ésteres: Análise técnico-econômica e ambiental de rotas enzimáticas

SÃO CARLOS - SP
2025

Ana Bárbara Moulin Cansian

Soybean Oil Deodorizer Distillate (SODD) as feedstock for esters production: Techno-economic-environmental analysis of enzymatic routes

Destilado da Desodorização do Óleo de Soja (DDOS) como matéria-prima na produção de ésteres: Análise técnico-econômica e ambiental de rotas enzimáticas

Tese apresentada ao Programa de Pós-Graduação em Engenharia Química da Universidade Federal de São Carlos como parte dos requisitos para a obtenção do título de Doutora em Engenharia Química.

Orientador: Prof. Dr. Paulo Waldir Tardioli

Coorientador: Prof. Dr. Ruy de Sousa Júnior

SÃO CARLOS - SP

2025

UNIVERSIDADE FEDERAL DE SÃO CARLOS

Centro de Ciências Exatas e de Tecnologia
Programa de Pós-Graduação em Engenharia Química

Folha de Aprovação

Defesa de Tese de Doutorado da candidata Ana Bárbara Moulin Cansian, realizada em 27/09/2024.

Comissão Julgadora:

Prof. Dr. Paulo Waldir Tardioli (UFSCar)

Prof. Dr. Andrew Milli Elias (EMBRAPA)

Profa. Dra. Simone de Carvalho Miyoshi (UFRJ)

Profa. Dra. Maria Carolina Pereira Gonçalves (Cargill)

Profa. Dra. Fernanda Perpétua Casciatori (UFSCar)

O Relatório de Defesa assinado pelos membros da Comissão Julgadora encontra-se arquivado junto ao Programa de Pós-Graduação em Engenharia Química.

AGRADECIMENTOS/ AKNOWLEDGEMENTS

A minha mãe, Janea, por me incentivar desde a infância a seguir meus sonhos e lutar pelo meu lugar na vida acadêmica, além de todo amor, carinho e apoio em cada momento difícil.

Ao meu pai, João Carlos, pelos ensinamentos, cuidado e apoio mesmo que de longe.

Ao meu irmão, Júnior, pelo companheirismo desde a infância.

Ao meu marido, Thiago, que conheci no meio dessa caminhada e esteve ao meu lado nos melhores e nos piores momentos, sem deixar de acreditar em mim. Seu amor me faz mais forte.

Aos meus sogros, Marcia e Kleber, que além de sempre me incentivarem me estenderam a mão nos momentos mais difíceis.

Ao meu orientador, Prof. Paulo, pela orientação, por todo ensinamento e paciência.

Ao meu coorientador, Prof. Ruy, pela orientação, por todo conhecimento transmitido, pela confiança, tempo em mim empregado e paciência.

Ao Prof. Felipe, pela paciência e disponibilidade em me ajudar com todos os problemas a ele levados.

Aos colegas de pesquisa Andrew, Ana Carolina, Nicole, Maria Carolina, Renato, entre outros, que me ensinaram muito nessa trajetória.

Aos meus colegas de Doutorado e de laboratório, por todo companheirismo e parceria ao longo desses dois anos.

A todos aqueles que fizeram parte e contribuíram para que este doutorado fosse finalizado, fica meu muito obrigada.

FINANCIAL SUPPORT

This study was financed in part by the Coordenação de Aperfeiçoamento de Pessoal de Nível Superior - Brasil (CAPES) - Finance Code 001. I would like to thank CNPq for the financial support with the PhD scholarship, category GM/GD and process number 11411112020-8.

To FAPESP for the financial support provided through inclusion in the thematic project with process grant number #2016/10636-8.

RESUMO

A demanda constante por processos viáveis que mantenham indicadores ambientais baixos tem sido incessante nas últimas décadas. Em resposta a esses objetivos, a economia circular emergiu, com um dos pilares sendo a reutilização de resíduos em todas as etapas de produção. No contexto da indústria do óleo de soja, a etapa de refino gera um coproduto com potencial significativo para aplicações em biorrefinarias, contribuindo ainda mais para a circularidade da produção e a redução de custos: o destilado da desodorização do óleo de soja (DDOS). As concentrações de ácidos graxos e mono-, di- e triglicerídeos presentes no DDOS tornam-no um candidato promissor para conversão em ésteres por meio de reações com álcoois ou açúcares, produzindo biodiesel ou biossurfactantes. Para que a pesquisa laboratorial seja aplicável em escala industrial, as análises técnico-econômico-ambientais devem indicar a viabilidade econômica do processo e os impactos ambientais. Existem vários estudos relacionados aos dados experimentais da produção de biodiesel. No entanto, eles são mais raros quando se utilizam matérias-primas que não competem com a indústria alimentícia. Da mesma forma, a pesquisa sobre a produção de biossurfactantes com esse tipo de matéria-prima é rara. Contudo, não há estudos que avaliem tais processos a partir de uma análise técnico-econômico-ambiental utilizando o DDOS. Neste contexto, este trabalho teve como objetivo apoiar o desenvolvimento e a escala da produção de biodiesel (ésteres etílicos de ácidos graxos) e biossurfactantes (éster de xilose) por meio de uma avaliação técnico-econômico-ambiental de processos enzimáticos utilizando um subproduto/resíduo de biorrefinarias (DDOS) como fonte de ácidos graxos. Inicialmente, o estudo concentrou-se na esterificação do ácido oleico com xilose utilizando lipase imobilizada, analisando fatores econômicos e ambientais. Usando terc-butanol como solvente, o Preço Mínimo de Venda de Biossurfactantes (PMVB) foi de US$ 72,37/kg com 86% de pureza. Quando se utilizou metil etil cetona e o investimento na purificação aumentou, o PMVB subiu para US$ 392,98/kg com 96% de pureza, adequado para aplicações em indústrias farmacêutica e cosmética. Além disso, a produção enzimática de biodiesel e biossurfactantes utilizando DDOS foi modelada. O biodiesel apresentou um PMVB de US$ 6.15/L e mostrou impactos ambientais inferiores ao método tradicional de produção, como o Potencial de Aquecimento Global em 100 anos (GWP100: 1.55 kg CO_2 eq.), Depleção Abiótica (AD: 27.66 MJ), e Acidificação (AC: $3.35 \cdot 10^{-3}$ kg SO_2 eq.). Três cenários para a produção de biossurfactantes foram avaliados, com PMVBs variando de US$ 5.82/kg a US$ 13.42/kg, dependendo da mistura de solventes. O processo com a razão de solventes tert-butanol: dimetilsulfóxido: água de 6,29:1,86:1,86 em volume apresentou os menores valores para os parâmetros ambientais (GWP100: 1.87 kg CO_2 eq., AD: 18.4 MJ; AC: $5.09 \cdot 10^{-3}$ kg SO_2 eq., EU: $2.54 \cdot 10^{-3}$ kg PO_4 eq.). A pesquisa concluiu que a otimização da mistura de solventes e o uso do DDOS podem agregar valor às biorrefinarias, melhorando a rentabilidade e a sustentabilidade ambiental.

Palavras-chave: Biossurfactantes; Biodiesel; Modelagem e simulação; Destilado da desodorização do óleo de soja (DDOS); Análise técnico-econômico-ambiental.

ABSTRACT

The constant demand for feasible processes maintaining low environmental indicators has been nonstop in recent decades. In response to these goals, the circular economy has emerged, with one of the pillars of coproduct reuse at all stages of production. In the soybean oil industry context, the refining stage produces a residue with significant potential for applications in a biorefinery, further contributing to the circularity of production and the reduction of costs: the soybean oil deodorizer distillate (SODD). The concentrations of fatty acids and mono-, di-, and triglycerides found in SODD make it an exciting prospect as an appealing candidate for conversion into esters through reactions with alcohols or sugars, producing biodiesel or biosurfactants. For laboratory research to be applicable on an industrial scale, techno-economic-environmental analyses must indicate the process's economic viability and environmental impacts. There are several studies related to the experimental data of biodiesel production. However, they are rarer when using raw materials that do not compete with the food industry. Likewise, research into the production of biosurfactants with this type of raw material is rare. Nevertheless, no studies evaluate processes from techno-economic-environmental analysis using SODD. In this context, this work aimed to support the development and scaling of biodiesel (fatty acid ethyl esters) and biosurfactants (fatty acid xylose ester) production by conducting a techno-economic and environmental assessment of enzymatic processes using a subproduct/ residue from biorefineries (SODD) as a material source of fatty acids. Initially, the study focused on the esterification of oleic acid with xylose using immobilized lipase, analyzing economic and environmental factors. Using tert-butanol as a solvent, the Minimum Biosurfactant Selling Price (MBSP) was US$72.37/kg with 86% purity. When methyl ethyl ketone was used instead, and investment in purification increased, the MBSP rose to US$392.98/kg with 96% purity, suitable for pharmaceutical and cosmetic industries. Additionally, enzymatic biodiesel and biosurfactant production using soybean oil deodorizer distillate (SODD) were modeled. The biodiesel had an MBSP of US$6.15/L and showed lower environmental impacts than traditional method, such as Global Warming Potential in 100 years (GWP100: 1.55 kg CO_2 eq.), Abiotic depletion (AD: 27.66 MJ), and Acidification (AC: $3.35 \cdot 10^{-3}$ kg SO_2 eq. Three scenarios for biosurfactant production were evaluated, with MBSPs ranging from US$5.82/kg to US$13.42/kg, depending on the solvent mixture. The process with solvent ratio tert-butanol: dimethyl sulfoxide: water of 6.29:1.86:1.86 in volume presented the lowest values of environmental parameters (GWP100: 1.87 kg CO_2 eq., AD: 18.4 MJ; AC: $5.09 \cdot 10^{-3}$ kg SO_2 eq., EU: $2.54 \cdot 10^{-3}$ kg PO_4 eq.). The research concluded that optimizing solvent mixture and using SODD can add value to biorefineries, improving profitability and environmental sustainability.

Keywords: Biosurfactants; Biodiesel; Modeling and simulation; Soybean oil deodorizer distillate (SODD); Techno-economic-environmental analysis.

SUMMARY

LIST OF FIGURES

CHAPTER 2

CHAPTER 3

CHAPTER 4

CHAPTER 6

LIST OF TABLES

CHAPTER 2

CHAPTER 3

7CHAPTER 4

CHAPTER 6

CHAPTER 1: Theme motivation

1.1 Introduction

In recent years, the challenge of achieving high-efficiency industrial production while minimizing environmental impact has become increasingly prominent. This way, processes are often optimized to enhance energy efficiency, utilize new materials, and reduce environmental consequences. A critical aspect of this effort is the effective management and reuse of by-products generated during processing, a concept central to the circular economy (DE ARAUJO-SILVA et al., 2022; FURLAN et al., 2012; GONÇALVES et al., 2023; VIEIRA et al., 2021; YIN et al., 2016). This approach, which emphasizes waste reuse at all production stages, could lower costs and increase production efficiency (ELDOS et al., 2024; FURLAN et al., 2016; PALUZAR, 2024). In the soybean oil industry context, the refining process generates residues with significant potential for biorefinery applications, further promoting production circularity and inspiring innovations in the industry (BEZERRA et al., 2022; D'AMATO VILLARDI et al., 2017; DE ARAUJO-SILVA et al., 2022; VIEIRA et al., 2021; VISIOLI et al., 2023; XIONG et al., 2022).

During the final stage of refining vegetable oils, particularly soybean oil, distillation removes compounds that contribute to undesirable aromas and flavors. This process involves the injection of direct steam or superheated nitrogen at temperatures between 220 and 260 °C, which varies depending on the oil's characteristics (BEZERRA et al., 2022; HIROTA et al., 2003; MARTINI; NERLI; MALPIEDI, 2022; WATANABE et al., 2004). This results in the formation of Soybean Oil Deodorizer Distillate (SODD), a by-product composed mainly of free fatty acids, mono-, di-, triglycerides, and tocopherols (D'AMATO VILLARDI et al., 2017; LIU; FU; LI, 2019; LV et al., 2021; VIEIRA et al., 2021; XIONG et al., 2022; YIN et al., 2016). SODD, accounting for 0.3% to 0.5% of processed soybean oil, is typically considered waste in the industry due to its lack of direct applications (WANG et al., 2006). In 2023, Brazil produced 10.8 million tons of refined soybean oil, generating approximately 43,200 tons of SODD, with projections indicating that this figure could double by 2030 (BRAZIL GOVERNMENT, 2024).

The diverse composition of SODD makes it a promising candidate for conversion into valuable biomolecules through enzymatic esterification or transesterification processes (VISIOLI et al., 2023; YIN et al., 2017). Potential products include tocopherol, biodiesel, lubricants, and biosurfactants derived from the esterification of acyl glyceride groups in SODD (ATABANI et al., 2012; DE ARAUJO-SILVA et al., 2022; HOSSEINZADEH-BANDBAFHA et al., 2022; LV et al., 2021; PARTOVI et al., 2013; REETU et al., 2023; SANTOS et al., 2024; VIEIRA et al., 2021; YIN et al., 2015, 2016). It opens new possibilities for utilizing it as a raw material in producing esters and other biomolecules, offering a sustainable alternative that does not compete directly with the food industry.

Biodiesel, a widely studied mono-alkyl ester of fatty acids, can commonly be produced through transesterification or esterification in enzymatic processes (BANCHERO; GOZZELINO, 2015; UDEH, 2018). Transesterification involves the reaction of mono-, di-, or triglycerides with low molecular weight alcohols like methanol or ethanol, resulting in a mixture of fatty acid methyl or ethyl esters, which constitutes biodiesel, along with glycerol as a by-product. In esterification, the process occurs in two stages: first, mono-, di-, and triglycerides are hydrolyzed into free fatty acids, and then these acids react with alcohol to produce biodiesel and water. Both processes require the use of catalysts and specific temperature and pressure conditions to be effective. The literature highlights various studies on biodiesel production from SODD (D'AMATO VILLARDI et al., 2017; LI et al., 2015a, 2015b, 2015c; PODDAR; JAGANNATH; ALMANSOORI, 2017; SOUZA et al., 2009; VENKATA SUBHASH; VENKATA MOHAN, 2011; VIEIRA et al., 2021; YIN et al., 2016; ZHENG et al., 2020).

Surfactants are amphiphilic compounds with both hydrophobic and hydrophilic properties. They are widely utilized in pharmaceuticals, cosmetics, and food industries because they reduce surface tension and emulsify and stabilize mixtures (BANAT et al., 2010; PERFUMO; BANAT; MARCHANT, 2018). Biosurfactants, produced through microbiological or enzymatic processes, share these properties but offer additional advantages like biodegradability, thermal stability, and low toxicity. However, their production costs are generally higher than synthetic surfactants (PANDEY et al., 2024; RAOUF et al., 2024). In particular, the enzymatic production of biosurfactants using SODD could be promising. Rich in mono-, di-, triglycerides, and free fatty acids, SODD can be converted into sugar esters through transesterification or hydrolysis followed by esterification. Despite the potential, the literature reports limited research on biosurfactant production from SODD (PARTOVI et al., 2013; VIEIRA et al., 2021).

Regarding the scaling up the production of both biodiesel and biosurfactants, modeling and simulation of these processes are crucially important. It is necessary to describe them mathematically, expand to industrial scales, and calculate the project's fixed and variable costs,

economic viability, and environmental impact indicators (ELIAS et al., 2021; FURLAN et al., 2016; LONGATI et al., 2018). The costs calculated in the economic analysis are divided into capital (CAPEX) and operational (OPEX). CAPEX is given by the cost of the physical plant, with dimensioning of equipment, connections, and electrical installations, among others. OPEX includes reagents, energy, utilities, labor, supervision, and maintenance costs. These cost analysis are based on mass and energy balances from process simulation (TURTON et al., 2009).

The Life Cycle Assessment (LCA) is a method used to calculate the impact of processes on the environment. The leading indicators are abiotic depletion - fossil fuels (AD), global warming potential (GWP100), ozone layer depletion (ODP), human toxicity (HT), freshwater aquatic ecotoxicity (FWAET), marine aquatic ecotoxicity (MAET), terrestrial ecotoxicity (TET), photochemical oxidation (PO), acidification (AC), and eutrophication (EU). They are also based on the mass and energy balances (simulation) (ARU; IKECHUKWU NE, 2018; BACCILE et al., 2017; BIPPUS et al., 2024; BRIÈRE et al., 2018; ELIAS et al., 2021; GUILBOT et al., 2013; HU et al., 2021; KOPSAHELIS et al., 2018; LOKESH et al., 2017).

1.2 Theme choosing

The thesis was based on the research insertion of the BIOENFAPESP Thematic Project (Proc. No. 2016/10636-8) “Da fábrica celular à biorrefinaria integrada biodiesel-bioetanol: uma abordagem sistêmica aplicada a problemas complexos em micro e macroescalas”. The Thematic Project aimed, among other objectives, to seek material and energetic integration of the processes in biorefineries, taking advantage of coproducts /waste and fully utilizing biomass to add value to the production chain.

In this context, the research group of the Enzyme Technology Laboratory of the Department of Chemical Engineering of the Federal University of São Carlos has been researching the use of SODD in the enzymatic production of biomolecules: biodiesel (VIEIRA et al., 2021), biosurfactants (VIEIRA, 2021), and lubricants (DE ARAUJO-SILVA et al., 2022). However, the demand for assessments of applicability on an industrial scale regarding economic and environmental viability is a gap in the area.

As mentioned, Brazil has a massive soybean oil production, with 10.8 million tons in 2023 alone (BRAZIL GOVERNMENT, 2024). It's worth noting that soybeans, among all vegetable oils, have a production that is 15 times greater than palm oil, the second highest in national production (SANTOS et al., 2022). Therefore, SODD is a significant residue for the quantity produced daily. Even so, no studies were found on the reuse of SODD in other processes at an

industrial scale. COCAMAR, a company in the sector, sells this residue to companies in China for low values.

Techno-economic-environmental analysis of enzymatic production routes in biodiesel and biosurfactants (using SODD as raw material) is an unprecedented subject in the literature. Since there is more experimental data on obtaining biodiesel in this context, the focus was on modeling and simulation. On the other hand, in the production of biosurfactants, only PARTOVI et al. (2013) and VIEIRA (2021) highlight some reaction conditions, and therefore experimental tests were associated with this topic in addition to simulations and numerical evaluations.

1.3 Research objectives

1.3.1 General objective

Perform techno-economic-environmental analyses for enzymatic production of esters (biodiesel and biosurfactants) using Soybean Oil Deodorizer Distillate (SODD) as a source of fatty acids.

1.3.2 Specific objectives

i) Perform modeling and simulation for xylose esters production (biosurfactants) using only commercial reagents (oleic acid, xylose, immobilized enzyme, and solvents); for xylose esters production using SODD; for fatty acid ethyl esters production (biodiesel) using SODD.

ii) Evaluate fixed and variable costs for each process plant, analyzing their viability.

iii) Perform a life cycle analysis to understand the environmental impact associated with each process.

1.4 Thesis structure

The following chapters of the thesis describe how the objectives were achieved. The first chapter contains an introduction to the topic, followed by the motivation for the research, the objectives, and the structure of the thesis. The second chapter contains a literature review incorporating principles of systematic mapping, in the format of a scientific article, containing the compositions of different SODDs and the products obtained from them with a description of the experimental conditions applied. The third chapter includes two scientific papers presenting

the methodology initially applied and further developed for the economic and environmental analysis of two simulations of xylose ester production, using only commercial reagents under reaction conditions reported in the literature.. The fourth chapter, also in the format of a scientific article, addresses the analysis of the production of fatty acid ethyl esters, from SODD, with experimental data from literature and also three different conditions for xylose ester production with experimental research. Finally, the fifth chapter includes final considerations and suggestions for future work.

REFERENCES

ARU, O. O.; IKECHUKWU NE, O. Life Cycle Assessment of the Environmental Impact of Biosurfactant Production from Oil Waste by a Diculture of Azotobacter vinelandii and Pseudomonas sp. **Journal of Bioremediation & Biodegradation**, v. 09, n. 03, 2018.

ATABANI, A. E.; SILITONGA, A. S.; BADRUDDIN, I. A.; MAHLIA, T. M. I.; MASJUKI, H. H.; MEKHILEF, S. A comprehensive review on biodiesel as an alternative energy resource and its characteristics. **Renewable and Sustainable Energy Reviews**, 2012.

BACCILE, N. et al. Development of a Cradle-to-Grave Approach for Acetylated Acidic Sophorolipid Biosurfactants. **ACS Sustainable Chemistry & Engineering**, v. 5, n. 1, p. 1186–1198, 3 jan. 2017.

BANAT, I. M. et al. Microbial biosurfactants production, applications and future potential. **Applied Microbiology and Biotechnology**, v. 87, p. 427–444, 2010.

BANCHERO, M.; GOZZELINO, G. Nb2O5-catalyzed kinetics of fatty acids esterification for reactive distillation process simulation. **Chemical Engineering Research and Design**, v. 100, p. 292–301, 1 ago. 2015.

BEZERRA, I. D.; BELISÁRIO, C. M.; FAVARETO, R.; TAHAM, T.; CASTEJON, L. V. Industrially concentrated tocopherols from soybean oil deodorizer distillate. **Brazilian Journal of Food Technology**, v. 25, 2022.

BIPPUS, L. et al. Life cycle assessment for early-stage process optimization of microbial biosurfactant production using kinetic models—a case study on mannosylerythritol lipids (MEL). **Frontiers in Bioengineering and Biotechnology**, v. 12, 23 fev. 2024.

BRAZIL GOVERNMENT. **ABIOVE**. Disponível em: <https://abiove.org.br/estatisticas/>. Accessed on: 20 jul. 2024.

BRIÈRE, R. et al. Life cycle assessment of the production of surface-active alkyl polyglycosides from acid-assisted ball-milled wheat straw compared to the conventional production based on corn-starch. **Green Chemistry**, v. 20, n. 9, p. 2135–2141, 2018.

D'AMATO VILLARDI, H. G.; LEAL, M. F.; DE AZEVEDO ANDRADE, P. H.; PESSOA, F. L. P.; SALGADO, A. M.; DE OLIVEIRA, A. R. G. Catalytic and non-catalytic esterification of soybean oil deodorizer distillate by ethanol: Kinetic modelling. **Chemical Engineering Transactions**, v. 57, p. 1999–2004, 2017.

DE ARAUJO-SILVA, R.; VIEIRA, A. C.; GIORDANO, R. DE C.; FERNANDEZ-LAFUENTE, R.; TARDIOLI, P. W. Enzymatic Synthesis of Fatty Acid Isoamyl Monoesters from Soybean Oil Deodorizer Distillate: A Renewable and Ecofriendly Base Stock for Lubricant Industries. **Molecules**, v. 27, n. 9, 2022.

ELDOS, H. I. et al. Isolation, identification, and characterization of potential biosurfactant-producing bacteria from processing wastewater for the development of eco-friendly green technology. **Bioresource Technology Reports**, v. 25, p. 101763, fev. 2024.

ELIAS, A. M.; LONGATI, A. A.; ELLAMLA, H. R.; FURLAN, F. F.; RIBEIRO, M. P. A.; MARCELINO, P. R. F.; et al. Techno-Economic-Environmental Analysis of Sophorolipid Biosurfactant Production from Sugarcane Bagasse. **Industrial & Engineering Chemistry Research**, v. 60, n. 27, p. 9833–9850, 2021.

FURLAN, F. F.; COSTA, C. B. B.; FONSECA, G. DE C.; SOARES, R. DE P.; SECCHI, A. R.; CRUZ, A. J. G. DA; GIORDANO, R. C. Assessing the production of first and second generation bioethanol from sugarcane through the integration of global optimization and process detailed modeling. **Computers and Chemical Engineering**, v. 43, p. 1–9, 2012.

FURLAN, F. F.; COSTA, C. B. B.; SECCHI, A. R.; WOODLEY, J. M.; GIORDANO, R. C. Retro-Techno-Economic Analysis: Using (Bio)Process Systems Engineering Tools to Attain Process Target Values. **Industrial & Engineering Chemistry Research**, v. 55, n. 37, p. 9865–9872, 2016.

GONÇALVES, M. C. P.; CANSIAn, A. B. M.; TARDIOLI, P. W.; SAVILLE, B. A. Production of sugars from mixed hardwoods for use in the synthesis of sugar fatty acid esters catalyzed by immobilized-stabilized derivatives of Candida antarctica lipase B. **Biofuel, Bioproducts and Biorefining**, v. 17, n. 5, p. 1236–1250, 2023.

GUILBOT, J. et al. Life cycle assessment of surfactants: the case of an alkyl polyglucoside used as a self emulsifier in cosmetics. **Green Chemistry**, v. 15, n. 12, p. 3337, 2013.

HIROTA, Y.; NAGAO, T.; WATANABE, Y.; SUENAGA, M.; NAKAI, S.; KITANO, M.; et al. Fractionation of soybean oil deodorizer distillate (SODD) by molecular distillation a content (wt%). **Journal of the American Oil Chemists' Society**, v. 80, n. 4, p. 341–346, 2003.

HOSSEINZADEH-BANDBAFHA, H. et al. Environmental life cycle assessment of biodiesel production from waste cooking oil: A systematic review. **Renewable and Sustainable Energy Reviews**, v. 161, 1 jun. 2022.

HU, X. et al. Bioconversion of Food Waste to produce Industrial-scale Sophorolipid Syrup and Crystals: dynamic Life Cycle Assessment (dLCA) of Emerging Biotechnologies. **Bioresource Technology**, v. 337, p. 125474, out. 2021.

KOPSAHELIS, A. et al. Gate-to-gate life cycle assessment of biosurfactants and bioplasticizers production via biotechnological exploitation of fats and waste oils. **Journal of Chemical Technology & Biotechnology**, v. 93, n. 10, p. 2833–2841, 23 out. 2018.

LI, L. et al. Efficient mono-acylation of fructose by lipase-catalyzed esterification in ionic liquid co-solvents. **Carbohydrate Research**, v. 416, p. 51–58, 30 out. 2015c.

LI, L. et al. Esterification degree of fructose laurate exerted by Candida antarctica lipase B in organic solvents. **Enzyme and Microbial Technology**, v. 69, p. 46–53, 1 fev. 2015a.

LI, L. et al. Esterification degree of fructose laurate exerted by Candida antarctica lipase B in organic solvents. **Enzyme and Microbial Technology**, v. 69, p. 46–53, 1 fev. 2015b.

LIU, W.; FU, X.; LI, Z. Extraction of tocopherol from soybean oil deodorizer distillate by deep eutectic solvents. **Journal of Oleo Science**, v. 68, n. 10, p. 951–958, 2019.

LOKESH, K. et al. Environmental impact assessment of wheat straw based alkyl polyglucosides produced using novel chemical approaches. **Green Chemistry**, v. 19, n. 18, p. 4380–4395, 2017.

LONGATI, A. A.; LINO, A. R. A.; GIORDANO, R. C.; FURLAN, F. F.; CRUZ, A. J. G. Defining research and development process targets through retro-techno-economic analysis: the sugarcane biorefinery case. **Bioresource Technology**, v. 263, p. 1–9, 2018.

LV, W.; WU, C.; LIN, S.; WANG, X.; WANG, Y. Integrated utilization strategy for soybean oil deodorizer distillate: synergically synthesizing biodiesel and recovering bioactive compounds by a combined enzymatic process and molecular distillation. **ACS Omega**, v. 6, n. 13, p. 9141–9152, 2021.

MARTINI, G.; NERLI, B. B.; MALPIEDI, L. P. A novel method based on saponification coupled to micelle-extraction for recovering valuable bioactive compounds from soybean oil deodorizer distillate. **Food Chemistry**, v. 384, 1 ago. 2022.

PALUZAR, H. Production of high quality biodiesel from sunflower soapstock acid oil as novel feedstock: Catalyzed by immobilized pancreatic lipase. **Journal of the American Oil Chemists' Society**, v. 101, n. 2, p. 251–265, 21 fev. 2024.

PANDEY, R. et al. Glycolipid biosurfactant production and petroleum hydrocarbon degradation by a new strain of Citricoccus zhacaiensis. **Biocatalysis and Agricultural Biotechnology**, v. 59, p. 103248, jul. 2024.

PARTOVI, M.; LOTFABAD, T. B.; ROOSTAAZAD, R.; BAHMAEI, M.; TAYYEBI, S. Management of soybean oil refinery wastes through recycling them for producing biosurfactant using Pseudomonas aeruginosa MR01. **World Journal of Microbiology and Biotechnology**, v. 29, n. 6, p. 1039–1047, 2013.

PERFUMO, A.; BANAT, I. M.; MARCHANT, R. Going Green and Cold: Biosurfactants from Low-Temperature Environments to Biotechnology Applications. **Trends in Biotechnology**, v. 36, n. 3, p. 277-289, 2018.

PODDAR, T.; JAGANNATH, A.; ALMANSOORI, A. Use of reactive distillation in biodiesel production: A simulation-based comparison of energy requirements and profitability indicators. **Applied Energy**, v. 185, p. 985–997, 1 jan. 2017.

RAOUF, S. et al. Screening of sustainable biosurfactant produced by indigenous bacteria isolated from Egyptian oil fields for microbial enhanced oil recovery. **Geoenergy Science and Engineering**, v. 239, p. 212974, ago. 2024.

REETU et al. Latest advances and status analysis of nanomaterials for microalgae photosystem, lipids and biodiesel: A state of art. **Journal of Environmental Chemical Engineering**, v. 11, n. 1, 1 fev. 2023.

SANTOS, A. C.; FERREIRA, P. M.; LOPES, C. L.; BRAGA, M.; VIANA, N. M. Estudo prospectivo de óleos vegetais: o caso da Embrapa Agroenergia [Internet]. Brasília, DF; 2022. Available from: https://ainfo.cnptia.embrapa.br/digital/bitstream/item/232384/1/-DOC41.pdf

SANTOS, B. L. P. et al. Unlocking the potential of biosurfactants: Production, applications, market challenges, and opportunities for agro-industrial waste valorization. **Environmental Research**, v. 244, p. 117879, mar. 2024.

SOUZA, M. S. et al. Biodiesel synthesis via esterification of feedstock with high content of free fatty acids. **Applied Biochemistry and Biotechnology**, v. 154, p.253–267, 2009.

TURTON, R.; BAILIE, R. C.; WHITING, W. B.; SHAEIWITZ, J. A. Analysis, synthesis and design of chemical processes. 3. ed. Upper Saddle River: **Pearson Education**, Inc, 2009. p. 1-1007.

UDEH, B. Bio-waste Transesterification Alternative for Biodiesel Production: A Combined Manipulation of Lipase Enzyme Action and Lignocellulosic Fermented Ethanol. **Asian Journal of Biotechnology and Bioresource Technology**, v. 3, n. 3, p. 1–9, 25 abr. 2018.

VENKATA SUBHASH, G.; VENKATA MOHAN, S. Biodiesel production from isolated oleaginous fungi Aspergillus sp. using corncob waste liquor as a substrate. **Bioresource Technology**, v. 102, n. 19, p. 9286–9290, out. 2011.

VIEIRA, A. C.; CANSIAN, A. B. M.; GUIMARÃES, J. R.; VIEIRA, A. M. S.; FERNANDEZ-LAFUENTE, R.; TARDIOLI, P. W. Performance of liquid eversa on fatty acid ethyl esters production by simultaneous esterification/transesterification of low-to-high acidity feedstocks. **Catalysts**, v. 11, n. 12, 2021.

VIEIRA, A. C. Produção enzimática de compostos de valor agregado a partir do destilado da desodorização do óleo de soja. Thesis. **UFSCar**, São Carlos, SP, Brazil, 2021.

VISIOLI, L. J.; NUNES, A. L. B.; WANCURA, J. H. C.; ENZWEILER, H.; VERNIER, L. J.; DE CASTILHOS, F. Batch and continuous γ-alumina-catalyzed FAME production from soybean oil deodorizer distillate by interesterification. **Fuel**, v. 351, 2023.

WANG, L.; DU, W.; LIU, D.; LI, L.; DAI, N. Lipase-catalyzed biodiesel production from soybean oil deodorizer distillate with absorbent present in tert-butanol system. **Journal of Molecular Catalysis B: Enzymatic**, v. 43, n. 1-4, p. 29-32, 2006.

WATANABE, Y.; NAGAO, T.; HIROTA, Y.; KITANO, M.; SHIMADA, Y. Purification of Tocopherols and Phytosterols by a Two-Step in situ Enzymatic Reaction. Press 339**. JAOCS**, **Journal of the American Oil Chemists' Society,** Vol. 81, no. 4, 2004.

XIONG, Y. W.; GO, A. W.; ALIVIO, R. K. O.; SANTOSO, S. P.; ANGKAWIJAYA, A. E.; SOETAREDJO, F. E. Non-isothermal (trans)esterification of linoleic acid and soybean oil deodorizer distillate with methanol under subcritical conditions. **Renewable Energy**, v. 197, p. 528–544, 2022.

YIN, X. et al. Biodiesel production from soybean oil deodorizer distillate enhanced by counter-current pulsed ultrasound. **Ultrasonics Sonochemistry**, v. 23, p. 53–58, 2015.

YIN, X. et al. Biodiesel production from soybean oil deodorizer distillate using calcined duck eggshell as catalyst. **Energy Conversion and Management**, v. 112, p. 199–207, 2016.

YIN, X. et al. Intensification of biodiesel production using dual-frequency counter-current pulsed ultrasound. **Ultrasonics Sonochemistry**, v. 37, p. 136–143, 2017.

ZHENG, J. et al. Immobilization of Lipozyme TL 100L for methyl esterification of soybean oil deodorizer distillate. **3 Biotech**, v. 10, n. 2, 2020.

CHAPTER 2: Literature review

Unlocking the Potential of Soybean Oil Deodorizer Distillate: A literature review of feedstock characteristics, production methods, and purification techniques

Under submission

2.1 Abstract

Soybean Oil Deodorizer Distillate (SODD) is a byproduct of soybean oil refining, mainly composed of free fatty acids, mono-, di-, and triglycerides, and tocopherols. Due to its rich composition, SODD has the potential to be converted into different value-added bioproducts. This literature review aimed to map the main bioproducts obtained from SODD, as well as the production and purification methods employed. A search in principal databases initially returned 277 articles from Web of Science, Scopus, and Science Direct. After screening and full-text analysis, 38 studies were selected. The mean composition was FFAs (46.30%), triglycerides (20.85%), sterols (11.21%), tocopherols (8.51%), phytosterols (8.27%), stearyl esters (4.83%), diglycerides (4.47%), monoglycerides (2.09%) and squalene (1.63%). The main reported bioproducts were biodiesel (25%), tocopherols (25%), phytosterols (9.1%), squalene (4.5%), lubricants (2.3%), biosurfactants (2.3%), among others. The most used methods were enzymatic esterification/transesterification for ester production and different physics separation/purification techniques for obtaining tocopherols. Statistical tests confirmed good agreement and reproducibility of the article selection. In essence, this review highlights the diverse potential applications of SODD, presenting various analyses and experimental results for numerous bioproducts. Despite these promising prospects, it is essential to emphasize that SODD requires treatment for contaminant removal before its utilization.

Keywords: soybean oil deodorizer distillate; bioproducts; literature review; esterification; purification.

2.2 Introduction

Today's most significant challenges are to combine high-efficiency industrial production with low levels of environmental impact. Therefore, processes are frequently optimized to improve energy efficiency and use new materials while reducing these impacts. In this context, an essential point for achieving such objectives is the destination and reuse of residues/by-products generated during processing (PALUZAR, 2024; DE ARAUJO-SILVA et al. 2022; GONÇALVES et al. 2023; VIEIRA et al. 2021; YIN et al. 2016; FURLAN et al. 2012; HRASTAR et al. 2011;).

Vegetable oils extracted from oilseeds are initially crude and need treatments before consumption. Due to their undesirable color, odor, and contaminants, most crude oils are unsuitable for direct consumption. The oil purification or refining process is a combination of the following process steps (VAN DUIJN, 2023): degumming, a pre-treatment process applied to seed oils to reduce the phosphorus content. It is a two-step process with addition of water and/or acid to hydrate phospholipids (the phospholipids are subsequently being removed by centrifugation); neutralization, whose purpose is to reduce the concentration of free fatty acids to maximum 0.10% with the use of a alkali solution, typically sodium hydroxide (and soapstock can be effectively upgraded with the right processes to add value (LAORETANI et al., 2017); bleaching, whose main purpose is to remove residual soap, pigments and oxidized components (addition of activated carbon in the bleaching process will also reduce the polycyclic aromatic hydrocarbon level, and an acid pre-treatment before bleaching earth addition will improve the removal of phosphorous and/or metals); deodorization, in which, under high vacuum, the oil is heated to 180–240°C and brought in contact with stripping steam to remove volatile components and to create an odorless oil with a bland taste and increased storage stability.

As seen, during the refining of vegetable oils, specifically soybean oil, there is the formation of a by-product from the distillation process, named Soybean Oil Deodorizer Distillate (SODD). SODD is mainly composed of free fatty acids (18 to 80%), mono-, di- and triglycerides (5 to 65%), and tocopherol (2 to 20%) (BEZERRA et al. 2022; XIONG et al. 2022; MARTINI et al. 2022; LV et al. 2021; VIEIRA et al. 2021; LIU et al. 2019; D'AMATO VILLARDI et al. 2017; YIN et al. 2016; HIROTA et al. 2003). In general, distillation is carried out to remove substances that give the oil an undesirable aroma and flavor, including aldehydes, ketones, sterols, unsaturated hydrocarbons, and fatty acids, among others. Direct steam or superheated nitrogen, between 220 and 260 °C, is injected to remove such compounds. This temperature varies according to the quality of the oil and odorants in the process. Subsequently, the volatile compounds pass through condensers and, finally, are collected, generating SODD (SHERAZI; MAHESAR; SIRAJUDDIN, 2016). The SODD generation reaches 0.3 to 0.5% (m/m) of the processed soybean oil, being treated as residue in the industry because it has no direct application

(WANG et al., 2006). According to ABIOVE (2024), refined soybean oil production reached 10.8 million tons in 2023 in Brazil, corresponding to an average of 43,200 tons of SODD per year, with a forecast that this value will double by 2030. It's worth noting that, in Brazil, soybeans have a production that is 15 times greater than palm oil, the second highest in national production (SANTOS et al., 2022). Therefore, SODD is a significant residue for the quantity produced daily. Even so, there are no studies or data where SODD is reused in other processes at industrial levels. Some companies in the sector sell this residue based on tocopherol content. The saponifiable material is typically recovered and utilized as an energy source (through combustion). However, this energy value is not commercially valued. Generally speaking, other potential applications can be limited due to pesticide contamination, dioxane, mineral oils, oxidation byproducts, and color compounds. This way, purification of SODD for contaminate removal is paramount when considering the possibility of other applications.

The concentrations of fatty acids and mono-, di- and triglycerides in SODD make it attractive for conversion into biomolecules through enzymatic processes of esterification/ transesterification of acyl glyceride groups (VISIOLI et al., 2023; YIN et al., 2017). Molecules such as biodiesel (fatty acid methyl and ethyl esters) (ATABANI et al., 2012; REETU et al., 2023; VIEIRA et al., 2021; YIN et al., 2015, 2016), lubricants (fatty acid isoamyl monoesters) (DE ARAUJO-SILVA et al., 2022), and biosurfactants (sugar fatty acid esters) (PARTOVI et al., 2013) can be obtained using SODD as raw material. Furthermore, physical separation/purification processes make it possible to obtain products such as tocopherol (Bezerra et al. 2022; Liu et al. 2019; Kordsmeier et al. 2015; Kasim et al. 2010; Fang et al. 2007), phytosterols (Zhao et al. 2014; Yan et al. 2012; Kasim et al. 2010; Khatoon et al. 2010; Moreira and Baltanás 2004), sterols (GÜÇLÜ-ÜSTÜNDAĞ; TEMELLI, 2007; TORRES et al., 2007), and squalene (CETINBAS; GUMUS-BONACINA; TEKIN, 2022; GUNAWAN; KASIM; JU, 2008) from ODD.

One of the products mentioned, biodiesel, widely reported in the literature, is a mono-alkyl ester of fatty acids that can be obtained through transesterification or esterification processes (BANCHERO; GOZZELINO, 2015). Transesterification occurs through the reaction of mono-, di- or triglycerides with low molecular weight alcohol (usually methanol or ethanol), producing a mixture of methyl (or ethyl) esters of fatty acids, which corresponds to biodiesel, together with glycerol. Esterification occurs in two stages, the first being responsible for hydrolyzing mono-, di- and triglycerides into free fatty acids, and the second for esterifying by reacting them with alcohol to produce biodiesel and water. Both processes require catalysts, besides specific temperature and pressure conditions (PODDAR; JAGANNATH; ALMANSOORI, 2017; VENKATA SUBHASH; VENKATA MOHAN, 2011; VIEIRA et al., 2021; YIN et al., 2016).

Tocopherol (α-, β-, δ- and ɣ-tocopherol), another value-added class of molecules present in DDOS, is commercially called vitamin E. As already mentioned, the price of ODD as a raw material is determined by its tocopherol content, starting at € 0.56 per kg of ODD for 5 wt% tocopherol, with an additional cost of € 0.13 per kg of ODD for each extra percentage of tocopherol (LAORETANI & IRIBARREN, 2014).

There are several characteristics relating to bioactivity in the intake of vitamin E in the human body; they have antioxidant, nephroprotective, neuroprotective, and anti-inflammatory activities, among others. They are used not only in pharmaceutical but also in food industry (SAINI; KEUM, 2016). As they are found in large quantities in SODD, they can be removed by different separation techniques such as saponification (YIN et al., 2017), liquid-liquid extraction (KASIM et al., 2010), supercritical CO2 extraction (LIU; FANG; DING, 2006), and molecular distillation (BEZERRA et al., 2022), among others.

The literature does not frequently cite biosurfactants and lubricants obtained from SODD. Biosurfactants are amphipathic molecules produced by enzymatic (CANSIAN et al., 2022; GONÇALVES et al., 2021b) or microbiological (PARTOVI et al., 2013) routes. They have hydrophobic and hydrophilic regions, reaching emulsification, stabilizing effect, surface tension reduction, and viscosity reduction (DÍAZ DE RIENZO et al., 2015). Furthermore, lubricants from vegetable oils are ester-based and can be enzymatically obtained through transesterification of mono-, di- and triglycerides or esterification of free fatty acids (DE ARAUJO-SILVA et al., 2022).

Based on the SODD composition, this study aims to perform a literature review, incorporating principles of systematic mapping, concerning using soybean oil deodorizer distillate (SODD) to synthesize different bioproducts. Additionally, it explores supposed knowledge gaps and literature findings regarding the use of this by-product.

2.3 Methodology

2.3.1 Literature searching

The design executed for the literature investigation was based on a systematic search in the leading scientific databases using a string that describes the SODD applications (GONÇALVES et al., 2021a, 2023; ROMANELLI et al., 2021).

Web of Science, Scopus, and Science Direct platforms were consulted using the following search string: “oil deodorizer distillate” AND (“bioproduct*” OR “bio*” OR “prod*”) AND (“prod*” OR “sep*” OR “purif*” OR “ext*”). The asterisks indicate that the term can be completed with any string, including plurals and variations of the main words. Furthermore, the terms "AND" and "OR" used in everyday programming logically indicate that the text must cover all terms (for "AND") and at least one of the terms (for "OR"). All papers presented as search results (from year 2000 to year 2024) on each platform had their primary information saved and are presented in Table S1 of the supplementary material.

2.3.2 Database construction

Once the papers resulting from the search were obtained from the platforms, the database needed to be carefully evaluated so that only relevant articles to the topic would be discussed in this review. Following the selection methodology described by (COLLABORATION FOR ENVIRONMENTAL EVIDENCE, 2018), Figure 1 indicates the flow diagram. The first step, "searching", returned 277 articles (database presented in Table S1). Then, by carrying out the "screening" step, the duplicated papers were excluded from the database generating Table S2 (at supplementary material), with 193 papers. Subsequently, these works' title/abstract analysis was performed according to a two-step inclusion criteria:

i. Studies that address the production of bioproducts from ODD and

ii. Studies that address SODD and have purification steps for products.

After title/abstract analysis, we obtained 118 articles sequentially assessed as full text (database available in Table S3). A total of 38 papers were selected after that step (database available in Table S4). Although those 118 articles met the two criteria, some of the 80 works were reviews, and others did not have DOI (Digital Object Identifier).

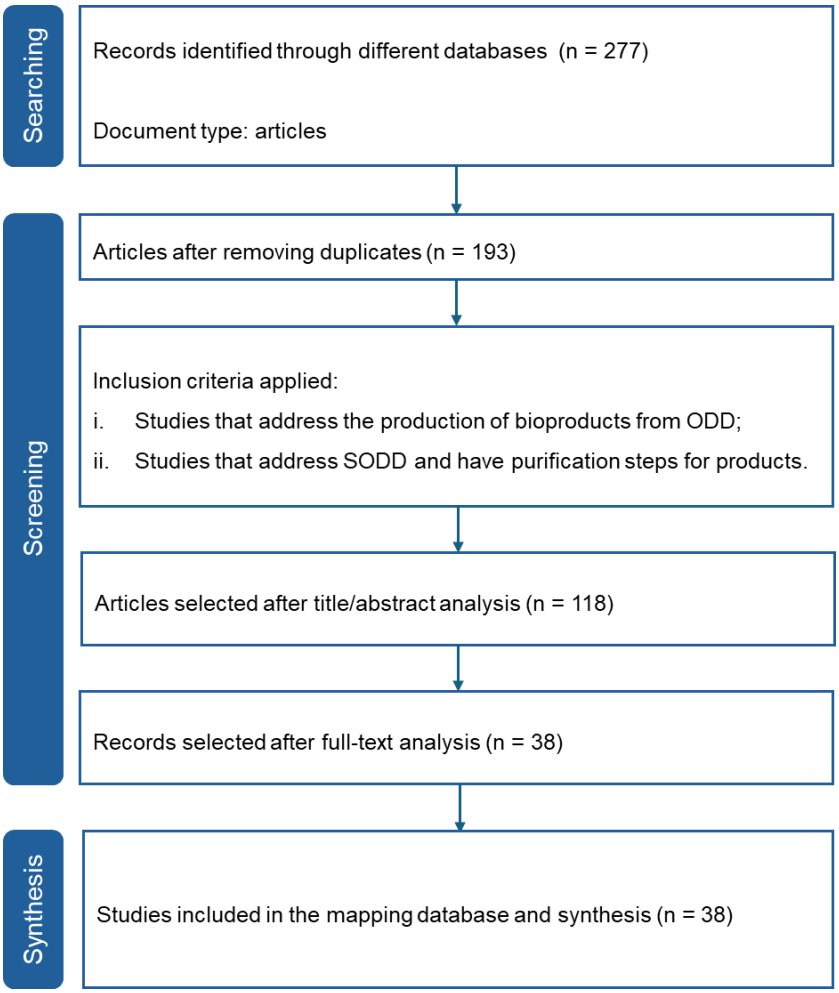

Figure 1. Flow diagram for works selection based on ROSES software.

2.3.3 Statistical tests

The screening steps were performed by the principal author and another coauthor so that the subjective decisions could be analyzed, checking if the hypotheses of disagreement/agreement between the authors are statistically significant. This way, Cohen's kappa statistic is a method that scores the agreement among raters. Essentially, kappa measures the extent to which observed agreement among raters exceeds agreement expected by chance alone. Coefficient kappa (k) can be calculated through Equation 1 (DEVELLIS, 2005). The interpretation of this metric is given in Table 1.

$$k = \frac{f_O - f_E}{N - f_E} \qquad (1)$$

f_O: Number of observed agreements;

f_E: Number of agreements expected by chance;

N: Total number of observations.

Table 1. Interpretation of Cohen's Kappa test. (KUSUMA; SUSONGKO; ARFIANI, 2019)

k	Strength of agreement
< 0.20	Poor
0.21 - 0.40	Fair
0.41 - 0.60	Moderate
0.61 - 0.80	Good
0.81 - 1.00	Very good

Another test that can estimate the reproducibility of this work is McNemar's. A chi-square ($\chi 2$) goodness-of-fit test compares the hypothesis's significant difference in the proportions of disagreement between evaluators under the null hypothesis. The test statistic, which includes a continuity correction and has 1 degree of freedom, is calculated using Equation 2 (KAVZOGLU, 2017; PANIGRAHI et al., 2023).

Null Hypothesis (H_0): The marginal proportions of the discordant pairs are not significantly different from each other, indicating that there is no significant difference between the marginal frequencies.

Alternative Hypothesis (H_1): The marginal proportions of the discordant pairs are significantly different from each other, suggesting that there is a significant difference between the marginal frequencies.

$$\chi^2 = \frac{(|n_{ij} - n_{ji}| - 1)^2}{n_{ij} + n_{ji}} \qquad (2)$$

n_{ij}: Number of articles rejected by author i but accepted by author j;

n_{ji}: Number of articles rejected by author j but accepted by author i.

The chi-square distribution with 1 degree of freedom is used to obtain the p-value corresponding to the calculated test statistic. If it is less than 0.05, the null hypothesis is rejected for a significance level of 95%. However, if the p-value exceeds 0.05, there is insufficient statistical evidence to reject the null hypothesis, in a way that we conclude there is no significant difference in the proportions of disagreement between evaluators for the categories considered. The tests were calculated based on the decisions made by two authors of this article, especially when screening step where n = 193. The Python programming language was used on Google Colab, employing available statistics community libraries.

2.3.4 Data analysis

After selecting the studies, 38 articles were separated for analysis. The data were synthesized to identify and highlight the most pertinent information and key findings related to using soybean oil deodorizer distillate (SODD) to synthesize different bioproducts.

We used the open software VOSviewer® (version 1.6.20) for bibliographic maps, applying co-occurrence analysis for the keywords presented in the papers to relate the bioproducts, reactions, and separation/purification methods. From the database's DOI list, VOSviewer can connect the papers and describe their relation to the main methods using SODD as raw material. The analysis measures the proximity and relation between the articles, identifying if bioproducts are synthesized together at the same process, if purification methods are applied in different works and the correlation between them.

Another software, OriginPro® (version 2024), was used to construct the Figures, and Microsoft® Excel® (version 2403 Build 16.0.17425.20124) was applied to data management.

2.4 Results and Discussion

Vegetable Oil Deodorizer Distillate (VODD) or just ODD can have different origins; they come from different plants. As shown in Figure 1, 277 articles were initially separated, and after removing duplicates, the database presented 193 works. Figure 2 shows the percentage distribution of these articles concerning deodorizer distillate origin. The dataset tells us that almost 50% of the studies report ODD originating from soybeans, while the rest are distributed in the other 50%. Around 10% of the articles do not specify the origin and use the generic term VODD, while another 10% report olive as the source. Intermediate amounts (7 - 8%) originate from palm, rapeseed, and sunflower; amounts less than 5% originate from canola, corn, rice bran, and cotton seed.

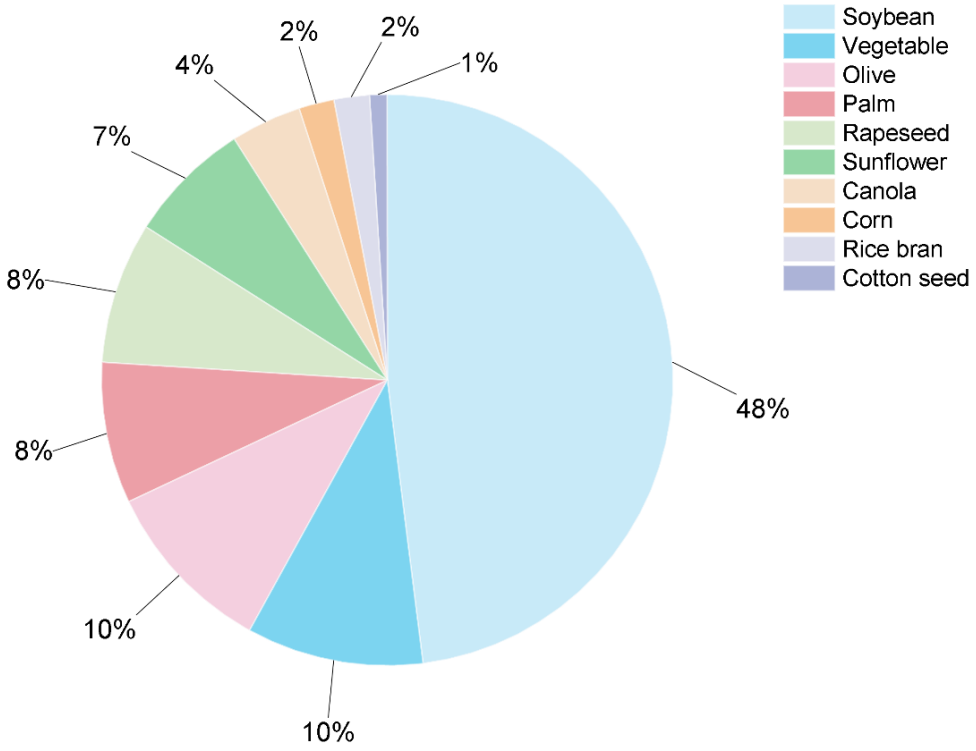

Figure 2. Percentage distribution of works regarding VODD sources.

2.4.1 Statistical tests

The algorithm presented in Figure 3 was written in Python to perform the Kappa and McNemar tests. It initially imports the necessary libraries, then reads the "statistic_test" file (see supplementary material) with each author's decision in the screening stage (yes = 1 and no = 2); the responses are saved in two different vectors for later use.

The kappa test's score is calculated directly from a function in the sklearn library. As seen in Figure 3, the value score is 0.77, which, according to Table 1, indicates a good strength of agreement between the evaluators. For the McNemar test, it is first necessary to construct a contingency matrix counting the divergences and agreements between the authors' responses. From there, a function from statsmodels library calculates the test value and the p-value. As Figure 3 indicates, p-value = 0.503 > 0.05, so there is insufficient statistical evidence to reject the null hypothesis, and there is no significant difference in the proportions of disagreement between authors, which guarantees the reproducibility of the systematic mapping that resulted in the final selection of 38 papers.

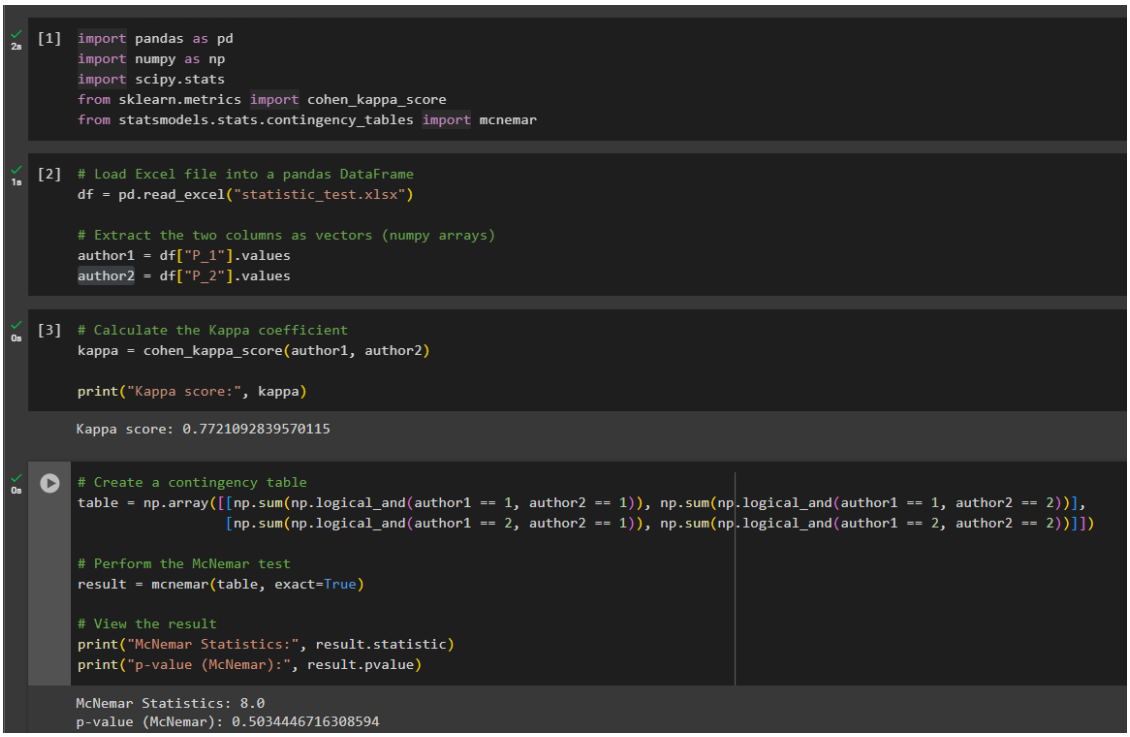

```
[1]  import pandas as pd
     import numpy as np
     import scipy.stats
     from sklearn.metrics import cohen_kappa_score
     from statsmodels.stats.contingency_tables import mcnemar

[2]  # Load Excel file into a pandas DataFrame
     df = pd.read_excel("statistic_test.xlsx")

     # Extract the two columns as vectors (numpy arrays)
     author1 = df["P_1"].values
     author2 = df["P_2"].values

[3]  # Calculate the Kappa coefficient
     kappa = cohen_kappa_score(author1, author2)

     print("Kappa score:", kappa)

     Kappa score: 0.7721092839570115

     # Create a contingency table
     table = np.array([[np.sum(np.logical_and(author1 == 1, author2 == 1)), np.sum(np.logical_and(author1 == 1, author2 == 2))],
                       [np.sum(np.logical_and(author1 == 2, author2 == 1)), np.sum(np.logical_and(author1 == 2, author2 == 2))]])

     # Perform the McNemar test
     result = mcnemar(table, exact=True)

     # View the result
     print("McNemar Statistics:", result.statistic)
     print("p-value (McNemar):", result.pvalue)

     McNemar Statistics: 8.0
     p-value (McNemar): 0.5034446716308594
```

Figure 3. Code for reading article selection data and calculating tests (kappa and McNemar); print screen from colab.

2.4.2 SODD composition

As it is a co-product of soybean oil refining, its composition depends on process conditions and may vary in different industries or regions. Tables 2 and 3 show the compositions of the SODDs made available by the works in our dataset. The components were: Free fatty acids (FFA), triglycerides, diglycerides, monoglycerides, squalene, sterols, Fatty Acid Stearyl Esters (FASE), tocopherols, free phytosterols and other substances in smaller quantities (hydrocarbons, aldehydes, ketones, pesticides, herbicides).

Based on the information in Tables 2 and 3, Table 4 brought the main statistical metrics of the SODD composition. Note that, according to both the main and the median, FFA's are in a higher percentage (18.47 – 79.66%). Then, triglycerides are in second place (0.94 – 69.5%). Sterols come in third place (1.69 – 27.1%). After that, there are Tocopherols (1.83 – 20.1%), followed by free phytosterols (5.36 – 10.32%), fatty acid stearyl esters (1.34 – 7.3%), diglycerides (0.88 – 10.17%), monoglycerides (0.15 – 5.37%), and, finally, squalene (0.55%– 2.82%). Note that if we consider the mono-, di- and triglycerides as a single group of acyl glycerides, it becomes the compound with the second percentage (1.97 – 85.04%).

Table 2. Composition of SODD from different sources (part 1).

SODD Compounds	(KASIM et al., 2010)	(BEZERRA et al., 2022)	(GUNAWAN; KASIM; JU, 2008)	(XIONG et al., 2022)	(LV et al., 2021)	(DE ARAUJO-SILVA et al., 2022; VIEIRA et al., 2021)	(HIROTA et al., 2003)	(MAYUMI ITO et al., 2006; XIONG et al., 2022)
Free fatty acids (FFA)	41.15 ± 0.39	76.61	45.38 ± 2.13	49.57 ± 2.70	44.70	18.47	30.1	53.98 ± 1.47
Triglycerides	5.90 ± 0.01	0.94	18.45 ± 2.20	7.51 ± 0.18	35.00	69.5	9.5	12.09 ± 1.46
Diglycerides	2.44 ± 0.03	0.88	4.85 ± 1.21	10.17 ± 0.26	2.00	4.39	3.5	8.53 ± 1.13
Monoglycerides	0.15 ± 0.01	0.83	-	3.78 ± 0.15	1.00	1.38	-	5.37 ± 0.19
Squalene	1.17 ± 0.13	0.55	1.83 ± 0.05	1.86 ± 0.04	1.55 ± 0.05	-	-	-
Sterols	9.75 ± 0.012	1.69	-	-	-	-	-	-
fatty acid stearyl esters	6.76 ± 0.08	1.34	3.91 ± 0.39	-	-	-	12.8	-
Tocopherols	9.13 ± 0.28	3.00	6.40 ± 0.85	5.26	6.85	1.83	10.4	4.06 ± 0.54
Free phytosterols	9.75 ± 0.12	-	5.36 ± 0.19	6.11 ± 0.3	-	-	10.3	-
Others*	23.54 ± 0.84	14.16	15.23 ± 0.16	28.96 ± 2.99	8.90 ± 0.20	4.43	19.3	20.03

*: Hydrocarbons, aldehydes, ketones, pesticides, herbicides etc.

Table 3. Composition of SODD from different sources (part 2).

SODD Compounds (%)	(TORRES et al., 2007, 2009)	(FANG et al., 2007)	(KHATOON; RAJAN; KRISHNA, 2010)	(D'AMATO VILLARDI et al., 2017)	(LIU; FANG; DING, 2006)	(SHIMADA et al., 2000)	(YIN et al., 2015, 2016)	(WATANABE et al., 2004)	(MARTINS et al., 2006)
Free fatty acids (FFA)	19.8	48.10	22.7 ± 0.3	79.66	31.53	66.3	53.8 ± 1.07	47.4	57.80 ± 1.2
Triglycerides	21.1	27.20	65.5± 2.0	-	-	-	28.53 ± 0.57	4.8	-
Diglycerides				-	-	-	-	3.5	-
Monoglycerides				-	-	4.1	-	-	-
Squalene	-	-	-	2.82	-	-	-	-	-
Sterols	27.1	9.45	-	10.25	7.11	13.1	-	-	-
fatty acid stearyl esters	7.3	-	-	-	-	-	-	-	-
Tocopherols	20.1	9.23	2.26 ± 0.020	7.27	7.67	16.5	-	17.2	8.97
Free phytosterols	-	-	7.80 ± 1.60	-	-	-	10.32 ± 0.35	-	-
Others*	4.5	6.02	-	-	26.25	-	7.35 ± 0.30	30.6	-

*: Hydrocarbons, aldehydes, ketones, pesticides, herbicides etc.

Table 4. Statistical metrics to SODD composition.

SODD Compounds (%)	Mean	Minimum	Maximum	Median	Mean deviation
Free fatty acids (FFA)	46.30	18.47	79.66	47.4	13.71
Triglycerides	20.85	0.94	69.5	15.27	14.14
Diglycerides	4.47	0.88	10.17	3.5	2.25
Monoglycerides	2.09	0.15	5.37	1.19	1.66
Squalene	1.63	0.55	2.82	1.69	0.54
Sterols	11.21	1.69	27.1	9.75	5.08
fatty acid stearyl esters	4.83	1.34	7.3	5.335	2.20
Tocopherols	8.51	1.83	20.1	7.47	4.00
Free phytosterols	8.27	5.36	10.32	8.775	1.85
Others	16.10	4.43	30.6	15.23	8.01

FFA is the compound present in the most significant quantity in SODD, and its composition also varies from one source to another. The articles that describe the composition of fatty acids in SODD are in Figure 4. Among the acids mentioned, linoleic acid appears in greater quantities in almost all studies, followed by oleic acid and then palmitic acid.

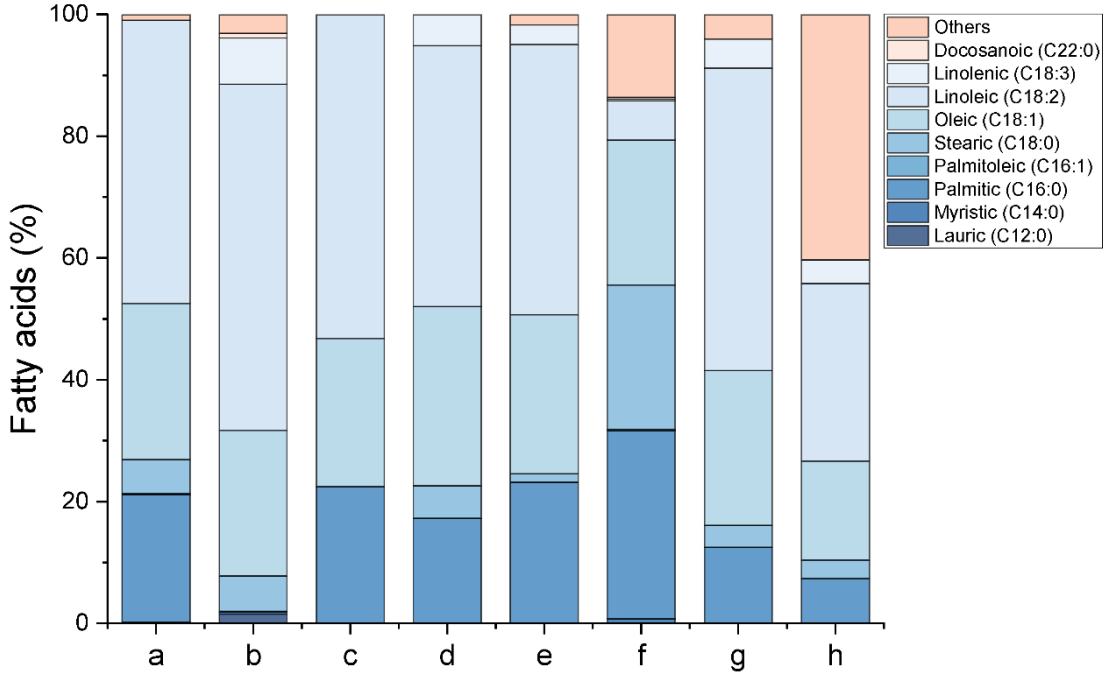

Figure 4. Percentage of Free Fatty Acids (FFA) in SODD; a: (XIONG et al., 2022); b: (LV et al., 2021); c: (D'AMATO VILLARDI et al., 2017); d: (VIEIRA et al., 2021); e: (KHATOON; RAJAN; KRISHNA, 2010); f: (SOUZA et al., 2009); g: (VERNIER et al., 2022); h: (SHIMADA et al., 2000).

Tocopherol is another important compound in SODD, popularly called vitamin E and has added market value in the pharmaceutical and food industries. It is composed of α-, β-, γ- and δ-tocopherol. Some works describe these components' partial or complete composition, and Table 5 summarizes this information. The share of γ-tocopherol is the largest ranging from 1.01 – 11.4%, followed by δ-tocopherol in the range of 0.36 – 5.69%, then α-tocopherol from 0.37 – 2.91% and, finally, β-tocopherol from 0.09 – 1.81%.

Table 5. Tocopherol composition.

Tocopherols	(LIU; FU; LI, 2019)	(MARTINS et al., 2006)	(XIONG et al., 2022)	(LV et al., 2021)	(VIEIRA et al., 2021)	(KASIM et al., 2010)	(WATANABE et al., 2004)	(SHIMADA et al., 2000)	(MARTINS et al., 2006)
α-tocopherol	0.83 ± 0.02	2.91 ± 0.29	0.82 ± 0.06	0.54 ± 0.00	0.37 ± 0.001	0.90 ± 0.10	1.5	2.3	1.41 ± 0.25
β-tocopherol	-	0.14 ± 0.07	-	1.81 ± 0.10	0.09 ± 0.005	-	-	-	0.12 ± 0.05
γ-tocopherol	6.84 ± 0.15	4.66 ± 0.19	1.86 ± 0.04	2.57 ± 0.02	1.01 ± 0.003	5.81 ± 0.01	11.4	9.9	1.95 ± 0.15
δ-tocopherol	5.69 ± 0.11	1.25 ± 0.08	2.58 ± 0.01	1.93 ± 0.03	0.36 ± 0.003	2.41 ± 0.17	4.3	4.3	0.58 ± 0.09

2.4.3 Contaminant removal

The results of this literature search concern different applications for SODD, bringing analysis and experiments for many bioproducts. Although these perspectives sound very promising, it is important to note that ODD needs treatment for contaminant removal before being utilized.

Since ODD results from the vegetable oil purification process, it contains contaminants previously in the oil. Among these, the most common are pesticides, polycyclic aromatic hydrocarbons, hydrocarbons of mineral origin, dioxins, furans, and dioxin-like PCBs (VAN DUIJN, 2016).

Throughout oil refining, pesticides in crude oil can be eliminated in several ways. They may be extracted with soap during neutralization, adsorbed by bleaching earth or activated carbon during bleaching, carried away by steam, condensed in fatty acids or cooling water, or released into the air as vapor during deodorization (VAN DUIJN, 2008). Still, a large portion of pesticides can end up in the ODD, making it necessary to remove them.

Regarding mineral oil hydrocarbons (MOH), they can mainly be present in extracted edible oils due to contamination during processing (lubricants and hydraulic oils). Contamination levels of oils and fats with MOH should be as low as reasonably achievable. This can be ensured by supply chain auditing and by setting customer limits (VAN DUIJN, 2023). Besides, different technologies and methods can be employed to remove hydrocarbon. For example, JU et al. (2012) managed to remove and identify hydrocarbons using modified Soxhlet extraction, followed by two chromatography methods (modified and classical preparative). This study demonstrated a procedure for purifying and identifying structures of hydrocarbons from SODD. Additionally, the findings on mineral oil contamination in SODD can be applied to various oil-based products. On the other side, GONG & WU (2024a) tested three graphene-based composites for the absorption of polycyclic aromatic hydrocarbons, including one with titanium dioxide, one with sepiolite, and one with iron oxide. The results showed that titanium dioxide-graphene achieved the highest removal rate. In turn, GONG & WU (2024b) used *E. coli* with rot fungus to degrade hydrocarbons. The findings revealed that polycyclic aromatic hydrocarbons degradation in ODD reached 59.28% when E. coli was engineered to express genes responsible for electron transfer, facilitating the breakdown process.

Several studies mention the purification of contaminants after obtaining the desired bioproducts. MEYER et al. (2011) reports the removal of traces of pesticides in the recovered polyphenols; SILVA et al (2012) managed to remove free fatty acids, hydrocarbons, herbicides, and residual pesticides by applying vacuum at the end of the transesterification reaction. TEIXEIRA et al. (2011) removed pesticides from ODD using membrane-based separation

processes after an enzymatic esterification reaction. The production of steryl esters enables the efficient removal of pesticides from the reaction product through nanofiltration. This efficiency is due to the significant difference in molecular weight between steryl esters (650–800 Da) and pesticides (150–420 Da), allowing nanofiltration membranes to selectively retain the larger steryl ester molecules while permitting the smaller pesticide molecules to pass through (TEIXEIRA et al. 2011). On the other hand, TEIXEIRA et al. (2014) investigated the removal of pesticides by diananofiltration process. This study explored solvent-resistant nanofiltration (SRNF) for the purification of products from deodorizer distillates, identifying three effective membranes: GMT-oNF2 (Borsig/GMT), PuraMemS600 (Evonik), and 030306F (Solsep). All membranes achieved high steryl ester retention (≥96%) while allowing the removal of pesticides (≤65%). The choice of solvent—hexane, ethanol, or oleic acid—significantly influenced membrane performance, with permeability strongly linked to solvent–membrane interactions. Operating in crossflow mode and optimizing process conditions, such as feed concentration and transmembrane pressure, further improved separation efficiency.

It is important to emphasize that all use of ODD, specifically SODD, must be careful with contaminant levels. Therefore, treatment processes aimed at removing them are essential. This is especially true when it comes to food or pharmaceutical-grade products.

2.4.4 Bioproducts from SODD

Before discussing the bioproducts generated using SODD as a raw material, it is worth highlighting that the analyzed initial dataset contains works from 2000 – 2024. The distribution of selected works overtime is shown in Figure 5. It is noticed that the most significant number of papers is located between 2005 – 2010 and 2020 – 2023.

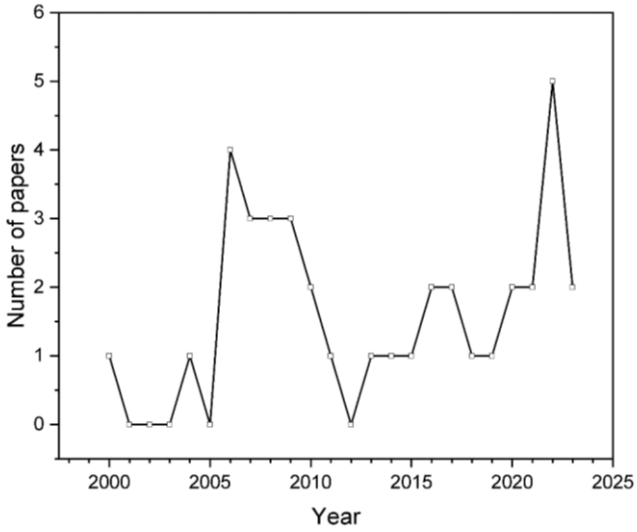

Figure 5. Papers distribution in time.

From the dataset, it was possible to identify the following products generated or purified from SODD: tocopherol, biodiesel, phytosterols, FFA, methyl and ethyl esters, scalene, fatty acids (stearyl and ethyl) esters, glycerides, phytosterols and sterol esters, and biosurfactants. Figure 6 shows the percentages of representation of these works in total. Biodiesel and tocopherol are the bioproducts most explored in the literature.

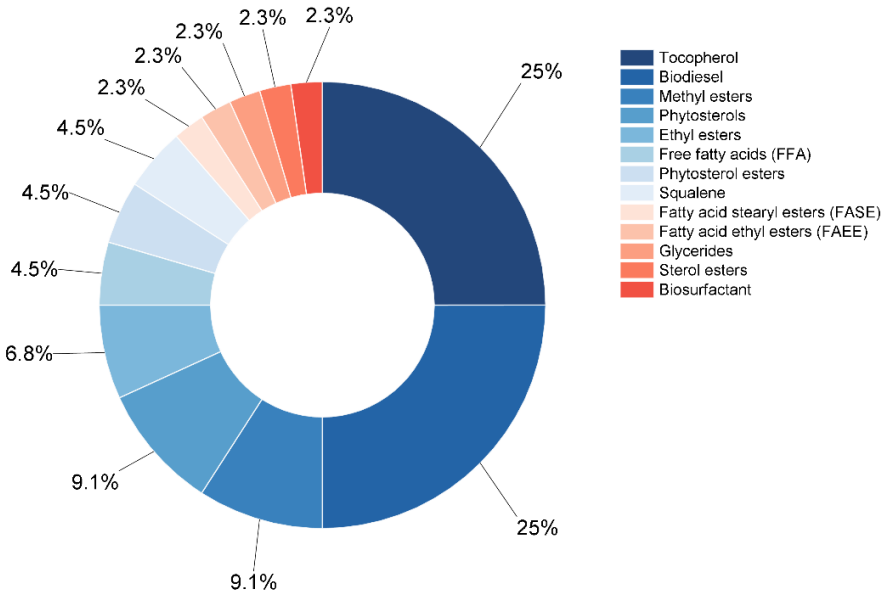

Figure 6. Percentage bioproducts from SODD.

2.4.5 Tocopherol

Between the products obtained or purified from SODD, tocopherol is the most explored in literature. Table 6 shows the primary methodologies for purifying tocopherol, sometimes consisting of a single step or several. Molecular distillation is the most used method within the works evaluated. It consists of a distillation of high molecular weight molecules, with a short path and high vacuum, occurring in a thin layer (LIU; FU; LI, 2019). Its main advantages are the degree of purity obtained and the prevention of decomposition of tocopherols when exposed to high temperatures, oxygen, and light. The disadvantage is the temperature gradient necessary to form a thin boiling layer since the tocopherol concentration changes throughout the process. As a result, the equipment becomes more complex to design and operate (BEZERRA et al., 2022; LUTIŠAN; CVENGROŠ; MICOV, 2002; MARTINS et al., 2006; MAYUMI ITO et al., 2006).

Another usual method for purifying tocopherol is the combination of chemical reactions with several processes. For instance, enzymatic esterification of FFA accompanied by distillation (WATANABE et al., 2004); saponification followed by micelle-extraction (MARTINI; NERLI; MALPIEDI, 2022); acid esterification combined with deacidification, methanolysis,

crystallization, filtration, extraction with supercritical carbon dioxide and distillation (SHI et al., 2011); and also saponification after soxhlet extraction which carries out a liquid-liquid extraction (KASIM et al., 2010). As seen in the fourth column of Table 6, the highest tocopherol degree of purity was obtained by (SHI et al., 2011) (the work with the largest set of steps), reaching 95% mass concentration despite its median recovery efficiency (~55%).

Well-known methods such as liquid-liquid extraction, chromatography, supercritical carbon dioxide, and centrifugation are also used to obtain tocopherol. Chromatography showed lower recovery efficiency 35.21% (α-tocopherol), 36.25% (γ-tocopherol) and 61.25% (δ-tocopherol) with a concentration of 92.35% (α-tocopherol), 91.23% (γ-tocopherol) and 89.95 % (δ-tocopherol) (WAN et al., 2008). At the same time, the lowest concentration was obtained by centrifugal molecular distillation, with 7.7% tocopherol and 90% recovery (MAYUMI ITO et al., 2006). Finally, (WATANABE et al., 2004) achieved a recovery efficiency of 89.6% with 76.4% tocopherol concentration, balancing both variables. Therefore, it is safe to conclude that the works composed by a sequence of treatments yield a purer tocopherol, but some of it is lost. Then, the choice of the process for obtaining this product must be oriented towards the objective and applicability.

Table 6. Main methods for tocopherol recovery.

Main method	**Equipment**	**Recovery efficiency**	**Tocopherol concentration (w/w)**	**Authors**
Enzymatic esterification and distillation	agitated reactor, distillatory vessel	<75%	65 %	(SHIMADA et al., 2000)
Two-step in situ enzymatic esterification, distillation	agitated reactor, distillatory vessel	89.6%	76.4%	(WATANABE et al., 2004)
Centrifugal molecular distillation	centrifugal molecular still	90%	7.7%	(MAYUMI ITO et al., 2006)
Molecular distillation	molecular distillatory vessel with vacuum system and agitation	81.23%	18.3%	(MARTINS et al., 2006)
Supercritical carbon dioxide	fractionation column	81.5%	57.1%	(FANG et al., 2007)

Chromatography	low pressure chromatography column	35.21% (α-tocopherol), 36.25% (γ-tocopherol) and 61.25% (δ-tocopherol)	92.35% (α-tocopherol), 91.23% (γ-tocopherol) and 89.95% (δ-tocopherol)	(WAN et al., 2008)
Soxhlet extraction, cold saponification, and liquid-liquid extraction	modified soxhlet extractor, agitated reactor, extractor balloon	94%	38.1%	(KASIM et al., 2010)
Two-step esterification, deacidification, methanolysis, crystallization, filtration, dual column supercritical carbon dioxide extraction-distillation	extraction-distillation dual column	55%	95%	(SHI et al., 2011)
Liquid-liquid extraction	ultrasonic vortex, centrifuge, rotary evaporator	77.6%	10.4%	(LIU; FU; LI, 2019)
Saponification, micelle-extraction	agitated reactor, mixed micellar systems	~100% (α- and δ-tocopherol), ~90% (γ-tocopherol)	11.0%	(MARTINI; NERLI; MALPIEDI, 2022)
Molecular distillation	patent conception	88.3%	15.8%	(BEZERRA et al., 2022)

2.4.6 Biodiesel (including methyl and ethyl esters)

As already mentioned, biodiesel is a mono-alkyl ester of fatty acids obtained through transesterification or esterification processes (MAZUBERT; POUX; AUBIN, 2013). Transesterification is a chemical process where mono-, di-, or triglycerides react with a low molecular weight alcohol, typically methanol or ethanol. This reaction yields a combination of fatty acid methyl or ethyl esters—commonly known as biodiesel—and glycerol. On the other hand, esterification unfolds in two phases: initially, mono-, di-, and triglycerides are hydrolyzed into free fatty acids; subsequently, these acids are esterified by combining them with alcohol, resulting in the production of biodiesel and water (PODDAR; JAGANNATH; ALMANSOORI, 2017).

Biodiesel from SODD is reported in 25% of the dataset, although the other 15% show the production of methyl and ethyl esters. Notice that we separate the nomenclature according to the authors of the works, though they all represent molecules present in biodiesel. Although all studies report the production of these molecules using SODD as a raw material (vide Table 7), some use a mixture with FFA, enriching this material and directly interfering with the kinetics and conversion. (YIN et al., 2016, 2017) report SODD pre-esterification processes but do not specify the experimental conditions; they only indicate the composition of the pre-esterified materials and the addition of FFAs to these reagents, reaching 94.6 % and 96.3% esterification conversions, respectively.

An esterification pre-treatment is reported by (YIN et al., 2015), followed by transesterification, both with chemical catalysis, achieving conversion of 96.1%. On other hand, (VIEIRA et al., 2021) indicates hydrolysis as pre-treatment followed by enzymatic esterification with 86.56% conversion. Although the two stages of chemical catalysis indicate ample conversion, hydrolysis catalysis followed by enzymatic esterification allows milder process conditions without acids in the medium that requires more complex and resistant equipment.

Single-step processes also present high conversions, as in (D'AMATO VILLARDI et al., 2017) – 99.7%, which uses chemical catalysis, and (ZHENG et al., 2020) – 98%, using enzymatic catalysis. However, some other points must be observed as they can contribute to reduce operational costs of the process, by means of lower molar ratio of reagents: (VERNIER et al., 2022) – 1:1, (VISIOLI et al., 2023) – 1.5:1, and (LV et al., 2021) – 1:2; mild process temperatures: (YIN et al., 2015, 2017) – 25ºC, (LV et al., 2021; VIEIRA et al., 2021) – 35ºC, and (WANG et al., 2006) – 40ºC; and reduced reaction time (VERNIER et al., 2022) – 10 min, (VISIOLI et al., 2016) – 20 min, and (YIN et al., 2017) – 30 min. However, minimizing all these variables will not necessarily be possible and rather an optimized balance focusing on the project objective must be taken into account.

Table 7. Main methods of biodiesel production.

	Main reaction				
Pre-treatment	**Catalyst**	**Proportion of reactants**	**Reaction conditions**	**Time/ Conversion**	**Authors**
-	3% lipozyme TL IM and 2% novozym 435 based on the oil weight	3.9:1(methanol/oil molar ratio), 80wt% tert-butanol	150 rpm 40 ºC	24 h 97%	(WANG et al., 2006)
-	4wt% novozym 435	3.9:1 (methanol to SODD molar ratio)	150 rpm 40 ºC	10 h 95%	(DU; WANG; LIU, 2007)
-	3 wt.% novozym 435	4:1 (g SODD: g ethanol)	50 ºC	90 min 83.5%	(SOUZA et al., 2009)
1.5% H_2SO_4 (v/w), 120 min, 12:1 (methanol/oil molar ratio), 60 °C	25% anhydrous sodium sulfate	10:1 (methanol to triglyceride molar ratio)	25 ºC	50 min 96.1%	(YIN et al., 2015)
pre-esterification	10wt% calcined duck eggshell	10:1(methanol to oil ratio – FFA + SODD)	60 ºC	80 min 94.6%	(YIN et al., 2016)
-	pressurized ethanol	7:1 (ethanol to FFA molar ratio)	20 MPa 275 ºC	20 min 87%	(VISIOLI et al., 2016)
pre-esterification	1.8wt% NaOH	8:1 (triglyceride to methanol molar ratio) FFA + SODD	20/28 kHz ultrasound 25 ºC	30 min 96.3%	(YIN et al., 2017)
-	3wt% sulfuric acid	10:1 (ethanol to SODD molar ratio)	100 ºC	3 h 99.7%	(D'AMATO VILLARDI et al., 2017)
-	lipozyme TL 100L on macroporous resin NKA	10 g of SODD, 5 mL of t-butanol, 4 mL of methanol, 0.5 g of enzyme	550 rpm 50 °C	8 h 98%	(ZHENG et al., 2020)

hydrolysis (4:1 water: SODD mass ratio)	8.36 wt.% liquid eversa	3.64:1 (ethanol:SODD molar ratio)	200 rpm 35 ºC	23 h 86.56 %	(VIEIRA et al., 2021)
-	self-prepared immobilized lipase MAS1-H108A (enzyme loading of 35 U/g SODD)	molar ratio of 1:2 (oil/methanol)	35 °C	24 h 97.08%	(LV et al., 2021)
-	-	FFA (25%, 50%, 90%) + SODD solvent-to-fatty acid ratio (1.5 mL/g) methanol	0 - 300 rpm 30–245 ◦C	100 min 87–89%	(XIONG et al., 2022)
-	-	1:1 (methyl acetate: SODD molar ratio)	20 kHz ultrasound 300 ºC	10 min 87.7%	(VERNIER et al., 2022)
-	0.70wt% γ-alumina	1.5:1 (methyl acetate: SODD)	300ºC	4 h 90.2%	(VISIOLI et al., 2023)

2.4.7 Other products

Sterol is a steroid molecule linked to alcohol, which has essential biological functions in animals, acting on hormonal function and immunity. Phytosterols are the sterols present in plants. Also produced by plants, squalene is an organic compound, a triterpene. When used in human alimentation, these compounds act as anti-inflammatory, antioxidant, antidiabetic, and antiatherosclerotic agents. In this context, the application of these compounds in the food and cosmetics industry is vast (FERRER et al., 2017; LOU-BONAFONTE et al., 2018; SALEHI et al., 2021).

Table 8 presents the main purification methods for obtaining phytosterols and squalene. The recovery techniques are very similar to the methods already described for tocopherol. (KASIM et al., 2010; WATANABE et al., 2004) are already mentioned in Table 6 since more than one product was obtained concomitantly.

Table 8. Main methods for phytosterols and squalene.

	Main method	**Recovery efficiency**	**Products concentration**	**Authors**
Phytosterols	Fermentation (*Candida tropicalis* 1253)	No significant loss	15.2 to 28.43 %	(ZHAO; HU; ZHAO, 2014)
	Alkali treatment, crystallization and organic solvent extraction	74.6%	87%	(KHATOON; RAJAN; KRISHNA, 2010)
	Soxhlet extraction, cold saponification, and liquid-liquid extraction	94%	55.51%	(KASIM et al., 2010)
	Two-step in situ enzymatic esterification, distillation	86.3%	97.2%	(WATANABE et al., 2004)
Squalene	Soxhlet and liquid-liquid extraction	-	1.83 to 6.29%	(GUNAWAN; KASIM; JU, 2008)
	Macroporous resin and thin-film evaporation, distillation	76.5%	98.5%	(YANG et al., 2020)

Crystallization, one of the methods presented in Table 8, occurs with solid particles forming from specific conditions of supersaturation or refrigeration, generating organized geometries, periodic arrangement of atoms, and named crystals. It is widely used in product purification stages in the food and pharmaceutical industries at purification steps (MULLIN, 2002). The driving force behind crystallization is the decrease in the system's free energy, which can be achieved by reducing the temperature, increasing the concentration, or altering the solvent

composition (MYERSON, 2019). This process involves two main steps: nucleation and crystal growth. Nucleation forms a small cluster of atoms or molecules that serves as a template for further crystal growth (KASHCHIEV, 2000). Once a stable nucleus is formed, crystal growth proceeds by adding atoms or molecules to the crystal surface. The growth rate depends on various factors, such as already mentioned, supersaturation, temperature, and impurities (DAVEY; GARSIDE, 2000). Controlling the crystallization process is essential for obtaining crystals with desired properties, such as size, shape, and purity. Various techniques have been developed to optimize crystallization conditions, including solvent selection, temperature control, and additives (TUNG et al., 2009). (KHATOON; RAJAN; KRISHNA, 2010) applied the crystallization on SODD to recover phytosterols, based on two patents that use this method to obtain sterols from deodorizer sludge and the like. The first, (WINTON AND SMITH, 1964), uses a methanol-water mixture with a concentration of about 5-10% by weight at 4°C for 24 hours to guarantee a maximum recovery of sterols. The other one, (SMITH, 1967), after an esterification reaction, add water in 5-60% in a temperature range of 0°C to 40ºC, crystallizing the sterols.

Adsorption on macroporous resin is a thermodynamically investigated method for purifying squalene from SODD (YANG et al., 2020). Macroporous resins have recently gained considerable interest due to their extensive use in various purification processes (WU et al., 2024; XUE et al., 2024; ZHANG; GONG; QU, 2024). These resins are characterized by their large pore sizes, high surface area, and excellent mechanical and chemical stability, making them suitable for separating and purifying a wide range of compounds (SUN; YANG, 2003; ZHANG et al., 2018). Despite the existence of numerous thoroughly studied technologies for purification, adsorption processes that utilize macroporous resins have gained heightened interest due to their distinctive adsorption characteristics and benefits such as reduced operational costs, decreased solvent usage, minimal presence residues in the final product, and the availability of commercially produced resins with diverse pore structures and internal surface areas (LI; CHASE, 2010).

Table 9 presents other products obtained from SODD. Esters of phytosterol, sterol, and stearyl have applications in food and cosmetic industries (FORNARI et al., 2009; GUNAWAN; FABIAN; JU, 2008; TORRES et al., 2007, 2009) since they have health-promoting uses such as reducing cholesterol and cardiovascular diseases (KORBER; KLEIN; DAUM, 2017; MOREAU et al., 2018; SENGUPTA; GHOSH, 2015). As seen in Table 9, some processes to obtain these esters from SODD are applying enzymatic reactions followed by extractions, while others combine just physics steps.

Table 9. Main methods for different esters and FFAs.

	Step 1	**Step conditions**	**Step 2**	**Step conditions**	**Purification/ Products concentration**	**Authors**
Phytosterol esters	Reaction with *candida rugosa* lipase liquid	10 wt-% of lipase, 200 rpm) at 35 ºC, 24h	Reaction with Novozym 435	10 wt-% of ethanol, 5 wt-% of Novozym 435, and 8 wt-% of hexadecane, 35 ºC, 24h	supercritical carbon dioxide and isothermal countercurrent column/ 82.4 %	(TORRES et al., 2009)
	-	-	Supercritical carbon dioxide extraction	Temperature at 328 K, pressures ranging from 200 to 280 bar and solvent-to-feed ratio around 25	94.2%	(FORNARI et al., 2009)
Sterol esters	Reaction with *candida rugosa* lipase liquid	10% of lipase, SODD mixed with oleic acid 200 rpm 35º C 24 h	Reaction with Novozym 435	OSODD 5% (w/w) of Novozym 435 200 rpm 35º C 24 h	-	(TORRES et al., 2007)
Stearyl esters	-	-	Modified soxhlet extraction, modified silica gel column chromatography and binary solvent extraction	-	86.74%	(GUNAWAN; FABIAN; JU, 2008)
Fatty Acid Isoamyl Monoesters	Reaction with *Eversa transform* immobilized	1:2.5 (fatty acids - based on the SODD to isoamyl alcohol molar ratio), 45 ◦C, and 6	Chromatographic analysis	-	70%	(DE ARAUJO-SILVA et al., 2022)

		wt.% enzymes 50h				
Biosurfactant	Fermentation with *Pseudomonas aeruginosa*	SOM culture medium, 30 °C, 200 rpm for 240 h	-	-	54.81%	(PARTOVI et al., 2013)
FFAs	multiple stages molecular distillation	-	-	-	95.8%	(LAORETANI; IRIBARREN, 2018)

Moreover, fatty acid isoamyl monoesters are bio-lubricants (DE ARAUJO-SILVA et al., 2022) obtained by enzymatic route (details in Table 9). obtained by enzymatic route (details in Table 9). The main advantage of obtaining lubricants from the modification of vegetable oils or residues of these oils is the reduction of the raw material used in this process, which is more than 90% petroleum-based (CECILIA et al., 2020). These formulations are non-renewable and toxic, riskng the human health and the environment owing to their low biodegradability and high toxicity. On the other hand, bio-lubricants, which are more readily biodegradable, have a lesser environmental impact despite also being reported to discharge contaminants into air, soil, and drinking water (SCHNEIDER, 2006).

Biosurfactants, specially obtained from SODD as bio-lubricants, are another product little discussed in the literature, according to our dataset. Table 9 demonstrates that fermentation can form them, producing the rhamnolipids class (PARTOVI et al., 2013). Biosurfactants are biomolecules obtained through microbiological or enzymatic routes as an alternative to chemical surfactants since the search for sustainability is becoming a more frequent industrial care subject (CERVELLON; CAREY, 2011; DRAKONTIS; AMIN, 2020). In the detergents industry, biosurfactants prevent surfactants' toxic effects on freshwater organisms (MD, 2012). In the pharmaceutical, they are utilized in formulations for color cosmetics and skin and hair care, justified for performance benefits, such as long-lasting effects, emulsion stability, rheology, and sensory experience (DRAKONTIS; AMIN, 2020). Biosurfactants in medicine are on the rise due to their antiviral, antibacterial, antifungal, anti-adhesive, and anticancer properties (JAHAN et al., 2020); Furthermore, remediation technologies employ aid in cleaning up hydrocarbons and metals from contaminated areas (JUWARKAR et al., 2007). It is essential to highlight that biosurfactants can also be obtained by enzymatic process (CANSIAN et al., 2022; GONÇALVES et al., 2021b), and using the SODD in this process is a potential application.

Finally, (LAORETANI; IRIBARREN, 2018) reports the production of FFAs through multiple stages molecular distillation. Although this is the only work on the subject, several others report this production as part of the process, once FFAs are amply employed in esters production.

2.5 Co-occurrence analysis of keywords

A co-occurrence analysis of the main keywords in our dataset was performed. Figure 7a shows the mapping of these words, divided into four clusters, where the size indicates the frequency of appearance, and the lines represent the occurrence together. It is noted that Soybean oil is at the center of this mapping, as it was the focus of the research. Observing Figure 7b, other words with high occurrence density are "chromatography" and "distillation", two well-known analysis and purification methods widely applied to SODD. Note that “food science” and “catalysis” also have high density, as the first indicates the great applicability of this raw material and the tool for converting it into products.

Figure 8a shows the co-occurrence analysis for the bioproducts obtained from SODD. It is noted that tocopherol and phytosterol are the products with the highest occurrence, followed by methyl esters, ethyl esters, and phytosterol esters. Note that biodiesel has a lower occurrence. However, several studies report this biofuel according to its components: fatty acids (methyl or ethyl) esters. Figure 8b reports the co-occurrence analysis of the purification methods covered throughout this review. Note that vortex ultrasonic, molecular distillation, soxhlet, supercritical carbon dioxide, and distillation are the most common methods, which agrees with the summary of the works discussed.

Finally, Figure 9 (a and b) shows the distribution of the dataset between countries. It is noted that China is the largest representative in the research, followed by Brazil and Portugal. This variety of countries throughout the dataset results in the different compositions of the SODD presented in this work, since the process conditions change it.

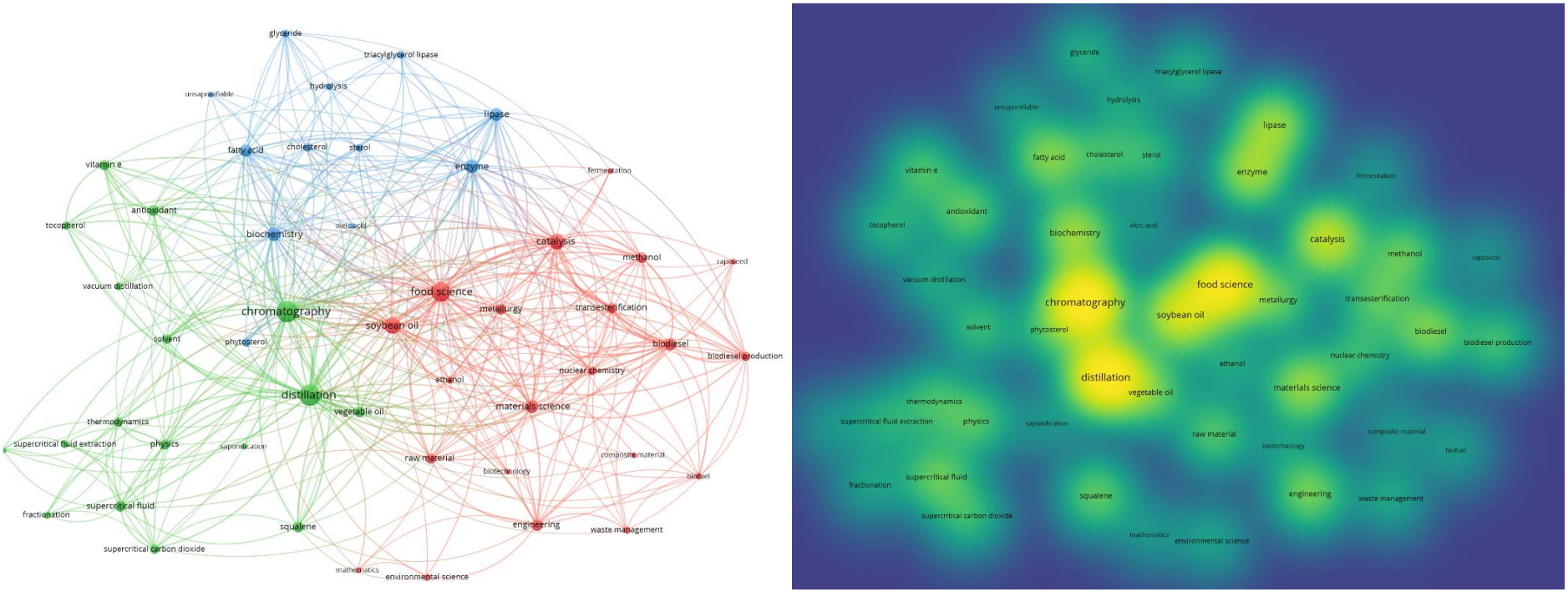

(a) (b)

Figure 7. Bibliometric analysis for keywords. (a) Co-occurrence analysis. (b) density mapping.

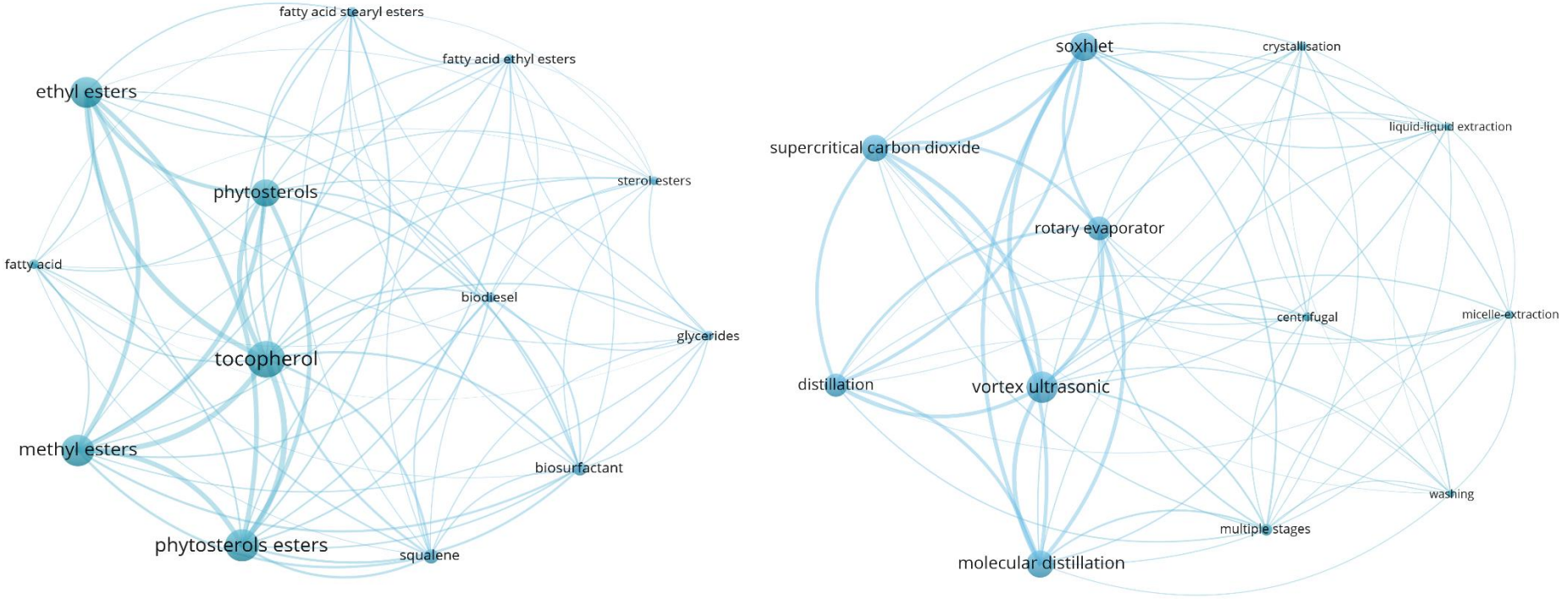

(a) (b)

Figure 8. Bibliometric analysis for: (a) bioproducts. (b) purification methods.

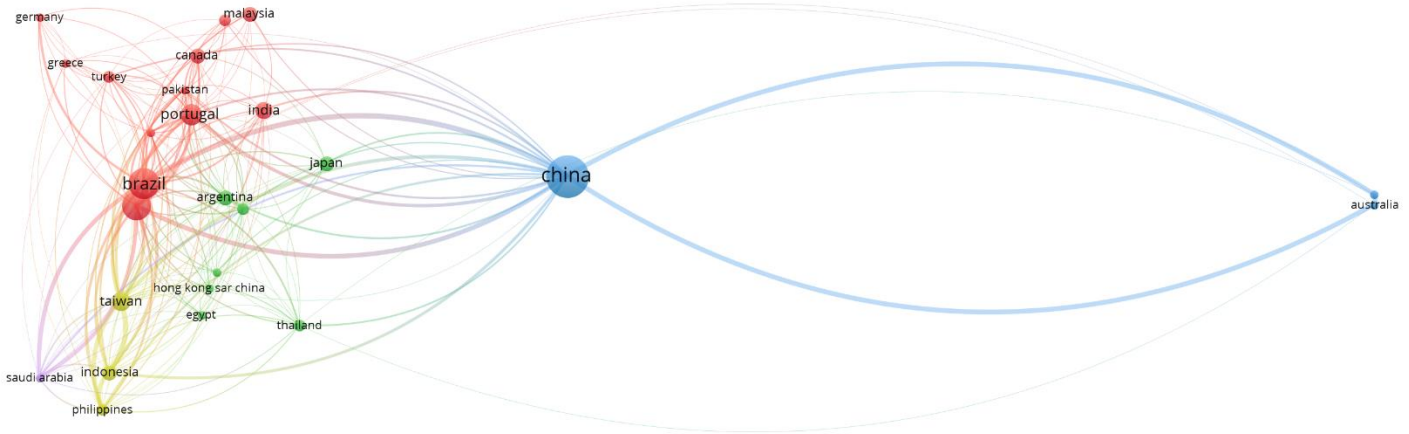

(a)

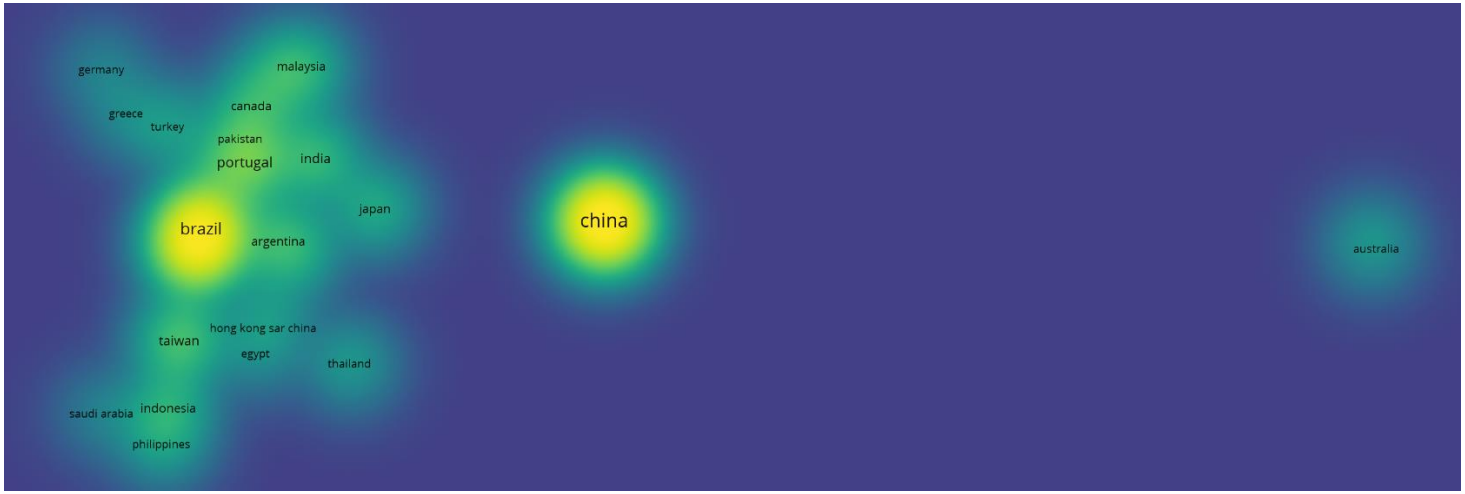

(b)

Figure 9. Bibliometric analysis for countries: (a) co-occurrence. (b) density.

2.6 Economic viability

When we think about scaling up the production of bioproducts from SODD, modeling and simulation of these processes are crucially important. It is necessary to describe them mathematically, expand to industrial scales, and calculate the project's fixed and variable costs, economic viability, and environmental impact parameters (ELIAS et al., 2021; FURLAN et al., 2016; LONGATI et al., 2018). The costs calculated in the economic analysis are divided into capital (CAPEX) and operational (OPEX). CAPEX is given by the cost of the physical plant, with dimensioning of equipment, connections, and electrical installations, among others. OPEX includes reagents, energy, utilities, labor, supervision, and maintenance costs. These cost analysis are based on mass and energy balances from process simulation (TURTON et al., 2009).

MARTINS (2023) conducted a technical-economic analysis of an enzymatic process for producing biolubricants from SODD. The work obtained a minimum biolubricant selling price of US$2.76 ± 0.27 per kg, 53.9% lower than traditional lubricants and 84.6% lower than biolubricants. BOURIAKOVA et al. (2020) assessed the economic viability of obtaining scalene from ODD and stated that there is profit in this process. The study by RAJENDRAN et al. (2024) analyzed the economic and environmental viability of a biodiesel production process, incorporating the simultaneous production of tocopherol, with a production capacity consuming 50 metric tons of rapeseed oil deodorizer distillate per day. In the economic sphere, the work demonstrated that the minimum biodiesel selling price necessary to make the process viable was US$0.67/kg. In contrast, the minimum sales price of tocopherol was $20.07/kg. However, it remains unclear whether the costs associated with contaminant removal were considered in the economic analysis of these processes, particularly for squalene and tocopherol, given their applications in the food and pharmaceutical industries.

2.7 Conclusions

From this literature review, it is safe to conclude that, on average, SODD is mostly composed of FFAs (46.30), triglycerides (20.85%), sterols (11.21%), tocopherols (8.51%), phytosterols (8.27%), stearyl esters (4.83%), diglycerides (4.47%), monoglycerides (2.09%) and squalene (1.63%). The composition of FFAs varies greatly; however, in most cases, linoleic acid appears in greater quantities, followed by oleic acid and then palmitic acid. This variation in composition is directly related to the great variation in works from different countries.

The best established and most cited bioproduct from SODD is biodiesel and/or component molecules. The main methods of obtaining it are through two-step esterification, both chemical and enzymatic. However, there are no reports of scale-up, economic or environmental analyzes for it. Tocopherol is another highly researched product, and the most cited methods are molecular distillation, liquid-liquid extraction, soxhlet, and supercritical carbon dioxide. Phytosterols are also represented in methodologies like tocopherols. It is noted that isoamyl esters, used as lubricants, and biosurfactants, are poorly explored in obtaining from SODD. This review highlights the diverse applications of SODD, presenting various analyses and experimental results for numerous bioproducts. Despite these promising prospects, it is essential to emphasize that SODD requires treatment for contaminant removal before its utilization.

SUPPLEMENTARY MATERIAL

“Table S1” Available on:

https://docs.google.com/spreadsheets/d/1Z52pTiydvrfCdxyLuifHZqNXBe1Y847J/edit?usp=drive_link&ouid=111021004072482321230&rtpof=true&sd=true

“Table S2” Available on:

https://docs.google.com/spreadsheets/d/1glh0rOHZZkMDw2pxjL8n3RwLNR5NyK3h/edit?usp=drive_link&ouid=111021004072482321230&rtpof=true&sd=true

“Table S3” Available on:

https://docs.google.com/spreadsheets/d/1EtPJd3oItmRLf-8xFsKSq--fTlwy4RJj/edit?usp=drive_link&ouid=111021004072482321230&rtpof=true&sd=true

“Table S4” Available on:

https://docs.google.com/spreadsheets/d/1d06L7mgduXIYen86xd-XEQY-RZjYbs1H/edit?usp=drive_link&ouid=111021004072482321230&rtpof=true&sd=true

“statistic_test” Available on:

https://docs.google.com/spreadsheets/d/1EYvU3xjv3DEzsL6_53FQzThcfnkTrVmZ/edit?usp=drive_link&ouid=111021004072482321230&rtpof=true&sd=true

REFERENCES

ATABANI, A. E.; SILITONGA, A. S.; BADRUDDIN, I. A.; MAHLIA, T. M. I.; MASJUKI, H. H.; MEKHILEF, S. A comprehensive review on biodiesel as an alternative energy resource and its characteristics. **Renewable and Sustainable Energy Reviews**, 2012.

BANCHERO, M.; GOZZELINO, G. Nb2O5-catalyzed kinetics of fatty acids esterification for reactive distillation process simulation. **Chemical Engineering Research and Design**, v. 100, p. 292–301, 2015.

BEZERRA, I. D.; BELISÁRIO, C. M.; FAVARETO, R.; TAHAM, T.; CASTEJON, L. V. Industrially concentrated tocopherols from soybean oil deodorizer distillate. **Brazilian Journal of Food Technology**, v. 25, 2022.

BOURIAKOVA, A.; MENDES, P. S. F.; ELST, K.; DE CLERCQ, J.; THYBAUT, J. W. Techno-economic evaluation of squalene recovery from oil deodorizer distillates. **Chemical Engineering Research and Design**, v. 154, p. 122–134, 2020.

BRAZIL GOVERNMENT. **ABIOVE**. Available in: <https://abiove.org.br/estatisticas/>. Accessed on: Jul. 20 2024.

CANSIAN, A. B. M.; TARDIOLI, P. W.; FURLAN, F. F.; DE SOUSA JÚNIOR, R. Modeling and simulation of the biosurfactant production by enzymatic route using xylose and oleic acid as reagents. **Chemical Industry and Chemical Engineering Quarterly**, v. 28, n. 4, p. 265–276, 2022.

CECILIA, J. A.; BALLESTEROS PLATA, D.; ALVES SABOYA, R. M.; TAVARES DE LUNA, F. M.; CAVALCANTE, C. L.; RODRÍGUEZ-CASTELLÓN, E. An Overview of the Biolubricant Production Process: Challenges and Future Perspectives. **Processes**, v. 8, n. 3, p. 257, 2020.

CERVELLON, M.-C.; CAREY, L. Consumers' perceptions of "green": Why and how consumers use eco-fashion and green beauty products. **Critical Studies in Fashion & Beauty**, v. 2, n. 1, p. 117–138, 2011.

CETINBAS, S.; GUMUS-BONACINA, C. E.; TEKIN, A. Separation of squalene from olive oil deodorizer distillate using short-pathmolecular distillation. **Journal of the American Oil Chemists' Society**, v. 99, n. 2, p. 175–179, 2022.

COLLABORATION FOR ENVIRONMENTAL EVIDENCE. **Guidelines and Standards for Evidence synthesis in Environmental Managemen**t, 2018.

D'AMATO VILLARDI, H. G.; LEAL, M. F.; DE AZEVEDO ANDRADE, P. H.; PESSOA, F. L. P.; SALGADO, A. M.; DE OLIVEIRA, A. R. G. Catalytic and non-catalytic esterification of soybean oil deodorizer distillate by ethanol: Kinetic modelling. **Chemical Engineering Transactions**, v. 57, p. 1999–2004, 2017.

DAVEY, R. J.; GARSIDE, J. **From Molecules to Crystallizers**. Oxford Chemistry Primers, 2000.

DE ARAUJO-SILVA, R.; VIEIRA, A. C.; GIORDANO, R. DE C.; FERNANDEZ-LAFUENTE, R.; TARDIOLI, P. W. Enzymatic Synthesis of Fatty Acid Isoamyl Monoesters from Soybean Oil Deodorizer Distillate: A Renewable and Ecofriendly Base Stock for Lubricant Industries. **Molecules**, v. 27, n. 9, 2022.

DEVELLIS, R. F. Inter-Rater Reliability. **Encyclopedia of Social Measurement**, v. 2p. 317–322, 2005.

DÍAZ DE RIENZO, M. A.; BANAT, I. M.; DOLMAN, B.; WINTERBURN, J.; MARTIN, P. J. Sophorolipid biosurfactants: Possible uses as antibacterial and antibiofilm agent. **New Biotechnology**, v. 32, n. 6, p. 720–726, 2015.

DRAKONTIS, C. E.; AMIN, S. Biosurfactants: Formulations, properties, and applications. **Current Opinion in Colloid & Interface Science**, v. 48, p. 77–90, 2020.

DU, W.; WANG, L.; LIU, D. Improved methanol tolerance during Novozym435-mediated methanolysis of SODD for biodiesel production. **Green Chemistry**, v. 9, n. 2, p. 173–17, 2007.

ELIAS, A. M.; LONGATI, A. A.; ELLAMLA, H. R.; FURLAN, F. F.; RIBEIRO, M. P. A.; MARCELINO, P. R. F.; et al. Techno-Economic-Environmental Analysis of Sophorolipid Biosurfactant Production from Sugarcane Bagasse. **Industrial & Engineering Chemistry Research**, v. 60, n. 27, p. 9833–9850, 2021.

FANG, T.; GOTO, M.; WANG, X.; DING, X.; GENG, J.; SASAKI, M.; et al. Separation of natural tocopherols from soybean oil byproduct with supercritical carbon dioxide. **Journal of Supercritical Fluids**, v. 40, n. 1, p. 50–58, 2007.

FERRER, A.; ALTABELLA, T.; ARRÓ, M.; BORONAT, A. Emerging roles for conjugated sterols in plants. **Progress in Lipid Research**, 2017.

FORNARI, T.; TORRES, C. F.; SEÑORÁNS, F. J.; REGLERO, G. Simulation and optimization of supercritical fluid purification of phytosterol esters. **AIChE Journal**, v. 55, n. 4, p. 1023–1029, 2009.

FURLAN, F. F.; COSTA, C. B. B.; FONSECA, G. DE C.; SOARES, R. DE P.; SECCHI, A. R.; CRUZ, A. J. G. DA; GIORDANO, R. C. Assessing the production of first and second generation bioethanol from sugarcane through the integration of global optimization and process detailed modeling. **Computers and Chemical Engineering**, v. 43, p. 1–9, 2012.

FURLAN, F. F.; COSTA, C. B. B.; SECCHI, A. R.; WOODLEY, J. M.; GIORDANO, R. C. Retro-Techno-Economic Analysis: Using (Bio)Process Systems Engineering Tools to Attain Process Target Values. **Industrial & Engineering Chemistry Research**, v. 55, n. 37, p. 9865–9872, 2016.

GONÇALVES, M. C. P.; AMARAL, J. C.; FERNANDEZ-LAFUENTE, R.; JUNIOR, R. DE S.; TARDIOLI, P. W. Lipozyme 435-mediated synthesis of xylose oleate in methyl ethyl ketone. **Molecules**, v. 26, n. 11, p. 1–18, 2021a.

GONÇALVES, M. C. P.; CANSIAn, A. B. M.; TARDIOLI, P. W.; SAVILLE, B. A. Production of sugars from mixed hardwoods for use in the synthesis of sugar fatty acid esters catalyzed by immobilized-stabilized derivatives of Candida antarctica lipase B. **Biofuel, Bioproducts and Biorefining**, v. 17, n. 5, p. 1236–1250, 2023.

GONÇALVES, M. C. P.; ROMANELLI, J. P.; GUIMARÃES, J. R.; VIEIRA, A. C.; DE AZEVEDO, B. P.; TARDIOLI, P. W. Reviewing research on the synthesis of CALB-catalyzed sugar esters incorporating systematic mapping principles. **Critical Reviews in Biotechnology**, p. 865–878, 2021b.

GONG, G.; WU, S. Lowering polycyclic aromatic hydrocarbon concentrations in vegetable oil deodorizer distillates and enhancing its utilization by graphene composites. **Food and Bioproducts Processing**, v. 143, p. 170–177, 2024a.

GONG, G.; WU, S. Degradation of polycyclic aromatic hydrocarbons in oil deodorizer distillates: kinetics, degradation product identification and toxicity. **International Biodeterioration & Biodegradation**, v. 187, p. 105718, 2024b.

GÜÇLÜ-ÜSTÜNDAĞ, Ö.; TEMELLI, F. Column Fractionation of Canola Oil Deodorizer Distillate Using Supercritical Carbon Dioxide. **Journal of the American Oil Chemists' Society**, v. 84, n. 10, p. 953–961, 2007.

GUNAWAN, S.; FABIAN, C.; JU, Y. H. Isolation and purification of fatty acid steryl esters from soybean oil deodorizer distillate. **Industrial and Engineering Chemistry Research**, v. 47, n. 18, p. 7013–7018, 2008.

GUNAWAN, S.; KASIM, N. S.; JU, Y. H. Separation and purification of squalene from soybean oil deodorizer distillate. **Separation and Purification Technology**, v. 60, n. 2, p. 128–135, 20 2008.

HIROTA, Y.; NAGAO, T.; WATANABE, Y.; SUENAGA, M.; NAKAI, S.; KITANO, M.; et al. Fractionation of soybean oil deodorizer distillate (SODD) by molecular distillation a content (wt%). **Journal of the American Oil Chemists' Society**, v. 80, n. 4, p. 341–346, 2003.

HRASTAR, R.; CHEONG, L.; XU, X.; MILLER, R. L.; KOŠIR, I. J. Camelina sativa oil deodorization: balance between free fatty acids and color reduction and isomerized byproducts formation. **Journal of the American Oil Chemists' Society**, v. 88, n. 4, p. 581–588, 2011.

JAHAN, R.; BODRATTI, A. M.; TSIANOU, M.; ALEXANDRIDIS, P. Biosurfactants, natural alternatives to synthetic surfactants: physicochemical properties and applications. **Advances in Colloid and Interface Science**, v. 275, p. 102061, 2020.

JU, Y.; HUYNH, L.; GUNAWAN, S.; CHERN, Y.; KASIM, N. S. Irresolvable complex mixture of hydrocarbons in soybean oil deodorizer distillate. **Journal of Separation Science**, v. 35, n. 2, p. 327–333, 2012.

JUWARKAR, A. A.; NAIR, A.; DUBEY, K. V.; SINGH, S. K.; DEVOTTA, S. Biosurfactant technology for remediation of cadmium and lead contaminated soils. **Chemosphere**, v. 68, n. 10, p. 1996–2002, 2007.

KASHCHIEV, D. Nucleation: basic theory with applications. 1. ed. Boston. ISBN: 978-0-7506-4682-6, **Elsevier Ltd**. 2000.

KASIM, N. S.; GUNAWAN, S.; YULIANA, M.; JU, Y. H. A simple two-step method for simultaneous isolation of tocopherols and free phytosterols from soybean oil deodorizer distillate with high purity and recovery. **Separation Science and Technology**, v. 45, n. 16, p. 2437–2446, 2010.

KAVZOGLU, T. Object-Oriented Random Forest for High Resolution Land Cover Mapping Using Quickbird-2 Imagery. Em: **Handbook of Neural Computation**. [s.l.] Elsevier Inc., 2017. p. 607–619.

KHATOON, S.; RAJAN, R. G. R.; KRISHNA, A. G. G. Physicochemical characteristics and composition of indian soybean oil deodorizer distillate and the recovery of phytosterols. **JAOCS, Journal of the American Oil Chemists' Society**, v. 87, n. 3, p. 321–326, 2010.

KORBER, M.; KLEIN, I.; DAUM, G. Steryl ester synthesis, storage and hydrolysis: A contribution to sterol homeostasis. **Biochimica et Biophysica Acta (BBA) - Molecular and Cell Biology of Lipids**, v. 1862, n. 12, p. 1534–1545, 2017.

KORDSMEIER, M.; HOWARD, L. R.; BROWNMILLER, C.; PROCTOR, A.; HAUER-JENSEN, M. Isolation of Gamma and Delta Tocotrienols from Rice Bran Oil Deodorizer Distillate Using Flash Chromatography. **Journal of the American Oil Chemists' Society**, v. 92, n. 9, p. 1243–1252, 2015.

KUSUMA, M.; SUSONGKO, P.; ARFIANI, Y. Validation of the instruments of learning readiness with e-learning using rasch modeling to empower technological content knowledge (TCK). **Journal Pena Sains**, v. 6, n. 1, p. 18, 2019.

LAORETANI, D. S.; FISCHER, C. D.; IRIBARREN, O. A. Selection among alternative processes for the disposal of soapstock. **Food and Bioproducts Processing**, v. 101, p. 177–183, 2017.

LAORETANI, D. S.; IRIBARREN, O. A. Optimization of the recycle structure of multiple stages molecular distillation. **Chemical Engineering Research and Design**, v. 130, p. 35–41, 2018.

LAORETANI, D. S.; IRIBARREN, O. A. Procedure for the selection among technologies. Treatment of deodorizer distillate oil. **Industrial & Engineering Chemistry Research**, v. 53, n. 43, p. 16803–16812, 2014.

LI, J.; CHASE, H. A. Development of adsorptive (non-ionic) macroporous resins and their uses in the purification of pharmacologically-active natural products from plant sources. **Natural Product Reports**, v. 27, n. 10, p. 1493, 2010.

LIU, W.; FU, X.; LI, Z. Extraction of tocopherol from soybean oil deodorizer distillate by deep eutectic solvents. **Journal of Oleo Science**, v. 68, n. 10, p. 951–958, 2019.

LIU, Y.; FANG, T.; DING, X. Phase equilibrium for supercritical co 2 and the methyl esterified product from soybean oil deodorizer distillate. **Journal of food Lipids**, v. 13, 4, p. 390-401, 2006.

LONGATI, A. A.; LINO, A. R. A.; GIORDANO, R. C.; FURLAN, F. F.; CRUZ, A. J. G. Defining research and development process targets through retro-techno-economic analysis: the sugarcane biorefinery case. **Bioresource Technology**, v. 263, p. 1–9, 2018.

LOU-BONAFONTE, J. M.; MARTÍNEZ-BEAMONTE, R.; SANCLEMENTE, T.; SURRA, J. C.; HERRERA-MARCOS, L. V.; SANCHEZ-MARCO, J.; ARNAL, C.; OSADA, J. Current insights into the biological action of squalene. **Molecular Nutrition & Food Research**, v. 62, n. 15, p. 1–59, ago. 2018.

LUTIŠAN, J.; CVENGROŠ, J.; MICOV, M. Heat and mass transfer in the evaporating film of a molecular evaporator. **Chemical Engineering Journal**, v. 85, p. 225–234, 2002.

LV, W.; WU, C.; LIN, S.; WANG, X.; WANG, Y. Integrated utilization strategy for soybean oil deodorizer distillate: synergically synthesizing biodiesel and recovering bioactive compounds by a combined enzymatic process and molecular distillation. **ACS Omega**, v. 6, n. 13, p. 9141–9152, 2021.

MARTINI, G.; NERLI, B. B.; MALPIEDI, L. P. A novel method based on saponification coupled to micelle-extraction for recovering valuable bioactive compounds from soybean oil deodorizer distillate. **Food Chemistry**, v. 384, 2022.

MARTINS C de O. Valorizando subprodutos das produções de óleo de soja e etanol: síntese e análise técnico-econômica da produção de biolubrificantes em biorrefinarias. Master's thesis. [chemical engineering]. [SP]: Universidade Federal de São Carlos; 2023.

MARTINS, P. F.; ITO, V. M.; BATISTELLA, C. B.; MACIEL, M. R. W. Free fatty acid separation from vegetable oil deodorizer distillate using molecular distillation process. **Separation and Purification Technology**, v. 48, n. 1, p. 78–84, 2006.

MAYUMI ITO, V; MARTINS, P. F.; BATISTELLA, C. B.; MACIEL FILHO, R.; MACIEL, M. R; W. Natural Compounds Obtained Through Centrifugal Molecular Distillation. **Applied Biochemistry and Biotechnology**. Vol. 129–132, 2006.

MAZUBERT, A.; POUX, M.; AUBIN, J. **Intensified processes for FAME production from waste cooking oil: A technological review**. **Chemical Engineering Journal**, 2013.

MD, F. Biosurfactant: Production and Application. **Journal of Petroleum & Environmental Biotechnology**, v. 03, n. 04, 2012.

MEYER, F.; EGGERS, R.; OEHLKE, K.; HARBAUM-PIAYDA, B.; SCHWARZ, K.; SIDDIQI, M. A. Application of short path distillation for recovery of polyphenols from deodorizer distillate. **European Journal of Lipid Science and Technology**, v. 113, n. 11, p. 1363–1374, 2011.

MOREAU, R. A.; NYSTRÖM, L.; WHITAKER, B. D.; WINKLER-MOSER, J. K.; BAER, D. J.; GEBAUER, S. K.; HICKS, K. B. Phytosterols and their derivatives: Structural diversity, distribution, metabolism, analysis, and health-promoting uses. **Progress in Lipid Research**, v. 70, p. 35–61, 2018.

MOREIRA, E. A.; BALTANÁS, M. A. Recovery of phytosterols from sunflower oil deodorizer distillates. **Journal of the American Oil Chemists' Society**, v. 81, n. 2, p. 161–167, 2004.

MULLIN, J. W. Crystallisation. **Organic Process Research & Development**, v. 6, n. 2, p. 201–202, 2002.

MYERSON A. Handbook of Industrial Crystallization. 3rd ed. Myerson AS, Erdemir D, Lee AY, editors. **Cambridge University Press**; 2019.

PALUZAR, H. Production of high quality biodiesel from sunflower soapstock acid oil as novel feedstock: Catalyzed by immobilized pancreatic lipase. **Journal of the American Oil Chemists' Society**, v. 101, n. 2, p. 251–265, 2024.

PANIGRAHI, S.; NANDA, B. S.; BHUYAN, R.; KUMAR, K.; GHOSH, S.; SWARNKAR, T. Classifying histopathological images of oral squamous cell carcinoma using deep transfer learning. **Heliyon**, v. 9, n. 3, 2023.

PARTOVI, M.; LOTFABAD, T. B.; ROOSTAAZAD, R.; BAHMAEI, M.; TAYYEBI, S. Management of soybean oil refinery wastes through recycling them for producing biosurfactant using Pseudomonas aeruginosa MR01. **World Journal of Microbiology and Biotechnology**, v. 29, n. 6, p. 1039–1047, 2013.

PODDAR, T.; JAGANNATH, A.; ALMANSOORI, A. Use of reactive distillation in biodiesel production: A simulation-based comparison of energy requirements and profitability indicators. **Applied Energy**, v. 185, p. 985–997, 2017.

RAJENDRAN, N.; PRIYANKA, R. B. S.; GURUNATHAN, B.; HAN, J. Techno-economic and environmental impact analysis of integrated biodiesel production and tocopherol separation from rapeseed oil deodorizer distillate. **Industrial Crops and Products**, v. 220, p. 119304, 2024.

REETU; CM, Prakash R; RAI, M. P. Latest advances and status analysis of nanomaterials for microalgae photosystem, lipids and biodiesel: A state of art. **Journal of Environmental Chemical Engineering**, v. 11, n. 1, 2023.

ROMANELLI, J. P.; SILVA, L. G. M.; GONÇALVES, M. C. P.; NAVES, R. P.; ALMEIDA, D. R. A.; RESENDE, A. F.; RODRIGUES, R. R. Repeatability of the searching process in reviews of restoration outcomes. **Restoration Ecology.** John Wiley and Sons Inc, 2021.

SAINI, R. K.; KEUM, Y. S. Tocopherols and tocotrienols in plants and their products: A review on methods of extraction, chromatographic separation, and detection. **Food Research International.** Elsevier Ltd, 2016.

SALEHI, B.; QUISPE, C.; SHARIFI-RAD, J.; CRUZ-MARTINS, N.; NIGAM, M.; MISHRA, A. P.; et al. Phytosterols: From Preclinical Evidence to Potential Clinical Applications. Frontiers in Pharmacology. **Frontiers Media S.A.**, 2021.

SANTOS, A. C.; FERREIRA, P. M.; LOPES, C. L.; BRAGA, M.; VIANA, N. M. Estudo prospectivo de óleos vegetais: o caso da Embrapa Agroenergia [Internet]. Brasília, DF; 2022. Available from: https://ainfo.cnptia.embrapa.br/digital/bitstream/item/232384/1/-DOC41.pdf

SCHNEIDER, M. P. Plant-oil-based lubricants and hydraulic fluids. **Journal of the Science of Food and Agriculture**, v. 86, n. 12, p. 1769–1780, 2006.

SENGUPTA, A.; GHOSH, M. Reduction of cardiac and aortic cholesterol in hypercholesterolemic rats fed esters of phytosterol and omega-3 fatty acids. **Journal of Food Science and Technology**, v. 52, n. 5, p. 2741–2750, 2015.

SHERAZI, S. T. H.; MAHESAR, S. A.; SIRAJUDDIN. Vegetable oil deodorizer distillate: A rich source of the natural bioactive components. **Journal of Oleo Science.** Japan Oil Chemists Society, v. 65, n. 12, p. 957-966, 2016.

SHI, B.; JIN, J.; YU, E.; ZHANG, Z. Concentration of Natural VitaminE Using a Continuous Countercurrent Supercritical CO2 Extraction-Distillation Dual Column. **Chemical Engineering and Technology**, v. 34, n. 6, p. 914–920, 2011.

SHIMADA, Y.; NAKAI, S.; SUENAGA, M.; SUGIHARA, A.; KITANO, M.; TOMINAGA, Y. Facile Purification of Tocopherols from Soybean Oil Deodorizer Distillate in High Yield Using Lipase**. JAOCS**, v. 77, n. 10, 2000.

SILVA, M. M. S.; NISHIAMA, H.; CAZZOLATO, A. S. Process for separating and purification of vod distilled vegetable oil components obtained from refined vegetable oil deodorization. **BR102012023398A2** (Patent), 2012.

SMITH, F. E. Separation of tocopherols and sterols from deodorizer sludge and the like. US, 1967.

SOUZA, M. S.; AGUIEIRAS, E. C. G.; DA SILVA, M. A. P.; LANGONE, M. A. P. Biodiesel synthesis via esterification of feedstock with high content of free fatty acids. **Applied Biochemistry and Biotechnology**, v. 154, p.253–267, 2009.

SUN, Q.; YANG, L. The adsorption of basic dyes from aqueous solution on modified peat–resin particle. **Water Research**, v. 37, n. 7, p. 1535–1544, 2003.

TEIXEIRA, A. R. S.; SANTOS, J. L. C.; CRESPO, J. G. Assessment of solvent resistant nanofiltration membranes for valorization of deodorizer distillates. **Journal of Membrane Science,** v. 470, p. 138–147, 2014.

TEIXEIRA, A. R. S.; SANTOS, J. L. C.; CRESPO, J. G. Production of Steryl Esters from Vegetable Oil Deodorizer Distillates by Enzymatic Esterification. **Industrial & Engineering Chemistry Research,** v. 50, n. 5, p. 2865–2875, 2011.

TORRES, C. F.; FORNARI, T.; TORRELO, G.; SEÑORÁNS, F. J.; REGLERO, G. Production of phytosterol esters from soybean oil deodorizer distillates. **European Journal of Lipid Science and Technology**, v. 111, n. 5, p. 459-463, 2009.

TORRES, C. F.; TORRELO, G.; SEÑORANS, F. J.; REGLERO, G. A two steps enzymatic procedure to obtain sterol esters, tocopherols and fatty acid ethyl esters from soybean oil deodorizer distillate. **Process Biochemistry**, v. 42, n. 9, p. 1335-1341, 2007.

TUNG, H.-H.; PAUL, E. L.; MIDLER, M.; MCCAULEY, J. A. Crystallization of Organic Compounds: An Industrial Perspective. New York: **John Wiley & Sons**, 2009.

TURTON, R.; BAILIE, R. C.; WHITING, W. B.; SHAEIWITZ, J. A. Analysis, synthesis and design of chemical processes. 3. ed. Upper Saddle River: **Pearson Education**, Inc, 2009. p. 1-1007.

VAN DUIJN, G. Fate of contaminants during the refining process of vegetable oils and fats: A calculation model. **European Journal of Lipid Science and Technology**, v. 118, n. 3, p. 353-360, 2016.

VAN DUIJN, G. Industrial experiences with pesticide removal during edible oil refining. **European Journal of Lipid Science and Technology**, v. 110, n. 11, p. 982-989, 2008.

VAN DUIJN, G. Vegetable Oils and Fats. In: **Food Safety Management**. Elsevier EBooks, p. 323-337, 2023.

VENKATA SUBHASH, G.; VENKATA MOHAN, S. Biodiesel production from isolated oleaginous fungi Aspergillus sp. using corncob waste liquor as a substrate. **Bioresource Technology**, v. 102, n. 19, p. 9286–9290, 2011.

VERNIER, L. J.; NUNES, A. L. B.; ALBARELLO, M.; DE CASTILHOS, F. Continuous production of fatty acid methyl esters from soybean oil deodorized distillate and methyl acetate at supercritical conditions. **Journal of Supercritical Fluids**, v. 186, 2022.

VIEIRA, A. C.; CANSIAN, A. B. M.; GUIMARÃES, J. R.; VIEIRA, A. M. S.; FERNANDEZ-LAFUENTE, R.; TARDIOLI, P. W. Performance of liquid eversa on fatty acid ethyl esters production by simultaneous esterification/transesterification of low-to-high acidity feedstocks. **Catalysts**, v. 11, n. 12, 2021.

VISIOLI, L. J.; NUNES, A. L. B.; WANCURA, J. H. C.; ENZWEILER, H.; VERNIER, L. J.; DE CASTILHOS, F. Batch and continuous γ-alumina-catalyzed FAME production from soybean oil deodorizer distillate by interesterification. **Fuel**, v. 351, 2023.

VISIOLI, L. J.; DE CASTILHOS, F.; CARDOZO-FILHO, L.; DE MELLO, B. T. F.; DA SILVA, C. Production of esters from soybean oil deodorizer distillate in pressurized ethanol. **Fuel Processing Technology**, v. 149, p. 326–331, 2016.

WAN, J.; ZHANG, W.; JIANG, B.; GUO, Y.; HU, C. Separation of individual tocopherols from Soybean distillate by low pressure column chromatography. **Journal of the American Oil Chemists' Society**, v. 85, n. 4, p. 331-338, 2008.

WANG, L.; DU, W.; LIU, D.; LI, L.; DAI, N. Lipase-catalyzed biodiesel production from soybean oil deodorizer distillate with absorbent present in tert-butanol system. **Journal of Molecular Catalysis B: Enzymatic**, v. 43, n. 1-4, p. 29-32, 2006.

WATANABE, Y.; NAGAO, T.; HIROTA, Y.; KITANO, M.; SHIMADA, Y. Purification of Tocopherols and Phytosterols by a Two-Step in situ Enzymatic Reaction. Press 339**. JAOCS**, **Journal of the American Oil Chemists' Society,** Vol. 81, no. 4, 2004.

WINTON, B.; SMITH, E. S. Process for separating tocopherols and sterols from deodorizer sludge and the like. US3153055A (Patent) 1964.

WU, Y.; MONDAL, J.; TAO, Y.; MARTIN, G. J. O.; ASHOKKUMAR, M. Ultrasound-enhanced adsorption of amino acids from aqueous solution onto macroporous resins for green separation: Mass transfer mechanism and acoustic cavitation properties. **Separation and Purification Technology**, v. 330, p. 125368, 2024.

XIONG, Y. W.; GO, A. W.; ALIVIO, R. K. O.; SANTOSO, S. P.; ANGKAWIJAYA, A. E.; SOETAREDJO, F. E. Non-isothermal (trans)esterification of linoleic acid and soybean oil deodorizer distillate with methanol under subcritical conditions. **Renewable Energy**, v. 197, p. 528–544, 2022.

XUE, J.; WU, S.; ZHU, Q.; LIU, X.; HE, Z.; YE, W.; WANG, P.; WU, F. Enrichment and purification of Torreya grandis peptides by macroporous resin and its hypoglycemic mechanism revealed by transcriptome analysis. **Industrial Crops and Products**, v. 213, p. 118445, 2024.

YAN, F.; YANG, H.; LI, J.; WANG, H. Optimization of Phytosterols Recovery from Soybean Oil Deodorizer Distillate. **Journal of the American Oil Chemists' Society**, v. 89, n. 7, p. 1363–1370, 2012.

YANG, Z.; LI, H.; DUAN, D.; YAO, X.; CHEN, J.; JI, H. Preparation of high purity squalene from soybean oil deodorizer distillate with the combination of macroporous resin and thin-film evaporation coupling distillation. **Separation Science and Technology (Philadelphia)**, v. 55, n. 9, p. 1611–1622, 2020.

YIN, X.; DUAN, X.; YOU, Q.; DAI, C.; TAN, Z.; ZHU, X. Biodiesel production from soybean oil deodorizer distillate using calcined duck eggshell as catalyst. **Energy Conversion and Management,** v. 112, p. 199-207, 2016.

YIN, X.; YOU, Q.; MA, H.; DAI, C.; ZHANG, H.; LI, K.; ZHU, X. Biodiesel production from soybean oil deodorizer distillate enhanced by counter-current pulsed ultrasound. **Ultrasonics Sonochemistry,** v. 23, p. 53-58, 2015.

YIN, X.; ZHANG, X.; WAN, M.; DUAN, X.; YOU, Q.; ZHANG, J.; LI, Y. Intensification of biodiesel production using dual-frequency counter-current pulsed ultrasound. **Ultrasonics Sonochemistry**, v. 37, p. 136-143, 2017.

ZHANG, L.; WU, T.; XIAO, W.; WANG, Z.; DING, G.; ZHAO, L. Enrichment and Purification of Total Ginkgo Flavonoid O-Glycosides from Ginkgo Biloba Extract with Macroporous Resin and Evaluation of Anti-Inflammation Activities In Vitro. **Molecules**, v. 23, n. 5, p. 1167, 2018.

ZHANG, S.; GONG, X.; QU, H. An effective and comprehensive optimization strategy for preparing *Ginkgo biloba* leaf extract enriched in shikimic acid by macroporous resin column chromatography. **Phytochemical Analysis**, 2024.

ZHAO, G.; HU, T.; ZHAO, L. Fermentation of soybean oil deodorizer distillate with Candida tropicalis to concentrate phytosterols and to produce sterols-rich yeast cells. **Journal of Industrial Microbiology and Biotechnology**, v. 41, n. 3, p. 579–584, 2014.

ZHENG, J.; WEI, W.; WANG, S.; LI, X.; ZHANG, Y.; WANG, Z. Immobilization of Lipozyme TL 100L for methyl esterification of soybean oil deodorizer distillate. **3 Biotech**, v. 10, n. 2, 2020.

CHAPTER 3: Biosurfactants

This chapter consists of two works evaluating the production of biosurfactants using commercial reagents with a high degree of purity. The first step in the methodological application of doctoral research was to study and perform a techno-economic analysis in the process proposed for the master's degree. The second step involved evaluating a second process and adding environmental assessment to the methodology.

Modeling and simulation of the biosurfactant production by enzymatic route using xylose and oleic acid as reagents

Published in Chemical Industry & Chemical Engineering Quarterly (CI&CEQ) - 7 February 2022

Doi: 10.2298/CICEQ210621001C

3.1 Abstract

The biosynthesis of sugar esters, molecules with biosurfactant properties, can occur through the esterification of sugars with fatty acids by enzymatic catalysis. An alternative to reduce the impact of raw materials on the final cost of biosurfactant production and reuse industrial waste is to use residues from vegetable oil industries as source of FFA (Free Fatty Acid, such as oleic acid) and lignocellulosic residues of 2G ethanol as source of sugar (xylose). In this scenario, the present work aimed to model the production process of biosurfactants via heterogeneous biocatalysis by lipase, using oleic acid and xylose. Product separation and purification was performed using a sequence of precipitations (by adding ethanol, water and methyl ethyl ketone). Simulation was performed using the equation-oriented software EMSO (Environment for Modeling, Simulation and Optimization), which is CAPE-OPEN compliant. The percentage of biosurfactants in the product was around 86%, with recovery of 88% in the purification. Regarding the study of energy expenditure, it was observed a value of -604.1 kW of heat associated with cooling and a value of 137.6 kW associated with heating. Developed mathematical models successfully described the process, making it possible to perform equipment sizing calculations, capital cost estimations, and operational costs determination.

Keywords: Biosurfactants; Esterification; Modeling and Simulation; Purification; Precipitation.

The complete scientific article can be found in the Appendix section of the thesis.

Sustainable Production of Xylose Ester Biosurfactant: A Techno-Economic-Environmental Analysis

Response to reviewers sent

3.2 Abstract

The search for alternatives that make the concept of a sustainable future conceivable and the possibility of having industries with low impact on global warming is among the most significant challenges today. The enzymatic production and application of xylose esters fit into this scenario as a potential sustainable biosurfactant with low environmental impact. Although several authors describe different possible operating conditions for the enzymatic production of xylose esters, studies that carry out techno-economic-environmental analysis (TEEA) for biosurfactant production are rare, and those that specifically apply TEEA for xylose esters production are even scarcer. In this context, this work aims to contribute to the development and scaling of the xylose ester production process by providing a TEEA of the biosurfactant production through enzymatic route using xylose and oleic acid as reagents. Phenomenological models were used to describe the process through mass and energy balances. The proposed process was simulated using EMSO, an equation-oriented simulator, from the esterification reaction to the downstream step, obtaining a biosurfactant with 96% purity. An economic analysis was also performed, which covered the installation and operating costs for a plant working throughout 25 years. In the life cycle assessment, the product showed low levels of ozone layer depletion, human toxicity, aquatic marine ecotoxicity, and photochemical oxidation, highlighting its environmental viability and lower impact.

Keywords: Xylose ester production; Technical-Economic-Environmental analysis; environmental viability.

3.3 Introduction

Surfactants are a chemical class with amphiphilic and surface-active characteristics used in multiple industries, such as pharmaceuticals, cosmetics, and food (BANAT et al., 2010). They have hydrophobic and hydrophilic regions in the same molecule, resulting in properties such as stabilizing effect, surface tension reduction, emulsifying capacity, solubilizing ionic strength, and viscosity reduction (SARUBBO et al., 2006). Biosurfactants, in turn, are amphipathic molecules produced by microbiological or enzymatic routes, presenting the same properties already mentioned for surfactants. Furthermore, these biomaterials have good biodegradability, thermal stability, specific bioactivity, low degradability when subjected to high pH values, and low toxicity. The main disadvantage is the production costs of the already established routes, which are usually still high, compared to those for synthetic surfactants (DÍAZ DE RIENZO et al., 2015; SANTOS et al., 2016).

In terms of products offered and used commercially, synthetic surfactants from petroleum derivatives are the main ones. However, social awareness and technological advances have led to a search for environmentally friendly reagents that can replace the chemical reagents used in the synthesis (JEMIL et al. 2016; PERFUMO et al. 2018).

The search for alternatives that make the concept of a sustainable future conceivable and the possibility of having industries with a low impact on global warming is among the most significant challenges today. The enzymatic production and application of xylose esters fit into this scenario as a potentially sustainable biosurfactant with low environmental impact. Specifically, xylose esters can be produced by enzymatic route using fatty acids and xylose as reagents, which, in turn, can be obtained from biorefinery residues (GONÇALVES et al., 2022; VIEIRA et al., 2021).

Table 1 summarizes the most recent and prominent works in producing xylose esters. As an acyl donor, some authors use lauric acid (BIDJOU-HAIOUR; KLAI, 2013; BOUZAOUIT; BIDJOU-HAIOUR, 2015; JOCQUEL et al., 2021; MARTINEZ-GARCIA et al., 2021), stearic acid (BIDJOU-HAIOUR; KLAI, 2013), capric acid (ABDULMALEK; HAMIDON; ABDUL RAHMAN, 2016), and oleic acid (DE LIMA et al., 2016; GONÇALVES et al., 2021; VESCOVI; DOS SANTOS; TARDIOLI, 2017). As for the esterification solvents, the most utilized are tert-butanol (DE LIMA et al., 2016; VESCOVI; DOS SANTOS; TARDIOLI, 2017), 2-methyl-2-butanol (JOCQUEL et al., 2021; MARTINEZ-GARCIA et al., 2021; MÉLINE et al., 2018), dimethyl sulfoxide (DMSO) and acetone (ABDULMALEK; HAMIDON; ABDUL RAHMAN, 2016), and methyl ethyl ketone (BIDJOU-HAIOUR; KLAI, 2013; BOUZAOUIT; BIDJOU-HAIOUR, 2015; GONÇALVES et al., 2021). Finally, the most often utilized enzymes are Porcine pancreas lipase (PPL) (BIDJOU-HAIOUR; KLAI, 2013; VESCOVI; DOS SANTOS;

TARDIOLI, 2017), Candida cylindracea lipase (BOUZAOUIT; BIDJOU-HAIOUR, 2015), Candida antartica B lipase (CALB) (BIDJOU-HAIOUR; KLAI, 2013; DE LIMA et al., 2016), Novozym 435 (JOCQUEL et al., 2021; MÉLINE et al., 2018), and Lipozyme 435 (ABDULMALEK; HAMIDON; ABDUL RAHMAN, 2016; GONÇALVES et al., 2021; MARTINEZ-GARCIA et al., 2021).

Although several authors describe different possible operating conditions for the enzymatic production of xylose esters, studies that carry out techno-economic-environmental analysis (TEEA) for biosurfactant production, summarized in Table 2, are rare (EKPENYONG et al., 2021; ELIAS et al., 2021; MOUTINHO et al., 2021), and those that specifically apply TEEA for xylose esters production are even scarcer (CANSIAN et al., 2022).

In this context, this work aims to contribute to the development and scaling of the xylose ester production process by providing a TEEA of the biosurfactant production through the enzymatic route using xylose and oleic acid as reagents. The process conditions found in (GONÇALVES et al., 2021) were chosen since it had the highest conversion rate (~98%), the immobilized enzyme can be recovered and reused, and the solvent used (methyl ethyl ketone) has low toxicity, making the biosurfactant suitable for cosmetics and food industries (BIDJOU-HAIOUR; KLAI, 2013; LI et al., 2015).

Table 1. Recent research on the xylose esters production.

Free fatty acid	Enzyme	Conversion	Esterification solvent	Source
Lauric acid/ Stearic acid	*Porcine pancreas lipase* (PPL)/ *Candida antartica B lipase* (CALB)	0.63/ 0.45	Methyl ethyl ketone	BIDJOU-HAIOUR and KLAI (2013)
Lauric acid	*Candida cylindracea lipase*	0.85	Methyl ethyl ketone	BOUZAOUIT and BIDJOU-HAIOUR (2015)
Capric acid	*Novozym* 435	0.64	DMSO: acetone (1:10 v/v)	ABDULMALEK et al. (2016)
Oleic acid	*Candida antartica B lipase* (CALB)	0.60	Tert-butanol	DE LIMA et al. (2016)
Caprylic acid/ Oleic acid/ Butyric acid	*Porcine pancreas lipase* (PPL)	0.62/ 0.70/ 0.68	Tert-butanol	VESCOVI et al. (2017)
Vinyl laurate	*Novozym* 435	0.748	2-Methyl-2-butanol	MÉLINE et al. (2018)
Oleic acid	*Lipozyme* 435	0.98	Methyl ethyl ketone	GONÇALVES et al. (2021)
Lauric acid	*Lipozyme* 435	0.72	2-Methyl-2-butanol	MARTINEZ-GARCIA et al. (2021)
Lauric acid	*Novozym* 435	0.134	2-Methyl-2-butanol	JOCQUEL et al. (2021)

Table 2. Recent research containing technical-economic-environmental analysis of the biosurfactant production.

Biosurfactant	Process	Purity	Price (Economic analysis)	(Environmental analysis)	Source
Glycolipopeptide	Microbial fermentation	110g/L	€ 570/kg	-	EKPENYONG et al. (2021)
Rhamnolipids	Microbial fermentation	60% (w/w)	US$ 60/kg	-	MOUTINHO et al. (2021)
Sophorolipid	Microbial fermentation	90% (w/w)	US$ 20/kg	17.1 (case A)/ 9.55 (case B) kg CO_2 eq. / kg biosurfactant	ELIAS et al. (2021)
Xylose ester	Enzymatic production	86% (w/w)	US$ 72.37/kg	-	CANSIAN et al. (2022)

3.4 Material and Methods

3.4.1 Process description

The xylose ester production process by enzymatic route is shown in Figure 1. Initially, xylose is added to the solvent, methyl ethyl ketone, and both (stream 3) remain under stirring at a temperature of 60 ºC for 24 hours to solubilize all sugar. Then, in the reactor, oleic acid, immobilized enzyme (lipozyme 435 from CALB), and molecular sieve (to retain water) are added (stream 8).

Operating conditions of esterification, such as temperature (60 ºC), pressure (1 atm), agitation (200 rpm), xylose to oleic acid molar ratio (1:5), xylose concentration (7 mM of xylose in methyl ethyl ketone), and enzymatic amount (0.5% w/v of lipozyme 435), are given by GONÇALVES et al. (2021). Esterification, in general, is represented by Equation 1.

$$C_5H_{10}O_5(l) + C_{18}H_{34}O_2(l) \overset{lipozyme\ 435}{\Longleftrightarrow} C_{23}H_{42}O_6(l) + H_2O(l) \quad (1)$$

The reaction takes place in 24 hours. After this, the molecular sieves are removed by filtration (stream 12), and the enzymes are recovered (also by filtration) and reinserted into the process (stream 16). As molecular sieve particles are much bigger than immobilized enzymes, filters with different granularities can remove them separately.

Then, in the downstream stage, the reaction medium passes through a cooler (stream 17), a centrifuge (stream 18), and a tank (stream 19), where the polar and ester phases are separated. The ester phase goes to a heat exchanger/evaporator (streams 20/22) to remove the esterification solvent. Next, water and alcohol (50:50, v/v) are added to the ester phase (stream 25), the mixture is centrifuged (stream 27), and the solid phase is collected in a precipitation tank (this entire step is performed twice) (streams 29/34). After that, methyl ethyl ketone is added to the solid phase (stream 35) and washed three times, also using centrifugation (streams 37/42/47) and collected in a precipitation tank (streams 39/44/49). Finally, the solid product passes through a heat exchanger/evaporator (streams 49/52) to complete the removal of precipitation solvent. In the described downstream stage, the precipitation steps to purify the biosurfactant were adapted from (WAGNER et al., 1991). The solution of ethanol/water (50:50, v/v) removes xylose from the process. Added methyl ethyl ketone solidifies xylose ester, while the oleic acid remains in the liquid phase. As mentioned, these steps are repeated multiple times to achieve high degree of the purification process.

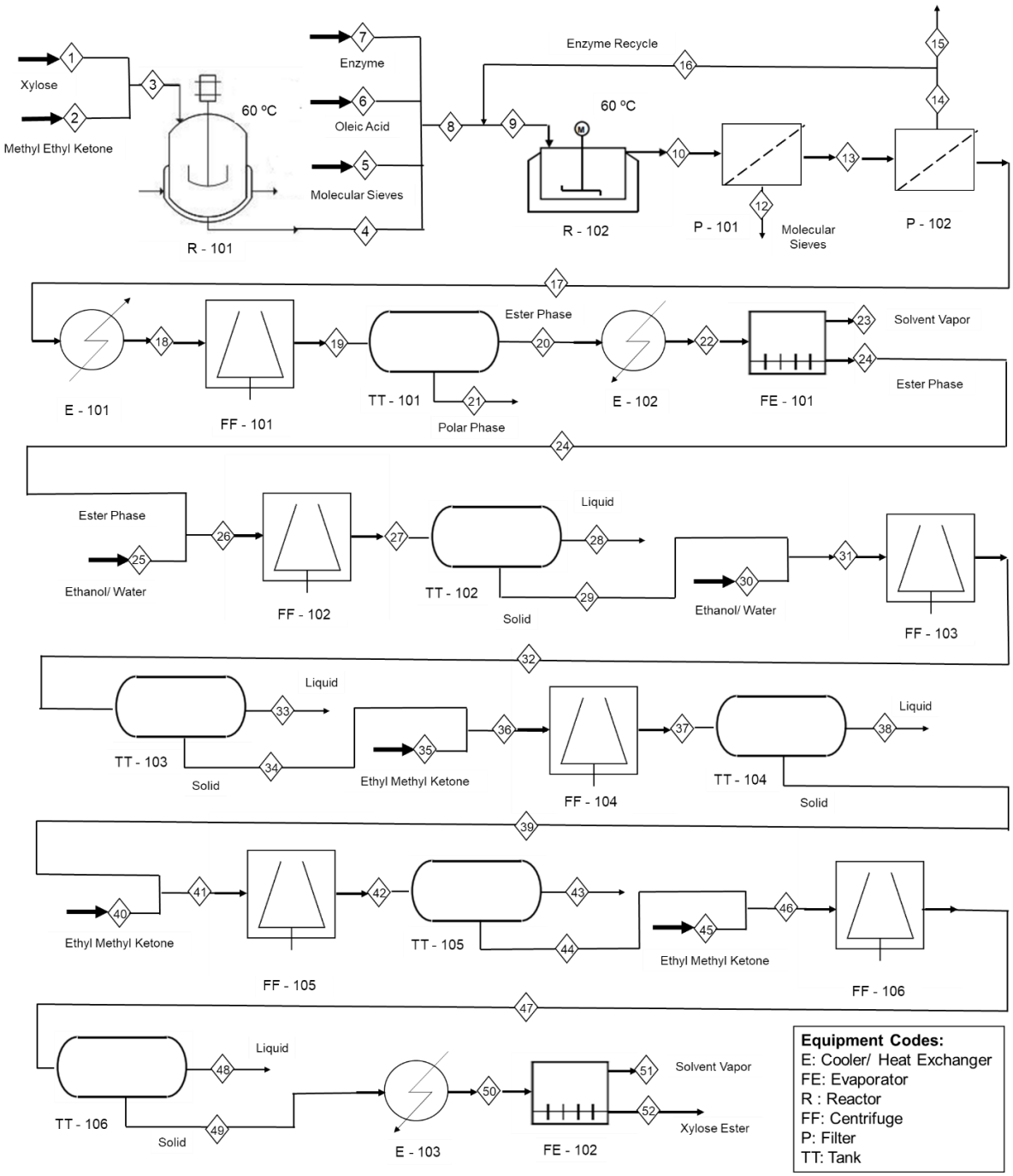

Figure 1. Representation of the production process of xylose ester by enzymatic route.

3.4.2 Modeling and simulation of the process

Phenomenological models were used to describe the process through mass and energy balances (Adapted from CANSIAN et al. (2022) and FURLAN et al. (2016). To simplify the system, considerations for pressure were performed. The reaction kinetics of the xylose ester is given by Equation 6, and GONÇALVES et al. (2021) obtained the parameters. Table 3 contains the main equations and equipment used in modeling the process.

Table 3. Main equations and equipment of the process.

Mixer	Global molar balance: $F_{in,1} + F_{in,2} = F_{out}$ (2)
	Molar balance per component: $F_{in,1} \times z_{in,1} + F_{in,2} \times z_{in,2} = F_{out} \times z_{out}$ (3)
	Pressure: $P_{out} = \min(P_{in,1}, P_{in,2})$ (4)
	Energy balance: $F_{out} \times h_{out} = F_{in,1} \times h_{in,1} + F_{in,2} \times h_{in,2}$ (5)
Reactor	Reaction rate: $v = \frac{v_{max} \cdot C_{OA} \cdot C_{Xyl}}{K_{m(OA)} \cdot C_{Xyl} + K_{m(Xyl)} \cdot C_{OA}}$ (6) $v_{max} = 1.57 \frac{mM}{min} \quad K_{m(OA)} = 1120.40\ mM \quad K_{m(Xyl)} = 754.16\ mM$
	Molar balance per component: $\frac{dC_{OA}}{dt} = -\frac{v_{max} \cdot C_{OA} \cdot C_{Xyl}}{K_{m(OA)} \cdot C_{Xyl} + K_{m(Xyl)} \cdot C_{OA}}$ (7) $\frac{dC_{Xyl}}{dt} = -\frac{1}{5}\frac{v_{max} \cdot C_{OA} \cdot C_{Xyl}}{K_{m(OA)} \cdot C_{Xyl} + K_{m(Xyl)} \cdot C_{OA}}$ (8) $\frac{dC_{Ester}}{dt} = \frac{v_{max} \cdot C_{OA} \cdot C_{Xyl}}{K_{m(OA)} \cdot C_{Xyl} + K_{m(Xyl)} \cdot C_{OA}}$ (9)
	Energy balance: $F_{out} \times h_{out} = F_{in} \times h_{in} + Q - F \times h_R \times X \times z_{limt}$ (10)
	Reactor pressure: $P_{in} = P_{out}$ (11)
Filter	Global molar balance: $F_{in} = F_{out,Solid} + F_{out,Fluid}$ (12)

	Efficiency of liquid separation: $Fw_{out,Fluid} = Fw_{in,Fluid} \times frac_{liq}$ (13)
	Efficiency of solid separation: $Fw_{out,Solid} = Fw_{in,Solid} \times frac_{sol}$ (14)
	Humidity in the solid stream: $humidity = \frac{Fw_{out,Fluid}}{Fw_{out}}$ (15)
	Impurity in the fluid stream: $impurity = \frac{Fw_{out,Solid}}{Fw_{out}}$ (16)
	Energy balance: $T_{out,Solid} = T_{out,Fluid} = T_{in}$ (17) $h_{out,Solid} = h_{out,Fluid} = h_{in}$ (18)
	Pressure: $P_{out,Solid} = P_{out,Fluid} = P_{in}$ (19)
Cooler/ Heater	Global molar balance: $F_{in} = F_{out}$ (20) $z_{in} = z_{out}$ (21)
	Heater: $\|Q\| = U \times A_e \times lmtd$ (22) $lmtd = \frac{\Delta T_1 - \Delta T_2}{\ln\left(\frac{\Delta T_1}{\Delta T_2}\right)}$ (23)
	Pressure: $P_{out} = P_{in} - P_{drop}$ (24)
Splitter	Global molar balance: $F_{in} = F_{out,1} + F_{out,2}$ (25)
	Molar balance per component: $F_{in} \times z_{in} = F_{out,1} \times z_{out,1} + F_{out,2} \times z_{out,2}$ (26)
	Energy balance: $F_{out,1} \times h_{out,1} + F_{out,2} \times h_{out,2} = F_{in} \times h_{in}$ (27)
	Pressure: $P_{out,1} = P_{out,2} = P_{in}$ (28)

The whole process is simulated as a continuous one, that is, the variables do not change over time. However, reaction kinetics did. So, to adapt the reactor equation to the process, a meta-model to these data was fitted to obtain the product's global conversion and insert it in the continuous problem. The universal Kriging meta-model employed is given by Equation 29. The term $\hat{\mu}(x)$ corresponds to the linear regression model and consists of a set of polynomial functions. Meanwhile, z(x) is a zero-mean stationary gaussian process.

$$\hat{y}(x) = \hat{\mu}(x) + z(x) \tag{29}$$

To obtain the meta-model, the initial concentrations of the reagents (C_{OA} and C_{Xyl}) were utilized as input data, while the final concentration of the product (C_{Ester} - xylose ester) was utilized as the output, with an integration period of 24 hours.

The basis of this simulation is calculated by the amount of biosurfactant produced per hour. It was considered a plant installed in São Paulo State, Brazil, operating every day, 24 hours per day, for 300 days a year (the days remaining are reserved for equipment cleaning and maintenance). Based on around 15% of surfactant imports (COMEXSTAT, 2022), a production value close to 2.5 tons per hour was reached.

The EMSO software was employed to solve the equations based on the modeling presented. The simulated process has 4257 equations, with 4386 variables and 129 specifications. Some of these specifications are presented in Table 4 while Table 5 shows the components used throughout the modeling and simulation processes.

Table 4. Main process specifications.

Equipment/ Stream	Variable	Name	Value	Unit
R - 102 / R - 101	T	Temperature	333.15	K
P - 101/ P - 102	frac_sol	Fraction of solids in the liquid stream	0.99	dimensionless
P - 101/ P - 102	humidity	Fraction of liquid in the solid stream	0.10	dimensionless
Splitter between streams 14 and 15	frac	Fraction of the stream that will be removed from the process	0.10	dimensionless
E - 101/ E - 102	Pdrop	Pressure loss	0	atm
E - 101	Outlet.T	Output temperature	383.15	K
E - 102	Outlet.T	Output temperature	298.15	K
E - 101/ E - 102	U	Global heat exchange coefficient	0.6945	kW/m²/K
E - 101/ E - 102	lmtd	Logarithmic mean temperature difference	10	K
Stream 1	F	Molar flow of xylose	7	kmol/h
Stream 2	F	Molar flow of methyl ethyl ketone	103.015	kmol/h
Stream 6	F	Molar flow of oleic acid	35	kmol/h
Stream 7	F	Molar flow of enzyme	0.0214	kmol/h
Streams 25 and 30 (total)	F	Molar flow of etanol/ water 50:50 (v:v)	30898.50	kmol/h
Streams 35, 40 and 45 (total)	F	Molar flow of methyl ethyl ketone	13412.70	kmol/h

Table 5. Components phase used in the simulation.

Components in the liquid phase	Components in the solid phase
Xylose	Xylose
Oleic Acid	Oleic Acid
Xylose Ester	Xylose Ester
Ethanol	Immobilized Lipase
Water	Molecular Sieves
Ethyl Methyl Ketone	-

3.4.3 Technical-economic analysis

The costs calculated in the economic analysis are divided into capital (CAPEX) and operational (OPEX). CAPEX is given by the cost of the physical plant, with dimensioning of equipment, connections, electrical installations, among others. OPEX includes reagents, energy, utilities, labor, supervision, and maintenance costs. These costs are based on the mass and energy balances from the process simulation.

The scheme in Figure 1 was evaluated according to the duration of each step to adjust the process. As shown in Figure 2, through Gantt chart, the purification steps require significantly less time than the others do: while the xylose solubilization and esterification take place, the equipment used in downstream can be reused. Figure 3 shows what the process looks like, and which equipment is reused. Therefore, CAPEX and OPEX are based on the process summarized in Figure 3.

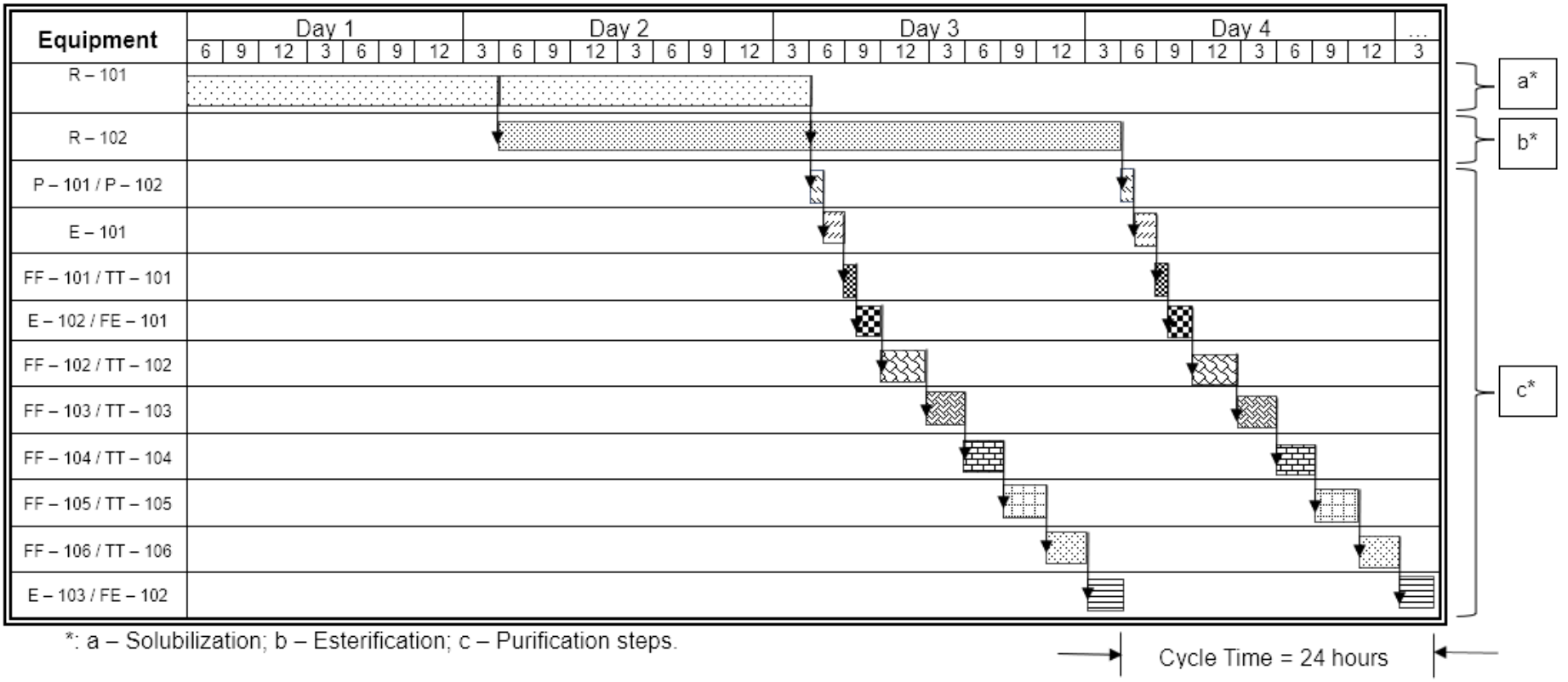

Figure 2. Gantt chart for production of xylose ester by enzymatic route.

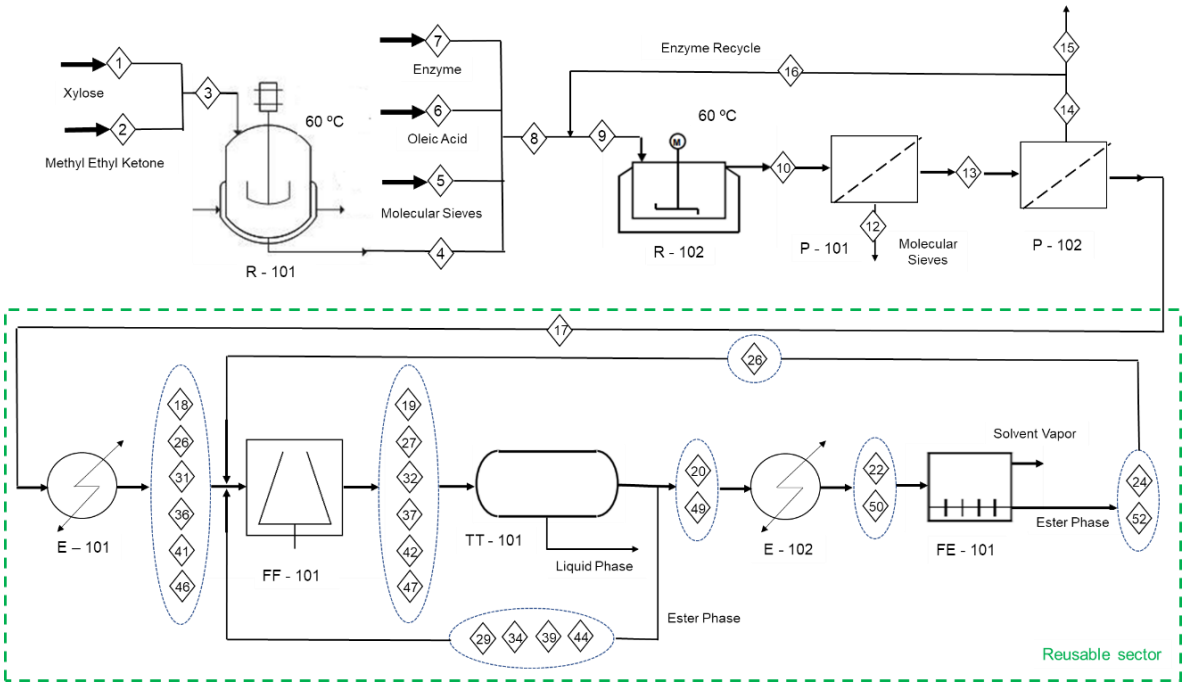

Figure 3. Representation of the equipment used in the production of xylose ester by enzymatic route.

3.4.4 Equipment cost

The equipment cost can be described by Equation 30 (presented in Table 6), with minimum and maximum size specifications. When the simulation indicates an area or volume above the specified maximum, the total number of equipment is adjusted accordingly.

The basic modular costs are calculated depending on the equipment type. Equation 31 is for reactors and filters, Equation 32 for exchangers and process vessels (TURTON et al., 2009).

Since the previous equations were generated in 2001, it is necessary to correct the estimative for the present time by applying Equation 33. It is also essential to adapt the prediction to the location where the equipment will be installed, using Equation 34. Finally, the total cost of installing the plant is given by Equation 35 (TURTON et al., 2009).

Table 6. Equations for equipment costs.

Equipment cost	$\log_{10} C_P^0 = K_1 + K_2 \log_{10}(A) + K_3[\log_{10}(A)]^2$ C_P^0: Equipment cost under standard conditions (carbon steel and atmospheric pressure); K_i: Specific constants for each equipment; A: Equipment cost attribute (area or volume).	(30)
Bare module equipment cost (sum of the direct and indirect costs of each unit)	$C_{BM} = C_P^0 \cdot F_{BM}$ C_{BM}: Bare module equipment cost; F_{BM}: Bare module equipment cost factor.	(31)
	$C_{BM} = C_P^0(B_1 + B_2)$ B_1: Bare module equipment cost factor 1; B_2: Bare module equipment cost factor 2.	(32)
Time-corrected cost	$C_2 = C_1\left(\frac{I_2}{I_1}\right)$ C_1: Cost of equipment at time 1; C_2: Cost of equipment at time 2; I_1: Price index (Chemical Engineering Plant Cost Index (CEPCI)) at time 1 (Sept 2001, CEPCI = 397); I_2: Price index at time 2 (March 2023, CEPCI = 799.3).	(33)
location-adjusted cost	$C_B = C_{USGC} \cdot LF_B$ C_B: Equipment cost in Brazil; C_{USGC}: Equipment price in USA gulf coast; LF_B: Brazil location factor: LF_B =1.14 (Turton et al. 2009).	(34)
Plant installation cost (CAPEX)	$C_{TM} = 1.18\sum_{i=1}^{n} C_{BMi}$ C_{TM}: Plant total cost; C_{BMi}: Equipament – i price (already corrected for time and location).	(35)

3.4.5 Labor costs

Labor costs can be estimated using Table 7, where the number of shift operators in a chemical plant is found and applies the information about each operator's fees for an employer. The medium employee salary who has completed high school in Brazil is about R$3641.50, besides 68.17% tax on this amount (CAGED, 2021).

Table 7. Direct Operating Labor Requirements for Chemical Processing Plants. Basis: Plant with Automatic Controls and 10–100 Ton/day of Product.

Type of Process	Number of Operators per Process Section
Continuous operation	
Fluids processing	1
Solids–fluids processing	2
Solids processing	3
Batch or semi-batch operation	
Fluids processing	2
Solids–fluids processing	3
Solids processing	4

Adapted from SEIDER et al. (2017).

3.4.6 Net Present Value (NPV) calculation

The NPV is a metric capable of determining the present value of future payments discounted at an appropriate interest rate, subtracting the cost of the initial investment. This metric indicates the viability of the investment when it is greater than zero. Therefore, the scenario with a minimum return on investment (NPV = 0) generated the minimum biosurfactant selling price (MBSP). NPV is calculated according to Equation 36, as in (PETERS et al. 2004). For this work, a minimum attractive rate of return of 11% per year was used, considering a project life of 25 years (LONGATI et al., 2018).

$$NPV(X) = \sum_{J=1}^{N} \frac{CF(X)}{(1+r)^j} - CAPEX(X) \tag{36}$$

3.4.7 Retro-Techno-Economic Analysis (RTEA)

RTEA is a methodology to assess the viability of any process to guide its implementation. Firstly, a traditional techno-economic analysis is performed based on the simulation data process. Then, a value of the economic metric is fixed (e.g. NPV = 0), and diagrams of the main process variables are obtained. These diagrams contain "isoeconomic" curves, representing a constant economic performance. They are built by varying x1 and x2 and then obtaining x3 (x1, x2, and x3 are process variables) (FURLAN et al., 2016).

Given the model size, many variables can be used in RTEA. However, not all variables available impact the response to the problem. Therefore, to select them, a local sensitivity analysis is carried out. This analysis shows how a minor disturbance in an input variable's value influences the output. Sensitivity analysis was performed using Equation 37.

$$S_{X_i} = \frac{d(\text{MBSP})}{\text{MBSP}} \frac{X_i}{d(X_i)} = \frac{d(\ln MBSP)}{d(\ln X_i)} \tag{37}$$

3.4.8 Life Cycle Assessment (LCA)

The LCA is a method used to calculate the impact of the process on the environment. The database Ecoinvent 3.0 and the software SimaPro 9.0.0.35 were used. The CML-IA baseline V3.04 (World 2000) method was applied to obtain the indicators below: abiotic depletion - fossil fuels (AD), global warming potential (GWP100), ozone layer depletion (ODP), human toxicity (HT), freshwater aquatic ecotoxicity (FWAET), marine aquatic ecotoxicity (MAET), terrestrial ecotoxicity (TET), photochemical oxidation (PO), acidification (AC), and eutrophication (EU). The parameters from the dataset were incorporated into the simulation at EMSO to calculate the indicators.

3.5 Results and discussion

3.5.1 Simulation

Initially, the reaction kinetics was modified from a time-varying model to a static meta-model. Then, the model for the enzyme kinetics was integrated for 24 h (Figure 4 (a)), with the concentration of reagents and product over time. The data were generated in the integration of this model for different initial conditions of reagents' concentration, and the Kriging meta-model was obtained. Figure 4 (b) compares the meta-model responses with those obtained from the rigorous enzyme kinetics model (both show the final concentration of xylose ester). The root-mean-square error (RMSE) for the validation was 0.4271 mM, which corresponds, on average, to approximately 10% relative error.

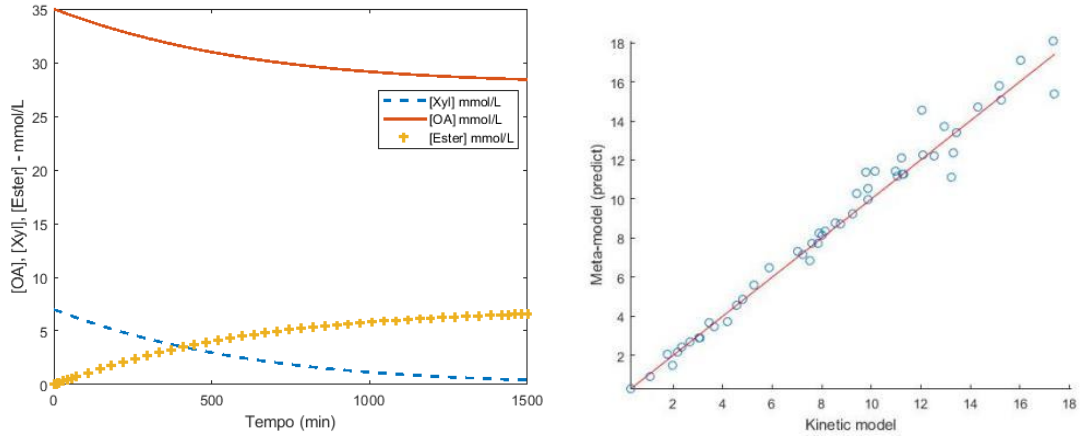

(a) (b)

Figure 4. (a) Model response simulated from the data of (GONÇALVES et al., 2021) for sugar ester production kinetics, showing reagents and product concentration for initial condition of $[C_{Xyl}]$ = 7 mM, $[C_{OA}]$ = 35 mM and 24h of reaction. (b) Correlation between data points obtained from the rigorous kinetic model and the responses predicted by the meta-model, for validation data related to the final concentration of ester ($[C_{Ester}]$ - mM) in a final time of 24h.

The RMSE for the validation was 0.4271, showing that the meta-model can predict the enzymatic kinetics of xylose ester production from oleic acid and xylose with good accuracy. Thus, the meta-model was incorporated in the steady-state simulation of the whole biosurfactant process to analyze the variables' effect on the process performance.

Table 8 shows the results for some streams in the process. The solution obtained from the simulation, specifically mass balances, is consistent with the data presented by (GONÇALVES et al., 2021). As the mass fraction of xylose ester in stream 24 is approximately 22%, purification steps are required to achieve higher concentrations of biosurfactant in the product.

First, as shown in Table 8, the product enters downstream at 21.8% in mass composition (stream 24) after enzyme removal in the reactor exit. Then, it reaches 73% (stream 34) with the precipitation process using ethanol/water. Then, applying methyl ethyl ketone comes to 95.02% (stream 49), and last, it reaches ~96% (stream 52) after the evaporator.

Table 8. Results for main streams.

Variable	Name	Unit	Stream 24	Stream 34	Stream 49	Stream 52
Fw	Mass flow	kg/h	11068.60	3240.81	2464.93	2440.29
T	Temperature	K	453.15	298.15	298.15	453.15
P	Pressure	atm	1	1	1	1
zw(1)*	Composition	dimensionless	0.0231	0.0009	0.0012	0.0012
zw(2)*	Composition	dimensionless	0.7358	0.2578	0.0369	0.0373
zw(3)*	Composition	dimensionless	0.2181	0.7300	0.9502	0.9598
zw(4)*	Composition	dimensionless	0.0000	0.0071	0.0000	0.0000
zw(5)*	Composition	dimensionless	0.0000	0.0028	0.0000	0.0000
zw(6)*	Composition	dimensionless	0.0226	0.0000	0.0100	0.0000
zw(7)*	Composition	dimensionless	0.0004	0.0014	0.0018	0.0018

* Component number: Liquids: 1-Xylose; 2-Oleic Acid; 3-Xylose Ester; 4-Ethanol; 5-Water; 6-Ethyl Methyl Ketone; 7-Immobilized Lipase.

3.5.2 Technical-economic analysis

3.5.2.1 Equipment cost

The equipment costs were calculated using Equation 30, the process stream values obtained in the simulation, equipment dimensions, and the parameters shown in Table 9. The results of the calculations are shown in Table 10. The total installation cost of the plant was approximately 6 million dollars, already considering all corrections and additions made by Equations 31, 32, 33, 34 and 35.

Figure 5 (a) presents the CAPEX distribution of equipment costs. The precipitation tank is the most impactful, followed by the heat exchanger, evaporator, reactors, centrifuge, and lastly, the filters. It indicates that precipitation for product purification is what most impacts CAPEX.

Table 9. Equipment cost parameters.

Equipaments	K_1	K_2	K_3	FBM	B1	B2	LF_B	A_{min}	A_{max}	Unit
Reactor (Jacketed agited)	4.1052	-0.4680	-0.0005	4.00	-	-	1.14	0.1	35	m^3
Filter (Gravity)	4.2756	-0.648	0.0714	1.65	-	-	1.14	0.5	80	m^2
Heat exchanger (Fixed tube)	4.3247	-0.3030	0.1634	-	1.63	1.66	1.14	10	1000	m^2
Tank (Fixed roof)	4.8509	-0.3973	0.1445	-	1.49	1.52	1.14	90	30000	m^3
Flash (Vaporizer)	3.8751	0.3328	0.1901	2.65	-	-	1.14	1	100	m^3
Centrifuge separator	4.3612	-0.1236	0.0049	1.57	-	-	1.14	0.5	1	m

Adapted from TURTON et al. (2009).

Table 10. Equipment capacity and costs.

Equipment	Category	Capacity	Cost
R - 101	Reactor - Jacketed agitated	178.27 m^3 (Volume)	MUS$ 0.1326
R - 102	Reactor - Jacketed agitated	440.54 m^3 (Volume)	MUS$ 0.2872
P - 101	Filter - Gravity	11.12 m^2 (Area)	MUS$ 0.0179
P - 102	Filter - Gravity	651.18 m^2 (Area)	MUS$ 0.0682
E - 101	Heat exchanger - Fixed tube	76.25 m^2 (Area)	MUS$ 0.1206
E - 102	Heat exchanger - Fixed tube	156.16 m^2 (Area)	MUS$ 0.3631
FE - 101	Flash - Vaporizer	23.86 m^3 (Volume)	MUS$ 0.3390
TT - 101	Tank (Fixed roof)	12205.64 m^3 (Volume)	MUS$ 3.6313
FF - 101	Centrifuge separator	0.1 m (Radius)	MUS$ 0.1113
	Total		MUS$ 5.0712
	Total plant installation		MUS$ 5.9840

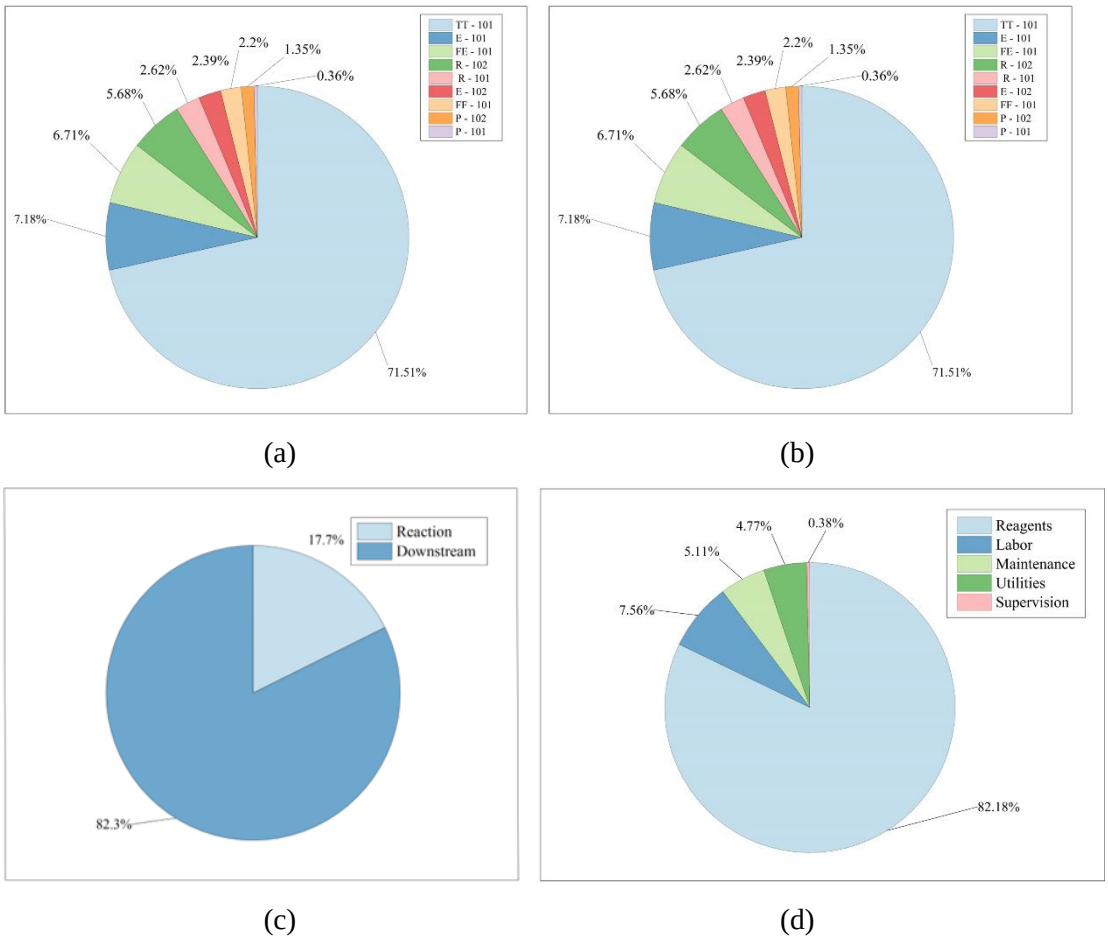

Figure 5. (a) Fraction representation of each equipment in the plant installation (CAPEX). **(b)** Fraction representation of each reagent in the process (OPEX). **(c)** Fraction representation of each sector in the plant installation (CAPEX). **(d)** Fraction representation of each sector in operating costs (OPEX).

3.5.2.2 Labor costs

The labor costs were calculated based on the values of an average Brazilian worker. As a result of using Table 7, and considering five daily shifts, government fees, and exchange rate, Table 11 summarizes information about operators and their costs. Ergo, it is necessary approximately U$ 0.4409 million to keep the plant in operation.

Table 11. Labor costs and calculations.

NOL (per turn)	Turns	Total workers	Salary per month	Taxes per month	Worker cost per month	Total (per year)
6	5	30	R$ 3641.50	3641.50 x 0.6817 = R$ 2482.41	US$ 1224.78	1224.78 x 30 x 12 = MUS$ 0.4409

3.5.2.3 Net Present Value (NPV) calculation

For the NPV to be calculated, it is necessary to have a well-defined cash flow. It considers not only the sale of the biosurfactant but also operating costs: reagents, utilities, labor, supervision, and maintenance. Table 12 contains reagent costs, and Table 13 presents energy costs. It is noteworthy that the operating supervision costs are about 5% of operating labor costs, and the maintenance costs are about 5% of capital cost (PETERS et al., 2004).

Regarding the raw material, the most significant impact on the process is given by the methyl ethyl ketone solvent, followed by the oleic acid reagent, and only then are the enzyme and other materials (See Figure 5 (b)). The impact of the solvent on the process costs is also visible in Figure 5 (c), which highlights the impact that the purification steps have on the process as a whole.

As for the operating costs, the largest fraction is given by reagents (Figure 5 (d)), followed by labor costs, maintenance, utilities, and supervision.

To find the minimum biosurfactant selling price (MBSP), we utilized the NPV = 0. With that, and from all the previously calculated costs, an MBSP of US$ 392.98 per kg of biosurfactant produced with 96% purity in xylose ester was found. The value is below that presented by (EKPENYONG et al., 2021) and above that of (MOUTINHO et al., 2021), (ELIAS et al., 2021), and (CANSIAN et al., 2022). Despite being above average, xylose ester is a product with different characteristics from the others, with a higher degree of purity, and which can be used in the food and cosmetics sectors since the solvent used, methyl ethyl ketone has lower toxicity and allows such applications. Therefore, all these characteristics add value to the product, making it competitive.

Table 12. Reagents costs.

Component	kg/h	US$/kg[+]
Xylose	1050.92	25.24
Enzyme	0.4896	173960.30
Ethanol	14234.60[*]	4.29
Ethyl Methyl Ketone	19491.50[*]	32.35
Oleic Acid	9886.28	15.71

*: It was considered the partial recovery of these reagents and was adopted 2% lost from initial simulation results (1% associated with recuperation costs and the other 1% with separation inefficiencies); +: Reagent prices were given from well-known brands (Sigma, Neon, Glasslab) and technical sources in the industry.

Table 13. Energy costs.

Type	Heat (MWh)	Total US$	
Hot	23962.18	23962.18 x 10.1 =	242018.02
Cold	6879.43	6879.43 x 5.26 =	36185.80
		Total	**US$ 278203.82/year**

3.5.3 Retro-Techno-Economic Analysis (RTEA)

Before performing the RTEA, it is necessary to choose which variables will be evaluated through local sensitivity analysis, applying Equation 37. As we can see in Table 14, the main variables that impact MBSP with higher sensitivity values are enzyme ratio, fraction of ester precipitation, methyl ethyl ketone ratio, molar ratio of reagents, esterification conversion and xylose solubilization. However, despite the values obtained in Table 14, the simulation does not present physically feasible scenarios regarding the numerical solution of the set of model equations when some of the most sensitive variables are set away from their values at the local solution. Therefore, only possible scenarios with feasible numerical solutions are presented, considering the fraction of ester precipitation and xylose solubilization to analyze the methyl ethyl ketone price, in Figure 6, and the fraction of ester precipitation and esterification conversion for MBSP, in Figure 7.

Figure 6 presents the RTEA results evaluating the market price of methyl ethyl ketone solvent (in US$/kg) as a function of the ester precipitation fraction (in the purification step) for

different values of xylose solubilization (in the first reactor), using MBSP = US$20/kg. In this situation, there is no scenario in which this process becomes practically feasible, because theoretical viable area would be associated with negative values for methyl ethyl ketone price (in the range of minus US$12-17/kg). This indicates that the path to make the process economically competitive is to reduce the amount of solvent used instead of maximizing the reactional conversion of the products.

Table 14. Sensitivity analysis normalized results.

Variables	Sensitivity	Variables	Sensitivity
Xylose price	0.0002	Fraction of ester precipitation	-0.9068
Enzyme price	0.0001	Evaporator outlet Temperature	-0.00054
Ethanol price	0.0029	Molar ratio of reagents	0.1412
Methyl ethyl ketone price	0.0039	Enzyme ratio	1
Oleic acid price	0.0020	Methyl ethyl ketone ratio	0.25209
Xylose solubilization	-0.0041	Outlet Temperature of heat exchanger	0.0000
Esterification conversion	-0.0801	Heat required in the Evaporator	0.0000

The RTEA were also evaluated in Figure 7 with the market price of biosurfactant in US$/kg as a function of a fraction of ester precipitation for different values of ester conversions, using NPV equal to zero. Here we observe that the higher the ester conversion and precipitation simultaneously, the lower the selling price of the biosurfactant that makes the process viable. For example, in a hypothetical scenario where there is conversion and precipitation of 100%, the MBSP reaches US$384.27. On the other hand, against a pessimistic scenario where ester conversion reaches 80% and precipitation 10%, the MBSP reaches a value of US$2533.74. In this perspective, for the price of the biosurfactant to follow the market and become competitive, a higher yield in reaction kinetics must be obtained in addition to the lower use of solvents.

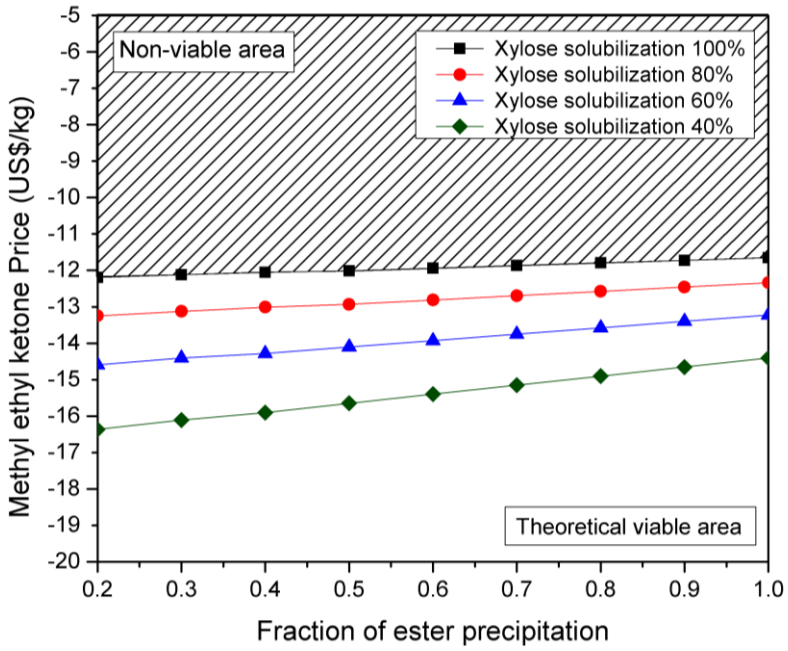

Figure 6. Market price of methyl ethyl ketone solvent in US$/kg as a function of fraction of ester precipitation for different values of xylose solubilization (with MBSP = US$20/kg).

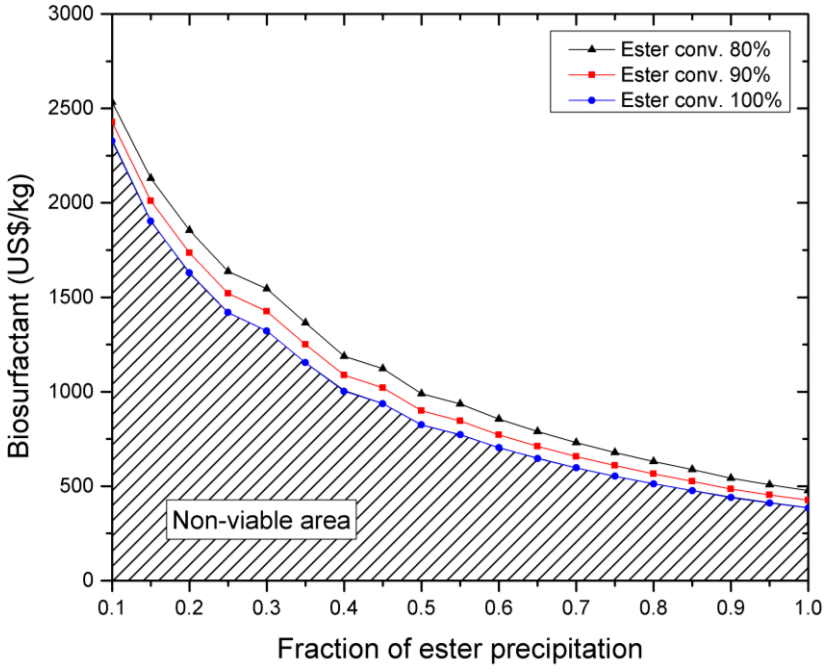

Figure 7. Market price of biosurfactant in US$/kg as a function of fraction of ester precipitation for different values of ester conversions (with NPV = 0).

3.5.4 Life Cycle Assessment (LCA)

The LCA results were obtained from the mass balances of the process and all calculated indicators are based on 1 kg of biosurfactant production. The absolute results for the environmental indicators are shown in Figure 8. For instance, the carbon emission calculated by the GWP100 is about 34 kg of carbon dioxide equivalent per kg of biosurfactant produced. This indicator is above that of (ELIAS et al., 2021) (~17.1 kg CO2 eq./kg of biosurfactant). On the other hand, other indicators showed lower values, such as ozone layer depletion (ODP), human toxicity (HT), marine aquatic ecotoxicity (MAET), photochemical oxidation (PO), acidification (AC) and eutrophication (EU).

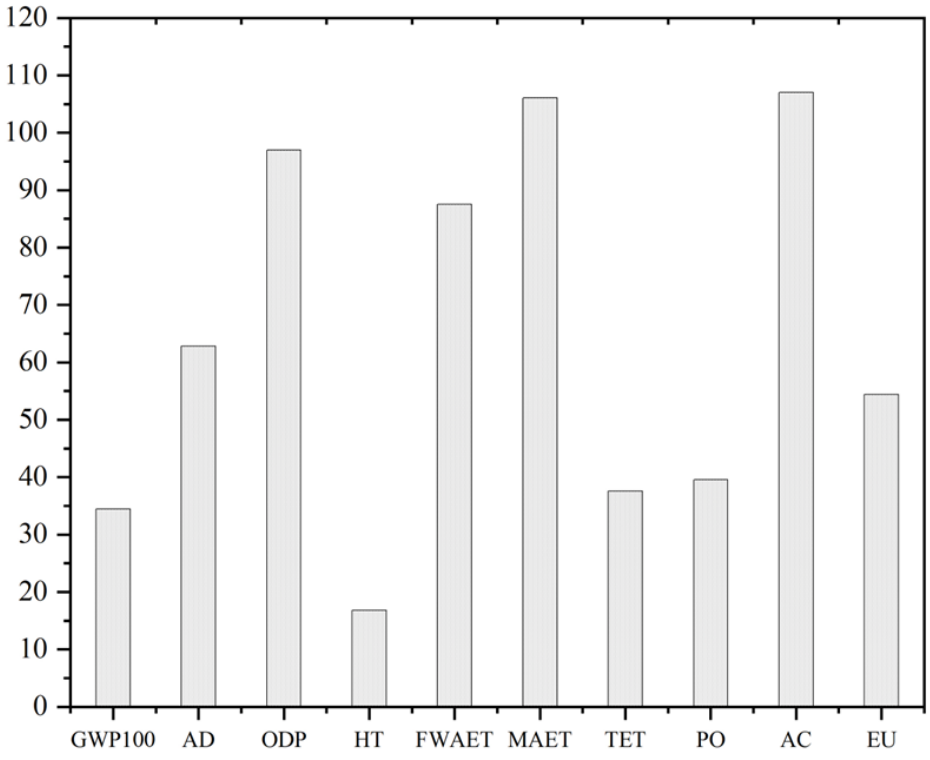

Figure 8. Environmental impact with absolute scores of the LCA for the process.

The human toxicity indicator reinforces the use of methyl ethyl ketone as a solvent and justifies the market value of xylose ester in its applicability in the food and esthetics industries. It is also worth highlighting the purity of the biosurfactant obtained in this work, which justifies a more significant impact of equivalent carbon dioxide, as it requires higher effort in the

downstream steps. This impact is shown in Figure 9, with the indices being presented in relative percentage values. We can see that the purification steps have a greater impact on all indicators except FWAET, TET and EU. Finally, Figure 10 also presents relative values of the environmental indicators, split regarding the percentages for energy, water, and reagents. The oleic acid has more impact on ODP, FWAET, TET, and EU. It is noticed that methyl ethyl ketone is the agent with the most significant effect on GWP100, AD, and MAET indicators. Finally, the ethanol impacts go on for just PO indicator. This is mainly due to the purification steps that require high use of solvents for the results to be achieved.

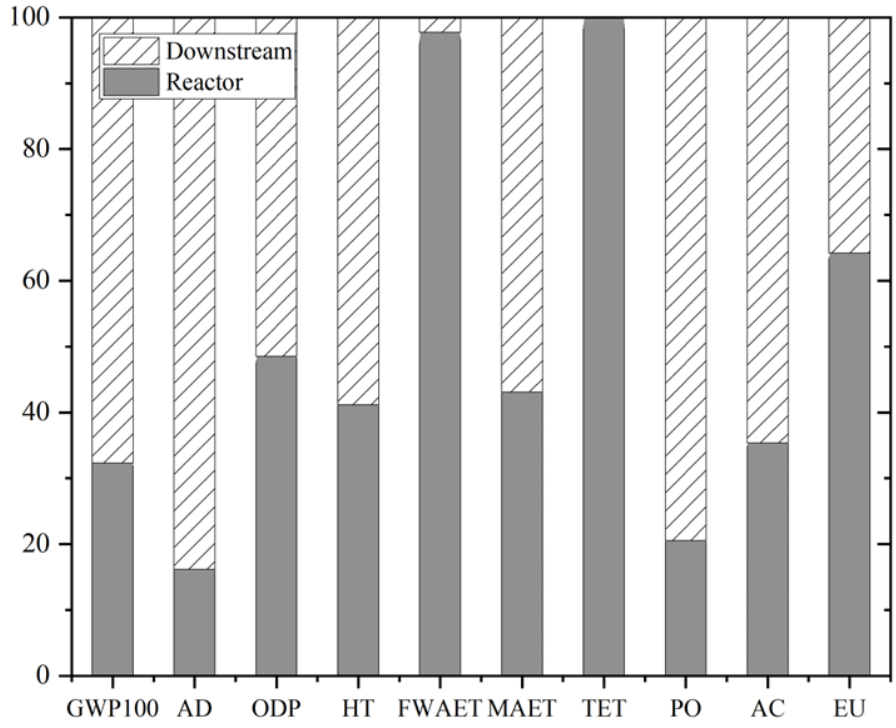

Figure 9. Environmental impact with percentage scores of the LCA for the process.

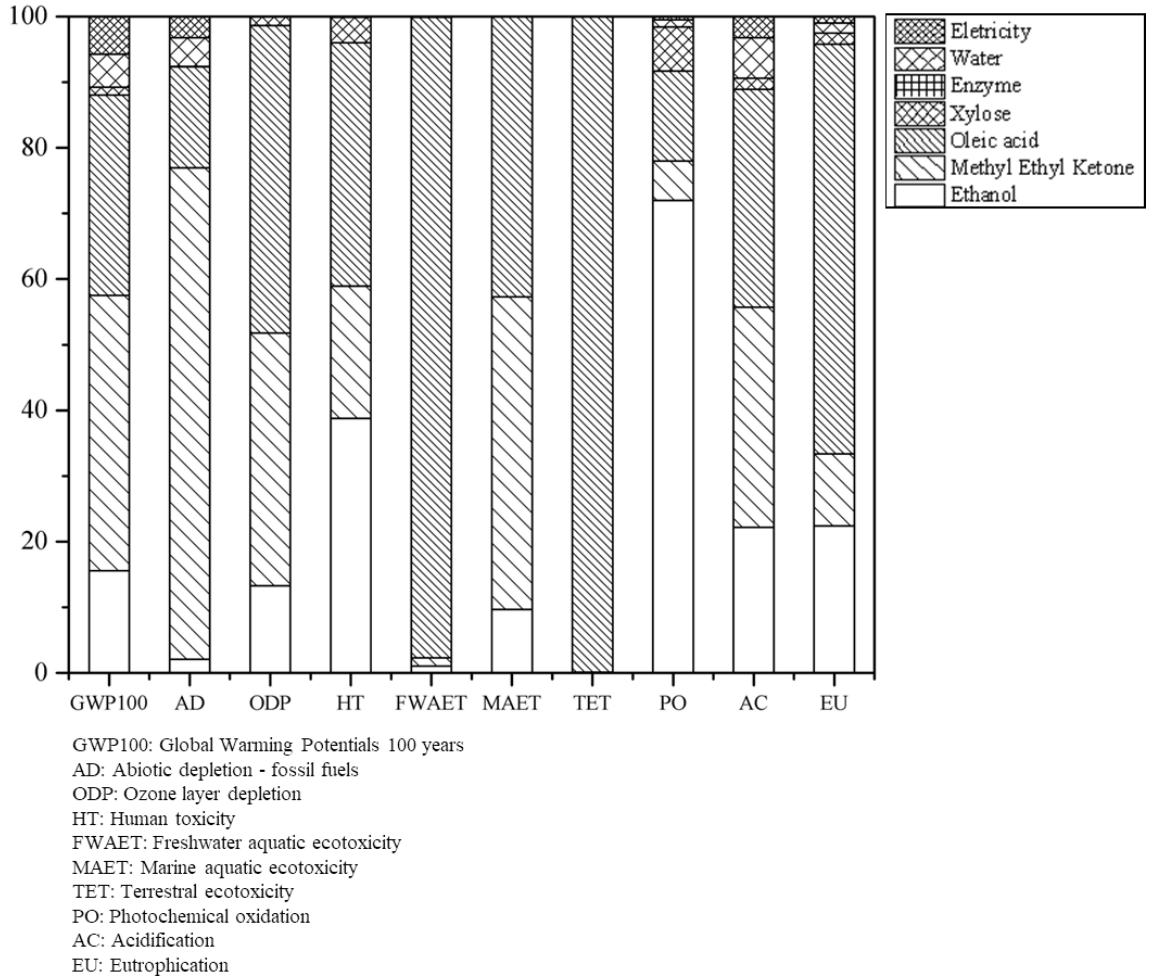

Figure 10. Environmental impact with percentage scores of the LCA for the process, separated by utilities and raw materials.

3.6 Conclusions

The enzymatic process for the biosurfactants production, in particular, xylose ester from oleic acid and xylose, was successfully described by the set of equations generated by the mathematical model developed. The simulation described the esterification reaction and the downstream purification steps to obtain a biosurfactant with approximately 96% purity. The economic analysis covered the CAPEX and OPEX cost calculations to assess a plant working throughout 25 years, obtaining a MBSP of US$ 392.98 per kg of biosurfactant produced. The process production cost obtained is justified by high biosurfactant purity and applicability in the pharmaceutical and cosmetic industries. On the other hand, RTEA indicated that process modifications could reduce this cost if carried out efficiently. Although the assays must be developed to investigate the theoretical RTEA results further, this is beyond the scope of this paper. As for LCA, the product showed low levels of ozone layer depletion, human toxicity, aquatic marine ecotoxicity, and photochemical oxidation, highlighting its environmental viability and lower impact. All these environmental indicators bring even more attractiveness to the product, given the current search for environmentally friendly products.

SYMBOLS

h_R	Reaction enthalpy
$h_{in,1}$	Enthalpy of stream at input 1 of the equipment
$h_{in,2}$	Enthalpy of stream at input 2 of the equipment
h_{in}	Enthalpy of stream at input of the equipment
$h_{out,1}$	Enthalpy of stream at output 1 of the equipment
$h_{out,2}$	Enthalpy of stream at output 2 of the equipment
$h_{out,Fluid}$	Enthalpy of stream at fluid output of the equipment
$h_{out,Solid}$	Enthalpy of stream at solid output of the equipment
h_{out}	Enthalpy of stream at output of the equipment
A_e	Heat exchange area
B_1	Bare module equipment cost factor 1
B_2	Bare module equipment cost factor 2
C_1	Cost of equipment at time 1
C_2	Cost of equipment at time 2
C_B	Equipment cost in Brazil
C_{BMi}	Equipment – i price (already corrected for time and location)
C_{Ester}	Xylose ester concentration
C_{OA}	Oleic acid concentration
C_P^0	Equipment cost under standard conditions (carbon steel and 1 atm pressure)
C_{TM}	Plant total cost
C_{USGC}	Equipment price in USA gulf coast
C_{Xyl}	Xylose concentration
F_{BM}	Bare module equipment cost factor
$F_{in,1}$	Molar flow of the stream at input 1 of the equipment
$F_{in,2}$	Molar flow of the stream at input 2 of the equipment
F_{in}	Molar flow of the stream at input of the equipment
$F_{out,1}$	Molar flow of the stream at output 1 of the equipment
$F_{out,2}$	Molar flow of the stream at output 2 of the equipment
$F_{out,Fluid}$	Molar flow of the fluid stream at output of the equipment
$F_{out,Solid}$	Molar flow of the solid stream at output of the equipment
F_{out}	Molar flow of the stream at output of the equipment
$Fw_{in,Solid}$	Mass flow of the solid stream at input of the equipment

$Fw_{in,Fluid}$	Mass flow of the fluid stream at input of the equipment
Fw_{in}	Mass flow of the stream at input of the equipment
$Fw_{out,Solid}$	Mass flow of the solid stream at output of the equipment
$Fw_{out,Fluid}$	Mass flow of the fluid stream at output of the equipment
Fw_{out}	Mass flow of the stream at output of the equipment
I_1	Price index (Chemical Engineering Plant Cost Index (CEPCI)) at time 1
I_2	Price index at time 2
K_i	Specific constants for each equipment
$K_{m(OA)}$	Michaelis constants for oleic acid
$K_{m(Xyl)}$	Michaelis constants for xylose
LF_B	Brazil location factor
P_{drop}	Pressure drop on the heat exchanger
$P_{in,1}$	Pressure at input 1 of the equipment
$P_{in,2}$	Pressure at input 2 of the equipment
P_{in}	Pressure at input of the equipment
$P_{out,1}$	Pressure at the output 1 of the equipment
$P_{out,Solid}$	Pressure at solid output of the equipment
$P_{out,2}$	Pressure at the output 2 of the equipment
$P_{out,Fluid}$	Pressure at fluid output of the equipment
P_{out}	Pressure at the output of the equipment
S_{X_i}	Sensitivity
T_{in}	Temperature of the stream at input of the equipment
$T_{out,Fluid}$	Temperature of the stream at fluid output of the equipment
$T_{out,Solid}$	Temperature of the stream at solid output of the equipment
X_i	Process variable under analysis
$frac_{sol}$	Fraction of input solids leaving the solid stream
v_{max}	The maximum velocity or limiting rate
$\hat{y}(x)$	Kriging meta-model
$z_{in,1}$	Molar composition of the stream at input 1 of the equipment
$z_{in,2}$	Molar composition of the stream at input 2 of the equipment
z_{in}	Molar composition of the stream at input of the equipment
z_{limt}	Composition of the limiting reagent
$z_{out,1}$	Molar composition of the stream at output 1 of the equipment
$z_{out,2}$	Molar composition of the stream at output 2 of the equipment
z_{out}	Molar composition of the stream at output of the equipment

$\hat{\mu}(x)$	Linear regression model
ΔT_1	Temperature difference on side 1
ΔT_2	Temperature difference on side 2
$humidity$	Fraction of liquids in the solids output of the equipment
A	Equipment cost attribute (area, volume, or radius)
$CAPEX(X)$	Capital investments as a function of process variables
$CF(X)$	Cash flow as a function of process variables
$MBSP$	Minimum biosurfactant selling price
N	Project lifetime
$NPV(X)$	Net present value as a function of process variables
Q	Output/Input heat at the equipment
U	Overall heat exchange coefficient
X	Reaction conversion
$frac_{liq}$	Fraction of input liquids leaving the liquid stream
$impurity$	Fraction of solids in the liquid output of the equipment
$lmtd$	Logarithmic average temperature difference
r	Minimum acceptable rate of return
t	Time
v	Reaction rate (esterification kinetic)
$z(x)$	Zero-mean stationary gaussian process

REFERENCES

ABDULMALEK, E.; HAMIDON, N. F.; ABDUL RAHMAN, M. B. Optimization and characterization of lipase catalysed synthesis of xylose caproate ester in organic solvents. **Journal of Molecular Catalysis B: Enzymatic**, v. 132, p. 1–4, 2016.

BANAT, I. M. et al. Microbial biosurfactants production, applications and future potential. **Applied Microbiology and Biotechnology**, v. 87, p. 427–444, 2010.

BIDJOU-HAIOUR, C.; KLAI, N. Lipase catalyzed synthesis of fatty acid xylose esters and their surfactant properties. **Asian Journal of Chemistry**, v. 25, n. 8, p. 4347–4350, 2013.

BOUZAOUIT, N.; BIDJOU-HAIOUR, C. Optimization of lipase catalyzed synthesis of fatty acid xylose ester using statistical experimental designs. **Scholars Research Library Der Pharma Chemica**, v. 7, p. 261-269, 2015.

CAGED. **Federal Government of Brazil**. **Cadastro Geral de Empregados e Desempregados**, 2021.

CANSIAN, A. B. M. et al. Modeling and simulation of the biosurfactant production by enzymatic route using xylose and oleic acid as reagents. **Chemical Industry and Chemical Engineering Quarterly**, v. 28, n. 4, p. 265–276, 2022.

COMEXSTAT. **Federal Government of Brazil**. In: Estatísticas de Comércio Exterior. http://comexstat.mdic.gov.br/pt/geral/44861.

DE LIMA, L. N. et al. Mono- and heterofunctionalized silica magnetic microparticles (SMMPs) as new carriers for immobilization of lipases. **Journal of Molecular Catalysis B: Enzymatic**, v. 133, p. S491–S499, 2016.

DÍAZ DE RIENZO, M. A. et al. Sophorolipid biosurfactants: Possible uses as antibacterial and antibiofilm agent. **New Biotechnology**, v. 32, n. 6, p. 720–726, 2015.

EKPENYONG, M. et al. Kinetic modeling and quasi-economic analysis of fermentative glycolipopeptide biosurfactant production in a medium co-optimized by statistical and neural network approaches. **Preparative Biochemistry and Biotechnology**, v. 51, p. 450–466, 2021.

ELIAS, A. M.; LONGATI, A. A.; ELLAMLA, H. R.; FURLAN, F. F.; RIBEIRO, M. P. A.; MARCELINO, P. R. F.; et al. Techno-Economic-Environmental Analysis of Sophorolipid Biosurfactant Production from Sugarcane Bagasse. **Industrial & Engineering Chemistry Research**, v. 60, n. 27, p. 9833–9850, 2021.

FURLAN, F. F.; COSTA, C. B. B.; SECCHI, A. R.; WOODLEY, J. M.; GIORDANO, R. C. Retro-Techno-Economic Analysis: Using (Bio)Process Systems Engineering Tools to Attain Process Target Values. **Industrial & Engineering Chemistry Research**, v. 55, n. 37, p. 9865–9872, 2016.

GONÇALVES, M. C. P.; AMARAL, J. C.; FERNANDEZ-LAFUENTE, R.; JUNIOR, R. DE S.; TARDIOLI, P. W. Lipozyme 435-mediated synthesis of xylose oleate in methyl ethyl ketone. **Molecules**, v. 26, n. 11, p. 1–18, 2021.

GONÇALVES, M. C. P.; ROMANELLI, J. P.; CANSIAN, A. B. M.; PUCCI, E. F. Q.; GUIMARÃES, J. R.; TARDIOLI, P. W.; SAVILLE, B. A. A review on the production and recovery of sugars from lignocellulosics for use in the synthesis of bioproducts. **Industrial Crops and Products,** 2022.

JEMIL, N. et al. Characterization and properties of biosurfactants produced by a newly isolated strain Bacillus methylotrophicus DCS1 and their applications in enhancing solubility of hydrocarbon. **World Journal of Microbiology and Biotechnology**, v. 32, n. 11, 2016.

JOCQUEL, C. et al. An Integrated Enzymatic Approach to Produce Pentyl Xylosides and Glucose/Xylose Laurate Esters From Wheat Bran. **Frontiers in Bioengineering and Biotechnology**, v. 9, 2021.

LI, L. et al. Esterification degree of fructose laurate exerted by Candida antarctica lipase B in organic solvents. **Enzyme and Microbial Technology**, v. 69, p. 46–53, 1 fev. 2015.

LONGATI, A. A.; LINO, A. R. A.; GIORDANO, R. C.; FURLAN, F. F.; CRUZ, A. J. G. Defining research and development process targets through retro-techno-economic analysis: the sugarcane biorefinery case. **Bioresource Technology**, v. 263, p. 1–9, 2018.

MARTINEZ-GARCIA, M. et al. Enzymatic Synthesis of Glucose- and Xylose Laurate Esters Using Different Acyl Donors, Higher Substrate Concentrations, and Membrane Assisted Solvent Recovery. **European Journal of Lipid Science and Technology**, v. 123, n. 2, 2021.

MÉLINE, T. et al. D-Xylose and L-arabinose laurate esters: Enzymatic synthesis, characterization and physico-chemical properties. **Enzyme and Microbial Technology**, v. 112, p. 14–21, 2018.

MOUTINHO, L. F. et al. Microbial biosurfactants: A broad analysis of properties, applications, biosynthesis, and techno-economical assessment of rhamnolipid production. **Biotechnology Progress**, v. 37, n. 2, 2021.

PETERS, M. S.; TIMMERHAUS, K. D.; WEST, R. E. **Plant design and economics for chemical engineers**. Boston: Mcgraw-Hill, 2004.

PERFUMO, A.; BANAT, I. M.; MARCHANT, R. Going Green and Cold: Biosurfactants from Low-Temperature Environments to Biotechnology Applications. **Trends in Biotechnology**, v. 36, n. 3, p. 277-289, 2018.

SANTOS, D. K. F. et al. Biosurfactants: Multifunctional biomolecules of the 21st century. **International Journal of Molecular Sciences.** MDPI AG, 2016.

SARUBBO, L. A.; DE LUNA, J. M.; DE CAMPOS-TAKAKI, G. M. Production and stability studies of the bioemulsifier obtained from a new strain of Candida glabrata UCP 1002. **Electronic Journal of Biotechnology**, v. 9, n. 4, p. 1–7, 2006.

SEIDER, W. D. et al. Product and Process Design Principles: Synthesis, Analysis, and Evaluation. New York: **John Wiley & Sons Inc**, 2017. v. 4, p. 500–505.

TURTON, R.; BAILIE, R. C.; WHITING, W. B.; SHAEIWITZ, J. A. Analysis, synthesis and design of chemical processes. 3. ed. Upper Saddle River: **Pearson Education**, Inc, 2009. p. 1-1007.

VESCOVI, V.; DOS SANTOS, J. B. C.; TARDIOLI, P. W. Porcine pancreatic lipase hydrophobically adsorbed on octyl-silica: A robust biocatalyst for syntheses of xylose fatty acid esters. **Biocatalysis and Biotransformation**, v. 35, n. 4, p. 298–305, 2017.

VIEIRA, A. C.; CANSIAN, A. B. M.; GUIMARÃES, J. R.; VIEIRA, A. M. S.; FERNANDEZ-LAFUENTE, R.; TARDIOLI, P. W. Performance of liquid eversa on fatty acid ethyl esters production by simultaneous esterification/transesterification of low-to-high acidity feedstocks. **Catalysts**, v. 11, n. 12, 2021.

WAGNER, W. F. W.; LINCOLN, M. A. D.; LINCOLN, V. H. S. Separation and Purification of sugar esters. **Patent** number: 4,983,731, USA, 1991.

CHAPTER 4: Esters from SODD

Soybean oil deodorizer distillate (SODD) as feedstock for esters production: Techno-Economic-Environmental evaluation of enzymatic routes

Under preparation

4.1 Abstract

The constant demand for feasible processes maintaining low environmental indicators has been nonstop in recent decades. In response to these goals, the circular economy has emerged, with one of the pillars of coproduct reuse at all stages of production. In the soybean oil industry context, the refining stage produces a coproduct with significant potential for applications in a biorefinery, further contributing to the circularity of production and the reduction of costs: the Soybean oil deodorizer distillate (SODD). The concentrations of fatty acids and mono-, di-, and triglycerides found in SODD make it as a promising candidate for conversion into esters through reactions with alcohols or sugars, producing biodiesel or biosurfactants. For laboratory research to be applicable on an industrial scale in industries, techno-economic-environmental analyses must indicate the process's economic viability and environmental impacts. There are several studies related to biodiesel containing these analyses. However, they are rarer when using raw materials that do not compete with the food industry. On the other hand, there is a wide variation in the types of biosurfactants, purity, and methods of obtaining them. Nevertheless, no studies that evaluate processes from techno-economic-environmental analysis using SODD were found. In this context, this study aimed to support the development and scaling of biodiesel (fatty acid ethyl esters) and biosurfactants (fatty acid xylose ester) production by conducting a techno-economic and environmental assessment (TEEA) of enzymatic processes using a coproduct from biorefineries (SODD) as a material source of fatty acids. The simulation for producing biodiesel from ethanol and SODD showed a product with approximately 81.57% (w/w) of ethyl esters (ethyl palmitate, ethyl stearate, ethyl oleate, ethyl linoleate, and ethyl linoleate), 0.99% acylglycerides, 14.79% of fatty acids and 1.91% tocopherol. The techno-economic evaluation of

the biodiesel route presented a Minimum Biodiesel Selling Price (MBSP) of approximately US$6.15/L or US$6.84/kg. Regarding the Life Cycle Assessment (LCA), our process has lower indicators than Brazil's chemical catalysis of biodiesel from soybean oil. It reinforces the importance of developing processes from coproduct in biodiesel production. Three scenarios containing different solvent mixtures were evaluated for biosurfactants (xylose esters) production through transesterification/ esterification reactions. When we compared all of them, the final purity in terms of mass of xylose esters decreased (process (a): 80.81%; process (b): 76.61%; process (c): 71.37%). We found a Minimum Biosurfactant Selling Price (MBSP) of $13.42/kg of product for the process (a), $5.82/kg for the process (b), and $6.56/kg for the process (c).

Keywords: Soybean oil deodorizer distillate (SODD); Biodiesel; Biosurfactants.

4.2 Introduction

The constant demand for feasible processes maintaining low environmental indicators has been nonstop in recent decades. In response to these goals, the circular economy has emerged, with one of the pillars of waste reuse at all stages of production. This approach reduces costs and enhances efficiency in the production line (ELDOS et al., 2024; MGBECHIDINMA et al., 2022; PALUZAR, 2024). In the soybean oil industry context, the refining stage produces a residue with significant potential for applications in a biorefinery, further contributing to the circularity of production and the reduction of costs. This potential is a source of optimism and inspiration for the industry's future (BEZERRA et al., 2022; D'AMATO VILLARDI et al., 2017; DE ARAUJO-SILVA et al., 2022; VIEIRA et al., 2021; VISIOLI et al., 2023; XIONG et al., 2022).

The last stage of refining vegetable oils consists of distillation, which aims to remove components that give the oil undesirable aromas and flavors. This way, other substances are carried together to form Vegetable Oil Deodorizer Distillate (VODD) (APOSTOLAKOU et al., 2009; MARTINS et al., 2006; SHERAZI; MAHESAR; SIRAJUDDIN, 2016). Specifically for soybean oil, direct steam or superheated nitrogen is injected to remove such compounds at a temperature range that varies between 220 and 260 °C depending on the characteristics of the oil. This temperature range is significant as it ensures the removal of undesirable compounds while preserving the beneficial ones, generating a subproduct/ residue named Soybean Oil Deod orizer Distillate (SODD) (BEZERRA et al., 2022; HIROTA et al., 2003; MARTINI; NERLI; MALPIEDI, 2022; WATANABE et al., 2004). The generation of SODD, which accounts for 0.3% to 0.5% (w/w) of processed soybean oil, is a factor that cannot be ignored. It is typically treated as waste in the industry due to its lack of direct applications (WANG et al., 2006). According to BRAZIL GOVERNMENT (2024), Brazil's refined soybean oil production reached 10.8 million tons in 2023, equating to an annual average of 43,200 tons of SODD. Projections indicate that this amount will double by 2030, underscoring the need for future planning to manage this potential growth.

As in the distillation process, the SODD composition depends on the oil characteristics. The literature reports Free Fatty Acids (FFAs) in higher percentage achieving values from 18 – 79%, then triglycerides from 0.94 – 69.5%, sterols from 1.69 – 27.1%, tocopherols 1.83 – 20.1%, free phytosterols 5.36 – 10.32%, fatty acid stearyl esters 1.34 – 7.3%, diglycerides 0.88 – 10.17%, monoglycerides 0.15 – 5.37%, and, lastly, squalene 0.55%– 2.82%. There are components such as hydrocarbons, aldehydes, ketones, pesticides, and herbicides, among others, in small quantities that the papers do not quantify (BEZERRA et al., 2022; D'AMATO VILLARDI et al., 2017; DE ARAUJO-SILVA et al., 2022; FANG et al., 2007; GUNAWAN; FABIAN; JU, 2008; GUNAWAN; KASIM; JU, 2008; HIROTA et al., 2003; KASIM et al., 2010; KHATOON; RAJAN; KRISHNA, 2010; LIU; FANG; DING, 2006; LV et al., 2021; MARTINS et al., 2006;

MAYUMI ITO et al., 2006; SHIMADA et al., 2000; TORRES et al., 2007, 2009; VIEIRA et al., 2021; WATANABE et al., 2004; XIONG et al., 2022; YIN et al., 2015, 2016, 2017). The concentrations of fatty acids and mono-, di-, and triglycerides found in SODD make it an exciting prospect. They make SODD an appealing candidate for conversion into esters through reactions with alcohols or sugars, producing biodiesel or biosurfactants (HOSSEINZADEH-BANDBAFHA et al., 2022; LV et al., 2021; PARTOVI et al., 2013; REETU et al., 2023; SANTOS et al., 2024; VIEIRA et al., 2021). This potential use of SODD opens new avenues for the industry and research, offering a raw material for producing esters that do not compete directly with the food industry.

Biodiesel is a mono-alkyl ester of fatty acids obtained through transesterification or esterification processes (BANCHERO; GOZZELINO, 2015; UDEH, 2018). Transesterification occurs through the reaction of mono-, di- or triglycerides with low molecular weight alcohol (usually methanol or ethanol), producing a mixture of methyl (or ethyl) esters of fatty acids, which corresponds to biodiesel, together with glycerol (VIEIRA et al., 2021). Esterification occurs in two stages, the first being responsible for hydrolyzing the mono-, di- and triglycerides into free fatty acids and the second for esterifying them by reacting them with alcohol and producing biodiesel and water (D'AMATO VILLARDI et al., 2017; DANG; OBIRI; HAYES, 2005; LI et al., 2015a, 2015b; PODDAR; JAGANNATH; ALMANSOORI, 2017; SOUZA et al., 2009; ZHENG et al., 2020). Both processes require catalysts and specific temperature and pressure conditions. Table 1 contains the main works that produced biodiesel from SODD. Note that VIEIRA et al. (2021) has higher conversion among reactions with ethanol (lower toxicity when compared with methanol), combining biocatalysis in mild reaction conditions.

Surfactants are amphiphilic compounds with surface-active properties used in various industries, as pharmaceuticals, food, and cosmetics. Their dual hydrophobic and hydrophilic nature allows them to reduce surface tension and emulsify and stabilize mixtures (BANAT et al., 2010; PERFUMO; BANAT; MARCHANT, 2018). Biosurfactants are sugar esters produced through microbiological or enzymatic processes and share these properties but offer additional benefits such as biodegradability, thermal stability, and low toxicity. However, their production costs are typically higher than those of synthetic surfactants (PANDEY et al., 2024; RAOUF et al., 2024). The enzymatic route to produce biosurfactants arises when SODD is used as a reagent. As a source of mono-, di-, triglycerides, and free fatty acids, it is possible to convert them into sugar esters (biosurfactants) through transesterification or hydrolysis followed by esterification (CANSIAN et al., 2022; GONÇALVES et al., 2021; VIEIRA et al., 2021). In the database evaluated in this study, only one research that produces biosurfactants from SODD was found, that it is through fermentation using *Pseudomonas aeruginosa* with 89% purity in final product (PARTOVI et al., 2013).

For laboratory research to be applicable on an industrial scale in industries, techno-economic-environmental analyses are necessary to indicate the process's economic viability and environmental impacts. There are several studies related to biodiesel containing these analyses. However, they are rarer when focusing on using raw materials that do not compete with the food industry. The potential of alternative raw materials, such as VODD, is promising. VILAS BÔAS et al. (2022) produced biodiesel using ethanol for US$ 2.60/ kg. RAJENDRAN et al. (2024) utilized a VODD from rapeseed oil with US$ 0.67/kg and 0.308 kg CO2 eq. / kg, demonstrating the potential ODD use for future biodiesel production.

Table 2 shows the main results of techno-economic-environmental analysis to produce biosurfactants in recent years. Note that there is a wide variation in the types of biosurfactants, purity, and methods of obtaining them. However, none of these studies evaluate processes from techno-economic-environmental analysis using SODD or VODD.

In this context, this study aims to support the development and scaling of biodiesel (fatty acid ethyl esters) and biosurfactants (fatty acid xylose ester) production by conducting a techno-economic and environmental assessment (TEEA) of enzymatic processes using a subproduct/ residue from biorefineries (SODD) as a material source of fatty acids. Although the main part of the work is related to computational simulations, experiments were conducted to supply information on the solubility of xylose in the reaction medium and on the reaction kinetics for biosurfactant production. For biodiesel production, on the other hand, available information from the research group were utilized (VIEIRA et al., 2021).

Table 1. Works that produced biodiesel from SODD.

Catalyst	Conversion	Reaction time	Temperature	Acyl group acceptor	Authors
Novozym 435	0.95	10 h	40 ºC	Methanol	(DU; WANG; LIU, 2007)
Novozym 435	0.835	90 min	50 ºC	Ethanol	(SOUZA et al., 2009)
Sulfuric acid/ anhydrous sodium sulfate	0.961	50 min	25 ºC	Methanol	(YIN et al., 2015)
Calcined duck eggshell	0.946	80 min	60 ºC	Methanol	(YIN et al., 2016)
Pressurized ethanol	0.87	20 min	275 ºC	Ethanol	(VISIOLI et al., 2016)
Sodium hydroxide/ ultrasound	0.963	30 min	25 ºC	Methanol	(YIN et al., 2017)
Sulfuric acid	0.997	3 h	100 ºC	Ethanol	(D'AMATO VILLARDI et al., 2017)
Lipozyme TL on macroporous resin	0.98	8 h	50 ºC	Methanol/ Tert-butanol	(ZHENG et al., 2020)
Liquid *Eversa*	0.866	23 h	35 ºC	Ethanol	(VIEIRA et al., 2021)
γ- alumina	0.902	4 h	300 ºC	Methyl acetate	(VISIOLI et al., 2023)
-	0.89	100 min	245 ºC	Methanol	(XIONG et al., 2022)
Calcium oxide synthesized	0.971	2 h	65 ºC	Methanol	(MAAFA et al., 2024)

Table 2. Recent research containing technical-economic-environmental analysis of the biosurfactant production.

Biosurfactant	Process	Purity	Price (Economic analysis)	(Environmental analysis)	Source
Di-Rhamnolipid	Microbial fermentation	-	US$ 12–56/kg	7.58 kg CO_2 eq. / kg biosurfactant	(NOLL et al., 2024)
Xylose ester	Enzymatic production	96% (w/w)	US$ 392.98/kg	34.43 kg CO_2 eq. / kg biosurfactant	(CANSIAN et al., 2024a)
Xylose ester	Enzymatic production	86% (w/w)	US$ 72.37/kg	-	(CANSIAN et al., 2022)
Surfactin and lichenysin	Microbial fermentation	85.04% (w/w)	US$ 836 - 2059.7/kg	-	(CZINKÓCZKY; NÉMETH, 2020)
Glycolipopeptide	Microbial fermentation	110g/L	€ 570/kg	-	(EKPENYONG et al., 2021)
Rhamnolipids	Microbial fermentation	60% (w/w)	US$ 60/kg	-	(MOUTINHO et al., 2021)
Sophorolipid	Microbial fermentation	90% (w/w)	US$ 20/kg	17.1 (case A)/ 9.55 (case B) kg CO2 eq. / kg biosurfactant	(ELIAS et al., 2021)

4.3 Material and Methods

4.3.1 Materials

The SODD was provided by COCAMAR, located in Maringá, Paraná, Brazil. The enzymes were *Candida antarctica* lipase B immobilized on Lewatit VP OC 1600 (Lipozyme 435) from Novozymes, A/S, Bagsværd, Denmark, Eversa Transform 2.0 liquid lipase from *Thermomyces lanuginosus*, Novozymes A/S, Bagsværd, Denmark, and free *Pseudomonas fluorescens* lipase from Sigma-Aldrich, St. Louis, USA. Tert-butanol, ethanol, xylose, heptane, dimethyl sulfoxide (DMSO) were obtained from Synth, São Paulo, Brazil. Chromatography standards, including α-, β-, γ-, and δ-tocopherols, methyl heptadecanoate, monoolein, diolein, triolein, butanethiol, tricarpine, and free fatty acids, along with N-methyl-N-(trimethylsilyl) trifluoroacetamide (MSTFA), were acquired from Sigma Chemical Co., St. Louis, USA. All other chemicals were of analytical grade and were used as provided.

4.3.2 Analytical methods of composition

Throughout all experiments, it was necessary to determine the concentration of the components (since the characterization of the SODD to the final processing steps). Table 3 shows all the methods used, all of which are based on established standards analysis or papers in the literature, reinforcing the credibility of our study.

Table 3. Main analyses for evaluating compositions in processes.

Compound analyzed	Method	Standard	Author
Lipid matter (expressed as FAME[a])	Gas chromatography	Ce 2-66 and EN 14103	(AOCS, 2004a; DUVEKOT, 2021)
Triglycerides	Gas chromatography	Ce 5-86	(AOCS, 2009a)
Mono and Diglycerides	Gas chromatography	Cd 11b-91	(AOCS, 2009b)
Fatty acids	Gas chromatography	-	(AGILENT TECHNOLOGIES, 2011)
Methyl and ethyl esters	Gas chromatography	EN 14103	(DUVEKOT, 2021)
α, β, ɣ e δ tocopherols	High performance liquid chromatography	Ce 8-89	(AOCS, 2004b)
Xylose	High performance liquid chromatography	-	(ARCENS et al., 2018)
Acidity index (mgKOH/g)	Gas chromatography	Ca 5a-40	(AOCS, 1990a)
Iodine (gI_2/100 g)	Wijs method	Cd 1-25	(AOCS, 1990b)
Saponification index (mg KOH/g)	Gas chromatography	Cd 3-25	(AOCS, 1990c)
Humidity (%)	Analytical	Ca 2b-38	(AOCS, 2004c)

[a]: Fatty Acid Methyl Esters.

4.3.3 Characterization of the SODD

SODD was characterized using several AOCS methods and based on VIEIRA et al. (2021): acidity index (Ca 5a-40) (AOCS, 1990a); iodine index (Cd 1-25) (AOCS, 1990b); saponification index (Cd 3-25) (AOCS, 1990c); Lipid matter expressed as FAME (Ce 2-66, EN 14103) (AOCS, 2004a; DUVEKOT, 2021); Mono-, Di- and Triglycerides (Cd 11b-91, Ce 5-86) (AOCS, 2004d, 2009b); FFAs (AGILENT TECHNOLOGIES, 2011); Humidity percentage (Ca 2b-38) (AOCS, 2004c); density (Cc 10a-25) (AOCS, 1990d); Viscosity using a Brookfield Rheometer (SC4-27 spindle); Heat capacity was determined using an isolated system with a 1000W resistance, a chronometer, and a thermometer (water was applied to calibrate o equipment).

4.3.4 Modeling and simulation

The primary equipment used for computational simulations included a desktop with an Intel Core i7 7700K processor running at 4.20 GHz and 32 GB of RAM. Additionally, a desktop with an AMD Ryzen 5600X 6-core processor at 3.7 GHz and 16 GB of RAM was utilized for the project. The software employed were EMSO academic beta version 0.10.9, SimaPro 9.0.0.35, OriginPro® 2024, and Microsoft® Excel® 2403 (Build 16.0.17425.20124).

Mass and energy balances and pressure considerations are the pillars of the equations. All equations used can be verified in supplementary material 1. The entire process was simulated as a continuous operation, meaning the variables remained constant over time.

The basis of this simulation was determined by the hourly. The scenario assumed facilities in São Paulo, Brazil, operating continuously for 24 hours a day, 300 days a year, with the remaining days allocated for equipment cleaning and maintenance. For both biodiesel and biosurfactants, projects operating with 10 kmol/h of SODD were considered.

4.3.4.1 Biodiesel from SODD

The modeling and simulation of the process took place as described in Figure 1, using the open software EMSO. In the first stage, corresponding to the R - 101 reactor, SODD-water (1:4 mass ratio), and the free enzyme PFL (*Pseudomonas fluorescens* lipase) (5g of enzyme mass for every 100g of SODD) are added at 37°C for 48 hours (hydrolysis occurs according to Equations 1, 2, and 3) (VIEIRA et al., 2021).

$$C_3H_5(RCOO)(RCOO)(RCOO)(l) + 3\,H_2O(l) \overset{PFL}{\longleftrightarrow} 3\,RCOOH(l) + C_3H_8O_3(l) \quad (1)$$
$$Triglycerides \qquad Water \qquad Fatty\ Acid \qquad Glycerol$$

$$C_3H_5(OH)(RCOO)(RCOO)(l) + 2\,H_2O(l) \overset{PFL}{\longleftrightarrow} 2\,RCOOH(l) + C_3H_8O_3(l) \quad (2)$$
$$Diglycerides \qquad Water \qquad Fatty\ Acid \qquad Glycerol$$

$$C_3H_5(OH)_2(RCOO)(l) + H_2O(l) \overset{PFL}{\longleftrightarrow} RCOOH(l) + C_3H_8O_3(l) \quad (3)$$
$$Monoglycerides \qquad Water \qquad Fatty\ Acid \qquad Glycerol$$

Water at 90°C is combined with the first reactor outlet (stream 6) in a mixer and goes to a centrifuge, where the oily phase is separated and rewashed. Stream 13 corresponds to the oil phase entering an evaporator to dry the remaining water. Afterwards, the second reaction stage takes place in R - 102, where a stream rich in FFA's from SODD is added to ethanol (1:3.64 molar ratio), and free *Eversa* enzyme at 8.5% (m/v), at 35°C for 48 hours (esterification occurs according to Equation 4).

$$RCOOH(l) + C_2H_6O(l) \overset{Eversa}{\longleftrightarrow} RCOOC_2H_5(l) + H_2O(l) \quad (4)$$
$$Fatty\ Acid \qquad Ethanol \qquad Ethyl\ ester \qquad Water$$

Washing occurs in the same way as the previous step, twice, and the oily phase passes through an evaporator to remove the remaining ethanol, generating a stream with a high content of ethyl esters of fatty acids. All proportions and conditions were experimentally tested by VIEIRA (2021). Table 4 lists the components utilized in the modeling and simulation of the biodiesel process. All MAGs and DAGs were considered TAGs (maintaining the proportions), especially Tripalmitin (the fifth compound in Table 4), to facilitate the numerical solution.

Table 4. Components phase used in the biodiesel process simulation.

Components	Components
SODD (1)	Linolenic acid (10)
Enzyme (2)	Ethyl palmitate (11)
Water (3)	Ethyl stearate (12)
Ethanol (4)	Ethyl oleate (13)
Tripalmitin (5)	Ethyl linoleate (14)
Palmitic acid (6)	Ethyl linolenate (15)
Stearic acid (7)	Tocopherol (16)
Oleic acid (8)	Hydrocarbon (17)
Linoleic Acid (9)	Glycerol (18)

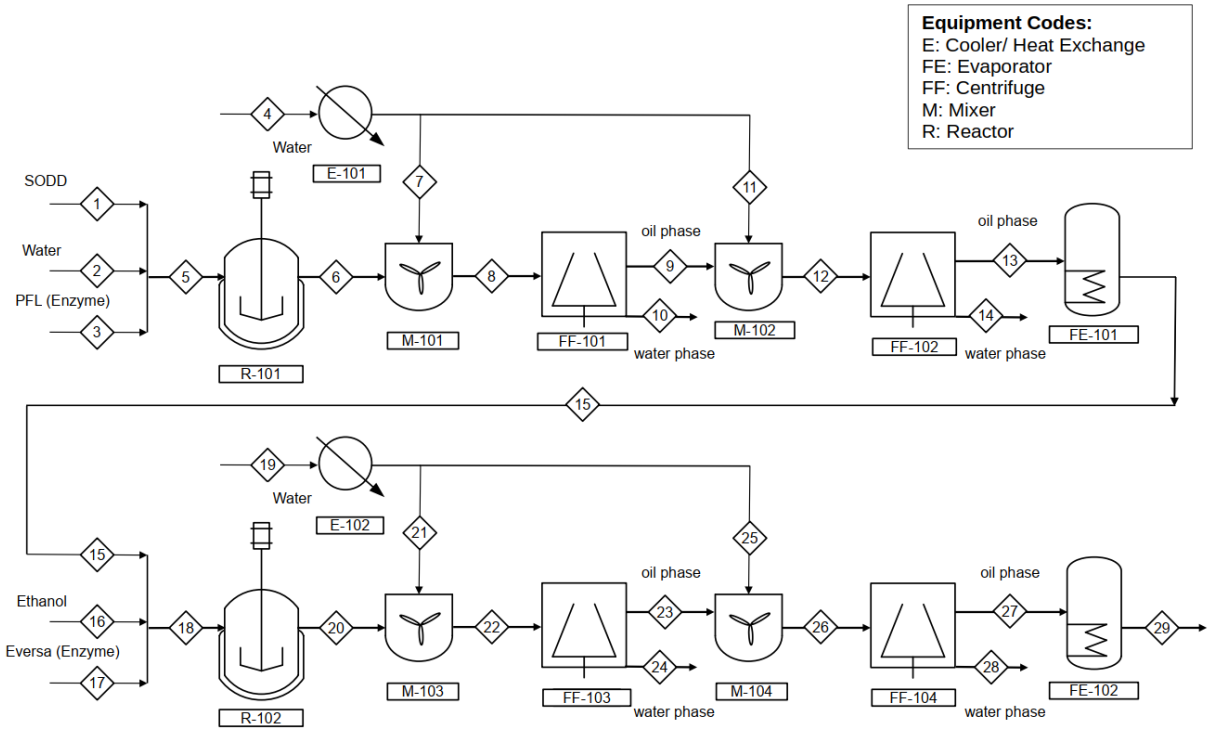

Figure 1. Process diagram for modeling and simulation of two-step fatty acid ethyl ester production (SODD hydrolysis followed by FFAs esterification).

4.3.4.2 Biosurfactant from SODD

Although GONÇALVES et al. (2021) experimentally obtained a low-toxicity, food-grade xylose ester, it is clear from CANSIAN et al. (2024) that the low solubility of xylose in methyl ethyl ketone make more expensive the final product. Thus, the present work aimed to find an alternative mixture.

Experiments to produce biosurfactants begin with the solubility of xylose in an organic solvent, specifically, a mixture of tert-butanol, DMSO, and water. The experiment was designed according to Table 5 to determine the solubility of xylose in the mixture. After evaluating the solubility, the reactions (transesterification/ esterification – look Equations 5 and 6) were tested for three different solvent ratios. The kinetics were evaluated with 1% (w/w) enzyme load and lipid matter in SODD: xylose (5:1) at 60ºC for 120 hours. The solvent ratio was based on the solubility of xylose in the medium. For separation and purification, WAGNER (1991) was experimental tested for data validation.

$$C_3H_5(RCOO)_3(l) + 3\ C_5H_{10}O_5(l) \xleftrightarrow{Novozyme\ 435} 3\ RCOO(C_5H_9O_5)(l) + C_3H_8O_3(l) \qquad (5)$$

$$Triglycerides \qquad Xylose \qquad\qquad Xylose\ ester \qquad Glycerol$$

$$RCOOH(l) + C_5H_{10}O_5(l) \xleftrightarrow{Novozyme\ 435} RCOO(C_5H_9O_5)(l) + H_2O(l) \quad (6)$$

Fatty acid *Xylose* *Xylose ester* *Water*

Table 5. Experimental design for xylose solubility.

Terc Butanol (mL)	DMSO (mL)	Water (mL)	Total (mL)
7.50	0.78	0.78	9.06
7.50	0.78	3.00	11.28
7.50	3.00	0.78	11.28
7.50	3.00	3.00	13.50
10.00	0.78	0.78	11.56
10.00	0.78	3.00	13.78
10.00	3.00	0.78	13.78
10.00	3.00	3.00	16.00
6.40	1.89	1.89	10.18
10.66	1.89	1.89	14.44
8.50	0.02	1.89	10.41
8.50	1.89	1.89	12.28
8.50	1.89	0.02	10.41
8.50	1.89	3.76	14.15
8.50	1.89	1.89	12.28

The modeling and simulation of the process took place as described in Figure 2. As explained in the previous section, EMSO was utilized. The process begins with xylose and solvent being added to the reactor R - 101 at 60 °C for 3 hours to solubilize all the sugar. The output from the reactor (stream 6) joins the SODD and immobilized enzyme sources and goes to the reactor R - 102. They remain there for 24 hours, at 60 ºC, so the esterification and transesterification reactions can occur. The output from the reactor enters to the filter P - 101 where the solid phase (enzymes) is collected and reinserted into the process for reuse (stream 12). Stream 11 is only added to the simulation and represents the discard and deactivation of the enzyme by 10%. However, in the real scenario, it is discarded after ten cycles and replaced. The liquid phase that leaves the filter (stream 13) enters the heat exchanger E - 101 to be cooled. After cooling, water is added, and the mixture is sent to enter the centrifuge FF - 101 and then to the settling tank TT - 101 so that the water phase containing xylose is collected below. The oily (ester) phase with the product and other reagents continues. The water phase (stream 18) is recovered and reused (xylose and water). The ester phase (stream 21) continues in the process and enters the heat exchanger E - 102 where the medium is heated and prepared for the flash tank F - 101. The tert-butanol solvent is recovered as a vapor phase (stream 23) and reinserted into the process (stream 3). Stream 24, now without solvent, enters the biosurfactant purification phase. Stream 25, with water and ethanol in a mass

fraction of 1:1, is mixed with stream 24 and enters the centrifuge FF - 102. All content leaves the equipment and goes to the settling tank TT - 102. In this phase, the xylose ester settles in the solid phase with some fatty acids and continues in the process (stream 29). Note that stream 28 is not connected in the diagram because it is assumed that the biosurfactant production unit is located inside a biorefinery and, therefore, the alcohol/water feed is one of the inputs to the distillation towers that diverts to this diagram and then returns to distillation. After this stage, methyl ethyl ketone is added, enters the centrifuge FF - 103, and then goes to the settling tank TT - 103. At this step, the fatty acids remaining in the solid phase go to the liquid phase, and the xylose ester (stream 35) becomes purer. The liquid phase is recovered so the methyl ethyl ketone can be reused. At the end of the process, the solid phase enters the heater E - 103 and ends up in the flash tank F - 102 that finishes evaporating the remaining solvents, obtaining the final product in stream 38. Notice that the solvent is recovered in stream 37 and reinserted in the process. Table 6 details the components used in the modeling and simulation of the biosurfactant process. As in the biodiesel simulation, all MAGs and DAGs were considered TAGs (maintaining the proportions), especially Tripalmitin (the sixth compound in Table 6), to facilitate the numerical solution.

Table 6. Components phase used in the biodiesel process simulation.

Components (liquid phase)	Components (solid phase)
SODD (1)	Enzyme (23)
Enzyme (2)	Xylose (24)
Tert-butanol (3)	Palmitic acid (25)
Xylose (4)	Stearic acid (26)
Dimethyl sulfoxide (5)	Xylose palmitate (27)
Tripalmitin (6)	Xylose stearate (28)
Palmitic acid (7)	Xylose linoleate (29)
Stearic acid (8)	Xylose linolenate (30)
Linoleic acid (9)	Xylose Oleate (31)
Linolenic acid (10)	-
Oleic acid (11)	-
Tocopherol (12)	-
Hydrocarbon (13)	-
Glycerol (14)	-
Water (15)	-
Xylose palmitate (16)	-
Xylose stearate (17)	-
Xylose linoleate (18)	-
Xylose linolenate (19)	-
Xylose Oleate (20)	-
Ethanol (21)	-
Methyl ethyl ketone (22)	-

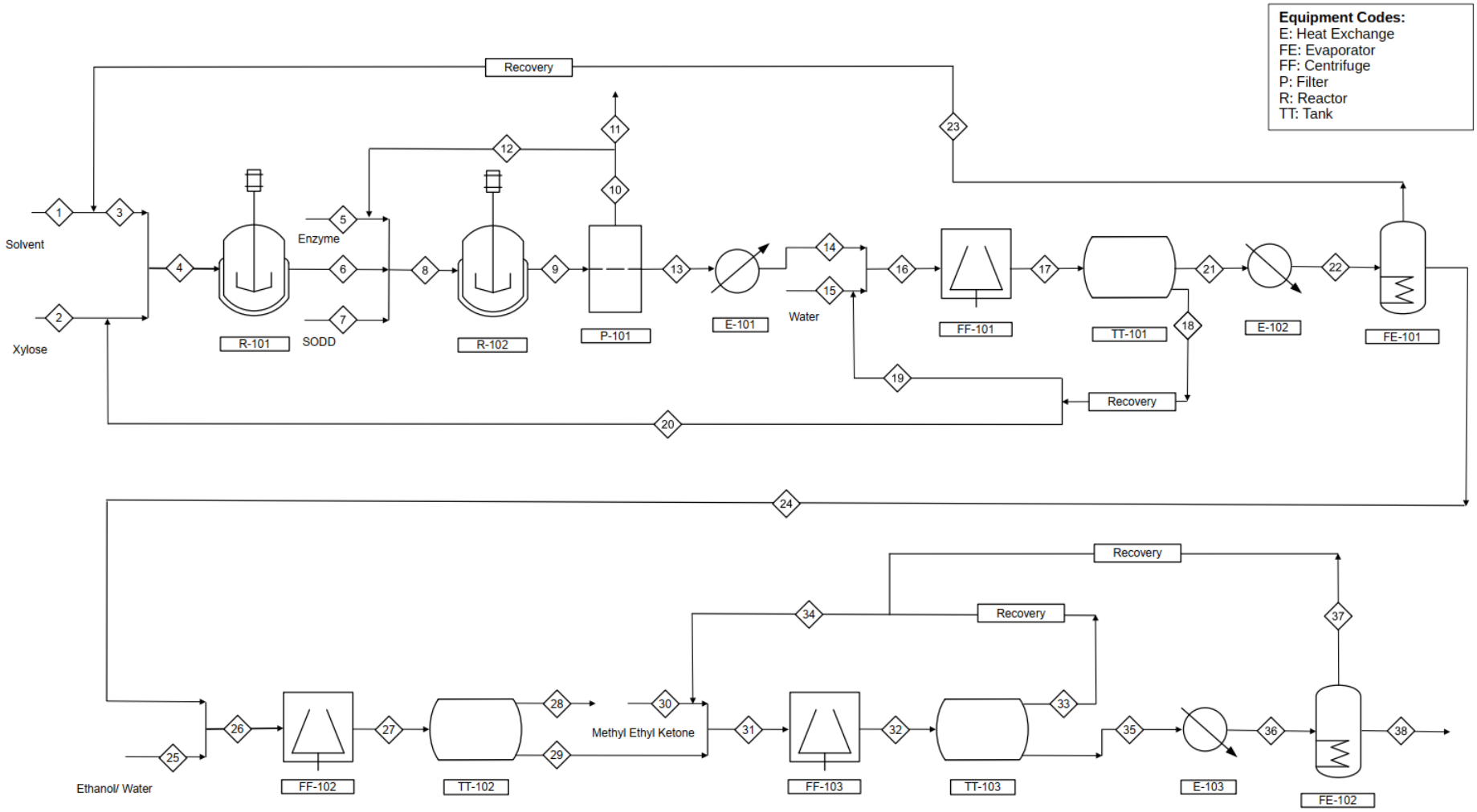

Figure 2. Process diagram for modeling and simulation of xylose ester production SODD trans/esterification).

4.3.5 Technical-economic analysis

The economic analysis categorizes costs into capital expenses (CAPEX) and operational expenses (OPEX). CAPEX encompasses the expenses of the physical plant, including equipment sizing, piping, electrical installations, and related infrastructure. OPEX covers the costs of reagents, energy, utilities, labor, supervision, and maintenance. These costs are derived from mass and energy balances obtained through process simulation, equipment sizing values, and process streams (mass and energy).

4.3.5.1 Equipment costs

The equipment costs were meticulously calculated using TURTON et al. (2009) methodology, with all equations detailed and applied in (CANSIAN et al., 2022, 2024a). Each equipment was dimensioned based on the information obtained in the simulation, and the initial modular cost was calculated. These costs were then corrected for time and location, ensuring the total installation cost was accurately determined using the Lang Factor of 5.03 for solid/liquid processes (TURTON et al., 2009).

4.3.5.1.1 Biodiesel

The Figure 1 outlines the process for ethyl esters, with some production steps naturally taking longer than others. The Gantt chart (Figure 3) clearly indicates the residence time for each piece of equipment. From one end of the cycle to the next, there are 48 hours, so the reactors cannot be used and must be independent units. However, the separation modules containing the mixer, centrifuge, heat exchanger, and evaporator can be reused, reducing CAPEX costs and optimizing plant use.

4.3.5.1.2 Biosurfactant

The same thing happens for the xylose esters production process. The cycle between two productions is 48 hours, and the limiting factor is the second reactor (R - 102). This way, the downstream equipment can be reused in the purification stages. Figure 4 summarizes the residence time of each equipment described in Figure 2.

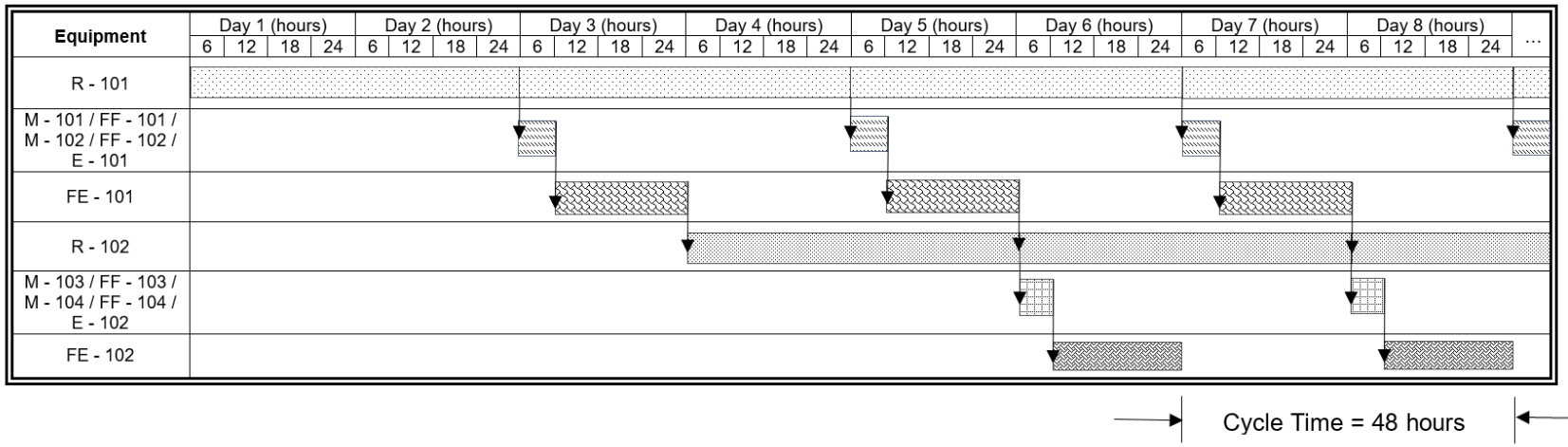

Figure 3. Gant chart for e Gant chart for equipment costs optimization (biodiesel process).

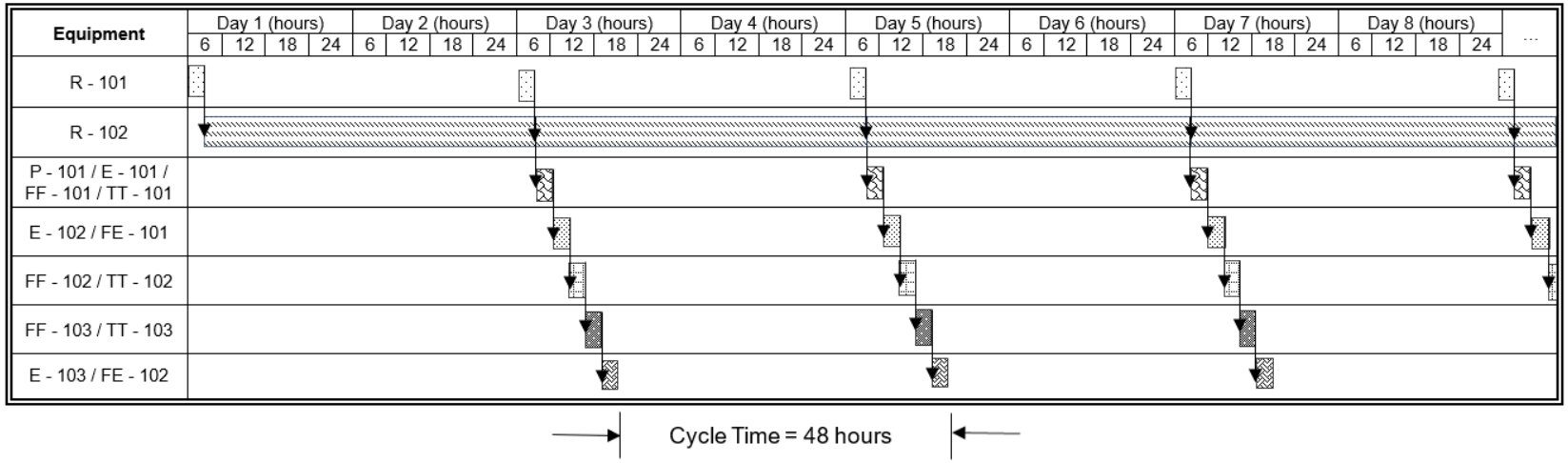

Figure 4. Gant chart for e Gant chart for equipment costs optimization (biosurfactant process).

4.3.5.2 Labor costs

SEIDER et al. (2017) indicate that plants with automatic controls and 10 – 100/ ton per day of product require approximately two operators per process section considering just fluids processing and three operators considering solids–fluids in batch or semi-batch operation. For biodiesel production, we consider two sections: one containing hydrolysis plus purification and another with esterification plus purification, since while each reaction occurs, those responsible for the sector can focus on the separation steps. Therefore, a total of four operators per shift are required for biodiesel production. In the production of biosurfactants, the sector with xylose dissolution and transesterification/esterification reactions is designated as the first, and the subsequent separations as the second, totaling a total of six operators per shift.

In 2023, the average monthly payment for an industrial worker in Brazil was R$2,297.19 (CAGED, 2023). However, in the state of São Paulo, the monthly payment for a chemical industry technician varied, as shown in Figure 5, with an average (SALÁRIO, 2024). So, we assumed a payment of US$ 3526.93 per month. Therefore, we will consider the highest payment, approximately 68.17% more than this, with taxes (CAGED, 2021).

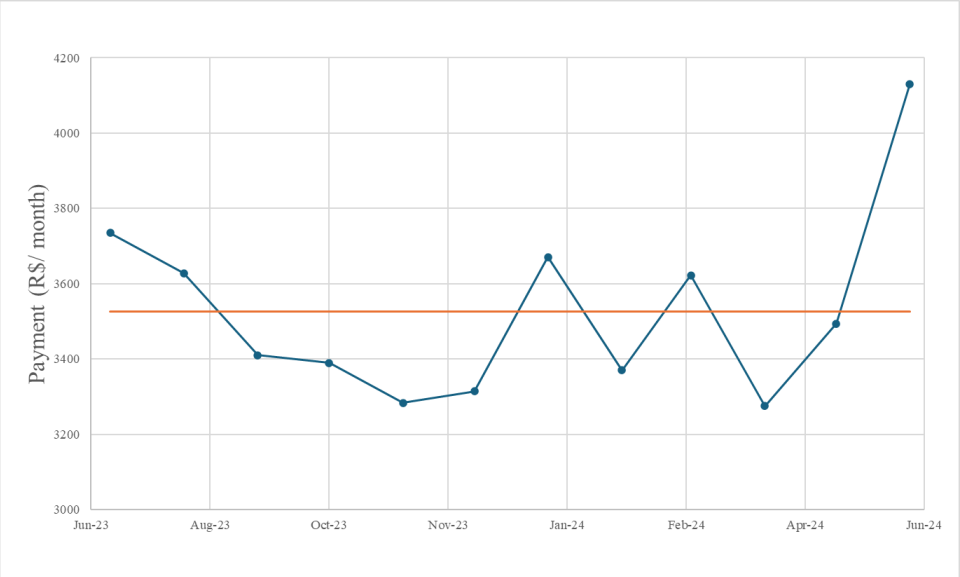

Figure 5. Labor payments over the last year - São Paulo - Brazil (SALÁRIO, 2024).

4.3.5.3 Net Present Value (NPV) calculation

The Net Present Value (NPV) is a metric that determines the current value of future payments by discounting them at an appropriate interest rate and subtracting the initial investment cost. When the NPV is greater than zero, it indicates that the investment is viable. In this context, the scenario with a break-even point (NPV = 0) led to the determination of the minimum biosurfactant selling price (MBSP). The NPV is calculated as shown in Equation 7, following the method outlined by PETERS et al. (2004). For this study, a minimum attractive rate of return of 11% per year was applied with a project lifespan of 25 years.

$$NPV(X) = \sum_{J=1}^{N} \frac{CF(X)}{(1+r)^j} - CAPEX(X) \quad (7)$$

4.3.5.4 Reagents costs

The cost of reagents was based on Brazilian imports in 2023, considering an average value presented on the government website COMEXSTAT. Table 7 shows the price per kilogram found for each reagent. Note that there is no information on the value of SODD since this considers a plant installed in a biorefinery using and integrating this coproduct into other processes. It is important to note that the work presented in the previous chapter considered reagent prices under a more conservative (i.e., less favorable) scenario compared to the one analyzed here. In high-volume demand scenarios, exploring suppliers that offer significant price discounts becomes feasible. Therefore, this chapter has based our analysis on the average prices of nationally imported reagents.

Table 7. Reagents costs.

Component	US$*/kg
Xylose	4.56
Tert butanol	6.25
Dimethyl sulfoxide	13.78
Water+	6.99×10^{-4}
Free enzyme	9.59
Immobilized enzyme	30.74
Ethanol+	3.07
Methyl Ethyl Ketone+	1.62

+: A partial recovery of these reagents was considered, with a 2% loss based on initial simulation results - 1% attributed to recovery costs and the other 1% to separation inefficiencies.

*: The dollar rate considered was 5.47 (1 US$/ R$).

4.3.6 Life Cycle Assessment (LCA)

Life Cycle Assessment (LCA) is a method employed to evaluate the environmental impact of a process. The Ecoinvent 3.0 database and SimaPro 9.0.0.35 software were utilized for this analysis. The CML-IA baseline V3.04 (World 2000) method was applied to calculate the following indicators: abiotic depletion - fossil fuels (AD), global warming potential (GWP100), ozone layer depletion (ODP), human toxicity (HT), freshwater aquatic ecotoxicity (FWAET), marine aquatic ecotoxicity (MAET), terrestrial ecotoxicity (TET), photochemical oxidation (PO), acidification (AC), and eutrophication (EU). The dataset parameters were integrated into the EMSO simulation to calculate these indicators.

4.4 Results and discussion

4.4.1 SODD properties

Initially, the characterization of SODD, provided by COCAMAR's company, was performed, and the results were presented in Table 8. In the same batch of SODD supplied, the degummed and refined oil parameters were also evaluated. The parameters evaluated are consistent with the average variation reported in the review literature (CANSIAN et al., 2024b).

Table 8. Characterization results for the SODD, Degummed and refined oil from COCAMAR company (chemical and physical parameters).

Parameters	SODD	Degummed oil	Refined oil
Heat Capacity (J/kg .K) (25 to 105ºC)	2889.06 ± 79.32	2640.28 ± 15.68	2100.12 ± 10.55
Density (g/cm³) (25°C)	0.9062 ± 0.0430	0.9156 ± 0.0512	0.9154 ± 0.0453
Dynamic Viscosity (mPa.s = cP) (40°C)	30.03 ± 0.11	36.41 ± 4.61	36.72 ± 4.82
Dynamic Viscosity (mPa.s = cP) (25°C)	284.51 ± 12.23	54.52 ± 0.15	57.38 ± 1.03
Kinematic Viscosity (mm²/s = cSt) (25°C)	313.94	59.55	62.68
Humidity (%) (130°C)	1.0463 ± 0.0705	0.5741 ± 0.0349	0.4738 ± 0.0349
Saponification Index (mgKOH/g) (25°C)	162.98 ± 4.07	196.51 ± 1.90	197.23 ± 2.56
Total saponifiable matter as % oleic acid	81.90 ± 2.04	98.75 ± 0.96	99.11 ± 1.29
Acidity Index (mgKOH/g) (25°C)	82.32 ± 0.46	1.43 ± 0.15	0.63 ± 0.16
Acidity Index (g oleic acid/100 g, %)	41.38 ± 0.23	0.72 ± 0.08	0.32 ± 0.08
Iodine Index (gI_2/100g) (25°C)	121.89 ± 2.83	133.07 ± 2.78	134.79 ± 2.47
Lipid as methyl esters (FAME) (% w/w)	66.43 ± 1.70	92.57 ± 7.05	95.11 ± 2.83
Alpha Tocopherol (% w/w)	0.7864 ± 0.0098	0.0182 ± 0.0026	0.0167 ± 0.0011
Beta Tocopherol (% w/w)	0.0864 ± 0.0017	$0.0017 \pm 1.40 \times 10^{-5}$	$0.0014 \pm 5.96 \times 10^{-5}$
Gamma Tocopherol (% w/w)	4.3579 ± 0.0219	0.0995 ± 0.0086	0.0863 ± 0.0007
Delta Tocopherol (% w/w)	1.6866 ± 0.0013	0.0333 ± 0.0027	0.0270 ± 0.0004
Total Tocopherol (% w/w)	6.9173	0.1527	0.1314

4.4.2 Biodiesel from SODD

After performing the simulation based on experimental data, the results of the main streams are presented in Table 9. Note that stream 6 is the result of the hydrolysis reaction. That is, the fatty acids now appear in the composition of the medium with (w/w) 7.46% palmitic acid, 2.31% stearic acid, 12.69% oleic acid, 18.49% linoleic acid and 2.22% linolenic acid. After the esterification reaction, stream 20 presents 50.3% fatty acid ethyl esters. Immediately after purification, the final process stream (stream 29) was 1046.96 kg/h of product with approximately 81.57% (w/w) of ethyl esters (ethyl palmitate, ethyl stearate, ethyl oleate, ethyl linoleate, and ethyl linoleate), 0.99% of MAGs, DAGs, and TAGs, 14.79% of fatty acids and 1.91% tocopherol. Although the product did not meet the biodiesel standards, it could be used as an alternative biofuel with improved lubricity capacity mainly due to its content of MAGs, DAGs, TAGs, and fatty acids (CALERO et al., 2020).

The techno-economic evaluation of the biodiesel route presented a Minimum Biodiesel Selling Price (MBSP) of approximately US$6.15/L or US$6.84/kg (for NPV = 0). When related to the cost of equipment (Table 10 and Figure 6a), it is noted that the most significant impact on CAPEX was related to the hydrolysis reactor. It occurred because the molar fraction of SODD: Water is 1:4, causing the mass of water present in the reaction to be very large. The depreciation of the plant was 10% per year. As for OPEX (vide Figure 6b), the annual cost of reagents was approximately US$47,672,556; labor was US$ 293,948; energy was US$1,640,180; supervision was US$14,697; and maintenance was US$97,472. Income taxes were only applied for years when cash flow was positive, which was applied to 34% of the total. The cash flow can be seen in Table 11. A plant with 25 years of operation was considered, adding the first three years for complete construction.

The MBPS found of US$6.15/L is below of HARUN et al. (2011) (US$75.77/L) and of RICHARDSON et al. (2012) (US$8.35/L), but it is above NAGARAJAN et al. (2013) (US$0.97/L), CASTRO et al. (2023) (US$3.31/L), DELRUE et al. (2012) (US$3.55/L), and AMER; ADHIKARI; PELLEGRINO (2011) (US$3.60/L).

Among the fixed costs, the hydrolysis reactor has the most significant impact, and reducing the proportion of water used in the reaction can reduce the investment costs in the plant, because it could reduce the reactor volume. As for operating costs, the energy spent in the process has a major impact on its cost, as does the liquid enzyme purchased and discarded with each batch. A possible future solution is the implementation of energy integration with the biorefinery; another is to produce the process energy in the plant; a third is immobilizing the enzyme used to reuse it. In this way, the process needs some optimizations to be competitive in the market.

Table 9. Result for main streams (biodiesel production).

Variable	Name	Unit	Stream 6	Stream 20	Stream 29
Fw	Mass flow	kg/h	2173.74	2129.20	1046.9600
T	Temperature	K	310.15	308.15	453.15
P	Pressure	atm	1	1	1
zw(1)*	Composition	dimensionless	0.0000	0.0000	0.0000
zw(2)*	Composition	dimensionless	0.0345	0.0009	0.0000
zw(3)*	Composition	dimensionless	0.0855	0.0789	0.0143
zw(4)*	Composition	dimensionless	0.0000	0.2879	0.0359
zw(5)*	Composition	dimensionless	0.0553	0.0532	0.0099
zw(6)*	Composition	dimensionless	0.0746	0.0142	0.0230
zw(7)*	Composition	dimensionless	0.0231	0.0040	0.0071
zw(8)*	Composition	dimensionless	0.1269	0.0200	0.0388
zw(9)*	Composition	dimensionless	0.1849	0.0401	0.0705
zw(10)*	Composition	dimensionless	0.0222	0.0052	0.0085
zw(11)*	Composition	dimensionless	0.0000	0.0890	0.1448
zw(12)*	Composition	dimensionless	0.0000	0.0275	0.0445
zw(13)*	Composition	dimensionless	0.0000	0.1500	0.2438
zw(14)*	Composition	dimensionless	0.0000	0.2111	0.3416
zw(15)*	Composition	dimensionless	0.0000	0.0254	0.0410
zw(16)*	Composition	dimensionless	0.0093	0.0101	0.0191
zw(17)*	Composition	dimensionless	0.0447	0.0070	0.0003
zw(18)*	Composition	dimensionless	0.3389	0.0000	0.0000

*Component number: SODD (1), Enzyme (2), Water (3), Ethanol (4), Tripalmitin (5), Palmitic acid (6), Stearic acid (7), Oleic acid (8), Linoleic Acid (9), Linolenic acid (10), Ethyl palmitate (11), Ethyl stearate (12), Ethyl oleate (13), Ethyl linoleate (14), Ethyl linolenate (15), Tocopherol (16), Hydrocarbon (17), glycerol (18).

Table 10. Equipment capacity and costs with installation included (CAPEX).

Equipment	number	Volume/ Area	Total cost (US$)
Reactor (R - 101)	1	1802.03 m^3	1,148,870
Reactor (R - 102)	1	85.09 m^3	66,281
Mixer - Agited tank (M - 10x)	2	0.5 m^3	44,187
Heat exchanger (E - 10x)	1	28.25 m^2	127,962
Vaporizer (FE - 10x)	1	1 m^3	45,622
Centrifuge (FF - 10x)	2	0.2 m	101,557

Table 11. Cash flow for biodiesel production.

Year	Cash Flow *	Year	Cash Flow *	Year	Cash Flow *	Year	Cash Flow *
1	-4.16915	8	0.613585	15	0.229767	22	0.110669
2	-3.75599	9	0.552779	16	0.206997	23	0.099702
3	-0.209794	10	0.497999	17	0.186484	24	0.089822
4	0.931464	11	0.448648	18	0.168004	25	0.08092
5	0.839157	12	0.404187	19	0.151355	26	0.072901
6	0.755997	13	0.364133	20	0.136356	27	0.065677
7	0.681079	14	0.255042	21	0.122843	28	0.06936

*: The values are expressed in million US$/ year and converted to present values.

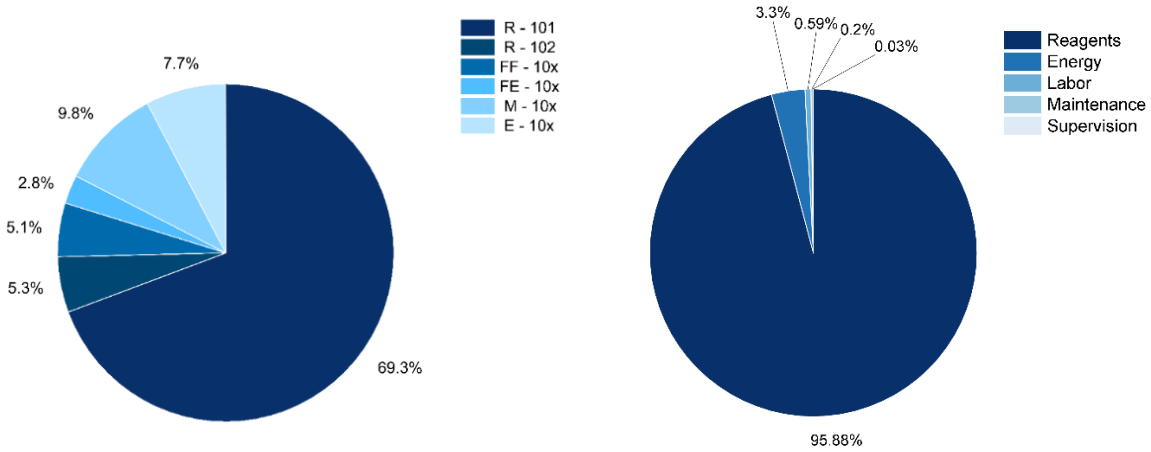

(a) (b)

Figure 6. (a) OPEX costs (b) CAPEX costs for biodiesel process.

The LCA results were obtained using mass and energy balances (simulation responses). Figure 7 shows the parameters calculated considering 1 kg of product. The Global Warming Potential in 100 years (GWP100: 1.55 kg CO_2 eq.), Abiotic depletion (AD: 27.66 MJ), Acidification (AC: $3.35 \cdot 10^{-3}$ kg SO_2 eq.), and Eutrophication (EU: $7.44 \cdot 10^{-4}$ kg PO_4 eq.) obtained per kg of product are close to AL-MUHTASEB et al. (2022) (GWP100: 1.15 kg CO_2 eq.; AD: 22.92 MJ; AC: $4.9 \cdot 10^{-3}$ kg SO_2 eq.; EU: $2 \cdot 10^{-4}$ kg PO_4 eq.) that produced biodiesel by transesterification of waste *Prunus Armeniaca* seeds oil. Despite this, when compared with the chemical catalysis of biodiesel from soybean oil in Brazil, the parameters provided by PEÑARRUBIA FERNANDEZ; LIU; ZHAO (2017) (GWP100: 1.69 kg CO_2 eq.; HT: $4.43 \cdot 10^{-1}$ 1,4-DB eq.; AC: $7.66 \cdot 10^{-3}$ kg SO_2 eq.) are higher than those calculated here. It reinforces the importance of developing processes from coproducts in biodiesel production.

Figure 8 presents the results for the LCA parameters with the impact of utilities and reagents. Note that the enzyme has the most significant impact on most parameters since its immobilization

involves other processes. Electricity has the greatest impact on GWP100, AC, and EU. Water does not impact toxicity parameters, as proven in the HT, FWAET, MAET, and TET calculations. Finally, an important point is that ethanol is largely responsible for ODP.

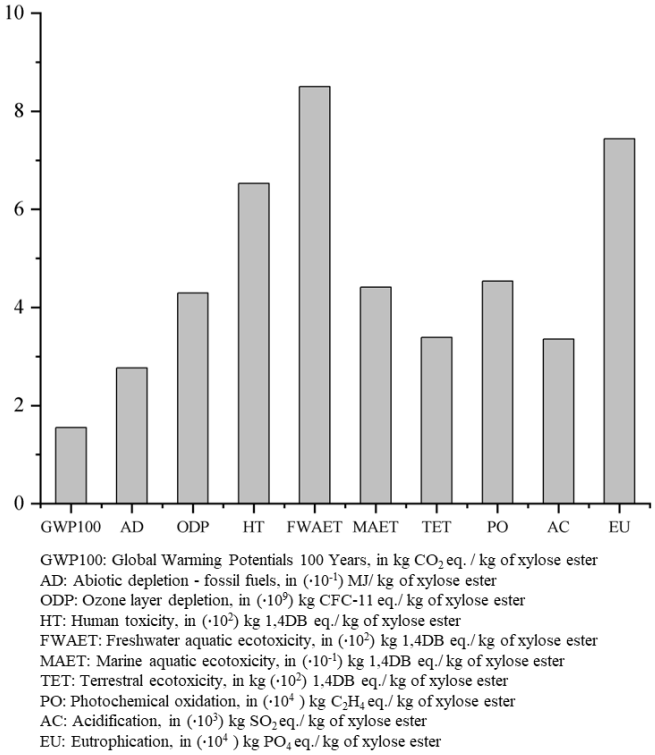

Figure 7. Environmental impact with absolute LCA scores for the biodiesel process.

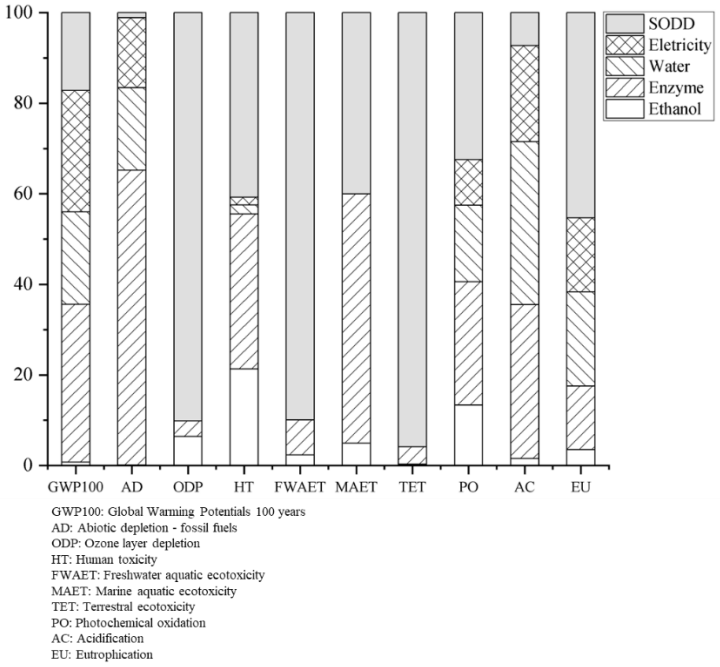

Figure 8. Environmental impact with percentage LCA scores for biodiesel process, separated by utilities and raw materials.

4.4.3 Biosurfactant from SODD

The results of the experiments evaluating the solubility of xylose in tert-butanol, DMSO, and water are shown in Table 12. Note that the highest solubilities were in the mixtures with the lowest proportion of tert-butanol and the highest proportions of DMSO and water. Three proportions were chosen to evaluate the conversion kinetics in terms of xylose, as shown in Table 13.

Table 12. Xylose solubility results for each point of the experimental design.

Tert-butanol (mL)	DMSO (mL)	Water (mL)	Xylose Concentration (g/L)
8.28	0.86	0.86	82.82 ± 3.41
6.65	0.69	2.66	91.02 ± 2.88
6.65	2.66	0.69	52.99 ± 0.78
5.56	2.22	2.22	98.53 ± 2.39
8.65	0.67	0.67	39.58 ± 6.22
7.26	0.57	2.18	60.83 ± 11.87
7.26	2.18	0.57	52.03 ± 2.49
6.25	1.88	1.88	98.84 ± 2.53
6.29	1.86	1.86	106.29 ± 2.66
7.38	1.31	1.31	94.27 ± 1.77
8.16	0.00	1.82	66.00 ± 7.89
6.92	1.54	1.54	67.36 ± 3.74
8.16	1.82	0.00	37.50 ± 3.45
6.01	1.34	2.66	70.65 ± 2.52

Table 13. Points chosen for collection of biosurfactant production kinetics.

Terc Butanol (mL)	DMSO (mL)	Water (mL)	Xylose concentration (g/L)	Process
10	0	0	10	(a)
8.28	0.86	0.86	82.82 ~ 80	(b)
6.29	1.86	1.86	106.29 ~105	(c)

The three scenarios that change in terms of solvent mixture (Table 13) were chosen for the kinetics evaluation and economic and environmental assessment of processes (a), (b), and (c). The kinetics for the solvent ratio (a) are shown in Figure 9. After 120 hours of reaction, approximately 94% conversion in terms of xylose was reached. In 48 hours, the conversion stabilizes at around 81% and increases slowly until the end of the reaction. The kinetic profile of process (b) is shown in Figure 10, in which the xylose conversion stabilizes after 48 hours at approximately 78%, with no significant changes after that. Finally, in Figure 11, process (c), the same thing happens as in the previous case, where the conversion reaches a maximum of 63% in 48 hours and stabilizes.

The literature reports similar results under other reaction conditions. BIDJOU-HAIOUR and KLAI (2013) achieved, in 72 hours at 60ºC, a conversion of 63% of xylose laurate using immobilized PPL and tert-butanol as solvent. However, their best result was using CALB in methyl ethyl ketone with 67% conversion. ABDULMALEK et al. (2016) employed a system with DMSO and acetone (1:10 v/v), 16% (w/v) of Novozym 435, and a molar ratio of xylose to caproic acid of 1:4, reaching after 24 hours a conversion of 64% in esters. GONÇALVES et al. (2021) used oleic acid and xylose in methyl ethyl ketone for 24 hours at 60°C, 0.5% (w/v) of Lipozyme 435, using a molecular sieve, achieved 98% xylose conversion. VIEIRA (2021) also tested xylose in methyl ethyl ketone and 0.5% (w/v) of enzymatic load, but used hydrolyzed SODD, obtaining in 24 hours 89.2% (PFL), 80.2% (TLL), and 51.8% (CALB) of conversion in terms of xylose.

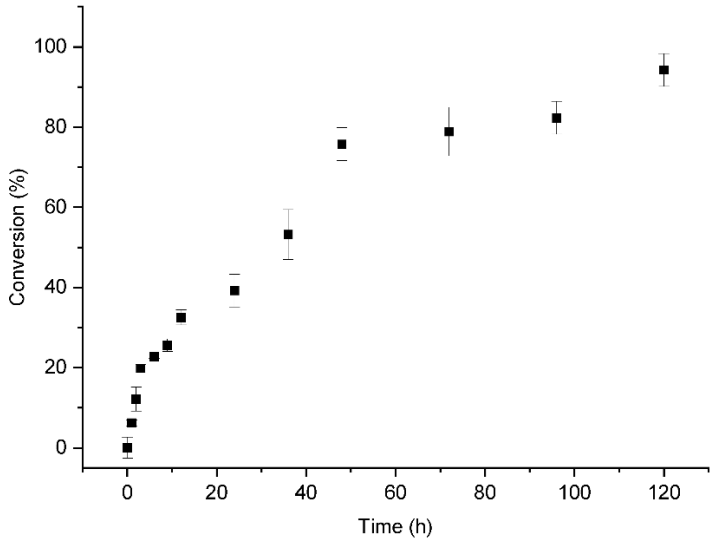

Figure 9. Conversion in terms of xylose consumption over time for transesterification/esterification reaction in the production of xylose esters. Reaction conditions: 120 h, 60ºC, 1% enzyme load (w/v), 10g/L xylose in tert-butanol, xylose: SODD (8.66 g: 100g).

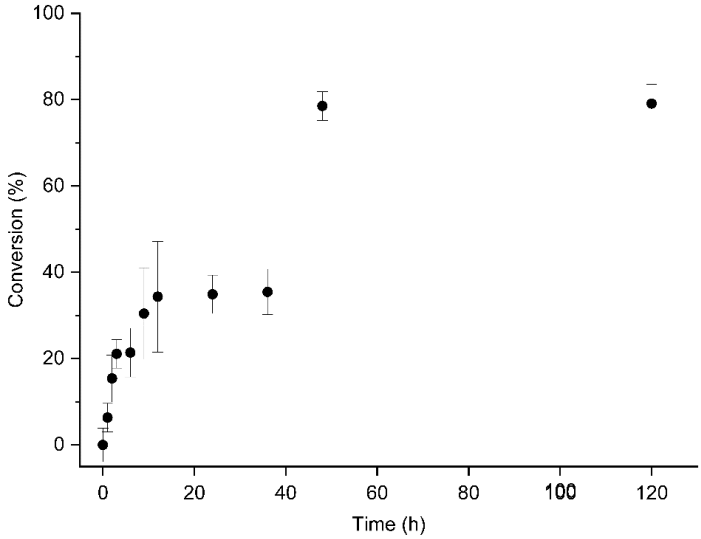

Figure 10. Conversion in terms of xylose consumption over time for transesterification/esterification reaction in the production of xylose esters. Reaction conditions: 120 h, 60ºC, 1% enzyme load (w/v), 80g/L xylose in tert-butanol: DMSO: water (8.28mL: 0.86mL: 0.86mL), xylose: SODD (8.66g: 100g).

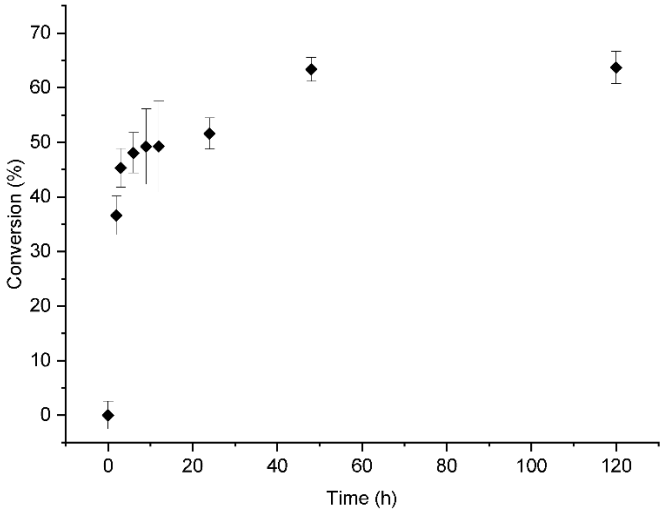

Figure 11. Conversion in terms of xylose consumption over time for transesterification/esterification reaction in the production of xylose esters. Reaction conditions: 120 h, 60ºC, 1% enzyme load (w/v), 105g/L xylose in tert-butanol: DMSO: water (6.29mL: 1.86mL: 1.86mL), xylose: SODD (8.66g: 100g).

Considering the stability of the conversion kinetics presented, a 48-h reaction cycle was considered for all simulations. For process (a), the simulation results are presented in Table 14. All SODD used in the process feed is composed of its constituent components. Note that stream 9,

immediately after the transesterification/esterification reactor (R - 102), has mainly the bulk component, tripalmitin (54.46%). Among the products, in the liquid phase only, there are xylose palmitate (6.34%), xylose stearate (0.27%), xylose linoleate (2.12%), xylose linolenate (0.26%), and xylose oleate (1.45%), totaling 10.44% (w/w) in xylose esters. After the solid enzyme is removed for recycling, water is added, and cooling is performed; stream 17 presents 10.67% esters. The first stage of purification by precipitation (stream 29) results in an ester content, now in the solid phase, increasing to 77.47%. Finally, at the end of the process (stream 38) there are 80.81% esters, 18.51% fatty acids, 0.04% TAGs, and traces of other components in negligible composition.

For the simulation of processes (b) and (c), the numerical results are presented in the supplementary material (Tables S2 and S3). For process (b), stream 9 presents 49.95% tripalmitin, 5.61% xylose palmitate, 0.24% xylose stearate, 1.87% xylose linoleate, 0.23% xylose linolenate, and 1.29% xylose oleate (totaling 9.24% esters w/w). At the end of the process, stream 38 presented 76.61% esters, 22.6% fatty acids, and 0.04% TAGs. Finally, in process (c), stream 9 presents 54.05% tripalmitin, 4.59% xylose palmitate, 0.20% xylose stearate, 1.54% xylose linoleate, 0.19% xylose linoleate, and 1.05% xylose oleate (totaling 7.57% esters w/w). At the end of the process, stream 38 presented 71.37% esters, 27.8% fatty acids, and 0.04% TAGs.

When we compare the three processes, the final purity in terms of mass of xylose esters decreases (process (a): 80.81%; process (b): 76.61%; process (c): 71.37%). This decrease in concentration was expected since the conversion is different in each case. The energy expended for each process can be found in Table S4 of the supplementary material. With NPV = 0, we find a Minimum Biosurfactant Selling Price (MBSP) of $13.42/kg of product for the process (a), $5.82/kg for the process (b), and $6.56/kg for the process (c). Therefore, compared with xylose esters, the use of SODD residue as a reagent managed to lower the value of CANSIAN et al. (2024a) (US$ 392.98/kg) and CANSIAN et al. (2022) (US$ 72.37/kg). As for biosurfactants from fermentation, our processes have a lower value than MOUTINHO et al. (2021) (US$ 60/kg), EKPENYONG et al. (2021) (€ 570/kg), CZINKÓCZKY and NÉMETH (2020) (US$ 836 - 2059.7/kg), ELIAS et al. (2021) (US$20/kg) and NOLL et al. (2024) (US$ 12–56/kg).

Table 14. Simulation results for main streams – process (a).

Variable	Name	Unit	Stream 9	Stream 17	Stream 29	Stream 38
Fw	Mass flow	kg/h	3297.12	3225.23	395.7530	372.0170
T	Temperature	K	333.15	298.15	298.15	333.15
P	Pressure	atm	1	1	1	1
zw(1)*	Composition	dimensionless	0.0000	0.0000	0.0000	0.0000
zw(2)*	Composition	dimensionless	0.0000	0.0000	0.0000	0.0000
zw(3)*	Composition	dimensionless	0.0355	0.0331	0.0004	0.0000
zw(4)*	Composition	dimensionless	0.0063	0.0013	0.0000	0.0000
zw(5)*	Composition	dimensionless	0.0000	0.0000	0.0000	0.0000
zw(6)*	Composition	dimensionless	0.5246	0.5363	0.0061	0.0004
zw(7)*	Composition	dimensionless	0.0284	0.0291	0.0001	0.0025
zw(8)*	Composition	dimensionless	0.0088	0.0090	0.0000	0.0004
zw(9)*	Composition	dimensionless	0.0705	0.0721	0.0008	0.0001
zw(10)*	Composition	dimensionless	0.0085	0.0087	0.0001	0.0000
zw(11)*	Composition	dimensionless	0.0484	0.0495	0.0006	0.0000
zw(12)*	Composition	dimensionless	0.0203	0.0208	0.0002	0.0000
zw(13)*	Composition	dimensionless	0.0782	0.0765	0.0009	0.0001
zw(14)*	Composition	dimensionless	0.0451	0.0461	0.0005	0.0000
zw(15)*	Composition	dimensionless	0.0108	0.0109	0.0002	0.0000
zw(16)*	Composition	dimensionless	0.0634	0.0648	0.0001	0.0003
zw(17)*	Composition	dimensionless	0.0027	0.0028	0.0000	0.0000
zw(18)*	Composition	dimensionless	0.0212	0.0216	0.0000	0.0001
zw(19)*	Composition	dimensionless	0.0026	0.0026	0.0000	0.0000
zw(20)*	Composition	dimensionless	0.0145	0.0149	0.0000	0.0001
zw(21)*	Composition	dimensionless	0.0000	0.0000	0.0001	0.0000
zw(22)*	Composition	dimensionless	0.0000	0.0000	0.0000	0.0058
zw(23)*	Composition	dimensionless	0.0017	0.0000	0.0000	0.0000
zw(24)*	Composition	dimensionless	0.0084	0.0000	0.0002	0.0002
zw(25)*	Composition	dimensionless	0.0000	0.0000	0.1642	0.1349
zw(26)*	Composition	dimensionless	0.0000	0.0000	0.0510	0.0472
zw(27)*	Composition	dimensionless	0.0000	0.0000	0.4703	0.4903
zw(28)*	Composition	dimensionless	0.0000	0.0000	0.0204	0.0213
zw(29)*	Composition	dimensionless	0.0000	0.0000	0.1571	0.1638
zw(30)*	Composition	dimensionless	0.0000	0.0000	0.0190	0.0198
zw(31)*	Composition	dimensionless	0.0000	0.0000	0.1079	0.1125

*Component number - Liquid phase: SODD (1), Enzyme (2), Tert-butanol (3), Xylose (4), Dimethyl sulfoxide (5), Tripalmitin (6), Palmitic acid (7), Stearic acid (8), Linoleic acid (9), Linolenic acid (10), Oleic acid (11), Tocopherol (12), Hydrocarbon (13), Glycerol (14), Water (15), Xylose palmitate (16), Xylose stearate (17), Xylose linoleate (18), Xylose linolenate (19), Xylose Oleate (20), Ethanol (21), Methyl ethyl ketone (22); Solid phase: Enzyme (23), Xylose (24), Palmitic acid (25), Stearic acid (26), Xylose palmitate (27), Xylose stearate (28), Xylose linoleate (29), Xylose linolenate (30), Xylose Oleate (31).

Table 15 shows the equipment dimensions and costs, and Table 16 the cash flow for 28 years, both to process (a). For the simulation of processes (b) and (c), these results are presented in the supplementary material (Tables S5, S6, S7 and S8). Figure 12 shows the distribution of CAPEX costs according to the plant equipment for each scenario. Note that transesterification/ esterification reactor (R - 102) burden the installation cost the most, presenting values above 22%. Figure 13 shows the distribution of operating costs (OPEX). Note that the cost of labor has the most significant impact in the three scenarios, followed by reagents.

Table 15. Equipment capacity and costs with installation included (CAPEX) – process (a).

Equipment	Volume/ Area	Total cost (US$)
Reactor (R - 101)	0.3513 m^3	190,801
Reactor (R - 102)	168.56 m^3	552,340
Filter (P - 101)	12.0000 m^2	17,288.3
Heat exchanger (E - 101)	12.4276 m^2	116,633
Centrifuge (FF - 101)	0.2000 m	111,282
Tank (TT - 101)	0.7027 m^3	292,230
Heat exchanger (E - 102)	6.7960 m^2	115,643
Vaporizer (FE - 101)	5.8740 m^3	106,530
Centrifuge (FF - 102)	0.2000 m	111,282
Tank (TT - 102)	3.2533 m^3	292,230
Centrifuge (FF - 103)	0.2000 m	111,282
Tank (TT - 102)	0.0371 m^3	292,230
Heat exchanger (E - 103)	8.0380 m^2	115,643
Vaporizer (FE - 102)	0.5324 m^3	45,621.5

Table 16. Cash flow for biosurfactant production – process (a).

Year	Cash Flow *	Year	Cash Flow *	Year	Cash Flow *	Year	Cash Flow *
1	-5.10337	8	0.751077	15	0.281254	22	0.135468
2	-4.59763	9	0.676646	16	0.253382	23	0.122043
3	-0.25681	10	0.609591	17	0.228272	24	0.109949
4	1.14019	11	0.549181	18	0.20565	25	0.099053
5	1.0272	12	0.494758	19	0.18527	26	0.089237
6	0.925402	13	0.445728	20	0.16691	27	0.080394
7	0.833696	14	0.312191	21	0.15037	28	0.084903

*: The values are expressed in million US$/ year and converted to present values.

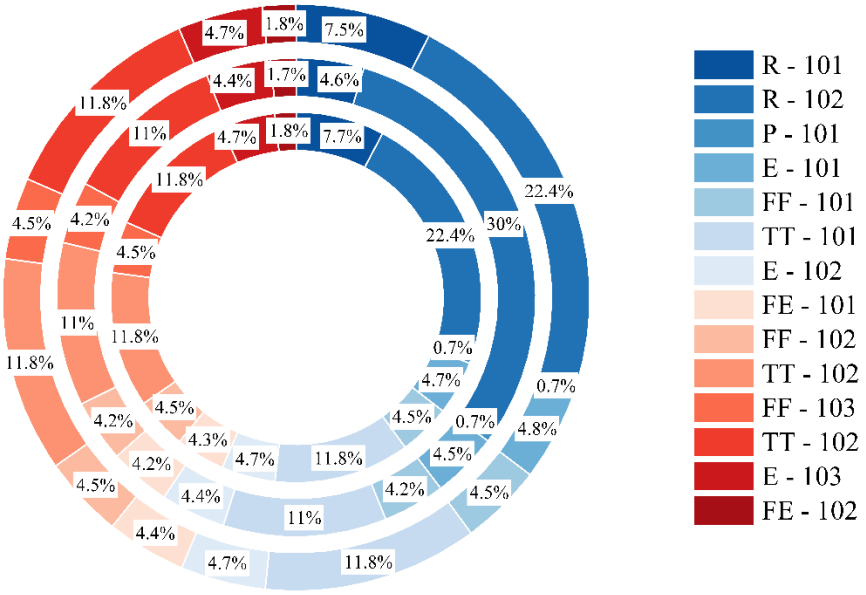

Figure 12. Fraction representation of each equipment in the plant installation (CAPEX): processes (a), (b) and (c).

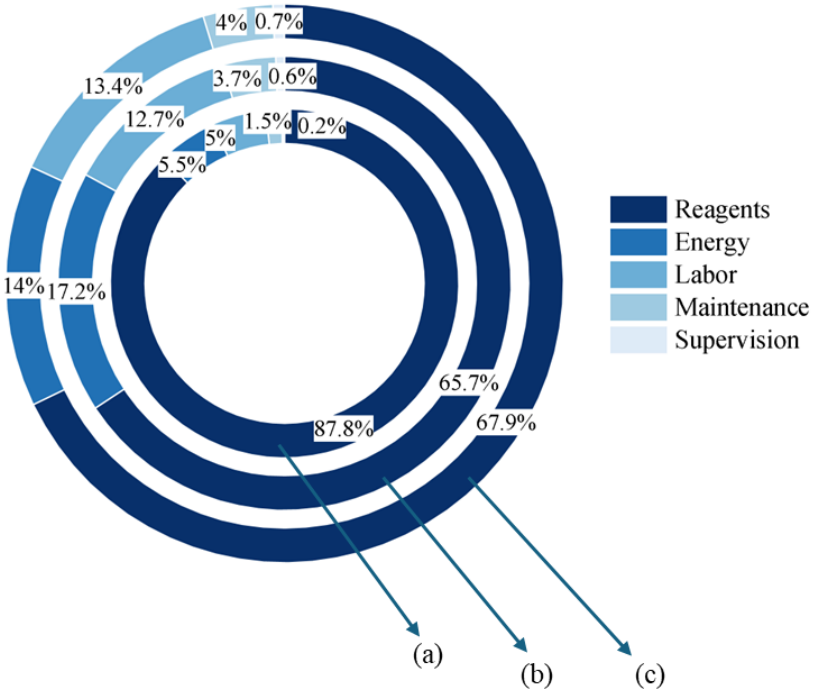

Figure 13. Fraction representation for operation costs (OPEX): processes (a), (b) and (c).

Since all three evaluated scenarios presented a Minimum Biosurfactant Selling Price (MBSP) below the market value, the cumulative discounted cash flow over the operational lifetime of the plants was assessed. Assuming a biosurfactant selling price of US$15/kg, the graphs in Figures 14 (a), (b), and (c) were generated. During the first two years, capital expenditures (CAPEX) were invested in the project, and only from the third year onward did the cash flow allow the plant to begin operations. From

that point on, a positive cash flow was maintained, and the break-even point was reached when the net present value (NPV) equaled zero. Among the three scenarios, process (b) had the shortest payback period, followed by scenario (c), and finally, scenario (a). Therefore, from the investors' perspective, scenario (b) offered the highest actual return.

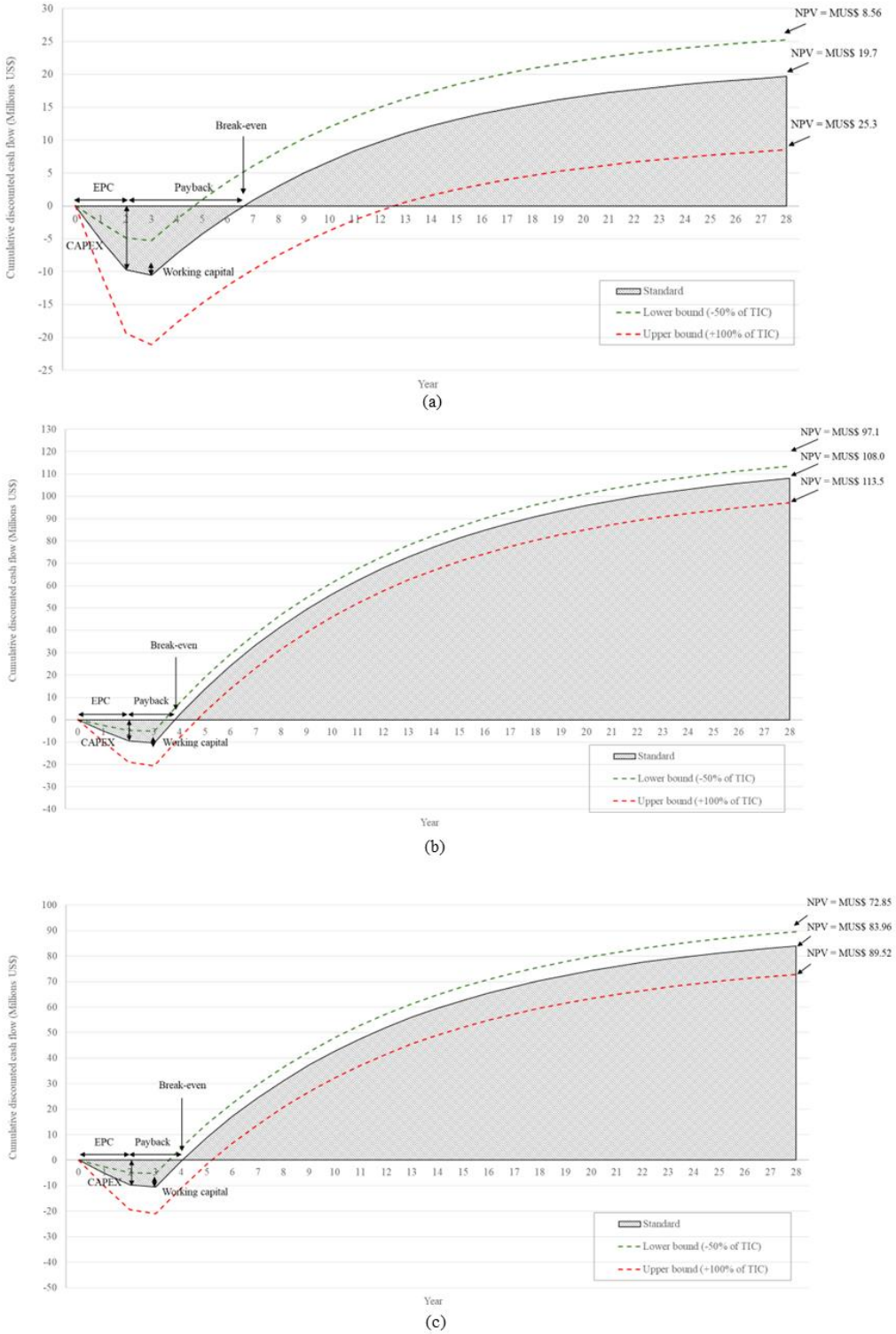

Figure 14. Cumulative discounted cash flow for processes: (a), (b) and (c). EPC: Engineering, Procurement and Construction; TIC: Total Installed Cost.

The last analysis of the three scenarios was that of environmental impact, shown in Figure 15. Note that there is a pattern of decrease in all parameters starting from process (a), decreasing in (b), and then in (c). However, scenarios (b) and (c) present similar values in most indicators. Compared to the xylose ester produced by CANSIAN et al. (2022), all indicators have lower values. They are also lower than those fermentation biosurfactants produced by KOPSAHELIS et al. (2018), GUILBOT et al. (2013), and NOLL et al. (2024). It is essential to highlight that all indicators have the same order of magnitude as ELIAS et al. (2021), being below them in almost all of them, excluding MAET in process (a). Only LOKESH et al. (2017) presented lower values of FWAET (6.21 x 10^{-2} kg 1,4DB eq.), TET (1.33 x 10^{-3} kg 1,4DB eq.), and AC (1.18 x 10^{-2} kg SO_2 eq.).

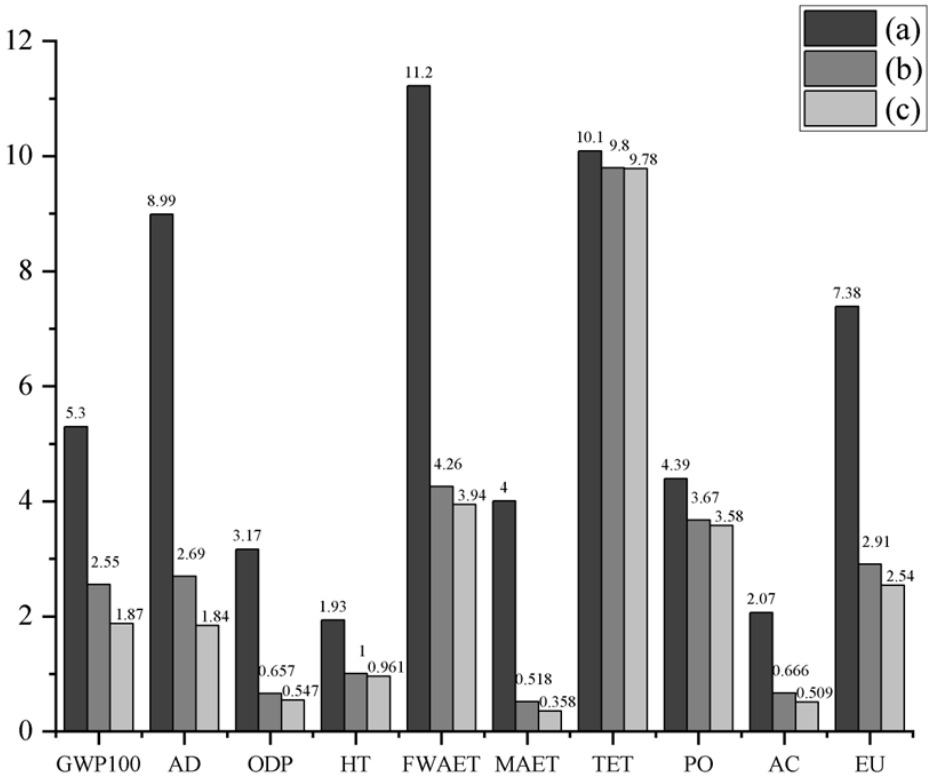

GWP100: Global Warming Potentials 100 Years, in kg CO_2 eq. / kg of xylose ester
AD: Abiotic depletion - fossil fuels, in ($\cdot 10^{-1}$) MJ/ kg of xylose ester
ODP: Ozone layer depletion, in ($\cdot 10^{7}$) kg CFC-11 eq./ kg of xylose ester
HT: Human toxicity, in kg 1,4DB eq./ kg of xylose ester
FWAET: Freshwater aquatic ecotoxicity, in ($\cdot 10^{1}$) kg 1,4DB eq./ kg of xylose ester
MAET: Marine aquatic ecotoxicity, in ($\cdot 10^{-3}$) kg 1,4DB eq./ kg of xylose ester
TET: Terrestral ecotoxicity, in kg ($\cdot 10^{2}$) 1,4DB eq./ kg of xylose ester
PO: Photochemical oxidation, in ($\cdot 10^{3}$) kg C_2H_4 eq./ kg of xylose ester
AC: Acidification, in ($\cdot 10^{2}$) kg SO_2 eq./ kg of xylose ester
EU: Eutrophication, in ($\cdot 10^{3}$) kg PO_4 eq./ kg of xylose ester

Figure 15. Environmental impact with LCA parameters calculated for process (a), (b), and (c).

It is important to emphasize that all SODD must be carefully monitored for contaminant levels. Although treatment processes aimed at contaminant removal are essential, the solvents employed in this study are not suitable for applications requiring food- or pharmaceutical-grade purity. Consequently, the resulting biodiesel and biosurfactants are intended for industrial applications in which such contaminants do not pose regulatory or functional limitations.

4.5 Conclusions

The enzymatic processes for producing biodiesel and biosurfactants were accurately described for the modeling in this work. So, the SODD proved an excellent reagent for producing these molecules. The simulation effectively represented the hydrolyzes and subsequent esterification reactions for producing biodiesel from ethanol and SODD, obtaining a product with approximately 81.57% (w/w) of ethyl esters (ethyl palmitate, ethyl stearate, ethyl oleate, ethyl linoleate, and ethyl linoleate), 0.99% of MAGs, DAGs, and TAGs, 14.79% of fatty acids and 1.91% tocopherol. Although the product did not meet the standards for biodiesel, it shows potential as an alternative biofuel with enhanced lubricity, primarily due to its content of MAGs, DAGs, TAGs, and fatty acids. The techno-economic evaluation of the biodiesel route presented a Minimum Biodiesel Selling Price (MBSP) of approximately US$6.15/L or US$6.84/kg. Regarding the Life Cycle Assessment (LCA), our process has lower indicators compared with the chemical catalysis of biodiesel from soybean oil in Brazil. It reinforces the importance of developing processes from coproduct in biodiesel production.

Three scenarios containing different solvent mixtures were evaluated for biosurfactants (xylose esters) production through transesterification/ esterification reactions. When we compared all of them, the final purity in terms of mass of xylose esters decreased (process (a): 80.81%; process (b): 76.61%; process (c): 71.37%). This decrease in ester concentration was expected since the conversion is different in each case. With NPV = 0, we found a Minimum Biosurfactant Selling Price (MBSP) of $13.42/kg of product for the process (a), $5.82/kg for the process (b), and $6.56/kg for the process (c). The production costs were comparable and competitive with others in the literature. The Life Cycle Assessment (LCA) reinforced the value of using SODD as a raw material for biosurfactants since all the parameters indicate an impactive reduction compared with almost all other works.

Supplementary material

Table S1. Equipment cost parameters.

Equipment	K_1	K_2	K_3	FBM	B1	B2	LF_B	A_{min}	A_{max}	Unit
Reactor (Jacketed agitated)	4.1052	-0.4680	-0.0005	4.00	-	-	1.14	0.1	35	m^3
Filter (Gravity)	4.2756	-0.648	0.0714	1.65	-	-	1.14	0.5	80	m^2
Heat exchanger (Fixed tube)	4.3247	-0.3030	0.1634	-	1.63	1.66	1.14	10	1000	m^2
Tank (Fixed roof)	4.8509	-0.3973	0.1445	-	1.49	1.52	1.14	90	30000	m^3
Flash (Vaporizer)	3.8751	0.3328	0.1901	2.65	-	-	1.14	1	100	m^3
Centrifuge separator	4.3612	-0.1236	0.0049	1.57	-	-	1.14	0.5	1	m

Adapted from TURTON et al. (2009).

Table S2. Simulation results for main streams – process (b).

Variable	Name	Unit	Stream 9	Stream 17	Stream 29	Stream 38
Fw	Mass flow	kg/h	3504.84	3373.06	395.7530	362.3980
T	Temperature	K	333.15	298.15	298.15	333.15
P	Pressure	atm	1	1	1	1
zw(1)*	Composition	dimensionless	0.0000	0.0000	0.00001	0.0000
zw(2)*	Composition	dimensionless	0.0000	0.0000	0.0000	0.0000
zw(3)*	Composition	dimensionless	0.0692	0.0625	0.0007	0.0001
zw(4)*	Composition	dimensionless	0.0081	0.0017	0.0000	0.0000
zw(5)*	Composition	dimensionless	0.0101	0.0103	0.0001	0.0000
zw(6)*	Composition	dimensionless	0.4995	0.5190	0.0058	0.0004
zw(7)*	Composition	dimensionless	0.0271	0.0281	0.0001	0.0003
zw(8)*	Composition	dimensionless	0.0084	0.0087	0.0000	0.0005
zw(9)*	Composition	dimensionless	0.0671	0.0698	0.0008	0.0001
zw(10)*	Composition	dimensionless	0.0081	0.0084	0.0001	0.0000
zw(11)*	Composition	dimensionless	0.0461	0.0479	0.0005	0.0000
zw(12)*	Composition	dimensionless	0.0191	0.0199	0.0002	0.0000
zw(13)*	Composition	dimensionless	0.0736	0.0713	0.0008	0.0001
zw(14)*	Composition	dimensionless	0.0425	0.0441	0.0005	0.0000
zw(15)*	Composition	dimensionless	0.0193	0.0124	0.0002	0.0000
zw(16)*	Composition	dimensionless	0.0561	0.0583	0.0001	0.0011
zw(17)*	Composition	dimensionless	0.0024	0.0025	0.0000	0.0000
zw(18)*	Composition	dimensionless	0.0187	0.0195	0.0000	0.0004
zw(19)*	Composition	dimensionless	0.0023	0.0023	0.0000	0.0000
zw(20)*	Composition	dimensionless	0.0129	0.0134	0.0000	0.0002
zw(21)*	Composition	dimensionless	0.0000	0.0000	0.0001	0.0000
zw(22)*	Composition	dimensionless	0.0000	0.0000	0.0000	0.0067
zw(23)*	Composition	dimensionless	0.0016	0.0000	0.0000	0.0000
zw(24)*	Composition	dimensionless	0.0079	0.0000	0.0003	0.0003
zw(25)*	Composition	dimensionless	0.0000	0.0000	0.1737	0.1760
zw(26)*	Composition	dimensionless	0.0000	0.0000	0.0539	0.0491
zw(27)*	Composition	dimensionless	0.0000	0.0000	0.4627	0.4642
zw(28)*	Composition	dimensionless	0.0000	0.0000	0.0201	0.0201
zw(29)*	Composition	dimensionless	0.0000	0.0000	0.1546	0.1551
zw(30)*	Composition	dimensionless	0.0000	0.0000	0.0187	0.0187
zw(31)*	Composition	dimensionless	0.0000	0.0000	0.1061	0.1065

*Component number - Liquid phase: SODD (1), Enzyme (2), Tert-butanol (3), Xylose (4), Dimethyl sulfoxide (5), Tripalmitin (6), Palmitic acid (7), Stearic acid (8), Linoleic acid (9), Linolenic acid (10), Oleic acid (11), Tocopherol (12), Hydrocarbon (13), Glycerol (14), Water (15), Xylose palmitate (16), Xylose stearate (17), Xylose linoleate (18), Xylose linolenate (19), Xylose Oleate (20), Ethanol (21), Methyl ethyl ketone (22); Solid phase: Enzyme (23), Xylose (24), Palmitic acid (25), Stearic acid (26), Xylose palmitate (27), Xylose stearate (28), Xylose linoleate (29), Xylose linolenate (30), Xylose Oleate (31).

Table S3. Simulation results for main streams – process (c).

Variable	Name	Unit	Stream 9	Stream 17	Stream 29	Stream 38
Fw	Mass flow	kg/h	3370.14	3324.75	320.2930	306.3580
T	Temperature	K	333.15	298.15	298.15	333.15
P	Pressure	atm	1	1	1	1
zw(1)*	Composition	dimensionless	0.0000	0.0000	0.0000	0.0000
zw(2)*	Composition	dimensionless	0.0000	0.0000	0.0000	0.0000
zw(3)*	Composition	dimensionless	0.0208	0.0211	0.0002	0.0000
zw(4)*	Composition	dimensionless	0.0159	0.0032	0.0000	0.0000
zw(5)*	Composition	dimensionless	0.0087	0.0088	0.0001	0.0000
zw(6)*	Composition	dimensionless	0.5405	0.5478	0.0062	0.0004
zw(7)*	Composition	dimensionless	0.0293	0.0297	0.0001	0.0003
zw(8)*	Composition	dimensionless	0.0091	0.0092	0.0000	0.0005
zw(9)*	Composition	dimensionless	0.0726	0.0736	0.0008	0.0001
zw(10)*	Composition	dimensionless	0.0087	0.0088	0.0001	0.0000
zw(11)*	Composition	dimensionless	0.0499	0.0505	0.0006	0.0000
zw(12)*	Composition	dimensionless	0.0199	0.0202	0.0002	0.0000
zw(13)*	Composition	dimensionless	0.0765	0.0776	0.0008	0.0001
zw(14)*	Composition	dimensionless	0.0442	0.0448	0.0005	0.0000
zw(15)*	Composition	dimensionless	0.0184	0.0279	0.0001	0.0000
zw(16)*	Composition	dimensionless	0.0459	0.0466	0.0001	0.0009
zw(17)*	Composition	dimensionless	0.0020	0.0020	0.0000	0.0000
zw(18)*	Composition	dimensionless	0.0154	0.0156	0.0000	0.0003
zw(19)*	Composition	dimensionless	0.0019	0.0019	0.0000	0.0000
zw(20)*	Composition	dimensionless	0.0105	0.0107	0.0000	0.0002
zw(21)*	Composition	dimensionless	0.0000	0.0000	0.0001	0.0000
zw(22)*	Composition	dimensionless	0.0000	0.0000	0.0000	0.0070
zw(23)*	Composition	dimensionless	0.0016	0.0000	0.0000	0.0000
zw(24)*	Composition	dimensionless	0.0082	0.0001	0.0007	0.0007
zw(25)*	Composition	dimensionless	0.0000	0.0000	0.2136	0.2167
zw(26)*	Composition	dimensionless	0.0000	0.0000	0.0663	0.0604
zw(27)*	Composition	dimensionless	0.0000	0.0000	0.4307	0.4324
zw(28)*	Composition	dimensionless	0.0000	0.0000	0.0187	0.0188
zw(29)*	Composition	dimensionless	0.0000	0.0000	0.1439	0.1445
zw(30)*	Composition	dimensionless	0.0000	0.0000	0.0174	0.0174
zw(31)*	Composition	dimensionless	0.0000	0.0000	0.0988	0.0992

*Component number - Liquid phase: SODD (1), Enzyme (2), Tert-butanol (3), Xylose (4), Dimethyl sulfoxide (5), Tripalmitin (6), Palmitic acid (7), Stearic acid (8), Linoleic acid (9), Linolenic acid (10), Oleic acid (11), Tocopherol (12), Hydrocarbon (13), Glycerol (14), Water (15), Xylose palmitate (16), Xylose stearate (17), Xylose linoleate (18), Xylose linolenate (19), Xylose Oleate (20), Ethanol (21), Methyl ethyl ketone (22); Solid phase: Enzyme (23), Xylose (24), Palmitic acid (25), Stearic acid (26), Xylose palmitate (27), Xylose stearate (28), Xylose linoleate (29), Xylose linolenate (30), Xylose Oleate (31).

Table S4. Energy for each process.

Process	Type	Heat (MWh) per month
(a)	Hot	154.53
	Cold	-62.14
(b)	Hot	187.97
	Cold	-75.85
(c)	Hot	137.39
	Cold	-70.92

Table S5. Equipment capacity and costs with installation included (CAPEX) – process (b).

Equipment	Volume/ Area	Total cost (US$)
Reactor (R - 101)	0.9308 m^3	120,965
Reactor (R - 102)	177.8340 m^3	795,372
Filter (P - 101)	12.0000 m^2	17,288.3
Heat exchanger (E - 101)	15.1696 m^2	118,244
Centrifuge (FF - 101)	0.2000 m	111,282
Tank (TT - 101)	1.8616 m^3	292,230
Heat exchanger (E - 102)	7.3148 m^2	115,643
Vaporizer (FE - 101)	6.2504 m^3	110,782
Centrifuge (FF - 102)	0.2000 m	111,282
Tank (TT - 102)	3.4011m^3	292,230
Centrifuge (FF - 103)	0.2000 m	111,282
Tank (TT - 102)	0.0370 m^3	292,230
Heat exchanger (E - 103)	8.4643 m^2	115,643
Vaporizer (FE - 102)	0.5211 m^3	45,621.5

Table S6. Cash flow for biosurfactant production – process (b)

Year	Cash Flow *	Year	Cash Flow *	Year	Cash Flow *	Year	Cash Flow *
1	-4.99802	8	0.735572	15	0.275448	22	0.132672
2	-4.50272	9	0.662678	16	0.248151	23	0.119524
3	-0.2515	10	0.597007	17	0.223559	24	0.107679
4	1.11665	11	0.537844	18	0.201405	25	0.097008
5	1.00599	12	0.484544	19	0.181446	26	0.087395
6	0.906299	13	0.436526	20	0.163465	27	0.078734
7	0.816485	14	0.305747	21	0.147266	28	0.08315

*: The values are expressed in million US$/ year and converted to present values.

Table S7. Equipment capacity and costs with installation included (CAPEX) – process (c).

Equipment	Volume/ Area	Total cost (US$)
Reactor (R - 101)	0.3781 m³	184,359
Reactor (R - 102)	168.9910 m³	552,340
Filter (P - 101)	12.0000 m²	17,288.3
Heat exchanger (E - 101)	14.1832 m²	117,624
Centrifuge (FF - 101)	0.2000 m	111,282
Tank (TT - 101)	0.7562 m³	292,230
Heat exchanger (E - 102)	6.9399 m²	115,643
Vaporizer (FE - 101)	6.0282 m²	108,275
Centrifuge (FF - 102)	0.2000 m	111,282
Tank (TT - 102)	3.2621 m³	292,230
Centrifuge (FF - 103)	0.2000 m	111,282
Tank (TT - 102)	0.0364 m³	292,230
Heat exchanger (E - 103)	8.0632 m²	115,643
Vaporizer (FE - 102)	0.4431 m³	45,621.5

Table S8. Cash flow for biosurfactant production – process (c).

Year	Cash Flow *	Year	Cash Flow *	Year	Cash Flow *	Year	Cash Flow *
1	-5.09404	8	0.749704	15	0.280739	22	0.13522
2	-4.58922	9	0.675409	16	0.252918	23	0.12182
3	-0.25634	10	0.608476	17	0.227854	24	0.109748
4	1.1381	11	0.548177	18	0.205274	25	0.098872
5	1.02532	12	0.493853	19	0.184932	26	0.089074
6	0.92371	13	0.444913	20	0.166605	27	0.080247
7	0.832171	14	0.311621	21	0.150095	28	0.084748

*: The values are expressed in million US$/ year and converted to present values.

REFERENCES

ABDULMALEK, E.; HAMIDON, N. F.; ABDUL RAHMAN, M. B. Optimization and characterization of lipase catalysed synthesis of xylose caproate ester in organic solvents. **Journal of Molecular Catalysis B: Enzymatic**, v. 132, p. 1–4, 2016.

AGILENT TECHNOLOGIES. **The Essential Chromatography and Spectroscopy Catalog**. Available in: <https://www.agilent.com/cs/library/catalogs/public/5991-1056EN%20General%20Catalog.pdf>. Accessed on: Augst 14, 2024.

AL-MUHTASEB, A. H. et al. Integrating life cycle assessment and characterisation techniques: A case study of biodiesel production utilising waste Prunus Armeniaca seeds (PAS) and a novel catalyst. **Journal of Environmental Management**, v. 304, p. 114319, 2022.

AMER, L.; ADHIKARI, B.; PELLEGRINO, J. Technoeconomic analysis of five microalgae-to-biofuels processes of varying complexity. **Bioresource Technology**, v. 102, n. 20, p. 9350–9359, 2011.

AOCS. Free Fatty Acids in Crude and Refined Fats and Oils. Ca 5a-40. Champaign, USA. **Official methods and recommended practices of the American Oil Chemists` Society**, 1990a.

AOCS. Wijs Method for Iodine Value. Cd 1-25. Champaign, USA. **Official methods and recommended practices of the American Oil Chemists` Society**, 1990b.

AOCS. Saponification Value. Cd 3-25. Champaign, USA. **Official methods and recommended practices of the American Oil Chemists` Society**,1990c.

AOCS. Specific Gravity of Oils and Liquid Fats. Cc 10a-25. Champaign, USA. **Official methods and recommended practices of the American Oil Chemists` Society**, 1990d.

AOCS. Preparation of Methyl Esters of Fatty Acids. Ce 2-66. Champaign, USA. **Official methods and recommended practices of the American Oil Chemists` Society**, 2004a.

AOCS. Tocopherols and Tocotrienols in Vegetable Oils and Fats by HPLC. Ce 8-89. Champaign, USA. **Official methods and recommended practices of the American Oil Chemists` Society**, 2004b.

AOCS. Moisture and Volatile Matter in Butter, Fats, Margarines, and Oils, Hot Plate. Ca 2b-38; Champaign, USA. **Official methods and recommended practices of the American Oil Chemists` Society**, 2004c.

AOCS. FAME. Ce 5-86. Champaign, USA**. Official methods and recommended practices of the American Oil Chemists` Society**, 2004d.

AOCS. Triglycerides by Gas Chromatography. Ce 5-86. Champaign, USA. **Official methods and recommended practices of the American Oil Chemists` Society**, 2009a.

AOCS. Determination of Mono- and Diglycerides by Capillary Gas Chromatography. Cd 11b-91. Champaign, USA. **Official methods and recommended practices of the American Oil Chemists` Society**, 2009b.

APOSTOLAKOU, A. A. et al. Techno-economic analysis of a biodiesel production process from vegetable oils. **Fuel Processing Technology**, v. 90, n. 7–8, p. 1023–1031, 2009.

ARCENS, D. et al. 6-O-glucose palmitate synthesis with lipase: Investigation of some key parameters. **Molecular Catalysis**, v. 460, p. 63–68, 2018.

ARTQUÍMICA. **Metil Etil Cetona**. Available in: <https://artquimicamaringa.com.br/produtos/metil-etil-cetona-pa-acs-1l-controlado-pela-policia-federal/>. Accessed on: Aug 28, 2024.

BANAT, I. M. et al. Microbial biosurfactants production, applications and future potential. **Applied Microbiology and Biotechnology**, v. 87, p. 427–444, 2010.

BANCHERO, M.; GOZZELINO, G. Nb2O5-catalyzed kinetics of fatty acids esterification for reactive distillation process simulation. **Chemical Engineering Research and Design**, v. 100, p. 292–301, 2015.

BEZERRA, I. D. et al. Industrially concentrated tocopherols from soybean oil deodorizer distillate. **Brazilian Journal of Food Technology**, v. 25, 2022.

BIDJOU-HAIOUR, C.; KLAI, N. Lipase catalyzed synthesis of fatty acid xylose esters and their surfactant properties. **Asian Journal of Chemistry**, v. 25, n. 8, p. 4347–4350, 2013.

BRAZIL GOVERNMENT. **ABIOVE**. Available in: <https://abiove.org.br/estatisticas/>. Accessed on: Jul 20, 2024.

CAGED. Federal Government of Brazil. **Cadastro Geral de Empregados e Desempregados**, 2021.

CAGED. **Federal Government of Brazil**. **Cadastro Geral de Empregados e Desempregados**, 2023. Available in: <https://www.gov.br/trabalho-e-emprego/pt-br/assuntos/estatisticas-trabalho/novo-caged/novo-caged-2023>. Accessed on: Aug 28, 2024

CALERO, J. et al. Optimization by response surface methodology of the reaction conditions in 1,3-selective transesterification of sunflower oil, by using CaO as heterogeneous catalyst. **Molecular Catalysis**, v. 484, p. 110804, 2020.

CANSIAN, A. B. M. et al. Modeling and simulation of the biosurfactant production by enzymatic route using xylose and oleic acid as reagents. **Chemical Industry and Chemical Engineering Quarterly**, v. 28, n. 4, p. 265–276, 2022.

CANSIAN, A. B. M. et al. Valuable bioproducts from Soybean Oil Deodorizer Distillate: A systematic review of feedstock characteristics, production methods, and purification techniques. **UFSCar**, São Carlos, SP, Brazil, 2024a.

CANSIAN, A. B. M. et al. Sustainable Production of Xylose Ester Biosurfactant: A Techno-Economic-Environmental Analysis. **UFSCar**, São Carlos, SP, Brazil, 2024b.

CASTRO, J. S. et al. Life cycle assessment and techno-economic analysis for biofuel and biofertilizer recovery as by-products from microalgae. **Renewable and Sustainable Energy Reviews**, v. 187, p. 113781, 2023.

CZINKÓCZKY, R.; NÉMETH, Á. Techno-economic assessment of Bacillus fermentation to produce surfactin and lichenysin. **Biochemical Engineering Journal**, v. 163, p. 107719, 2020.

D'AMATO VILLARDI, H. G. et al. Catalytic and non-catalytic esterification of soybean oil deodorizer distillate by ethanol: Kinetic modelling. **Chemical Engineering Transactions**, v. 57, p. 1999–2004, 2017.

DANG, H. T.; OBIRI, O.; HAYES, D. G. Feed Batch Addition of Saccharide During Saccharide-Fatty Acid Esterification Catalyzed by Immobilized Lipase: Time Course, Water Activity, and Kinetic Model. **JAOCS,** v. 82, n. 7, 2005.

DE ARAUJO-SILVA, R. et al. Enzymatic Synthesis of Fatty Acid Isoamyl Monoesters from Soybean Oil Deodorizer Distillate: A Renewable and Ecofriendly Base Stock for Lubricant Industries. **Molecules**, v. 27, n. 9, 2022.

DELRUE, F. et al. An economic, sustainability, and energetic model of biodiesel production from microalgae. **Bioresource Technology**, v. 111, p. 191–200, 2012.

DEPARTAMENTO DE ÁGUA E ESGOTO. **Tarifa industrial**. 2024. Available in: <https://www.deagua.com.br/public/admin/globalarq/uploads/files/tarifa-industrial-1.pdf>. Accessed on: Aug 28, 2024

DU, W.; WANG, L.; LIU, D. Improved methanol tolerance during Novozym435-mediated methanolysis of SODD for biodiesel production. **Green Chemistry**, v. 9, n. 2, p. 173–17, 1 2007.

DUVEKOT, C. Determination of Total FAME and Linolenic Acid Methyl Esters in Biodiesel According to **EN-14103. 2021**. Available in: <https://www.agilent.com/cs/library/applications/5990-8983EN.pdf>. Accessed on: June 17, 2020

EKPENYONG, M. et al. Kinetic modeling and quasi-economic analysis of fermentative glycolipopeptide biosurfactant production in a medium co-optimized by statistical and neural network approaches. **Preparative Biochemistry and Biotechnology**, v. 51, n. 5, p. 450–466, 2021.

ELDOS, H. I. et al. Isolation, identification, and characterization of potential biosurfactant-producing bacteria from processing wastewater for the development of eco-friendly green technology. **Bioresource Technology Reports**, v. 25, p. 101763, 2024.

ELIAS, A. M.; LONGATI, A. A.; ELLAMLA, H. R.; FURLAN, F. F.; RIBEIRO, M. P. A.; MARCELINO, P. R. F.; et al. Techno-Economic-Environmental Analysis of Sophorolipid Biosurfactant Production from Sugarcane Bagasse. **Industrial & Engineering Chemistry Research**, v. 60, n. 27, p. 9833–9850, 2021.

FANG, T. et al. Separation of natural tocopherols from soybean oil byproduct with supercritical carbon dioxide. **Journal of Supercritical Fluids**, v. 40, n. 1, p. 50–58, 2007.

GONÇALVES, M. C. P. et al. Lipozyme 435-mediated synthesis of xylose oleate in methyl ethyl ketone. **Molecules**, v. 26, n. 11, 2021.

GUILBOT, J. et al. Life cycle assessment of surfactants: the case of an alkyl polyglucoside used as a self emulsifier in cosmetics. **Green Chemistry**, v. 15, n. 12, p. 3337, 2013.

GUNAWAN, S.; FABIAN, C.; JU, Y. H. Isolation and purification of fatty acid steryl esters from soybean oil deodorizer distillate. **Industrial and Engineering Chemistry Research**, v. 47, n. 18, p. 7013–7018, 2008.

GUNAWAN, S.; KASIM, N. S.; JU, Y. H. Separation and purification of squalene from soybean oil deodorizer distillate. **Separation and Purification Technology**, v. 60, n. 2, p. 128–135, 2008.

HARUN, R. et al. Technoeconomic analysis of an integrated microalgae photobioreactor, biodiesel and biogas production facility. **Biomass and Bioenergy**, v. 35, n. 1, p. 741–747, 2011.

HIROTA, Y. et al. Fractionation of Soybean Oil Deodorizer Distillate (SODD) by Molecular Distillation a Content (wt%). **JAOCS**, Vol. 80, no. 4, 2003.

HOSSEINZADEH-BANDBAFHA, H. et al. Environmental life cycle assessment of biodiesel production from waste cooking oil: A systematic review. **Renewable and Sustainable Energy Reviews**, v. 161, 2022.

KASIM, N. S. et al. A simple two-step method for simultaneous isolation of tocopherols and free phytosterols from soybean oil deodorizer distillate with high purity and recovery. **Separation Science and Technology**, v. 45, n. 16, p. 2437–2446, 2010.

KHATOON, S.; RAJAN, R. G. R.; KRISHNA, A. G. G. Physicochemical characteristics and composition of indian soybean oil deodorizer distillate and the recovery of phytosterols. **JAOCS, Journal of the American Oil Chemists' Society**, v. 87, n. 3, p. 321–326, 2010.

KOPSAHELIS, A. et al. Gate-to-gate life cycle assessment of biosurfactants and bioplasticizers production via biotechnological exploitation of fats and waste oils. **Journal of Chemical Technology & Biotechnology**, v. 93, n. 10, p. 2833–2841, 2018.

LI, L. et al. Esterification degree of fructose laurate exerted by Candida antarctica lipase B in organic solvents. **Enzyme and Microbial Technology**, v. 69, p. 46–53, 2015a.

LI, L. et al. Efficient mono-acylation of fructose by lipase-catalyzed esterification in ionic liquid co-solvents. **Carbohydrate Research**, v. 416, p. 51–58, 2015b.

LIU, Y.; FANG, T.; DING, X. Phase equilibrium for supercritical co 2 and the methyl esterified product from soybean oil deodorizer distillate. **Journal of food Lipids**, v. 13, 4, p. 390-401, 2006.

LOJA QUÍMICA. **Álcool absoluto**. **Álcool Absoluto 99,3% - 50 Litros (Etanol)**, 2024b. Available in: <https://www.lojaquimica.com.br/alcool-absoluto-99-3-50-litros-etanol>. Accessed on: Aug 28, 2024

LOJA QUÍMICA. **DMSO**. **Dimetilsulfóxido P.A. 99,9% (DMSO) - 1 Litro**, 2024a. Available in: <https://www.lojaquimica.com.br/dmso-1litro>. Accessed on: Aug 28, 2024

LOKESH, K. et al. Environmental impact assessment of wheat straw based alkyl polyglucosides produced using novel chemical approaches. **Green Chemistry**, v. 19, n. 18, p. 4380–4395, 2017.

LV, W. et al. Integrated Utilization Strategy for Soybean Oil Deodorizer Distillate: Synergically Synthesizing Biodiesel and Recovering Bioactive Compounds by a Combined Enzymatic Process and Molecular Distillation. **ACS Omega**, v. 6, n. 13, p. 9141–9152, 2021.

MAAFA, I. M. et al. Eco-friendly self-terminated process for preparation of CaO catalyst based on chitosan production wastes for biodiesel production. **Journal of Materials Research and Technology**, v. 30, p. 1217–1227, 2024.

MARTINI, G.; NERLI, B. B.; MALPIEDI, L. P. A novel method based on saponification coupled to micelle-extraction for recovering valuable bioactive compounds from soybean oil deodorizer distillate. **Food Chemistry**, v. 384, 2022.

MARTINS, P. F. et al. Free fatty acid separation from vegetable oil deodorizer distillate using molecular distillation process. **Separation and Purification Technology**, v. 48, n. 1, p. 78–84, 2006.

MAYUMI ITO, V. et al. Natural Compounds Obtained Through Centrifugal Molecular Distillation. **Applied Biochemistry and Biotechnology**. Vol. 129–132, 2006.

MGBECHIDINMA, C. L. et al. Integration of green economy concepts for sustainable biosurfactant production – A review. **Bioresource Technology**, v. 364, p. 128021, 2022.

MOUTINHO, L. F. et al. Microbial biosurfactants: A broad analysis of properties, applications, biosynthesis, and techno-economical assessment of rhamnolipid production. **Biotechnology Progress**, v. 37, n. 2, 2021.

NAGARAJAN, S. et al. An updated comprehensive techno-economic analysis of algae biodiesel. **Bioresource Technology**, v. 145, p. 150–156, 2013.

NOLL, P. et al. Limits for sustainable biosurfactant production: Techno-economic and environmental assessment of a rhamnolipid production process. **Bioresource Technology Reports**, v. 25, p. 101767, 2024.

ORION PRODUTOS CIENTIFICOS. **Tert Butanol**. **Alcool Butilico Terc (3-Butanol) Pa 1L Exodo Cientifica**, 2024. Available in: <https://www.orionprodutoscientificos.com.br/alcool-butilico-terciario-p-a-terc-butanol-1l-exodo-cientifica>. Accessed on: Aug 28, 2024

PALUZAR, H. Production of high quality biodiesel from sunflower soapstock acid oil as novel feedstock: Catalyzed by immobilized pancreatic lipase. **Journal of the American Oil Chemists' Society**, v. 101, n. 2, p. 251–265, 2024.

PANDEY, R. et al. Glycolipid biosurfactant production and petroleum hydrocarbon degradation by a new strain of Citricoccus zhacaiensis. **Biocatalysis and Agricultural Biotechnology**, v. 59, p. 103248, 2024.

PARTOVI, M. et al. Management of soybean oil refinery wastes through recycling them for producing biosurfactant using Pseudomonas aeruginosa MR01. **World Journal of Microbiology and Biotechnology**, v. 29, n. 6, p. 1039–1047, 2013.

PEÑARRUBIA FERNANDEZ, I. A.; LIU, D.-H.; ZHAO, J. LCA studies comparing alkaline and immobilized enzyme catalyst processes for biodiesel production under Brazilian conditions. **Resources, Conservation and Recycling**, v. 119, p. 117–127, 2017.

PETERS, M. S.; TIMMERHAUS, K. D.; WEST, R. E. **Plant design and economics for chemical engineers**. Boston: Mcgraw-Hill, 2004.

PERFUMO, A.; BANAT, I. M.; MARCHANT, R. Going Green and Cold: Biosurfactants from Low-Temperature Environments to Biotechnology Applications. **Trends in Biotechnology**, v. 36, n. 3, p. 277-289, 2018.

PODDAR, T.; JAGANNATH, A.; ALMANSOORI, A. Use of reactive distillation in biodiesel production: A simulation-based comparison of energy requirements and profitability indicators. **Applied Energy**, v. 185, p. 985–997, 2017.

RAJENDRAN, N. et al. Techno-economic and environmental impact analysis of integrated biodiesel production and tocopherol separation from rapeseed oil deodorizer distillate. **Industrial Crops and Products**, v. 220, p. 119304, 2024.

RAOUF, S. et al. Screening of sustainable biosurfactant produced by indigenous bacteria isolated from Egyptian oil fields for microbial enhanced oil recovery. **Geoenergy Science and Engineering**, v. 239, p. 212974, 2024.

REETU et al. Latest advances and status analysis of nanomaterials for microalgae photosystem, lipids and biodiesel: A state of art. **Journal of Environmental Chemical Engineering**, v. 11, n. 1, 2023.

RICHARDSON, J. W.; JOHNSON, M. D.; OUTLAW, J. L. Economic comparison of open pond raceways to photo bio-reactors for profitable production of algae for transportation fuels in the Southwest. **Algal Research**, v. 1, n. 1, p. 93–100, 2012.

SALÁRIO. **Portal Salário**. Available in: <https://www.salario.com.br/graficos-da-pesquisa-salarial/>. Accessed on: Aug 20, 2024.

SANTOS, B. L. P. et al. Unlocking the potential of biosurfactants: Production, applications, market challenges, and opportunities for agro-industrial waste valorization. **Environmental Research**, v. 244, p. 117879, 2024.

SEIDER, W. D. et al. Product and Process Design Principles: Synthesis, Analysis, and Evaluation. New York: **John Wiley & Sons Inc**, 2017. v. 4, p. 500–505.

SHERAZI, S. T. H.; MAHESAR, S. A.; SIRAJUDDIN. Vegetable oil deodorizer distillate: A rich source of the natural bioactive components. **Journal of Oleo Science.** Japan Oil Chemists Society, v. 65, n. 12, p. 957-966, 2016.

SHIMADA, Y. et al. Facile Purification of Tocopherols from Soybean Oil Deodorizer Distillate in High Yield Using Lipase**. JAOCS**, v. 77, n. 10, 2000.

SIGMA ALDRICH. **Enzyme**. **Amano Lipase from Pseudomonas fluorescens**, 2024a. Available in: <https://www.sigmaaldrich.com/BR/pt/product/aldrich/534730>. Accessed on: Aug 28, 2024.

SIGMA ALDRICH. **Enzyme**. **Lipase, produced by Aspergillus oryzae**, 2024b. Available in: <https://www.sigmaaldrich.com/BR/pt/product/sigma/sae0065>. Accessed on: Aug 28, 2024.

SIGMA ALDRICH. **Enzyme**. **Lipase immobilized from Candida antarctica**, 2024c. Available in: <https://www.sigmaaldrich.com/BR/pt/product/sigma/73940>. Accessed on: Aug 28, 2024.

SOUZA, M. S. et al. Biodiesel synthesis via esterification of feedstock with high content of free fatty acids. **Applied Biochemistry and Biotechnology**, v. 154, p.253–267, 2009.

SYNTH. **Loja Synth**. 2024. Available in: <https://www.lojasynth.com/reagentes-analiticosmaterias-primas/reagentes-analiticosmaterias-primas/xilose-d-extra-pura>. Accessed on: Aug 28, 2024

TORRES, C. F. et al. A two steps enzymatic procedure to obtain sterol esters, tocopherols and fatty acid ethyl esters from soybean oil deodorizer distillate. **Process Biochemistry**, v. 42, n. 9, p. 1335–1341, 2007.

TORRES, C. F. et al. Production of phytosterol esters from soybean oil deodorizer distillates. **European Journal of Lipid Science and Technology**, v. 111, n. 5, p. 459–463, 2009.

TURTON, R.; BAILIE, R. C.; WHITING, W. B.; SHAEIWITZ, J. A. Analysis, synthesis and design of chemical processes. 3. ed. Upper Saddle River: **Pearson Education**, Inc, 2009. p. 1-1007.

UDEH, B. Bio-waste Transesterification Alternative for Biodiesel Production: A Combined Manipulation of Lipase Enzyme Action and Lignocellulosic Fermented Ethanol. **Asian Journal of Biotechnology and Bioresource Technology**, v. 3, n. 3, p. 1–9, 2018.

VIEIRA, A. C.; CANSIAN, A. B. M.; GUIMARÃES, J. R.; VIEIRA, A. M. S.; FERNANDEZ-LAFUENTE, R.; TARDIOLI, P. W. Performance of liquid eversa on fatty acid ethyl esters production by simultaneous esterification/transesterification of low-to-high acidity feedstocks. **Catalysts**, v. 11, n. 12, 2021.

VIEIRA, A. C. Produção enzimática de compostos de valor agregado a partir do destilado da desodorização do óleo de soja. Thesis. **UFSCar**, São Carlos, SP, Brazil, 2021.

VILAS BÔAS, R.; ALMEIDA, L. DE A. DE; MENDES, M. F. Techno-economic evaluation of biodiesel production using by-product as raw material and hydrotalcite-hydroxyapatite as catalyst. **Research, Society and Development**, v. 11, n. 4, p. e0511426977, 2022.

VISIOLI, L. J. et al. Batch and continuous γ-alumina-catalyzed FAME production from soybean oil deodorizer distillate by interesterification. **Fuel**, v. 351, 1 nov. 2023.

VISIOLI, L. J. et al. Production of esters from soybean oil deodorizer distillate in pressurized ethanol. **Fuel Processing Technology**, v. 149, p. 326–331, 2016.

WAGNER, W. F. W.; LINCOLN, M. A. D.; LINCOLN, V. H. S. Separation and Purification of sugar esters. **Patent** number: 4,983,731, USA, 1991.

WANG, L. et al. Lipase-catalyzed biodiesel production from soybean oil deodorizer distillate with absorbent present in tert-butanol system. **Journal of Molecular Catalysis B: Enzymatic**, v. 43, n. 1–4, p. 29–32, 2006.

WATANABE, Y. et al. Purification of Tocopherols and Phytosterols by a Two-Step in situ Enzymatic Reaction. Press 339**. JAOCS**, **Journal of the American Oil Chemists' Society,** Vol. 81, no. 4, 2004.

XIONG, Y. W. et al. Non-isothermal (trans)esterification of linoleic acid and soybean oil deodorizer distillate with methanol under subcritical conditions. **Renewable Energy**, v. 197, p. 528–544, 2022.

YIN, X. et al. Biodiesel production from soybean oil deodorizer distillate enhanced by counter-current pulsed ultrasound. **Ultrasonics Sonochemistry**, v. 23, p. 53–58, 2015.

YIN, X. et al. Biodiesel production from soybean oil deodorizer distillate using calcined duck eggshell as catalyst. **Energy Conversion and Management**, v. 112, p. 199–207, 2016.

YIN, X. et al. Intensification of biodiesel production using dual-frequency counter-current pulsed ultrasound. **Ultrasonics Sonochemistry**, v. 37, p. 136–143, 2017.

ZHENG, J. et al. Immobilization of Lipozyme TL 100L for methyl esterification of soybean oil deodorizer distillate. **3 Biotech**, v. 10, n. 2, 2020.

CHAPTER 5: Final considerations

5.1 Conclusions

The research successfully described all the studied processes using the mathematical models developed, with the simulations and numerical results aligning with the compositions obtained in experimental data and tests. This thorough description allowed for effective economic and environmental assessments of the plants, providing reliable basis for comparison.

For the proposed process of esterification, by immobilized lipase, of oleic acid with xylose (tert-butanol as solvent), followed by recovery and reuse of enzymes and separation/purification of the product, the initial economic analysis indicates an MBPS of US$72.37/kg with 86% de purity (Appendices). When we replaced the solvent in the reaction medium with methyl ethyl ketone and increased investment in the purification stages, the MSBP became US$ 392.98 per kg of biosurfactant with 96% purity (Chapter 3). The process production cost obtained is justified by high biosurfactant purity and applicability in the pharmaceutical and cosmetic industries. As for LCA, the product showed low levels of ozone layer depletion, human toxicity, aquatic marine ecotoxicity, and photochemical oxidation, highlighting its environmental viability and lower impact. Given the current search for environmentally friendly products, all these environmental indicators bring even more attractiveness to the product.

The enzymatic processes for producing biodiesel and biosurfactants utilizing SODD as raw material were also accurately described for the modeling and simulation. The techno-economic evaluation of the biodiesel route presented a Minimum Biodiesel Selling Price (MBSP) of approximately US$6.15/L or US$6.84/kg (Chapter 4). Regarding the Life Cycle Assessment (LCA), our process has lower indicators than Brazil's chemical catalysis of biodiesel from soybean oil.

Three scenarios containing different solvent mixtures were evaluated for biosurfactants (xylose esters) production through transesterification/ esterification reactions from SODD (Chapter 4). When we compared all of them, the final purity in terms of mass of xylose esters decreased (process (a): 80.81%; process (b): 76.61%; process (c): 71.37%). This decrease in ester concentration was expected

since the conversion is different in each case. We found a Minimum Biosurfactant Selling Price (MBSP) of $13.42/kg of product for the process (a), $5.82/kg for the process (b), and $6.56/kg for the process (c). The production costs were comparable and competitive with others in the literature. The Life Cycle Assessment (LCA) reinforced the value of using SODD as a raw material for biosurfactants since all the parameters indicate an impactive reduction compared with almost all other works.

The research showed that improving the use of an optimized solvent mixture associated with the reuse of SODD can make this residue viable and add value to the biorefinery, bringing not only profit but also a more careful view of the environmental impacts that the industry causes.

5.2 Future work

For future work, the following are suggested:

- Evaluation of separation methods such as vacuum distillation to increase the concentration of biodiesel produced;
- Evaluate other drying options for the material, such as flash or rinse dryers;
- Research the production of enzymes with less environmental impacts;
- Research other paths and optimize experimental parameters for biodiesel production from SODD to reduce costs;
- Investigate methods that are not costly but increase the degree of purity of biosurfactants;
- Develop kinetic models for biosurfactant production from SODD;
- Perform a techno-economic-environmental analysis of xylose production from other biorefinery residues, such as sugarcane bagasse.

APPENDICES

APPENDIX A

Modeling and simulation of the biosurfactant production by enzymatic route using xylose and oleic acid as reagents

Ana Bárbara Moulin Cansian, Paulo Waldir Tardioli, Felipe Fernando Furlan, Ruy de Sousa Júnior

A.1 Introduction

Biosurfactants are amphipathic molecules obtained by enzymatic or microbiological routes. Like surfactants, they have amphiphilic structures, which means that the molecules have hydrophobic and hydrophilic regions (SANTOS et al., 2016). This duality generates interfaces with different degrees of polarity, bringing the substance adsorption characteristic (MARCELINO et al., 2016). Among the main characteristics of these molecules are emulsification capability, reduction of viscosity, reduction of surface tension, stabilizing effect and solubilizing ionic strength (SARUBBO, et al., 2006). Based on these characteristics, biosurfactants can be applied in pharmaceutical, oil, textile, food and cosmetics industries, among others (EL-SHESHTAWY et al., 2015). However, despite presenting low toxicity, good degradability, thermal stability, specific bioactivity, among other advantages, biosurfactants still lose market share to synthetic surfactants due to their high production cost (DÍAZ DE RIENZO et al., 2015).

It is important to note that the cost-benefit ratio in the application of biosurfactants can be valued for processes that require a lower degree of purity, since the separation and purification steps represent about 60% of the final operational cost of production (SARUBBO et. al, 2015). Another important point that impacts production costs is the choice of reagents, which can reach 50% (RUFINO et al., 2014).

The literature reports different studies on the production of sugar esters (biosurfactants) by microbiological route, involving steps of purification by means of solvent extraction, acid precipitation, centrifugation, filtration, gel filtration chromatography and lyophilization (MUKHERJEE et al., 2009; SATPUTE et al,, 2010; VARJANI et al, 2014; 2016).

For the production of biosurfactants by enzymes, several studies are reported focusing on the development or immobilization of the catalyst. The synthesis process can occur through the esterification of sugars with fatty acids, with lipase as the main enzyme that catalyzes the reaction (PAULA et al., 2005). Lipases are part of a group of hydrolytic enzymes, found in animals or produced from fermentation using some species of microorganisms. They are able to catalyze interesterification, transesterification and esterification reactions (CARVALHO et al., 2003). In particular, the immobilization of enzymes appears as a solution for the structural conformation of lipases in environments not conducive to them. In this way, through immobilization, they become stable for catalysis with their active sites exposed (DALLA-VECCHIA et al., 2004). Another advantage brought by immobilization is the inssolubilization of the enzyme in the liquid phase. Depending on the system, it facilitates their separation and reuse for long periods, contributing to the reduction of process costs. The work GUO et al. (2015) achieved a good conversion in the production of glucose esters under specific conditions of enzymatic reaction. Some other studies also use enzymes for the production of sugar esters, but none of them focuses on the separation/purification process of the product obtained (HA et al., 2010; ZAIDAN et al., 2012; MAI et al., 2014; TORRES et al., 2020).

There are several possibilities for employing less costly alternatives to the process as to the reagents used, being possible to integrate the production of biosurfactants within a concept of biorefinery. More specifically, within the framework of a biodiesel-bioethanol biorefinery, using by-products such as SODD (Soybean Oil Deodorization Distillate), obtained in the refining stage of soybean oil, and biomass residues, obtained in the production of bioethanol (HIRALES et al., 2020; PRATTO et al., 2020; RANKOVIĆ et al., 2014; MARZO et al., 2019).

Brazil has geographic and climatic factors that favours the cultivation of various oleaginous species that can be used in the production of oils. These species include pine nuts, castor beans, palm kernels, babassu coconuts, sunflower seeds, cotton, peanuts, linseeds, canola seeds, soybeans, corn, etc. On the other hand, residual vegetable oils are the result of domestic or industrial processes, citing as examples frying oils, industrial wastewater or by-products originating from refining stages, as SODD cited previously). Vegetable oils and their residues are mostly composed of mono, di and triglycerides and fatty acids, justifying their use as raw material in the esters production (MORAES, 2003; PARENTE, 2024.

Process residues involving biomass (such as sugarcane bagasse), in turn, have a high potential for conversion into renewable products with high commercial value (LAVARACK et al., 2000). In

particular, it is possible to obtain xylose from these residues. Lignocellulosic biomass needs pre-treatment that aims to disorganize the lignocellulosic complex and increase its surface area (HIRALES et al., 2020). Following the pre-treatment, hydrolysis occurs. Cellulose and hemicellulose are hydrolyzed and generate several products. Cellulose generates glucose and hemicellulose is broken down into hexoses and pentoses (like xylose), glucuronic acid and acetic acid (DUSSAN et al., 2013).

Thus, in order to contribute to the study of the production of biosurfactants in the context of a biodiesel-bioethanol biorefinery, the present paper aimed to model and simulate a process producing biosurfactants via heterogeneous biocatalysis with immobilized lipases, using oleic acid and xylose as reagents. The work was modelled and simulated in EMSO environment (Environment for Modeling, Simulation and Optimization). EMSO simulator is an equation-oriented process simulator for modeling steady-state and dynamic processes. It is CAPE-OPEN standard compliant. Pre-built models are available in the EMSO Modeling Library (EML). Besides, new models can be written in the EMSO modeling language. The behavior of the variables for the route under development was verified, as well as the energy costs were assessed throughout the process. Furthermore, the work aimed to simulate a separation/purification process as an alternative to the more complex and costly steps mentioned in the literature. Such alternative for the separation/purification of the product is a sequence of precipitation processes.

A.2 Material and methods

The main equipment used for computational simulations was a desktop with an Intel 7700K core I7 4.20 GHZ processor, 32 GB of RAM. In addition, a notebook with an Intel 3210M core I5 2.5 GHZ, 4 GB of RAM, was also employed in the project. The software used was EMSO academic beta version 0.10.9.

The route evaluated in this work encompasses the process of producing biosurfactants via heterogeneous biocatalysis, using immobilized lipases. Oleic acid and xylose were used directly as reagents. The process follows by recovery and reuse of the lipases and separation / purification of the product by a sequence of precipitations. This production route is presented in detail in Figure 1.

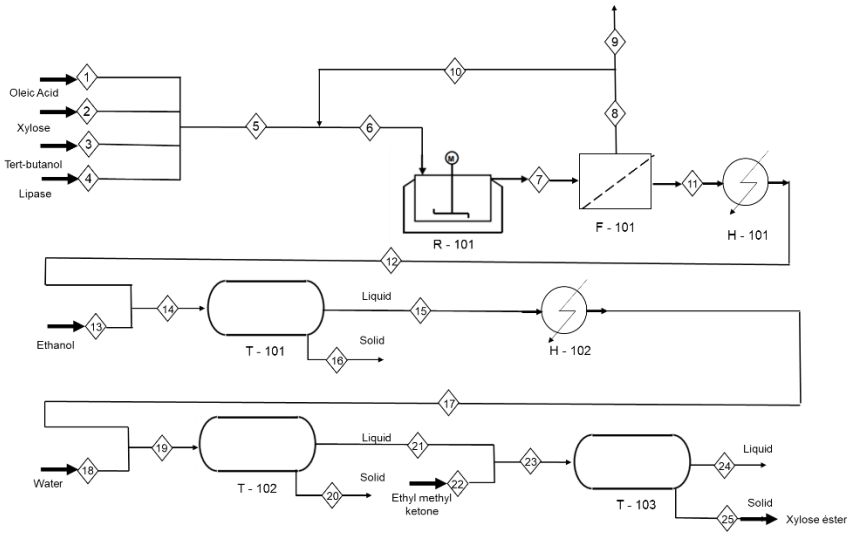

Figure 1. Representation of the production process of biosurfactants by enzymatic route.

A.2.1 Modeling

For the simulation of the process to be possible, it is necessary to model each equipment, as well as specify the operating conditions and considerations used in the models. The main equations on which the models are based will be presented. Table 1 shows the components used throughout the modeling and simulation processes.

Table 1. Components phase used in the simulation.

Components in the liquid phase	Components in the solid phase
Xylose	Immobilized Lipase
Oleic Acid	Xylose
Xylose Ester	Oleic Acid
Tert-butanol	Xylose Ester
Ethanol	-
Water	-
Ethyl Methyl Ketone	-

A.2.1.1 Mixer

The mixers used in this work were assumed to be static and adiabatic. This equipment has two inputs and one output and are considered the solid and liquid phases. Thus, each balance is carried out for both phases.

“Global molar balance”

$$Inlet1.F + Inlet2.F = Outlet.F \quad (1)$$

Where,

Inlet1.F: Molar flow of the input 1 of the equipment (kmol/h);

Inlet2.F: Molar flow of the input 2 of the equipment (kmol/h);

Outlet.F: Molar flow of the outlet of the equipment (kmol/h).

“Molar balance per component”

$$Inlet1.F \times Inlet1.z + Inlet2.F \times Inlet2.z = Outlet.F \times Outlet.z \quad (2)$$

Inlet1.z: Molar composition of the input 1 of the equipment (kmol of i component/kmol total);

Inlet2.z: Molar composition of the input 2 of the equipment (kmol of i component/kmol total);

Outlet.z: Molar composition of the output of the equipment (kmol of i component/kmol total).

“Consideration for pressure”

$$Outlet.P = \min[(Inlet1.P, Inlet2.P)] \quad (3)$$

Outlet.P: Pressure of the outlet stream of the equipment (kPa);

Inlet1.P: Pressure of the input stream 1 of the equipment (kPa);

Inlet2.P: Pressure of the input stream 2 of the equipment (kPa).

"Energy balance"

$$Outlet.F \times Outlet.h = Inlet1.F \times Inlet1.h + Inlet2.F \times Inlet2.h \quad (4)$$

Outlet.h: Enthalpy of the output stream of the equipment (kJ/kmol);

Inlet1.h: Enthalpy of the input stream 1 of the equipment (kJ/kmol);

Inlet2.h: Enthalpy of the input stream 2 of the equipment (kJ/kmol).

A.2.1.2 Esterification reactor

The reactor was assumed to be stoichiometric and in steady state, with conversion that could be specified based on the reaction limiting reagent. This equipment has a single input and one output. The solid and liquid phases are considered, so each balance is carried out for both phases.

“Reaction rate”

$$r = stoic \times conv \times z(\text{limit}) \quad (5)$$

r: Reaction rate (dimensionless);

stoic: Matrix of stoichiometric coefficients (dimensionless);

conv: Reaction conversion (dimensionless);

z (limit): Molar fraction of the limiting reagent for each reaction (dimensionless).

“Molar balance per component”

$$Outlet.F \times Outlet.z = Inlet.F \times Inlet.z + F \times r \quad (6)$$

F: Total molar flow of the equipment inlet (kmol/h).

"Energy balance"

$$Outlet.F \times Outlet.h = Inlet.F \times Inlet.h + Q - F \times sum(h_R \times conv \times z(\text{limit})) \quad (7)$$

Q: Heat removed from the reactor so that the temperature is maintained (kW or kJ/h);

h_R: Enthalpy of reaction (kJ/kmol).

“Reactor pressure”

$$Inlet.P = Outlet.P \quad (8)$$

A.2.1.3 Filter

The filtration employed separates the solids present from the liquid phase, in steady state and in adiabatic conditions. This equipment has a single inlet and two outlets, one with a higher concentration of solids and the other of liquids. The solid and liquid phases are considered, so each balance is carried out for both phases.

“Global molar balance”

$$Inlet.F = OutletS.F + OutletL.F \quad (9)$$

OutletS.F: Molar flow of solids output from the equipment (kmol/h);

OutletL.F: Molar flow of liquids output from the equipment (kmol/h).

"Efficiency of liquid separation"

$$OutletL.Fluid.Fw = Inlet.Fluid.Fw \times frac\_liq \quad (10)$$

OutletL.Fluid.Fw: Mass flow of the fluid in the liquid outlet stream (kg/h);

Inlet.Fluid.Fw: Mass flow of the fluid in the equipment inlet stream (kg/h);

frac_liq: Fraction of liquids from the inlet that leaves the equipment in the liquid stream (kg of liquids/kg total).

“Efficiency of solid separation”

$$Outlet.Solid.Fw = Inlet.Solid.Fw \times frac\_sol \quad (11)$$

OutletS.Solid.Fw: Mass flow of solids in the equipment solids outlet (kg/h);

Inlet.Solid.Fw: Mass flow of solids in the equipment entrance (kg/h);

frac_sol: Fraction of solids from the inlet that leaves the equipment in the solid stream (kg of solids/ kg total).

“Humidity in the solid stream”

$$humidity = \frac{OutletS.Fluid.Fw}{OutletS.Total.Fw} \quad (12)$$

humidity: Fraction of liquids in the equipment solids outlet (kg of liquids/kg total).

“Impurities in the liquid stream”

$$Outlet.Solid.Fw = impurity \times (OutletL.Total.Fw) \quad (13)$$

OutletL.Solid.Fw: Mass flow of solids in the liquid outlet of the equipment (kg/h);

Impurity: Fraction of solids in the liquid outlet of the equipment (kg of solids/kg total);

OutletL.Total.Fw: Total mass flow of the equipment liquid outlet (kg/h).

"Thermal balance"

$$OutletS.T = Inlet.T \quad (14)$$

$$OutletL.T = Inlet.T \quad (15)$$

"Mechanical balance"

$$OutletS.P = Inlet.P \quad (16)$$

$$OutletL.P = Inlet.P \quad (17)$$

“Enthalpy of the streams”

$$OutletS.h = Inlet.h \quad (18)$$

$$OutletL.h = Inlet.h \quad (19)$$

A.2.1.4 Cooler

The cooler was used to cool the process stream in a steady state and with no heat loss to the environment. This device has a single input and one output, without changing the stream mass. The solid and liquid phases are considered, so each balance is carried out for both phases.

“Molar balance”

$$Inlet.F = Outlet.F \quad (20)$$

"Composition"

$$Outlet.z = Inlet.z \quad (21)$$

“Pressure Delta”

$$Outlet.P = Inlet.P - Pdrop \quad (22)$$

Pdrop: Head loss in the heat exchanger (kPa).

“Heat exchanged”

$$Q = U \times A \times lmtd \quad (23)$$

$$lmtd = \frac{\Delta T_1 - \Delta T_2}{\ln\left(\frac{\Delta T_1}{\Delta T_2}\right)} \quad (24)$$

Q: Heat exchanged in the equipment (kW);

U: Global coefficient of thermal exchange (kW/m²/K);

A: Heat exchange area (m²);

lmtd: Logarithmic mean temperature difference (K).

A.2.1.5 Splitter

The separators used in this work were assumed to be static and adiabatic. This equipment has a single input and two outputs. The solid and liquid phases are considered, so each balance is carried out for both phases.

“Global molar balance”

$$Inlet.F = Outlet1.F + Outlet2.F \quad (25)$$

“Molar balance per component”

$$Inlet.F \times Inlet.z = Outlet1.F \times Outlet1.z + Outlet2.F \times Outlet2.z \quad (26)$$

“Consideration for pressure”

$$Outlet1.P = Inlet.P \quad (27)$$

$$Outlet2.P = Inlet.P \quad (28)$$

"Energy balance"

$$Outlet1.F \times Outlet1.h + Outlet2.F \times Outlet2.h = Inlet.F \times Inlet.h \quad (29)$$

A.2.1.6 Pump

The pump operates in steady state with the aim of correcting a certain pressure drop. The equipment has a single entrance and a single exit. There is no heat exchange with the environment and, again, all balances occur for liquid and solid phases.

“Molar balance for liquid phase”

$$Inlet.Fluid.F = Outlet.Fluid.F \quad (30)$$

“Molar balance for solid phase”

$$Inlet.Solid.F = Outlet.Solid.F \quad (31)$$

“Molar fraction for liquid phase”

$$Outlet.Fluid.z = Inlet.Fluid.z \quad (32)$$

“Molar fraction for solid phase”

$$Outlet.Solid.z = Inlet.Solid.z \quad (33)$$

"Head loss"

$$Outlet.P = Inlet.P + PIn \quad (34)$$

PIn: Pressure delta.

"Energy balance"

$$Inlet\_p.W = Inlet.Fluid.F \times (Outlet.Fluid.h - Inlet.Fluid.h) + Inlet.Solid.F \times (Outlet.Solid.h - Inlet.Solid.h) \quad (35)$$

“Work”

$$Inlet\_p.W = (Inlet.Fluid.Fw + Inlet.Solid.Fw) \times \frac{PIn}{n \times density} \quad (36)$$

n: pump efficiency (dimensionless).

A.2.2 Simulation

According to Figure 1, the process starts with the reactants (oleic acid and xylose), the solvent (tert-butanol) and the enzyme (lipase) being mixed to form stream 5 that joins to the system recycle and enters the bioreactor. In the reactor, the reaction takes place and there is consumption of reagents and formation of product. Stream 7 goes downstream to filtration, where part of the immobilized enzyme is recycled (a fraction is removed from the process (stream 9) while another is reinserted (stream 10)). Afterwards, the enzyme-free stream goes to the purification process, where stream 11 is cooled and mixed with ethanol in a separation tank. After the equilibrium is established, a solid phase is formed at the bottom of the tank, which is removed from the process. In the sequence, stream 15 is cooled and water is added to the stream to form a new equilibrium in a tank where the solid formed is removed. Soon after, ethyl methyl ketone is inserted into the process in a way that the precipitated formed contains the product of interest, xylose ester (stream 25).

The process simulation occurs in order to approximate the operating conditions of a given operational scheme and to verify the behavior of some variables. Thus, the EMSO software was used to solve the set of equations that describe the process based on the modeling presented previously. Tables 2 and 3 present the main specifications for the process simulation. As the simulated process has 2554 variables and 2419 equations, 135 specifications are needed. Thus, the remaining specifications are found in the supplementary material (Table S1).

Table 2. Variables specified in the process input streams.

Stream	Phase	Variable	Name	Unit	Value
Streams 1, 2,3 and 4	All	T	Temperature	K	333.15
Streams 1, 2,3 and 4	All	P	Pressure	atm	1
Streams 1, 2 and 3	Solid	F	Molar flow	kmol/h	1×10^{-6}
Stream 1	Liquid	F	Molar flow	kmol/h	50
Stream 2	Liquid	F	Molar flow	kmol/h	10
Stream 3	Liquid	F	Molar flow	kmol/h	175
Stream 4	Liquid	F	Molar flow	kmol/h	1×10^{-6}
Source 4	Solid	F	Molar flow	kmol/h	79.6
Stream 1	Solid	z(1)*	Composition	dimensionless	1
Stream 1	Solid	z(2 - 4)*	Composition	dimensionless	0
Stream 1	Liquid	z(1)*	Composition	dimensionless	0
Stream 1	Liquid	z(2)*	Composition	dimensionless	1
Stream 1	Liquid	z(3 - 7)*	Composition	dimensionless	0
Streams 2, 3 and 4	Solid	z(1)*	Composition	dimensionless	1
Streams 2, 3 and 4	Solid	z(2 - 4)*	Composition	dimensionless	0
Stream 2 and 4	Liquid	z(1)*	Composition	dimensionless	1
Stream 2 and 4	Liquid	z(2 - 7)*	Composition	dimensionless	0
Stream 3	Liquid	z(1 - 2)*	Composition	dimensionless	0
Stream 3	Liquid	z(3)*	Composition	dimensionless	0
Stream 3	Liquid	z(4)*	Composition	dimensionless	1
Stream 3	Liquid	z(5 - 7)*	Composition	dimensionless	0

* Component number: Liquids: 1-Xylose; 2-Oleic Acid; 3-Xylose Ester; 4-Tert-butanol, 5-Ethanol; 6-Water; 7-Ethyl Methyl Ketone. Solid: 1-Immobilized Lipase; 2-Xylose; 3-Oleic Acid; 4-Xylose Ester.

Table 3. Variables specified for the equipment.

Equipment	Variable	Name	Unit	Value
Reactor 101	conv	Conversion	dimensionless	0.7
Reactor 101	T	Temperature	K	333.15
Filter 101	frac_sol	Fraction of solids in the liquid stream	dimensionless	0.99
Filter 101	humidity	Fraction of liquid in the solid stream	dimensionless	0.10
Splitter between streams 8 and 9	frac	Fraction of the stream that will be removed from the process	dimensionless	0.10
Cooler 101	Pdrop	Pressure loss	atm	0
Cooler 101	Outlet.T	Output temperature	K	323.15
Cooler 101	U	Global heat exchange coefficient	kW/m²/K	0.6945
Cooler 101	lmtd	Logarithmic mean temperature difference	K	10

It is worth mentioning that the value of 1×10^{-6} present throughout the tables refers to the value zero and is used to avoid convergence problems. The information present in VESCOVI et al. (2017) was used for the reaction conditions, with the xylose to FFA (here represented by the Oleic Acid) molar ratio of 1:5, so for each 2.16 mmoles of xylose-FFA there is 6 mL of tert-butanol (as organic solvent) and 0.6 g of lipase, temperature of 60 ºC and conversion of 70%. The reaction of esterification of xylose with FFA follows the stoichiometry of Equation 37.

In the second stage of the process, there are precipitation tanks to purify the biosurfactant (Figure 1). WAGNER et al. (1991) presented a method for the separation and purification of sugar esters based on the precipitation of compounds. That method consisted of adding ethanol, water and ethyl methyl ketone, so that the ester was purified (a sucrose ester, in the specific case addressed by the authors (WAGNER et al., 1991)). Here, the first tank aims to precipitate the xylose (by adding ethanol), which is removed from the process, following Equation 38. The next two tanks (the second and the third) are intended to precipitate/purify the xylose ester. In the second tank the ester precipitation occurs with the presence of water, but part of the FFA is precipitated together with the ester. To achieve a higher level of purification, the last precipitation tank uses ethyl methyl ketone, which solubilizes part of the FFA, leaving the xylose ester more concentrated in the solid phase. The second process separation tank has three equations to represent what happens in precipitations and solubilizations. Equation 39 is the representation of the xylose ester precipitation. Equation 40 represents the precipitation of the FFA, and

Equation 41 the solubilization of xylose in water. The third and last separation tank aims to solubilize the FFA and thus increase the concentration of ester in the product. Equation 42 represents the solubilization of FFA in ethyl methyl ketone.

$$\underset{(Xylose)}{C_5H_{10}O_5(l)} + \underset{(Oleic\ Acid)}{C_{18}H_{34}O_2(l)} \Leftrightarrow \underset{(Xylose\ ester)}{C_{23}H_{42}O_6(l)} + \underset{(Water)}{H_2O(l)} \quad (37)$$

$$\underset{(Liquid\ xylose)}{C_5H_{10}O_5(l)} \Leftrightarrow \underset{(Solid\ xylose)}{C_5H_{10}O_5(s)} \quad (38)$$

$$\underset{(Liquid\ xylose\ ester)}{C_{23}H_{42}O_6(l)} \Leftrightarrow \underset{(Solid\ xylose\ ester)}{C_{23}H_{42}O_6(s)} \quad (39)$$

$$\underset{(Liquid\ FFA)}{C_{18}H_{34}O_2(l)} \Leftrightarrow \underset{(Solid\ FFA)}{C_{18}H_{34}O_2(s)} \quad (40)$$

$$\underset{(Solid\ xylose)}{C_5H_{10}O_5(s)} \Leftrightarrow \underset{(Liquid\ xylose)}{C_5H_{10}O_5(l)} \quad (41)$$

$$\underset{(Solid\ FFA)}{C_{18}H_{34}O_2(s)} \Leftrightarrow \underset{(Liquid\ FFA)}{C_{18}H_{34}O_2(l)} \quad (42)$$

A.3 Results and Discussion

A.3.1 Simulation

Table S2 presented in the supplementary material presents the data for stream 7, which is found immediately after the reactor output. It is noticed that in the process there is recovery and recycling of enzymes. The flow rate of the lipase source (line 8 of Table 2) was adjusted so that the flow of the enzyme into the esterification reactor (line 15 of Table S2) was in accordance with the literature, since 10% of this current is removed from the process. It is important to note that the lipase loses activity during the reactions and, therefore, the splitter is present in the simulation, representing a fraction of the enzyme stream that is removed from the process. In the study by VESCOVI et al. (2017), the immobilized enzyme loses its total activity in about 100h of reactions. The results for the recycle stream (Stream 10) and the stream that removes lipase from the process (Stream 9) are shown in Table S2. In

the simulation, it was necessary to add a pump that would correct the numerical errors inserted in the pressures. As in some cases of mechanical equilibrium the pressure at the output of the equipment was given by the minimum between the pressures of the inlet streams, the solution of the set of equations subtly modified these pressures, and, with this, modified the minimum pressure. This phenomenon led to the numerical non-convergence of the simulation. After countless tests and verifications to identify the problem, a loss of pressure was noticed throughout the process, which was the result of the numerical solution. To circumvent this problem, a pump was used in the recycle. The pump is located before the reactor, just after the separator (Stream 10).

After the esterification reaction and the filtration for reuse of the enzymes, the stream has the composition shown in Table 4. Notice that FFA is in greater quantity since it was placed in excess to get the degree of conversion of 70%.

Table 4. Results for stream 12.

Phase	Variable	Name	Unit	Value
Liquid	Fw	Mass flow	kg/h	28408.4
Solid	Fw	Mass flow	kg/h	166.793
All	T	Temperature	K	323.15
All	P	Pressure	atm	1
Liquid	zw(1)*	Composition	dimensionless	0.0154
Liquid	zw(2)*	Composition	dimensionless	0.4236
Liquid	zw(3)*	Composition	dimensionless	0.1030
Liquid	zw(4)*	Composition	dimensionless	0.4537
Liquid	zw(5)*	Composition	dimensionless	0
Liquid	zw(6)*	Composition	dimensionless	0.0045
Liquid	zw(7)*	Composition	dimensionless	0
Solid	zw(1)*	Composition	dimensionless	1
Solid	zw(2 - 4)*	Composition	dimensionless	0

* Component number: Liquids: 1-Xylose; 2-Oleic Acid; 3-Xylose Ester; 4-Tert-butanol, 5-Ethanol; 6-Water; 7-Ethyl Methyl Ketone. Solid: 1-Immobilized Lipase; 2-Xylose; 3-Oleic Acid; 4-Xylose Ester.

Mass balances are consistent with the results presented by VESCOVI et al. (2017), obtaining the production described by the authors. As the mass fraction of xylose ester in the stream is approximately 10.3% some purification steps are necessary in order to achieve higher concentrations of

biosurfactant in the product. Therefore, the reaction followed by the enzyme filtration step alone is not sufficient for this process.

The purification of the xylose ester consists of consecutive steps of addition of precipitant followed by precipitation. Figure 2 shows a graph of the composition of the streams after each purification step. The product enters this process at 10.3% (step 1: reactor exit after enzyme removal) in mass composition and reaches 10.4% in the first stage (1 → 2: first precipitation process with ethanol). In the second stage it reaches 37.6% (2 → 3: second precipitation process with water), and in the third (last) stage it reaches 85.7% (3 → 4: third precipitation process with ethyl methyl ketone, Table 5).

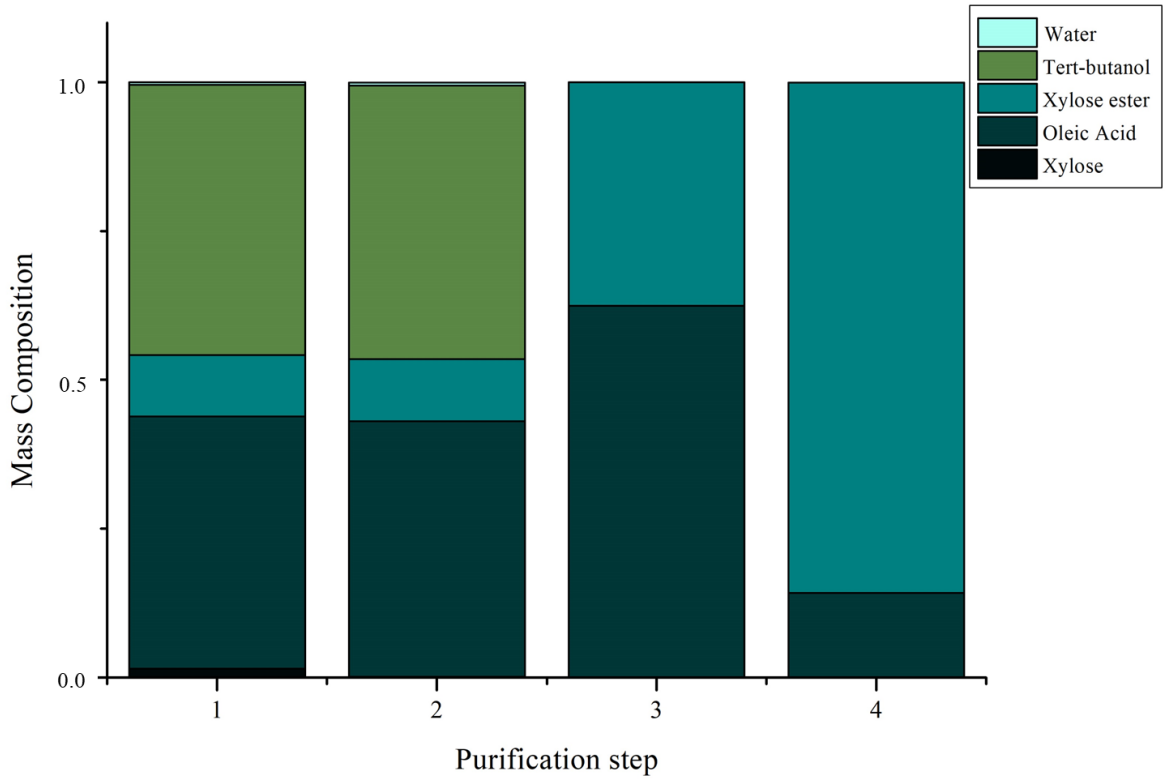

Figure 2. Mass composition of the streams after each stage (1, 2, 3 and 4) of purification.

Table 5. Results for stream 25.

Phase	Variable	Name	Unit	Value
Liquid	Fw	Mass flow	kg/h	367.413
Solid	Fw	Mass flow	kg/h	3306.72
All	T	Temperature	K	298.15
All	P	Pressure	atm	1
Liquid	zw(1)*	Composition	dimensionless	0.0004
Liquid	zw(2)*	Composition	dimensionless	0.8860
Liquid	zw(3)*	Composition	dimensionless	0.0002
Liquid	zw(4)*	Composition	dimensionless	0.1037
Liquid	zw(5)*	Composition	dimensionless	0.0002
Liquid	zw(6)*	Composition	dimensionless	0.0011
Liquid	zw(7)*	Composition	dimensionless	0.0084
Solid	zw(1)*	Composition	dimensionless	0.0005
Solid	zw(2)*	Composition	dimensionless	0
Solid	zw(3)*	Composition	dimensionless	0.1424
Solid	zw(4)*	Composition	dimensionless	0.8571

*Component number: Liquids: 1-Xylose; 2-Oleic Acid; 3-Xylose Ester; 4-Tert-butanol, 5-Ethanol; 6-Water; 7-Ethyl Methyl Ketone. Solid: 1-Immobilized Lipase; 2-Xylose; 3-Oleic Acid; 4-Xylose Ester.

Thus, the purification process indicates an overall efficiency of 88% ((0.857-0.103)/0.857). The literature does not report purification processes for obtaining biosurfactants by enzymatic route, using oleic acid and xylose as reagents. However, MUKHERJEE et al. (2009) report purification for biosurfactants obtained by microbiological route. The separation proceeds from several complex steps (acidification, cooling, gel filtration chromatography and lyophilization) up to reaching a lyophilized product with a high degree of purity. Regarding the degree of complexity of the proposed steps, the present work has reached a satisfactory purity, using simpler equipment. Energy costs throughout the process are shown in Table 6, separated by equipment.

In general, there is a greater absolute amount of heat associated with cooling (coolers 101 and 102, -604.14 kW) than heating (esterification reactor, 137.58 kW), with total heat of -466.56 kW. The energy expenditure figures exposed do not consider an energy integration of the process. If a possible energy integration is evaluated in order to feedback heat into the process, expenses can be significantly reduced, contributing to a reduction in operating costs. However, when assessing global energy costs,

the equipment used requires less heat than equipment used in the process of producing biosurfactants by microbiological routes, as mentioned in MUKHERJEE et al. (2009).

Table 6. Energy costs of the simulated process.

Equipment	Heat (kW)
Esterification reactor	137.58
Cooler 101	- 178.74
Cooler 102	- 425.39

Finally, to demonstrate the potential of the developed tool, a simple sensitivity analysis was carried out, showing the effect of the conversion of the esterification reactor on the mass composition of the final product.

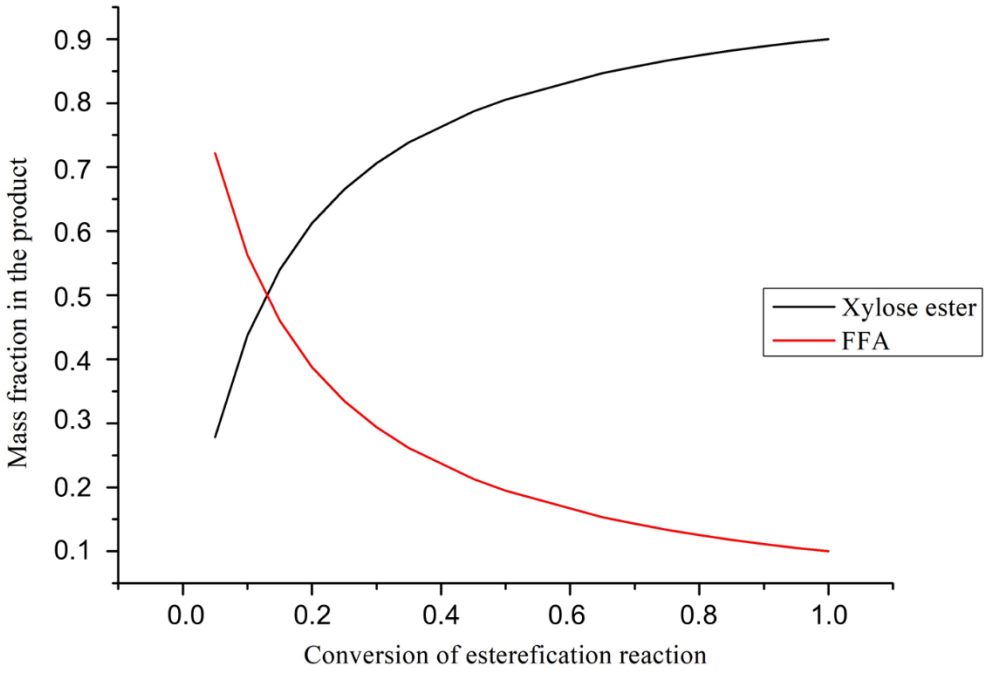

Figure 3. Ester/FFA fraction in the final stream of process versus conversion of the reactor.

From Figure 3 it is concluded that the gain of purity of xylose ester in the final product increases according to the conversion of reagents to ester in the reactor. Note that the behavior of the final product concentration has an exponential correlation with the conversion of the esterification reaction. For values around 15% conversion, the concentration of esters is greater than FFA in the final stream. It is worth mentioning that the final product concentration increases subtly at conversion values close to 100%. Therefore, there is no need for further research to increase the conversion above 70% in order to impact the final purity of the product.

From Figure 3 it is concluded that the gain of purity of xylose ester in the final product increases according to the conversion of reagents to ester in the reactor. Note that the behavior of the final product

concentration has an exponential correlation with the conversion of the esterification reaction. For values around 15% conversion, the concentration of esters is greater than FFA in the final stream. It is worth mentioning that the final product concentration increases subtly at conversion values close to 100%. Therefore, there is no need for further research to increase the conversion above 70% in order to impact the final purity of the product.

A.3.2 Economic analysis

Plant and operating costs for the process simulated in this work were calculated and analyzed. All the details of the calculations for this analysis are in the supplementary material. For equipment costs, the methodology from TURTON (2009) was used. Their parameters are shown in Table 7. The capacity of the equipment and their calculated costs are shown in Table 8.

Table 7. Equipment cost parameters to be used in economic analysis.

Equipaments	**K_1**	**K_2**	**K_3**	**FBM or (B1 and B2)**		**LF_B**	**A_{min}**	**A_{max}**	**Unit**
Esterification reactor (Jacketed agited)	4.1052	-0.4680	-0.0005	4.00		1.14	0.1	35	m^3
Filter (Gravity)	4.2756	-0.648	0.0714	1.65		1.14	0.5	80	m^2
Heat exchanger (Fixed tube)	4.3247	-0.3030	0.1634	1.63	1.66	1.14	10	1000	m^2
Process Vessel (Horizontal)	3.5565	0.3776	0.0905	1.49	1.52	1.14	0.1	628	m^3

Adapted from TURTON (2009).

For the operating costs evaluated in the economic analysis of the process, the raw material, labor, utility, operating supervision and maintenance costs were considered. These costs are presented in Table 9. Table 10, in turn, shows the cash flow for the process.

As can be seen, the cash flow obtained in the analysis was positive and the sales value of the product (for a return of 11% per year in a 25 years old plant) was US$72.37/kg. This price is coherent with some references presented in the literature (SIGMA ALDRICH, 2021; SOARES et al., 2018)

As a last effort, it was assessed the process from the point of view of its production scale (Figure 4).

Table 8. Equipments capacity according to process simulation and associated costs obtained.

Equipaments	Capacity	Cost
Esterefication reactor (Jacketed agited)	1451.87 m³ (Volume)	US$ 793083.09
Filter (Gravity)	39.75 m² (Area)	US$ 8550.56
Heat exchanger 1 (Fixed tube)	25.74 m² (Area)	US$ 107706.73
Heat exchanger 2 (Fixed tube)	61.26 m² (Area)	US$ 130288.61
Process Vessel 1 (Horizontal)	28.43 m³ (Volume)	US$ 116924.83
Process Vessel 2 (Horizontal)	27.99 m³ (Volume)	US$ 115763.22
Process Vessel 3 (Horizontal)	0.89 m³ (Volume)	US$ 20360.82
Total	-	US$ 1292677.87
Total plant installation	-	US$ 1525359.90

Table 9. Operating costs.

Raw material costs	US$ 1.024 x 10^9/year
Labor costs	US$ 511928.07/year
Utility costs	US$ 19730.66/year
Operating supervision costs	US$ 25596.40/year
Maintenance costs	US$ 76267.99/year
Total operating costs	US$ 1024271301.05/year

Table 10. Process cash flow.

Total operation cost	US$ 1024271301.05/year
Total revenue	US$ 1033841576.24/year
Cash flow	US$ 9570275.19/year

It can be seen that from 20% of the original scale to around 120%, the value of the product that brings profitability to the process remains practically unchanged. This value only changes when the process scale becomes between 0.75% and 20% of the original plant size.

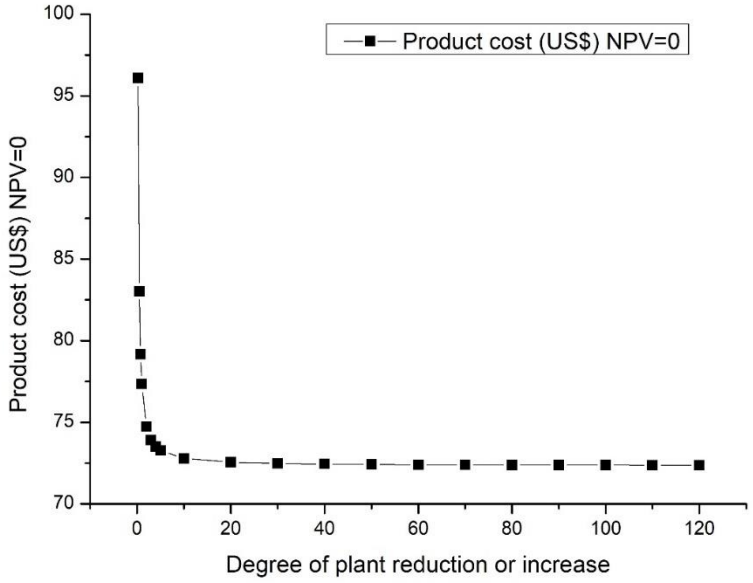

Figure 4. Product sales value depending on the degree of reduction or increase of the original plant (100%), with NPV = 0.

A.4 Conclusions

For the proposed process of esterification, by immobilized lipase, of oleic acid with xylose, followed by recovery and reuse of enzymes and separation/purification of the product, it was possible to develop mathematical models that successfully described the process. The simulation of the purification steps indicated a product with 86% in biosurfactants, which increased their recovery by 88%. It was also possible to obtain estimates of energy costs for the process. When compared to the works reported in the literature, the proposal presents itself as a more energy efficient and less complex alternative that uses cheaper equipment for the purification of biosurfactants. In addition, it is a suggested use for co-products from soy oil and 2G ethanol productions. It is worth mentioning that energy expenditure does not yet consider an integration of the process, therefore, these can still be significantly reduced by using energy integration analyzes in future works. The initial economic analysis of the process indicates a minimum profitability of around 11% in the plant for a product value of US$72.37/kg.

SUPPLEMENTARY MATERIAL

Table S1. Remaining variables specified for the simulation.

Stream or Equipment	Variable	Name	Unit	Value
Stream 13	F	Molar flow of ethanol	kmol/h	0.52
Stream 13	T	Temperature	K	323.15
Stream 13	P	Pressure	atm	1
Tank 101	Conv	Conversion	dimensionless	0.90
Splitter after T 101	frac_sol	Fraction of solids in the liquid stream	dimensionless	0.99
Splitter after T 101	humidity	Fraction of liquid in the solid stream	dimensionless	0.10
Stream 18	F	Molar flow of water	kmol/h	0.30
Stream 18	T	Temperature	K	298.15
Stream 18	P	Pressure	atm	1
Cooler 102	Pdrop	Pressure loss	atm	0
Cooler 102	Outlet.T	Output temperature	K	323.15
Cooler 102	U	Global heat exchange coefficient	kW/m²/K	0.6945
Cooler 102	Lmtd	Logarithmic mean temperature difference	K	10
Tank 102	Conv(1)	Conversion of FFA precipitation	dimensionless	0.40
Tank 102	Conv(2)	Conversion of xylose ester precipitation	dimensionless	0.99
Tank 102	Conv(3)	Conversion of xylose solubilization	dimensionless	0.99
Splitter after T 102	frac_sol	Fraction of solids in the liquid stream	dimensionless	0.99
Splitter after T 102	humidity	Fraction of liquid in the solid stream	dimensionless	0.10
Stream 22	F	Molar flow of ethyl methyl ketone	kmol/h	0.60
Stream 22	T	Temperature	K	298.15
Stream 22	P	Pressure	atm	1
Tank 103	Conv	Conversion of FFA solubilization	dimensionless	0.90
Splitter after T 103	frac_sol	Fraction of solids in the liquid stream	dimensionless	0.99
Splitter after T 103	humidity	Fraction of liquid in the solid stream	dimensionless	0.10

Table S2. Results for different process streams.

Stream	Phase	Variable	Name	Unit	Value
Stream 5	Liquid	F	Molar flow	kmol/h	235
Stream 5	Solid	F	Molar flow	kmol/h	79.6
Stream 5	Liquid	Fw	Mass flow	kg/h	28596
Stream 5	Solid	Fw	Mass flow	kg/h	1818.05
Stream 5	All	P	Pressure	atm	1
Stream 5	All	T	Temperature	K	333.15
Stream 5	Liquid	zw(1)*	Composition	dimensionless	0.0525
Stream 5	Liquid	zw(2)*	Composition	dimensionless	0.4939
Stream 5	Liquid	zw(3)*	Composition	dimensionless	0
Stream 5	Liquid	zw(4)*	Composition	dimensionless	0.4536
Stream 5	Liquid	zw(5 - 7)*	Composition	dimensionless	0
Stream 5	Solid	zw(1)*	Composition	dimensionless	1
Stream 5	Solid	zw(2 - 4)*	Composition	dimensionless	0
Stream 6	Liquid	F	Molar flow	kmol/h	248.572
Stream 6	Solid	F	Molar flow	kmol/h	730.275
Stream 6	Liquid	Fw	Mass flow	kg/h	30247.2
Stream 6	Solid	Fw	Mass flow	kg/h	16679.3
Stream 6	All	T	Temperature	K	333.15
Stream 6	All	P	Pressure	atm	1
Stream 6	Liquid	zw(1)*	Composition	dimensionless	0.0505
Stream 6	Liquid	zw(2)*	Composition	dimensionless	0.4901
Stream 6	Liquid	zw(3)*	Composition	dimensionless	0.0056
Stream 6	Liquid	zw(4)*	Composition	dimensionless	0.4536
Stream 6	Liquid	zw(5 - 7)*	Composition	dimensionless	0
Stream 6	Solid	zw(1)*	Composition	dimensionless	1
Stream 6	Solid	zw(2 - 4)*	Composition	dimensionless	0
Stream 9, 10	Liquid	zw(1)*	Composition	dimensionless	0.0151
Stream 9, 10	Liquid	zw(2)*	Composition	dimensionless	0.4237
Stream 9, 10	Liquid	zw(3)*	Composition	dimensionless	0.1030
Stream 9, 10	Liquid	zw(4)*	Composition	dimensionless	0.4537

Stream 9, 10	Liquid	zw(5)*	Composition	dimensionless	0
Stream 9, 10	Liquid	zw(6)*	Composition	dimensionless	0.0045
Stream 9, 10	Liquid	zw(7)*	Composition	dimensionless	0
Stream 9, 10	Solid	zw(1)*	Composition	dimensionless	1
Stream 9, 10	Solid	zw(2 - 4)*	Composition	dimensionless	0
Tank 101	Liquid	F	Molar flow	kmol/h	231.434
Tank 101	Solid	F	Molar flow	kmol/h	9.8812
Tank 101	Liquid	Fw	Mass flow	kg/h	28045.2
Tank 101	Solid	Fw	Mass flow	kg/h	533.899
Tank 101	All	T	Temperature	K	323.15
Tank 101	All	P	Pressure	atm	1
Tank 101	Liquid	zw(1)*	Composition	dimensionless	0.0015
Tank 101	Liquid	zw(2)*	Composition	dimensionless	0.4291
Tank 101	Liquid	zw(3)*	Composition	dimensionless	0.1044
Tank 101	Liquid	zw(4)*	Composition	dimensionless	0.4595
Tank 101	Liquid	zw(5)*	Composition	dimensionless	0.0008
Tank 101	Liquid	zw(6)*	Composition	dimensionless	0.0045
Tank 101	Liquid	zw(7)*	Composition	dimensionless	0
Tank 101	Solid	zw(1)*	Composition	dimensionless	0.3011
Tank 101	Solid	zw(2)*	Composition	dimensionless	0.6989
Tank 101	Solid	zw(3 - 4)*	Composition	dimensionless	0
Tank 102	Liquid	F	Molar flow	kmol/h	207.265
Tank 102	Solid	F	Molar flow	kmol/h	24.0645
Tank 102	Liquid	Fw	Mass flow	kg/h	20298.1
Tank 102	Solid	Fw	Mass flow	kg/h	7697.17
Tank 102	All	T	Temperature	K	298.15
Tank 102	All	P	Pressure	atm	1
Tank 102	Liquid	zw(1)*	Composition	dimensionless	0.0023
Tank 102	Liquid	zw(2)*	Composition	dimensionless	0.3550
Tank 102	Liquid	zw(3)*	Composition	dimensionless	0.0014
Tank 102	Liquid	zw(4)*	Composition	dimensionless	0.6336
Tank 102	Liquid	zw(5)*	Composition	dimensionless	0.0012
Tank 102	Liquid	zw(6)*	Composition	dimensionless	0.0065

Tank 102	Liquid	zw(7)*	Composition	dimensionless	0
Tank 102	Solid	zw(1)*	Composition	dimensionless	0.0002
Tank 102	Solid	zw(2)*	Composition	dimensionless	0
Tank 102	Solid	zw(3)*	Composition	dimensionless	0.6241
Tank 102	Solid	zw(4)*	Composition	dimensionless	0.3757
Tank 103	Liquid	F	Molar flow	kmol/h	24.3982
Tank 103	Solid	F	Molar flow	kmol/h	8.6713
Tank 103	Liquid	Fw	Mass flow	kg/h	5170.03
Tank 103	Solid	Fw	Mass flow	kg/h	3340.12
Tank 103	All	P	Pressure	atm	1
Tank 103	All	T	Temperature	K	298.15
Tank 103	Liquid	zw(1)*	Composition	dimensionless	0.0004
Tank 103	Liquid	zw(2)*	Composition	dimensionless	0.8860
Tank 103	Liquid	zw(3)*	Composition	dimensionless	0.0002
Tank 103	Liquid	zw(4)*	Composition	dimensionless	0.1037
Tank 103	Liquid	zw(5)*	Composition	dimensionless	0.0002
Tank 103	Liquid	zw(6)*	Composition	dimensionless	0.0011
Tank 103	Liquid	zw(7)*	Composition	dimensionless	0.0084
Tank 103	Solid	zw(1)*	Composition	dimensionless	0.0005
Tank 103	Solid	zw(2)*	Composition	dimensionless	0
Tank 103	Solid	zw(3)*	Composition	dimensionless	0.1423
Tank 103	Solid	zw(4)*	Composition	dimensionless	0.8571

*Component number: Liquids: 1-Xylose; 2-Oleic Acid; 3-Xylose Ester; 4-Tert-butanol, 5-Ethanol; 6-Water; 7-Ethyl Methyl Ketone. Solid: 1-Immobilized Lipase; 2-Xylose; 3-Oleic Acid; 4-Xylose Ester.

APPENDIX B

Tecno-economic analysis methodology for Appendix A.

B1. Equipment Cost

According to TURTON (2009), the cost of equipment can be described by Equation B.1. To apply Equation B.1, the equipment has minimum and maximum size specifications. When it is necessary, a correction is made to take into account the appropriate number of equipments to match the total area or volume that satisfies the process specifications. The modular basic cost is calculated by Equation B.2 (for Reactor and Filter) or by Equation B.3 (for Exchangers and Process Vessels). Since Equations B.1, B.2 and B.3 were exposed in 2001 for the first time, it is necessary to correct the estimative for the present time (Equation B.4). Finally, it is also important to adapt the prediction to the location where the equipment will be installed (Equation B.5).

$$\log_{10} C_P^0 = K_1 + K_2 \log_{10}(A) + K_3 [\log_{10}(A)]^2 \qquad (B.1)$$

C_P^0: Equipment cost under standard conditions (carbon steel and atmospheric pressure);

K_i: Specific constants for each equipment;

A: Equipment cost attribute (area or volume).

$$C_{BM} = C_P^0 \cdot F_{BM} \qquad (B.2)$$

C_{BM}: Bare module equipment cost;

F_{BM}: Bare module equipment cost factor.

$$C_{BM} = C_P^0 (B_1 + B_2) \qquad (B.3)$$

B_1: Bare module equipment cost factor 1;

B_2: Bare module equipment cost factor 2.

$$C_2 = C_1 \left(\frac{I_2}{I_1} \right) \qquad (B.4)$$

C_1: Cost of equipment at time 1;

C_2: Cost of equipment at time 2;

I_1: Price index (Marshall and Swift Equipment Cost Index (M&S)) at time 1;

I_2 : Price index at time 2.

For the both price indexes, it was utilized information from CAMARAZA-MEDINA et al. (2020).

$$C_B = C_{USGC} \cdot LF_B \qquad (B.5)$$

C_B : Equipment cost in Brazil;

C_{USGC}: Equipment price in USA gulf coast;

LF_B: Brazil location factor.

B.1.1 Esterification reactor (Jacketed agitated – carbon steel)

$$K_1 = 4.1052; \quad K_2 = -0.4680; \quad K_3 = -0.0005; \quad A_{\min} = 0.1m^3; \quad A_{\max} = 35m^3$$

$$\log_{10} C_P^0 = K_1 + K_2 \log_{10}(A) + K_3 [\log_{10}(A)]^2$$

$$\log_{10} C_P^0 = 4.1052 - 0{,}4680 \times \log_{10}(35) - 0.0005 \times [\log_{10}(35)]^2$$

$$C_P^0 = US\$2406.49$$

Each reactor has 35 m³, for A=1451.87 m³, we have 42 reactors:

$$C_P^0 = US\$2406.49 \times 42$$

$$C_P^0 = US\$101072.58$$

For bare module:

$$F_{BM} = 4.00; \quad C_P^0 = US\$101072.58;$$

$$C_{BM} = C_P^0 \cdot F_{BM}$$

$$C_{BM} = US\$101072.58 \times 4.00$$

$$C_{BM} = US\$404290.34$$

For time effect:

$$I_1 = 1262; \quad I_2 = 2171.6; \quad C_1 = US\$404290.34$$

$$C_2 = C_1 \left(\frac{I_2}{I_1} \right)$$

$$C_2 = US\$404290.34 \left(\frac{2171.6}{1262} \right)$$

$$C_2 = US\$695868.93$$

For location purposes: (USA – BRA):

$$C_{USGC} = US\$695868.93; \quad LF_B = 1.14$$

$$C_B = C_{USGC} \cdot LF_B$$

$$C_B = US\$695868.93 \times 1.14$$

$$C_B = US\$793083.10$$

B.1.2 Filter (Gravity – carbon steel)

$$K_1 = 4.2756; \quad K_2 = -0.6480; \quad K_3 = 0.0714; \quad A_{\min} = 0.5m^2; \quad A_{\max} = 80m^2; \quad A = 39.74m^2$$

$$\log_{10} C_P^0 = K_1 + K_2 \log_{10}(A) + K_3 [\log_{10}(A)]^2$$

$$\log_{10} C_P^0 = 4.2756 - 0.6480 \times \log_{10}(39.74) + 0.0714 \times [\log_{10}(39.74)]^2$$

$$C_P^0 = US\$2641.71$$

For bare module:

$$F_{BM} = 1.65; \quad C_P^0 = US\$2641.71$$

$$C_{BM} = C_P^0 \cdot F_{BM}$$

$$C_{BM} = US\$2641.71 \times 1.65$$

$$C_{BM} = US\$4358.82$$

For time effect:

$$I_1 = 1262; \quad I_2 = 2171.6; \quad C_1 = US\$4358.82$$

$$C_2 = C_1 \left(\frac{I_2}{I_1} \right)$$

$$C_2 = US\$4358.82 \left(\frac{2171.6}{1262} \right)$$

$$C_2 = US\$7500.49$$

For location purposes: (USA – BRA):

$$C_{USGC} = US\$7500.49; \quad LF_B = 1.14$$

$$C_B = C_{USGC} \cdot LF_B$$

$$C_B = US\$7500.49 \times 1.14$$

$$C_B = US\$8550.56$$

B.1.3 Heat exchanger 1 (Fixed tube – carbon steel)

$K_1 = 4.3247$; $K_2 = -0.3030$; $K_3 = 0.1634$; $A_{\min} = 10\,m^2$; $A_{\max} = 1000\,m^2$; $A = 25.74\,m^2$

$$\log_{10} C_P^0 = K_1 + K_2 \log_{10}(A) + K_3 [\log_{10}(A)]^2$$

$$\log_{10} C_P^0 = 4.3247 - 0.3030 \times \log_{10}(25.74) + 0.1634 \times [\log_{10}(25.74)]^2$$

$$C_P^0 = US\$16688.67$$

For bare module:

$B_1 = 1.63$; $B_2 = 1.66$; $C_P^0 = US\$16688.67$

$$C_{BM} = C_P^0 (B_1 + B_2)$$

$$C_{BM} = US\$16688.67(1.63 + 1.66)$$

$$C_{BM} = US\$54905.71$$

For time effect:

$I_1 = 1262$; $I_2 = 2171.6$; $C_1 = US\$54905.71$

$$C_2 = C_1 \left(\frac{I_2}{I_1} \right)$$

$$C_2 = US\$54905.71 \left(\frac{2171.6}{1262} \right)$$

$$C_2 = US\$94479.59$$

For location purposes: (USA – BRA):

$C_{USGC} = US\$94479.59$; $LF_B = 1.14$

$$C_B = C_{USGC} \cdot LF_B$$

$$C_B = US\$94479.59 \times 1.14$$

$$C_B = US\$107706.73$$

B.1.4 Heat exchanger 2 (Fixed tube – carbon steel)

$K_1 = 4.3247;\quad K_2 = -0.3030;\quad K_3 = 0.1634;\quad A_{\min} = 10 m^2;\quad A_{\max} = 1000\, m^2;\quad A = 61.26 m^2$

$$\log_{10} C_P^0 = K_1 + K_2 \log_{10}(A) + K_3 [\log_{10}(A)]^2$$

$$\log_{10} C_P^0 = 4.3247 - 0.3030 \times \log_{10}(61.26) + 0.1634 \times [\log_{10}(61.26)]^2$$

$$C_P^0 = US\$20187.63$$

For bare module:

$$B_1 = 1.63;\quad B_2 = 1.66;\quad C_P^0 = US\$20187.63$$

$$C_{BM} = C_P^0 (B_1 + B_2)$$

$$C_{BM} = US\$20187.63(1.63 + 1.66)$$

$$C_{BM} = US\$66417.29$$

For time effect:

$$I_1 = 1262;\quad I_2 = 2171.6;\quad C_1 = US\$66417.29$$

$$C_2 = C_1 \left(\frac{I_2}{I_1} \right)$$

$$C_2 = US\$66417.29 \left(\frac{2171.6}{1262} \right)$$

$$C_2 = US\$114288.26$$

For location purposes: (USA – BRA):

$$C_{USGC} = US\$114288.26;\quad LF_B = 1.14$$

$$C_B = C_{USGC} \cdot LF_B$$

$$C_B = US\$114288.26 \times 1.14$$

$$C_B = US\$130288.61$$

B.1.5 Process Vessel 1 (Horizontal – carbon steel)

$K_1 = 3.5565;\quad K_2 = 0.3776;\quad K_3 = 0.0905;\quad A_{\min} = 0.1 m^3;\quad A_{\max} = 628 m^3;\quad A = 28.43 m^3$

$$\log_{10} C_P^0 = K_1 + K_2 \log_{10}(A) + K_3 [\log_{10}(A)]^2$$

$$\log_{10} C_P^0 = 3.5565 + 0.3776 \times \log_{10}(28.43) + 0.0905 \times \left[\log_{10}(28.43)\right]^2$$

$$C_P^0 = US\$19802.27$$

For bare module:

$$B_1 = 1.49; \quad B_2 = 1.52; \quad C_P^0 = US\$19802.27$$

$$C_{BM} = C_P^0 (B_1 + B_2)$$

$$C_{BM} = US\$19802.27(1.49 + 1.52)$$

$$C_{BM} = US\$59604.82$$

For time effect:

$$I_1 = 1262; \quad I_2 = 2171.6; \quad C_1 = US\$59604.82$$

$$C_2 = C_1 \left(\frac{I_2}{I_1} \right)$$

$$C_2 = US\$59604.82 \left(\frac{2171.6}{1262} \right)$$

$$C_2 = US\$102565.64$$

For location purposes: (USA – BRA):

$$C_{USGC} = US\$102565.64; \quad LF_B = 1.14$$

$$C_B = C_{USGC} \cdot LF_B$$

$$C_B = US\$102565.64 \times 1.14$$

$$C_B = US\$116924.83$$

B.1.6 Process Vessel 2 (Horizontal – carbon steel)

$$K_1 = 3.5565; \quad K_2 = 0.3776; \quad K_3 = 0.0905; \quad A_{\min} = 0.1 m^3; \quad A_{\max} = 628 m^3; \quad A = 27.99 m^3$$

$$\log_{10} C_P^0 = K_1 + K_2 \log_{10}(A) + K_3 \left[\log_{10}(A)\right]^2$$

$$\log_{10} C_P^0 = 3.5565 + 0.3776 \times \log_{10}(27.99) + 0.0905 \times \left[\log_{10}(27.99)\right]^2$$

$$C_P^0 = US\$19605.54$$

For bare module:

$$B_1 = 1.49; \quad B_2 = 1.52; \quad C_P^0 = US\$19605.54$$

$$C_{BM} = C_P^0 (B_1 + B_2)$$

$$C_{BM} = US\$19605.54(1.49 + 1.52)$$

$$C_{BM} = US\$59012.67$$

For time effect:

$$I_1 = 1262; \quad I_2 = 2171.6; \quad C_1 = US\$59012.67$$

$$C_2 = C_1 \left(\frac{I_2}{I_1} \right)$$

$$C_2 = US\$59012.67 \left(\frac{2171.6}{1262} \right)$$

$$C_2 = US\$101546.68$$

For location purposes: (USA – BRA):

$$C_{USGC} = US\$101546.68; \quad LF_B = 1.14$$

$$C_B = C_{USGC} \cdot LF_B$$

$$C_B = US\$101546.68 \times 1.14$$

$$C_B = US\$115763.22$$

B.1.7 Process Vessel 3 (Horizontal – carbon steel)

$$K_1 = 3.5565; \quad K_2 = 0.3776; \quad K_3 = 0.0905; \quad A_{\min} = 0.1 m^3; \quad A_{\max} = 628 m^3; \quad A = 0.89 m^3$$

$$\log_{10} C_P^0 = K_1 + K_2 \log_{10}(A) + K_3 [\log_{10}(A)]^2$$

$$\log_{10} C_P^0 = 3.5565 + 0.3776 \times \log_{10}(0.89) + 0.0905 \times [\log_{10}(0.89)]^2$$

$$C_P^0 = US\$3448.29$$

For bare module:

$$B_1 = 1.49; \quad B_2 = 1.52; \quad C_P^0 = US\$3448.29$$

$$C_{BM} = C_P^0 (B_1 + B_2)$$

$$C_{BM} = US\$3448.29(1.49 + 1.52)$$

$$C_{BM} = US\$10379.34$$

For time effect:

$$I_1 = 1262; \quad I_2 = 2171.6; \quad C_1 = US\$10379.34$$

$$C_2 = C_1\left(\frac{I_2}{I_1}\right)$$

$$C_2 = US\$10379.34\left(\frac{2171.6}{1262}\right)$$

$$C_2 = US\$17860.37$$

For location purposes: (USA – BRA):

$$C_{USGC} = US\$17860.37; \quad LF_B = 1.14$$

$$C_B = C_{USGC} \cdot LF_B$$

$$C_B = US\$17860.37 \times 1.14$$

$$C_B = US\$20360.82$$

B.2 Plant installation cost (CAPEX - capital investments)

TURTON (2009) describes the cost of installing the plant as in Equation B.6:

$$C_{TM} = 1.18 \times \sum_{i=1}^{n} C_{BM,i} \qquad (B.6)$$

C_{TM} : Plant total cost;

$C_{BM,i}$: Equipament – i price (already corrected for time and location).

$$\sum_{i=1}^{n} C_{BM,i} = US\$129267.87$$

$$C_{TM} = 1.18 \times \sum_{i=1}^{n} C_{BM,i}$$

$$C_{TM} = 1.18 \times US\$129267.87$$

$$C_{TM} = US\$152535.90$$

B.3 NPV (Net present value) calculation

NPV is calculated according to Equation B.7, according to PETERS (2004):

$$NPV(X) = \sum_{j=1}^{N} \frac{CF(X)}{(1+r)^j} - CAPEX(X) \qquad (B.7)$$

$NPV(X)$: Net present value as a function of process variables;

$CF(X)$: Cash flow as a function of process variables;

r: Minimum acceptable rate of return;

N: Project lifetime;

$CAPEX(X)$: Capital investments as a function of process variables.

$r = 0.11; \quad N = 25 \ \ years$ (LONGATI et al., 2018) $NPV(X) = 0$

The value of NPV = 0 indicates that the project has obtained the stipulated minimum rate of return. Therefore, the NPV was zeroed in order to obtain the value of the product (US$ 72.37/kg) that makes the process profitable.

B.4 Raw material costs

Table B.1 shows all the calculations about the raw material.

Component	kg/h	R$/kg	US$/kg	R$/h	US$/h	
Xylose	1501.32	126.2[a]	21.94	189466.58	32944.41	
PPL enzyme	9.66 +	3048[b]	529.99	29436.00	5118.33	
Tert-butanol	259.43 *	131.51[c]	22.87	34117.60	5932.36	
Ethanol	0.4791 *	21.47[d]	3.73	10.287	1.79	
Ethyl Methyl Ketone	0.1081 *	161.74[e]	28.12	17.48	3.04	
Oleic Acid	14123.3	78.57[f]	13.66	1109693.52	192953.27	**US$/year**
Output product	3306.72	416.22[g]	72.37	1376305.80	239311.75	1.034×10^9
Total without product				1362741.49	236953.19	1.024×10^9

+: The calculation for PPL enzyme was performed considering its concentration in the immobilized support such as proposed by VESCOVI et al. (2017) (0.53% of PPL w/w); *: It was considered partial recovery of this reagents (for tert-butanol, ethanol and ethyl methyl ketone). Thus, it was adopted 2% from original simulation flows (for tert-butanol, ethanol and ethyl methyl ketone), being 1% associated with recuperation costs and other 1% with separation inefficiencies; a, e: SYNTH (2021); b: GLASSLAB (2021); c: NEON (2021); d, f: SIGMA ALDRICH (2021); g: value of the product obtained in the analysis (NPV=0).

Table B.1. Raw Material cost (per hour and per year).

B.5 Labor costs

The following equation can be used to estimate the number of shift operators in a chemical plant PETERS (2004):

$$N_{OL} = \left(6.29 + 31.7P^2 + 0.23N_{np}\right)^{0.5} \qquad (B.8)$$

N_{OL}: Number of shift operators;

P: Number of steps involving solids;

N_{np}: It is given by the sun of equipments.

$$N_{OL} = \left(6.29 + 31.7P^2 + 0.23N_{np}\right)^{0.5}$$

$P = 2$ (Two steps involve solids: enzymes, in the reactor, and purification step)

$N_{np} = 48$ (number of equipments)

$$N_{OL} = \left(6.29 + 31.7(2)^2 + 0.23 \times 48\right)^{0.5}$$

$$N_{OL} = 12.002 \approx 12 \, workes/turn$$

In three turns: 36 workers

In Brazil, the average salary of an employee who has completed high school is around R$1658.19 with 37% tax on this amount CAGED (2018). Considering the exchange rate of 5.7511 US$/R$ and the period of one year, it is possible to calculate the operating cost (BCB, 2021). See Table B.2.

Table B.2. Labor costs with descriptions and calculations.

NOL	11.61 = 12		workers/per turn
12h (3 turns)	36		workers
Salary	1658.19		R$/month
Taxes	0.37		%
Taxes	1658.19 x 0.37 =	613.53	R$/month
Worker cost per month	1658.19 + 613.53 =	2271.72	R$/month
Worker cost per month	2271.72/5.7511 =	395.01	US$/month
Total (per month)	395.01 x 36 =	14220.22	US$/month
Total (per year)	14220.22 x 12 =	**511928.07**	US$/year

B.6 Utility costs

Table B.3 and Table B.4 present all the information and calculations about the utility costs.

Table B.3. Utility costs with information and calculation.

	Heat (kWh)	US$/MWh (OLIVEIRA et al., 2018)	12h per day/ 30 days per month	Total Heat (MWh)	
Cold utility	-604.13	5.26		$\frac{604.13 \times 12 \times 30}{1000} =$	-217.49
Hot utility	137.58	10.1		$\frac{137.58 \times 12 \times 30}{1000} =$	49.53

Table B.4. Total utility costs.

Heat (MWh)	Total US$/month	
-217.49	$217.49 \times 5.26 =$	1143.98
49.53	$49.53 \times 10.1 =$	500.24
	Total	US$ 1644.22/month
	Total	**US$ 19730.66/year**

B.7 Total operating costs

According to PETERS (2004), the operating supervision costs are about 5% of operating labor costs and the maintenance costs are about 5% of capital cost. See Table B.5.

Table B.5. Total operating costs with calculations.

Operating labor cost	US$ 511928.07/year
Capital cost (Plant installation cost)	US$ 152359.90/25 years
Operating supervision costs	511928.07 x 0.05 = US$ 25596.40/year
Maintenance costs	152359.90 x 0.05 = US$ 76267.99/year

REFERENCES

CARVALHO, P. O.; CAMPOS, P. R. B.; NOFFS, M. D.; OLIVEIRA, J. G.; SHIMIZU, M. T.; SILVA, D. M. Aplicação de lipases microbianas na obtenção de concentrados de ácidos graxos poliinsaturados. **Química Nova**, v. 26, p. 75-80, 2003.

DALLA-VECCHIA, R.; NASCIMENTO, M. G.; SOLDI, V. Aplicações sintéticas de lipases imobilizadas em polímeros. **Química Nova**, v. 27, p. 623-630, 2004.

DÍAZ DE RIENZO, M. A. et al. Sophorolipid biosurfactants: Possible uses as antibacterial and antibiofilm agent. **New Biotechnology**, v. 32, n. 6, p. 720–726, 2015.

EL-SHESHTAWY, H. S. et al. Production of biosurfactant from Bacillus licheniformis for microbial enhanced oil recovery and inhibition the growth of sulfate reducing bacteria. **Egyptian Journal of Petroleum**, v. 24, n. 2, p. 155–162, jun. 2015.

GUO, D. et al. Scaling-up the synthesis of myristate glucose ester catalyzed by a CALB-displaying Pichia pastoris whole-cell biocatalyst. **Enzyme and Microbial Technology**, v. 75-76, p. 30–36, 2015.

HA, S. H.; HIEP, N. M.; KOO, Y.-M. Enhanced production of fructose palmitate by lipase-catalyzed esterification in ionic liquids. **Biotechnology and Bioprocess Engineering**, v. 15, n. 1, p. 126–130, 2010.

HILARES, R. T. et al. Hydrodynamic cavitation-assisted continuous pre-treatment of sugarcane bagasse for ethanol production: Effects of geometric parameters of the cavitation device. **Ultrasonics Sonochemistry**, v. 63, p. 104931–104931, 2020.

MAI, N. L., AHN, K., BAE, S. W., SHIN, D. W., MORYA, V. K., & KOO, Y.-M. Ionic liquids as novel solvents for the synthesis of sugar fatty acid ester. **Biotechnology Journal**, v. 9, p. 1565–1572, 2014.

MARCELINO, P. R. F. Produção de biossurfactantes de segunda geração por leveduras em hidrolisado hemicelulósico de bagaço de cana-de-açúcar. 2016. Thesis. Escola de Engenharia de Lorena, **Universidade de São Paulo**, Lorena, 2016.

MARZO, C. et. al. Status and Perspectives in Bioethanol Production From Sugar Beet. **Bioethanol Production from Food Crops**, chapter 4, p. 61–79, 2019.

MORAES, C. M. B. Vitamina e do destilado da desodorização do óleo de soja e sob forma de fármaco na prevenção à oxidação dos lípides e da necrose hepática decorrente de dieta deficiente em cistina para ratos. **Dissertation**. Unicamp, Campinas, 2003.

MUKHERJEE, S.; DAS, P.; SEN, R. Rapid quantification of a microbial surfactant by a simple turbidometric method. **Journal of Microbiological Methods**, v. 76, n. 1, p. 38–42, 2009.

PARENTE, J. S. Biodiesel: uma aventura tecnológica num país engraçado. 2003. Available in: <https://books.google.com.br/books/about/Biodiesel.html?id=FaAjYAAACAAJ&redir_esc=y>. Accessed on: Sep 4, 2024.

PAULA, A. V.; BARBOZA, J. C. S.; CASTRO, H. F. Estudo da influência do solvente, carboidrato e ácido graxo na síntese enzimática de ésteres de açúcares. **Química Nova**, v. 28, p. 792-796, 2005.

PRATTO, B. et al. Experimental optimization and techno-economic analysis of bioethanol production by simultaneous saccharification and fermentation process using sugarcane straw. **Bioresource Technology**, v. 297, p. 122494, 2020.

RANKOVIĆ, J. et al. Bioethanol production from intermediate products of sugar beet processing with different types of Saccharomyces cerevisiae. **Core.ac.uk**, 2014.

RUFINO, R. D. et al. Characterization and properties of the biosurfactant produced by Candida lipolytica UCP 0988. **Electronic Journal of Biotechnology**, v. 17, n. 1, p. 34–38, 2014.

SANTOS, D. K. F.; RUFINO, R. D.; LUNA, J. M.; SANTOS, V. A.; SARUBBO, L. A. Biosurfactants: Multifunctional Biomolecules of the 21st Century. **International Journal of Molecular Sciences**, v. 17, p 401-432, 2016.

SARUBBO, L. A.; DE LUNA, J. M.; DE CAMPOS-TAKAKI, G. M. Production and stability studies of the bioemulsifier obtained from a new strain of Candida glabrata UCP 1002**. Electronic Journal of Biotechnology**, v. 9, n. 4, p. 1–7, 15 jul. 2006.

SARUBBO, L. A.; LUNA, J. M.; RUFINO, R. D. Application of a biosurfactant produced in low-cost substrates in the removal of hydrophobic contaminants. **Chemical Engineering Transactions**, v. 43, p. 295–300, 2015.

SATPUTE, S. K. et al. Biosurfactants, bioemulsifiers and exopolysaccharides from marine microorganisms. **Biotechnology Advances**, v. 28, n. 4, p. 436–450, 2010.

TORRES, A.D.C.L.; DE LIMA, L.N.; TARDIOLI, P.W.; JÚNIOR, R.D.S. Mathematical modeling of enzymatic syntheses of biosurfactants catalyzed by immobilized lipases. **React. Kinet. Catal. Lett.** v. 130, p.699–712, 2020.

VARJANI, S. J., & UPASANI, V. N. Carbon spectrum utilization by an indigenous strain of Pseudomonas aeruginosa NCIM 5514: Production, characterization and surface active properties of biosurfactant. **Bioresource Technology**, v. 221, p. 510-516, 2016.

VARJANI, S.J., RANA, D.P., BATEJA, S., SHARMA, M.C., UPASANI, V.N. Screening and identification of biosurfactant (bioemulsifier) producing bacteria from crude oil contaminated sites of Gujarat, India. **International Journal of Innovative Research in Science, Engineering Technol**, n. 3, n. 2, p. 9205–9213, 2014.

ZAIDAN, U. H. et al. Biocatalytic production of lactose ester catalysed by mica-based immobilised lipase. **Food Chemistry**, v. 131, n. 1, p. 199–205, 2012.